National Library of Canada
Bibliothèque nationale du Canada

Canadian Theses Service
Service des thèses canadiennes

Ottawa, Canada
K1A 0N4

NOTICE

The quality of this microform is heavily dependent upon the quality of the original thesis submitted for microfilming. Every effort has been made to ensure the highest quality of reproduction possible.

If pages are missing, contact the university which granted the degree.

Some pages may have indistinct print especially if the original pages were typed with a poor typewriter ribbon or if the university sent us an inferior photocopy.

Reproduction in full or in part of this microform is governed by the Canadian Copyright Act, R.S.C. 1970, c. C-30, and subsequent amendments.

AVIS

La qualité de cette microforme dépend grandement de la qualité de la thèse soumise au microfilmage. Nous avons tout fait pour assurer une qualité supérieure de reproduction.

S'il manque des pages, veuillez communiquer avec l'université qui a conféré le grade.

La qualité d'impression de certaines pages peut laisser à désirer, surtout si les pages originales ont été dactylographiées à l'aide d'un ruban usé ou si l'université nous a fait parvenir une photocopie de qualité inférieure.

La reproduction, même partielle, de cette microforme est soumise à la Loi canadienne sur le droit d'auteur, SRC 1970, c. C-30, et ses amendements subséquents.

Canada

NL-339 (r. 88/04) c

GEOLOGY OF THE MOUNT COSTIGAN Pb-Zn DEPOSIT, WEST-CENTRAL NEW BRUNSWICK

by

Nicholas David Cox

A thesis
presented to the University of Ottawa
in partial fulfilment of the
requirements for the degree of
Master of Science
in Geology

Ottawa, Ontario

© Nicholas David Cox, Ottawa, Canada, 1990

National Library of Canada
Bibliothèque nationale du Canada

Canadian Theses Service
Service des thèses canadiennes

Ottawa, Canada
K1A 0N4

NOTICE

The quality of this microform is heavily dependent upon the quality of the original thesis submitted for microfilming. Every effort has been made to ensure the highest quality of reproduction possible.

If pages are missing, contact the university which granted the degree.

Some pages may have indistinct print especially if the original pages were typed with a poor typewriter ribbon or if the university sent us an inferior photocopy.

Reproduction in full or in part of this microform is governed by the Canadian Copyright Act, R.S.C. 1970, c. C-30, and subsequent amendments.

AVIS

La qualité de cette microforme dépend grandement de la qualité de la thèse soumise au microfilmage. Nous avons tout fait pour assurer une qualité supérieure de reproduction.

S'il manque des pages, veuillez communiquer avec l'université qui a conféré le grade.

La qualité d'impression de certaines pages peut laisser à désirer, surtout si les pages originales ont été dactylographiées à l'aide d'un ruban usé ou si l'université nous a fait parvenir une photocopie de qualité inférieure.

La reproduction, même partielle, de cette microforme est soumise à la Loi canadienne sur le droit d'auteur, SRC 1970, c. C-30, et ses amendements subséquents.

ISBN 0-315-60550-2

NL-339 (r. 88/04) c

Canada

UNIVERSITÉ D'OTTAWA
UNIVERSITY OF OTTAWA

But each one should be careful how he builds. For no one can lay any foundation other than the one already laid, which is Jesus Christ. If any man builds on this foundation using gold, silver, precious jewels, wood, hay or straw, his work will be shown for what it is, because the Day will bring it to light. It will be revealed with fire and the fire will test the quality of each man's work. If what he has built survives, he will receive his reward. If it is burned up, he will suffer loss; he himself will be saved, but only as one escaping through the flames.

1 Corinthians 3:10b-15

ABSTRACT

The Mount Costigan Pb-Zn deposit is located about 40km east of Plaster Rock, New Brunswick within the Early Devonian Costigan Mountain Formation, in the Matapedia Cover Sequence (formerly the Chaleur Bay Synclinorium). It occurs about 250m east of the summit of Mount Costigan within a series of brecciated and unbrecciated crystal and lapilli tuff, rhyolite and minor siltstone which are exposed in six trenches (North, South, East, West, Southwest and Central). To the west the Costigan Mountain Formation is overlain by the Wapske Formation.

The most significant feature of the deposit is the large amount of brecciation, which, in the Central Trench, also serves as the main sulphide host. Petrographic studies indicate that the breccia consists of angular to subangular blocks of massive and banded crystal tuff, massive to spherulitic to flow-banded rhyolite and minor lapilli tuff. It consists of two main types: 1. a polymictic allochthonous breccia exposed in the Central Trench and, 2. a monomictic crackle breccia, exposed in the North Trench. The latter type is interpreted to be autochthonous in origin.

The broadly circular plan shape of the breccia body led previous investigators to suggest it represents a breccia pipe associated with the Redstone Mountain Granite to the east. However, in this study, analysis of drill hole data show zones of breccia commonly separated by up to 70 metres of unbrecciated rock. Similarly, surface exposures of brecciated and unbrecciated rock occur outside of and within the limits originally defined for the breccia. Also, fractures in the trenches define two predominant directions (northwest to north-northwest and northeast to east-northeast) which are, in general, traceable through all of the trenches, suggesting they are a regional feature and not associated with the brecciation. The highly angular nature of the fragments in the allochthonous breccia, as well as the predominance of crystal tuff and rhyolite as fragment lithologies suggest that the breccia could have resulted from explosive volcanic activity or be a lag deposit on the flanks of a small rhyolite dome.

Mineralisation consists of fine- to coarse-grained sphalerite and galena (up to 20% Pb+Zn) and pyrite, with minor chalcopyrite and fluorite. Silver (1.5 to 32.6g/t) is most closely associated with the galena. Although most of the mineralisation in the Central Trench is essentially trace and disseminated in nature, approximately twenty areas of higher sulphide content are recognised. Sulphide textures in these areas occur in four styles: 1. Filling of fractures and between breccia fragments; 2. replacement of pumice fragments in rhyolite and crystal tuff, and replacement of compositional banding in crystal tuff; 3. Pods and veinlets in crystal tuff breccia fragments and/or matrix; 4. Fine-grained disseminations in breccia fragments and matrix.

Mineralisation at Mount Costigan has occurred in at least two phases. The earliest phase, prior to development of the breccia, is represented by disseminated sulphides in unbrecciated blocks of crystal tuff

within and outside of the breccia zone. The second, principal mineralising phase, which occurred either after or in the late stages of the brecciation is represented by fracture filling and replacement sulphides. The occurrence, within the stratigraphy, of successive mineralised breccia zones separated by poorly mineralised unbrecciated zones suggests that the mineralising fluids moved vertically along faults and fractures across the less permeable unbrecciated horizons and into the porous breccia.

Since epithermal systems commonly develop in the waning stages of explosive volcanism, the Mount Costigan deposit is interpreted to represent a base metal variety of epithermal deposit. The rocks were brecciated during the initial phase, while sulphide deposition occurred during the later, mature stages.

RÉSUMÉ

Le gisement de Pb-Zn du Mont Costigan est situé à 40km à l'est de Plaster Rock, Nouveau-Brunswick, à l'intérieur de la Formation Dévonienne Costigan Mountain, dans la séquence de couverture Matapédia (anciennement le synclinorium de la Baie-des-Chaleurs). Le gisement se situé à 250m à l'est du sommet du Mont Costigan, parmi une série brechifiée ou non de tufs à cristaux et à lapilli, de rhyolites et quelques aleuronites qui affleure dans six tranchées (nord, sud, est, ouest, sud-ouest et centrale). À l'ouest, la Formation Costigan Mountain est recouverte par la formation Wapske.

La caractéristique la plus importante de ce gisement est la grande quantité des brèches, qui dans la tranchée centrale encaissent principalement les sulphures. Les études pétrographique indiquent que les brèches sont composées de fragments angulaires ou subangulaires de tufs à cristaux, massive et laminée, de rhyolite massive, laminée ou sphérulitique et de quelques tufs à lapilli. Deux types principaux sont reconnus: 1. une brèche polymictique allochtone qui affleure dans la tranchée centrale et; 2., une brèche craquelée monomictique et autochtone qui affleure dans la tranchée nord.

Plusieurs chercheurs ont conclu dans des études antérieures que la brèche était une pipe associée au granite Redstone Mountain, dû à son allure circulaire en plan. Cependant, dans cette étude, l'analyse des trous de forages indique des zones de bréches espacées par jusqu'à 70 mètres de roches non-bréchiques. De même, l'on retrouve à la surface plusieurs affleurements non-bréchiques à l'intérieur de la zone originalement définie pour la pipe. Aussi, les fractures définissent deux directions prédominantes (NO-NNO et NE-NNE) qui sont, en général, continuent dans toutes les tranchées, suggérent qu'elles sont des structures régionales indépendante de la brèche. La forte angularité des fragments de la brèche allochtone ainsi que la prédominance des fragments de tufs à cristaux et rhyolite suggèrent que la brèche résulte d'une explosion volcanique ou d'une déflation sur les flancs d'un petit dôme rhyolitique.

La minéralisation se compose de sphalérite et de galène finement à grossièrement grenues (jusqu'à 20% Pb+Zn), de pyrite et d'un peu de chalcopyrite et fluorite. L'argent (1.5 à 32.6g/t) est étroitement associé à la galène. Malgré que la majeure partie de la minéralisation dans la tranchée centrale est de nature disseminée, on reconnait tout de même une vingtaire de zones à hautes teneurs en sulphures. Dans ces zones, les sulphures se classifient en quatre styles de textures: 1. remplissagede fractures et matrice des brèches; 2. remplacement de fragments de pierre ponce dans les tufs à cristaux et les rhyolites et remplacement de bands compositionelle dans les tufs à cristaux; 3. amas et veines dans les fragments et/ou la matrice de la brèche; 4. disséminations finement grenues dans les fragments et la matrice de la brèche.

Au Mont Costigan, la minéralisation est survenue en deux étapes. La première, avant la formation de la brèche, est répresentée par des sulphures disséminés dans les blocs de tufs à cristaux non-brèchique

plissages de fractures. La présence, parmi la séquence stratigraphique, de zones successives de brèche minéralisée séparées par des zones légèrement minéralisées et non-brèchiques suggère que les fluides minéralisateurs ont traversé les zones non-brèchiques et imperméables le long de failles et fractures verticales pour atteindre les zone brèchiques poreuses.

Puisque les systèmes épithermiaux sont communément associés à la fin des épisodes volcaniques explosifes, le gîte du Mont Costigan est interprété comme étant un gîte de métaux commun épithermal. Les roches furent brèchifiées durant la phase initiale, alors que la déposition des sulphures se produisit durant les phases tardives, évoluées, du volcanisme explosifs.

ACKNOWLEDGEMENTS

I would firstly like to give thanks to the Lord for being a continual source of strength (regrettably, at times, overlooked) during the time I spent completing this thesis. The Geological Survey of Canada is thanked for its support during the first two years of this project and permission to publish the data enclosed herein. Specifically, I would like to thank Drs. G.P. Watson and D.F. Sangster who served as my co-supervisors for this project. Their keen insight into Pb-Zn deposits in general and Mount Costigan in particular, led to many profitable discussions which resulted in significant improvements to the final version of this manuscript. I am indebted to them for their consistent encouragement to persevere and see this project through to the end. I would also like to thank Dr. Jim Franklin of the Geological Survey of Canada for allowing me access to his computer work station and assisting me in learning Autocad and Sect so I could produce the geological cross-sections through Mount Costigan, without which much of my interpretation of the breccia would be meaningless. I thank Lac Minerals Ltd. for allowing me access to their property, permission to sample their drill core and for providing me with copies of the maps accompanying Crevier (1984). They are also thanked for providing me with copies of the original Amoco Canada Petroleum Ltd. drill logs, which made up a large part of the study on distribution of the sulphide mineralisation. Lastly, I would like to thank Dr. André Lalonde for translating the abstract into French, as well as Georges, Robert and Don for proofreading the translated abstract and catching my numerous typographical errors.

TABLE OF CONTENTS

LIST OF FIGURES

LIST OF FIGURES (Con't)

LIST OF PLATES

LIST OF TABLES

CHAPTER 1

INTRODUCTION

a. Location and Access

The Mount Costigan area (Figure 1) in west-central New Brunswick, is roughly 40km east of the town of Plaster Rock and includes several mountains collectively referred to as the Costigan Mountains, a name derived from the highest peak in the region (Mount Costigan, elevation 670m). The deposit is accessible via Highway 109 east from Plaster Rock (approximately 35km) and then north along Fraser Company logging roads (24km) to the Mount Costigan fire tower road that leads to the summit of Mount Costigan.

b. Previous Work

Initial interest in the mineral potential of the Mount Costigan area developed through a geochemical stream sediment sampling program conducted by Selco in 1955, which outlined numerous Pb-Zn anomalies in the streams draining Mount Costigan (Lock, 1956). Selco staked the eastern base of Mount Costigan but follow-up geophysics (EM) were not encouraging and the property was dropped (Fyffe and Pronk, 1985).

Mount Costigan Mines re-staked the area in 1960 and re-surveyed the area using soil geochemistry to determine if the Selco anomalies had come from higher up on the mountain (Maclean, 1963). Their results showed Pb-Zn-Ag anomalies surrounding the mountain with the most anomalous areas occurring on the eastern flank. In 1969 International Geochemical Associates did a stream sediment geochemical survey over the area and in late 1969, early 1970, Silcan Mines Ltd. staked the area in order to investigate Pb-Zn-Ag anomalies (Riddell, 1971).

From 1970 to 1971 Amoco Canada Petroleum Ltd. did an extensive stream silt survey that indicated several possible targets, and in 1973 the area was staked (Maingot, 1974). In 1974 Amoco conducted a detailed soil sampling program over the area and found anomalous Pb, Zn, Cu and Ag values in streams draining the eastern portion of Mount Costigan as well as in the region to the northeast of the fire tower. The anomaly was found to have a shape elongated north-south and dominated by Pb and Zn (Bjornson, 1975). Electromagnetic (EM) and magnetometer surveys over the area in 1974 proved disappointing, but an Induced Polarisation (IP) survey showed several small anomalies that coincided with the soil geochemical anomalies (Maingot, 1974; Bjornson, 1975). In 1974 five diamond drill holes were sunk to test these anomalies and later a further twenty-three holes were drilled (NB-T-O-1 to NB-T-O-28) in an attempt to define the deposit. The last work Amoco did on the property was in 1979 when they drilled four holes (TNB-79-1 to TNB 79-4).

In 1982 Lac Minerals Ltd. developed six trenches over the area indicated by the previous Amoco Canada drilling. The trenching involved a Central Trench (96m x 32m) with five smaller outlying trenches (North, South, East, West, Southwest and Central) surrounding it (author's terminology). The outlying trenches were located to determine the extent of the breccia zone. Mapping was done at a scale of 1:200 in the outlying trenches and at 1:50 in the Central Trench (Crevier, 1984). Geological mapping of the area surrounding the breccia (1:2500) involved mapping boulder fields and the few existing outcrops. VLF-EM, magnetometer and IP surveys were also conducted (Crevier, 1983). As of 1982, Amoco had drilled 33 holes on the property (Figure 2), with some cutting significant economic (e.g., 7.8% Zn, 4.2% Pb, 15.5ppm Ag) abundances of base metal sulphide minerals (Fyffe and Pronk, 1985). Lac Minerals Ltd. re-logged the Amoco core and in 1983 drilled 10 holes (LCO-1 to LCO-10) in order to determine the limits of the breccia and sulphide zone. In 1984 Lac Minerals Ltd. drilled 5 more holes (84-1 to 84-5) after which they allowed their option on the property to lapse. Although control of the property reverted back to Amoco in December 1987, Lac Minerals Ltd. took out a mining lease on the property in 1988 and are now sole owners of the deposit.

The Mount Costigan area has been mapped by New Brunswick Department of Natural Resources and Energy geologists St. Peter (1978) at a scale of 1:25,000 and by Fyffe and Pronk (1985) at a scale of 1:50,000. Regional mapping of the area at 1:50,000 was done by Skinner (1974, 1982) for the Geological Survey of Canada.

c. Current Work

i. Objectives

The purpose of this study was to: **a.** produce an up-to-date geological map of the Mount Costigan deposit and immediate area; **b.** attempt to develop a model to explain the formation of the breccia as well as the genesis of the mineralisation.

ii. Method

In August 1986 four days were spent investigating the Mt. Costigan deposit. Over the four day period, through consultation with Drs. G.P. Watson and D.F. Sangster, the rocks exposed in the trenched areas were observed and Lac Minerals detailed and regional mapping of the area examined. Lac Minerals 1984 assessment report on the area, drill logs and re-logging of previous Amoco holes were examined in order to understand the nature of the breccia and any relationship with the lithology and mineralisation. Preliminary representative samples (approximately thirty) and photographs were taken of drill core and outcrop in order to document the rock types, alteration, and variations in styles of mineralisation and breccia.

Work on the Lac Minerals maps during the ensuing months involved transferring lithologic, textural (including breccia) and sulphide grade data to separate overlays so any inter-relationships at the outcrop

Figure 1:Location Map.

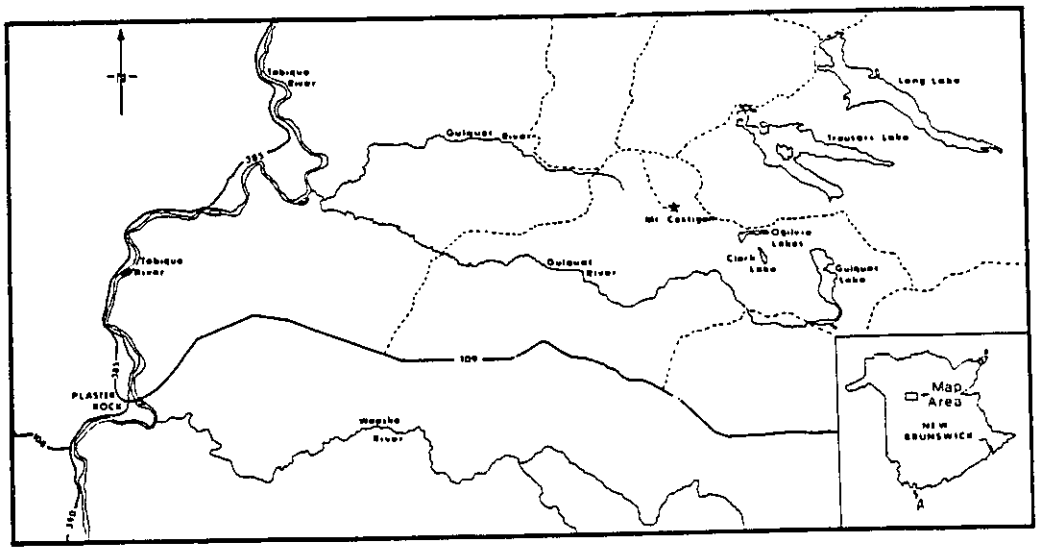

LEGEND

—— - Paved roads & Highways

------ - Unpaved roads

- - - - - Track

★ - Study area

5 4 3 2 1 0 5

kilometres

Figure 2: Generalised geology of the Mount Costigan property area. (After Crevier, 1985).

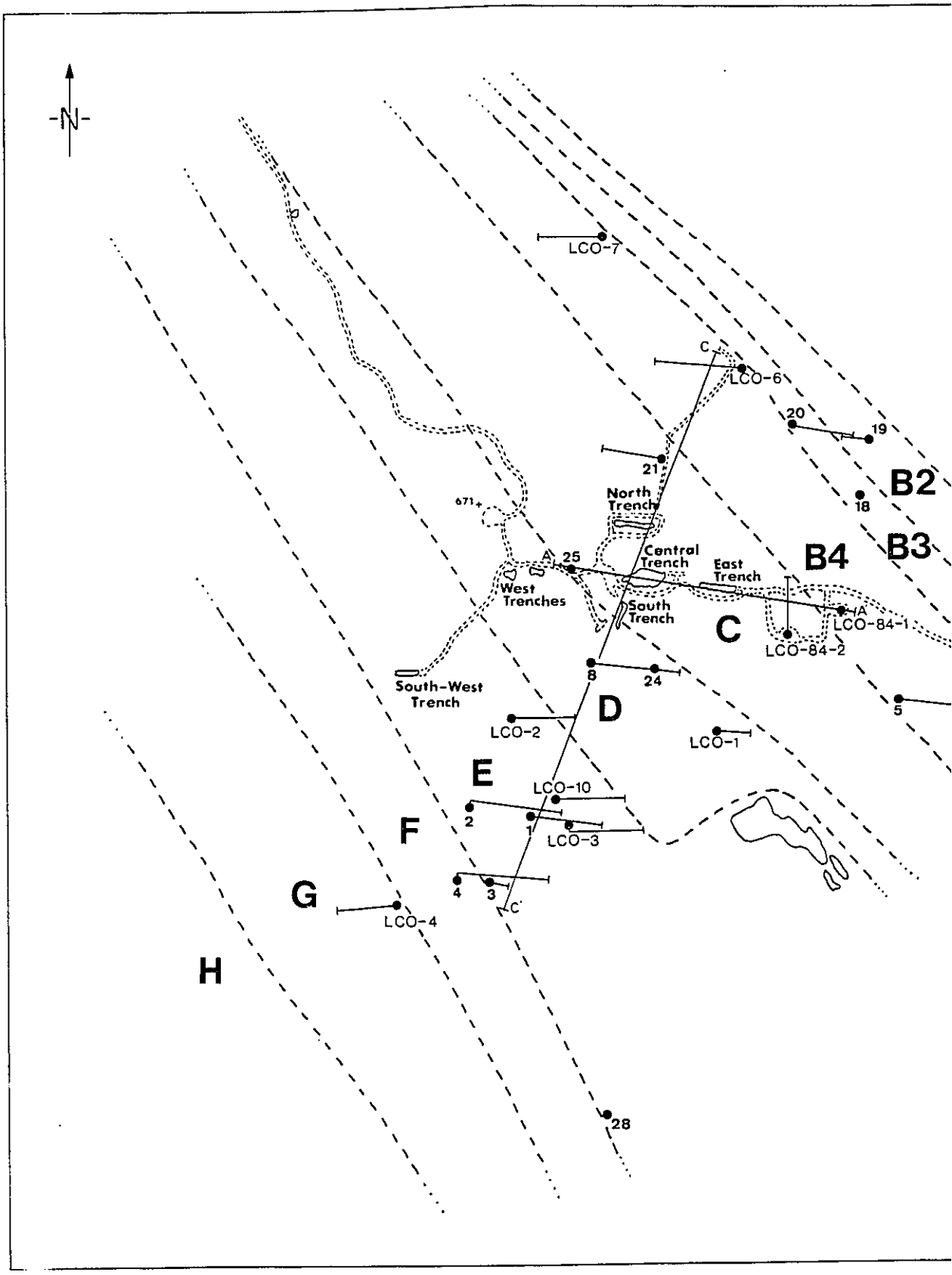
N
LCO-7
C
LCO-6
20
19
21
18
B2
North Trench
671+
B3
B4
Central Trench
East Trench
25
A
West Trenches
South Trench
C
LCO-84-1
LCO-84-2
South-West Trench
8
24
D
5
LCO-2
LCO-1
E
LCO-10
2
1
LCO-3
F
4
3
C'
G
LCO-4
H
28

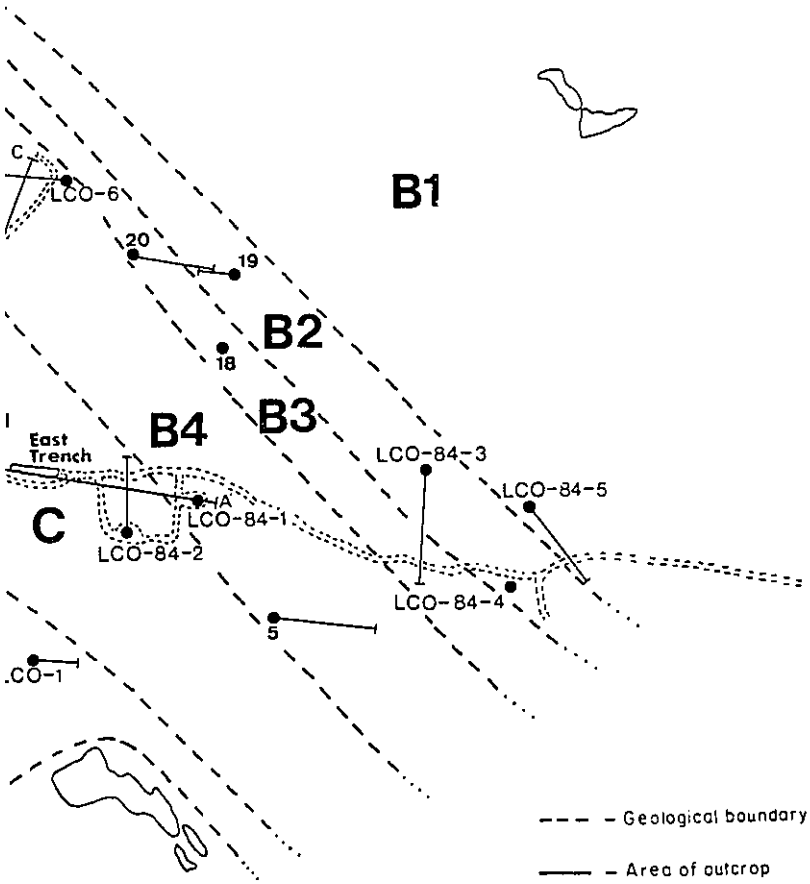

LEGEND

LOWER DEVONIAN

H	Siltstone
G	Siltstone & Lapilli tuff
F	Crystal tuff
E	Rhyolite, minor crystal & lapilli tuff
D	Lapilli tuff, minor siltstone & rhyolite
C	Crystal tuff, minor siltstone, rhyolite & lapilli tuff
B4	Lapilli tuff
B3	Greywacke
B2	Crystal tuff
B1	Conglomerate

& Siltstone

– Geological boundary (approximate)

– Area of outcrop

– Diamond drill hole & number (vertical, inclined)

671 – Bench mark & elevation (m)

– Access road

A A' – Cross-section

50 0 50 100 200 300m

PROPERTY GEOLOGY

scale might be observed. The same procedure was carried out for the Lac Minerals Ltd. and Amoco drill hole cross sections to observe the presence or absence of similar relationships at depth. Compilation maps of the trenched areas showing geology, breccia, alteration and mineralisation were drawn from Lac Minerals Ltd. maps to see if there was any correlation between trenches.

Petrographic work consisted of examining thin sections in both transmitted and reflected light. The remainder of the rock slabs were stained for plagioclase and K-feldspar to determine the extent of the alteration. Lastly, a preliminary classification of breccia types was devised, based on observations made in the field and descriptions found in Lac Minerals Ltd. drill logs and reports.

In order to produce an accurate geologic map of the area and develop a model for the breccia and mineralisation, approximately four weeks of field work in 1987 were spent mapping the geology, re-logging selected drill holes, collecting structural data, photographs and samples. The bulk of the mapping began with establishing a baseline, by transit, along the east-west axis of the Central Trench. This baseline was tied into the previous grid established by Lac Minerals in 1984, for reference and simplicity of comparing data. Reference stations at the outlying trenches surrounding the Central Trench were sighted in, in order to produce a large scale map of the trenched area. Once the east-west baseline in the Central Trench was constructed, a north-south baseline was established with cross-lines at 4 metre intervals.

Following completion of the grid, about 4 days were spent conducting a series of short traverses across the property in an attempt to define the extent of the brecciation exposed in outcrop and boulder fields. Boulder fields were used as an indication of bedrock lithology since it has been interpreted that there was little glaciation of the summit of Mount Costigan (Fyffe and Pronk, 1985). Individual boulder fields were only accepted as being reliable if boulder sizes exceeded 1m and over 80% were of the same lithology. Following this, 5 to 6 days were spent mapping the outlying trenches. A baseline was constructed along the length of each trench and their general shape determined. Two or three points along each baseline were sighted in from the earlier established reference points in order to locate the exact position of the trenches. Lithology, textures (including brecciation), alteration, structure and mineralisation were mapped; samples and photographs were taken to document characteristic or unusual features observed.

Once the outlying trenches were mapped, approximately two weeks were spent mapping the Central Trench. Prior to and during this time 2 to 3 days were spent examining selected Lac Minerals Ltd. and Amoco drill holes in order to observe and identify the breccia types reported by Lac Minerals Ltd. in their maps and assessment report. This was also done to compare the observed breccia types with the breccia classification established earlier.

Structural measurements taken on the Central and outlying trenches consisted of measuring possible bedding planes (West Trench only), and the trend of fracture sets. Fracture sets were considered important since their orientation might give clues to the origin of the breccia and help define a model for its

formation. Should the breccia be associated with a pipe-shaped structure then fractures occurring along the edge of the breccia should be sheet-like, with steep dips and circumferentially oriented with respect to the breccia (Norton and Cathles, 1973). Once these data had been collected they were plotted and contoured on stereonets. Alteration was mapped concurrently with textures and lithology, since it was decided that a study of alteration effects was not to be a major part of this project. The emphasis placed on alteration was limited to identifying the mineralogy, limits of various alteration types, including their effects on their host rocks.

CHAPTER 2

REGIONAL GEOLOGY

The Mount Costigan deposit occurs in the Costigan Mountain Formation within the Siluro-Devonian Tobique Group, part of the Matapedia Cover Sequence (Figure 3), a northeast to southwest trending belt of volcanic rocks, slate, sandstone, minor limestone, conglomerate, gabbro and granite. It is bounded to the south by the Miramichi terrane (Fyffe and Fricker, 1987).

The Miramichi terrane consists of a northeast trending belt of polydeformed rocks intruded by Devonian granites and gabbros (St. Peter, 1978). It is faulted against the younger volcanic and sedimentary rocks of the Matapedia Cover Sequence which were openly folded during the Acadian Orogeny. Unconformably overlying the Matapedia Cover Sequence rocks are gently dipping sandstones and conglomerates of the Mississippian Plaster Rock Basin (St. Peter, 1978).

Intrusive activity in the Matapedia Cover Sequence consisted mainly of granite (i.e. Redstone Mountain Granite; a pale pink, medium-grained, subporphyritic biotite granite), originally considered early to late Devonian and diabase dykes, sills and stocks (Skinner, 1982). The metamorphic grade in the area varies from amphibolite facies in the Tuadook Lake area through greenschist facies in the study area (indicated by the presence of albite, actinolite and epidote in the basalts) to prehnite-pumpellyite facies in the Wapske Formation (Skinner, 1982).

Recent work by Bevier and Whalen (1989) on the Mount Elizabeth and North Pole granites (similar in composition to the Redstone Mountain granite) north of the study area have shown that these intrusions are Late Silurian and not Late Devonian as was originally interpreted. This would suggest that the Costigan Mountain Formation is actually Silurian in age and not Early Devonian as has been previously interpreted (Skinner, 1974).

Figure 3: Main tectonic elements of the central Matapedia Cover Sequence (formerly Aroostook - Matapedia Anticlinorium and Chaleur Bay Synclinorium) and the Miramichi terrane (formerly Miramichi Anticlinorium) showing the location of Mount Costigan and its proximity to the contact with the Matapedia terrane. (After Fyffe and Pronk, 1985; Skinner, 1982).

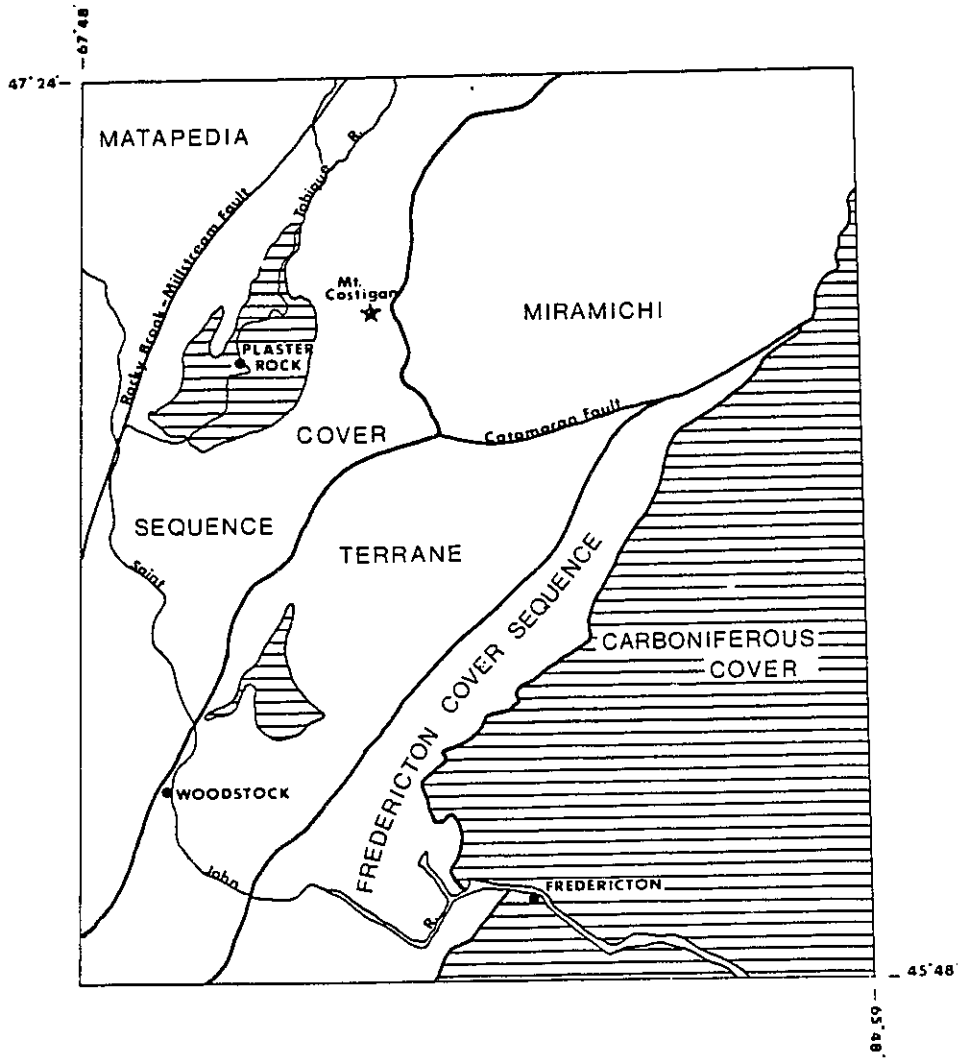
67°48'
47°24'
MATAPEDIA
Tobique R.
Rocky Brook - Millstream Fault
Mt. Costigan
MIRAMICHI
PLASTER ROCK
COVER
Catamaran Fault
SEQUENCE
TERRANE
Saint
FREDERICTON COVER SEQUENCE
CARBONIFEROUS COVER
WOODSTOCK
John R.
FREDERICTON
45°48'
65°48'

CHAPTER 3

MOUNT COSTIGAN DEPOSIT

a. Introduction

The Mount Costigan deposit is situated on the east face of Mount Costigan and is located about 200m from the summit, where six trenches were developed by Lac Minerals Ltd. between 1983 and 1984. The trenched area consists of a large Central Trench (author's terminology) 96m long by 32m wide, surrounded on the north, south, east, west and south-west by smaller peripheral trenches (Figure 4). The deposit is comprised of massive, coarse- to fine-grained sphalerite and galena hosted in a breccia that consists of angular blocks of fine- to medium-grained, massive and banded crystal tuff and massive and flow-banded rhyolite. Sulphide mineralisation is found primarily as a filling between breccia fragments, but also occurs as a replacement of banding in crystal tuff and of the quartzofeldspathic matrix.

b. Host Rocks

i. Stratigraphy

The Mount Costigan deposit occurs within the Costigan Mountain Formation (Figure 5), a series of felsic (rhyolitic), pyroclastic (crystal and lapilli tuff) and mafic volcanic rocks. It occurs within the felsic portion of the formation (Figure 2) and is underlain to the east by fine-grained siltstones and basalts. To the west the deposit is overlain by another suite of siltstones and felsic volcanic rocks belonging to the Wapske Formation.

Basalts of the Costigan Mountain Formation (stratigraphic unit A, Figure 5) represent the base of the formation. Although not exposed on the property, they outcrop to the east along the base of Mt. Costigan and are fine-grained, green-grey, massive and amygdaloidal (Skinner, 1982).

Overlying the basalts to the west is a thick sequence of siltstones intercalated with conglomerate, greywacke and lapilli and crystal tuff (stratigraphic units B1 to B4, Figure 5). Although the siltstone is best observed in drill core, minor amounts interlayered with crystal tuff are exposed in the East trench. The siltstone commonly is fine-grained, dark grey to brown weathering, featureless and extremely friable in outcrop, although more competent in drill core.

Lac Minerals reported a thin conglomerate (unit B1) at the base of DDH #84-5 intercalated with siltstone and greywacke. The conglomerate commonly is polymictic and consists of sub-rounded, green volcanic (basalt?) fragments approximately 1cm in size in a fine-grained silty matrix. Above this unit is a thick sequence of interlayered siltstone and crystal tuff (unit B2) referred to as tuffaceous siltstone or impure siltstone by Lac Minerals Ltd., siltstone and greywacke (Unit B3) and siltstone and lapilli tuff (Unit B4). Unit B2 varies from 1.5 to 20m thick and consists of locally brecciated, massive quartz and

Figure 4: Trench Location Map - Note the distribution of brecciated versus unbrecciated rock in the East Trench and its similarity to the pattern observed in drill core (see inset Figure 16). Note also the boundary between stratigraphic units C and D as represented by the lapilli tuff in the West Trenches and the sharp contact between lapilli and crystal tuff in the South Trench.

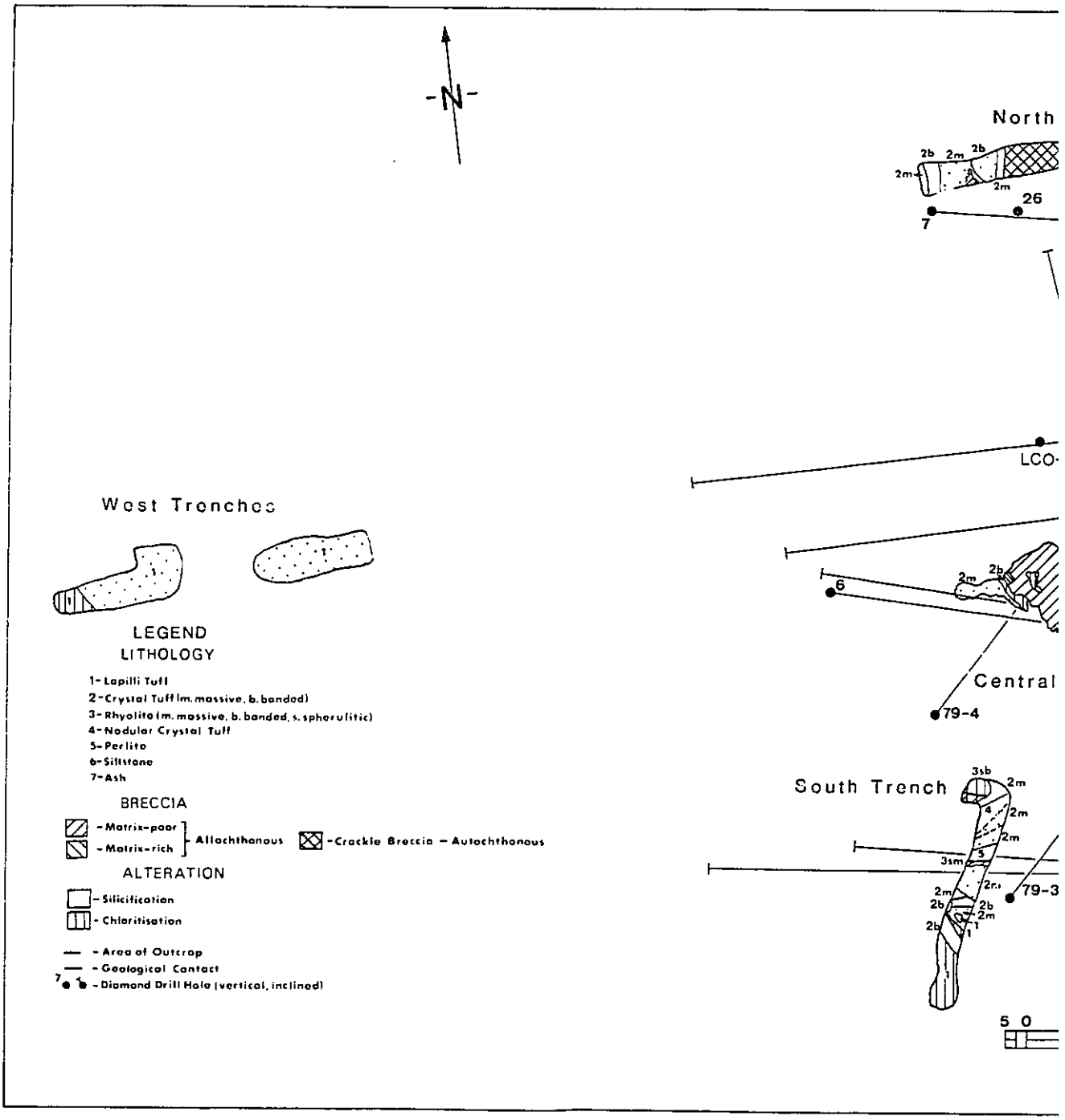
N
North
2b
2m
2b
2m
2m
26
7
LCO-
6
2m
2b
Central
79-4
West Trenches
LEGEND
LITHOLOGY
1-Lapilli Tuff
2-Crystal Tuff (m. massive, b. banded)
3-Rhyolite (m. massive, b. banded, s. spherulitic)
4-Nodular Crystal Tuff
5-Perlite
6-Siltstone
7-Ash
BRECCIA
-Matrix-poor
-Matrix-rich
Allochthonous
-Crackle Breccia – Autochthonous
ALTERATION
-Silicification
-Chloritisation
-Area of Outcrop
-Geological Contact
-Diamond Drill Hole (vertical, inclined)
South Trench
3sb
2m
4
2m
2m
5
3sm
2m
2b
2b
2m
2b
79-3
5 0

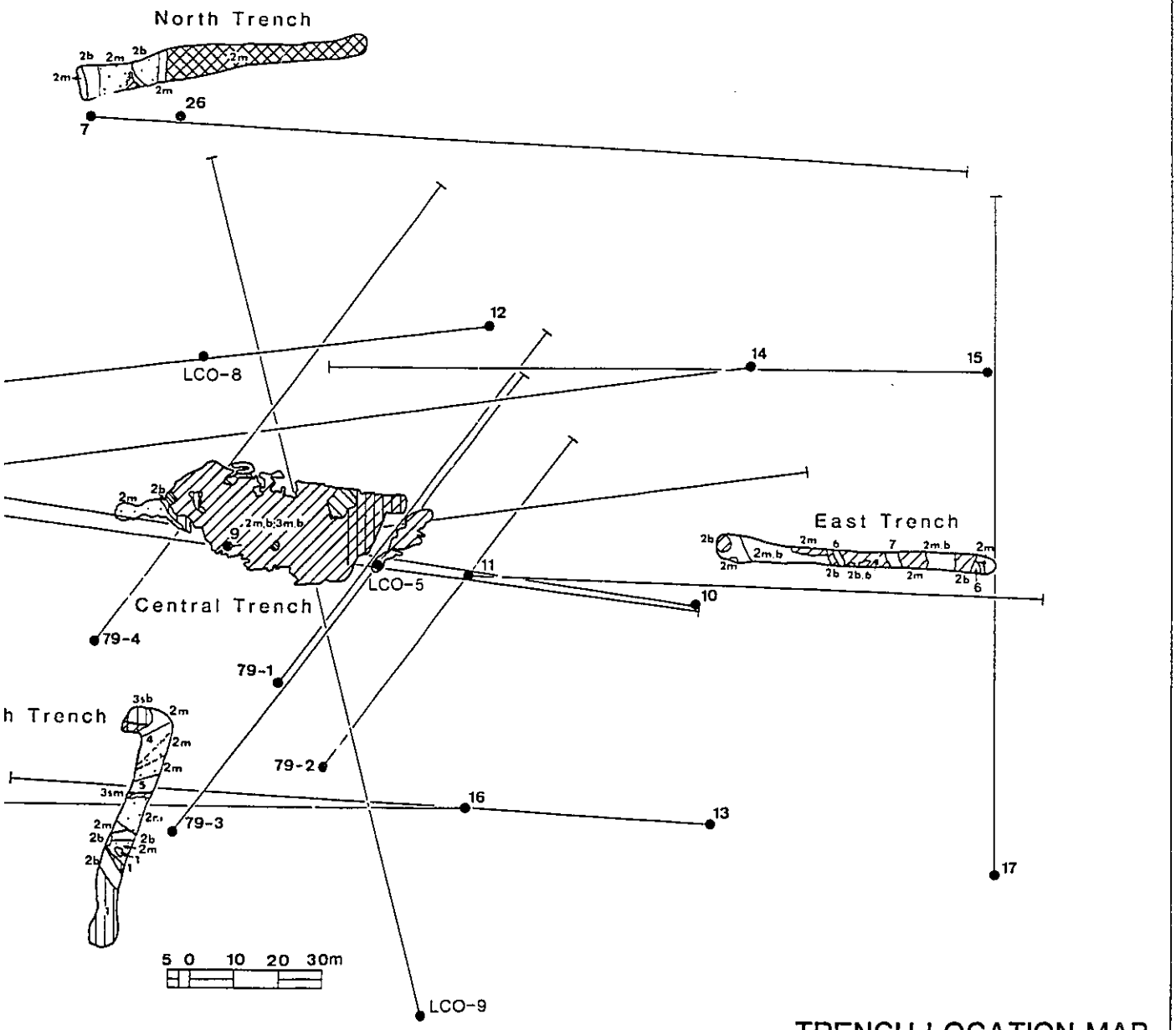

TRENCH LOCATION MAP

Figure 5: Stratigraphic column of the Mount Costigan property area as assembled from surface exposures and drill hole information. Note the transition in the Costigan Mountain Formation from mafic volcanic rocks and interlayered siltstone and pyroclastic rocks to dominantly felsic volcanic rocks with interlayered siltstone and pyroclastic rocks. The Wapske Formation probably begins with the siltstones near the top of the stratigraphy (after St. Peter, 1978).

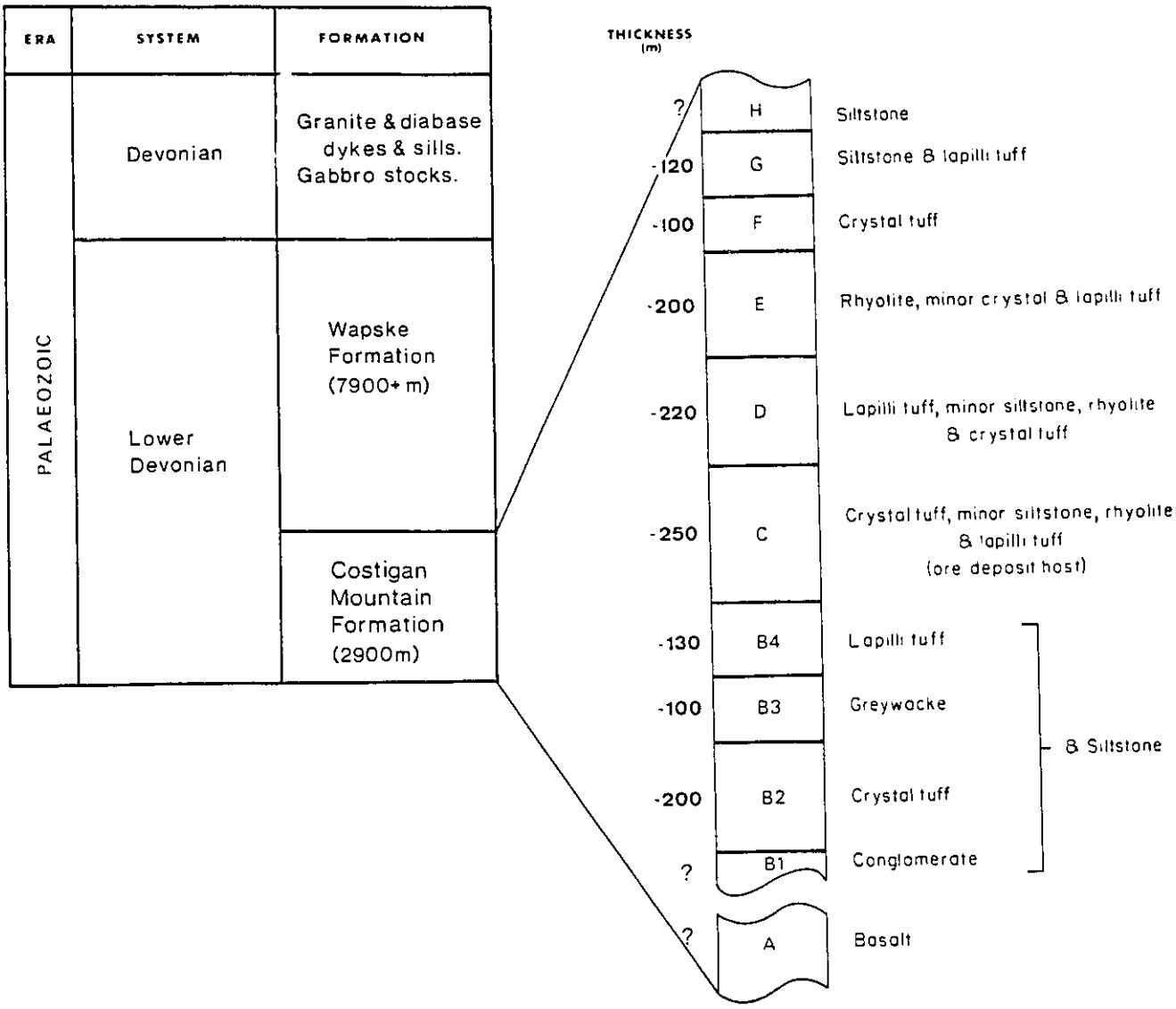
ERA
SYSTEM
FORMATION
PALAEOZOIC
Devonian
Granite & diabase dykes & sills. Gabbro stocks.
Lower Devonian
Wapske Formation (7900+ m)
Costigan Mountain Formation (2900m)
THICKNESS (m)
?
H
Siltstone
-120
G
Siltstone & lapilli tuff
-100
F
Crystal tuff
-200
E
Rhyolite, minor crystal & lapilli tuff
-220
D
Lapilli tuff, minor siltstone, rhyolite & crystal tuff
-250
C
Crystal tuff, minor siltstone, rhyolite & lapilli tuff (ore deposit host)
-130
B4
Lapilli tuff
-100
B3
Greywacke
-200
B2
Crystal tuff
?
B1
Conglomerate
& Siltstone
?
A
Basalt

K-feldspar rich crystal tuff, interlayered with grey to grey-brown siltstone. The siltstone is commonly banded (possible bedding) with dips varying from 35° to 60° (e.g., DDH LCO-84-4). This unit is overlain by fine-grained grey siltstone and interlayered greywacke (unit B3) that varies from 2 to about 160m thick. The greywacke is dark grey, and massive to weakly laminated and consists of fine-grained quartz and K-feldspar which give it a gritty appearance. The overlying lapilli tuff unit (unit B4) ranges from 5 to 20m thick, is also interlayered with siltstone and consists of grey to dark green, sub-angular to cuspate lapilli (0.5 to 1cm in size) in a fine-grained, massive, grey to cream coloured quartz and K-feldspar rich groundmass.

Overlying unit B4 is a thick sequence of interlayered siltstone, rhyolite flows and pyroclastic rocks that represent the main crystal tuff unit (unit C) (Figure 5). This unit is approximately 250m thick and contains most of the breccia and mineralisation. The crystal tuffs are fine- to medium-grained, both massive and banded, and contain quartz and K-feldspar of which only about 5% of the crystals are broken. In the vicinity of the breccia, the crystal tuff is locally moderately to intensely silicified, a process which has destroyed much of the original texture (banding etc.). While the breccia consists dominantly of chloritised banded crystal tuff fragments (up to 50cm), it also contains large blocks of massive crystal tuff (up to 4m x 8m in size). Massive crystal tuff is also present as small fragments, but these are a relatively minor component of the breccia. Other lithologies found in the breccia are flow-banded and massive rhyolite and agglomerate. Flow-banded rhyolite commonly contains small, rounded, pumice fragments which were likely incorporated into the rhyolite while it was still fluid, since the pumice commonly distorts and disrupts the banding. Massive rhyolite occurs as small, (36cm) angular, grey, featureless fragments commonly supported by a massive crystal tuff matrix. West of the Central Trench, pink flow-banded to massive spherulitic rhyolite occurs at the top of the unit and is best exposed in the South-west Trench and the top 60m of DDH #25. Agglomerate is a minor part of this unit and is only observed in the Central Trench where it consists of angular to sub-rounded fragments (12cm in size) of grey, massive rhyolite, crystal tuff in a fine-grained, grey-white matrix.

Immediately overlying the main crystal tuff (stratigraphic unit C) are four units:

1. Lapilli tuff with minor amounts of grey to pink, massive to flow-banded rhyolite, quartz and K-feldspar rich crystal tuff and massive, grey siltstone (unit D, Figure 5) which is best exposed in the West Trench and the southern 15m of the South Trench. Drill core shows that the lapilli tuff is interlayered, at depth, with massive to flow-banded rhyolite (3 to 30m thick), crystal tuff (2 to 15m thick) and massive siltstone (5 to 10m thick).

2. Massive, spherulitic rhyolite (unit E, Figure 5) (220m thick) which is best exposed in a large outcrop (200 x 100 x 50m) southwest of the trenched area. The rocks in this unit are interlayered with massive and banded crystal tuff (5 to 20m thick) and massive, weakly to very silicified lapilli tuff (5 to 40m thick). This rhyolite is similar to that in the main crystal tuff unit but is thought to represent different flows based on the reduced volume of inter-flow pyroclastic material present and its massive

texture. In addition to this, the rhyolite flows in the main crystal tuff unit are predominantly banded and individual flow layers are much thinner that those in the upper rhyolite.

3. Crystal tuff (unit F, Figure 5), approximately 100m thick and lithologically similar to that in the Central Trench, but thinner and consisting dominantly of massive crystal tuff with minor banded crystal tuff. This unit also contains minor, thin (3 to 5m) interbeds of grey to black siltstone. Brecciation is locally developed here, but not to the extent of that in the Central Trench.

4. Lapilli tuff and siltstone (unit G, Figure 4, 120m thick) similar to that at the base of the section (unit B4, Figure 5). The most significant difference here is that the siltstone is black and might represent the first stages of the overlying Wapske Formation siltstone. The lapilli tuff in this unit is basically the same as that observed in the West and South Trenches. Black, massive to poorly-bedded siltstone (unit H, Figure 5) overlies the entire stratigraphic section and likely belongs to the Wapske Formation. Although the rocks in the Costigan Mountain Formation and the Wapske Formation are similar the division between the two formations was established by St. Peter (1978) to the south of the study area and is represented by the presence of siltstone in the Wapske Formation and the lack thereof in the Costigan Mountain Formation. Recent work by New Brunswick Department of Mines and Energy geologists in the Mount Costigan area and this study indicate that here there is such a similarity between the Wapske and Mount Costigan Formations that the presence or lack of siltstone cannot be used to divide the formations.

The presence of weakly graded beds in the silicified lapilli tuff of the West Trenches, along with load casts and flame structures in the laminated siltstones, indicate that the entire sequence of tuffs, rhyolite and siltstones tops toward the northwest, and is a normal, not an overturned, succession.

ii. Lithology

1. Crystal Tuff

Crystal tuff is the dominant pyroclastic rock at Mount Costigan and occurs as two basic types: massive and banded. Massive crystal tuff is less common than banded crystal tuff, and is most abundant in the North Trench (Figure 6). Where it is found in the Central Trench it is a minor component (small subangular fragments) of the breccia. The massive crystal tuff is commonly fine- to medium-grained to equigranular (as observed in the eastern portion of the North Trench (Figure 6)) with a microcrystalline quartzofeldspathic groundmass that supports larger (up to 3mm) quartz and K-feldspar crystals (Plate 1A,B). These phenocrysts are typically subhedral to euhedral and only an average of 5% are broken. Rims of graphically intergrown quartz and K-feldspar surrounding K-feldspar phenocrysts are also typical of these rocks. Massive crystal tuff, although present in the South Trench is not as common as that in the North Trench and is interlayered with the lapilli tuff of stratigraphic unit D (Figure 7). It also occurs as distinct sub-units interlayered with brecciated banded crystal tuff.

In some of the massive crystal tuffs in the Central Trench groundmass quartz commonly contains small (<1mm) mineral inclusions. This occurs most commonly in moderate to strongly silicified tuffs

Plate 1

A: Typical massive crystal tuff, North Trench.

B: Photomicrograph of A showing fine-grained quartzofeldspathic groundmass supporting coarser quartz crystals (with fine-grained overgrowths). Note the chloritic alteration of the groundmass K-feldspar (dark patches interstitial to groundmass quartz).

C: Typical banded crystal tuff. East Trench.

D: Nodular crystal tuff showing development of "felsic" nodules with quartz cores (white) and K-feldspar rims (beige). South Trench.

E: Photomicrograph of D, showing the quartz-rich core and K-feldspar rich rim.

F: Chloritic lapilli tuff from the West Trenches. Note the dark, chloritised, cuspate lapilli characteristic of this rock. Scale in centimetres.

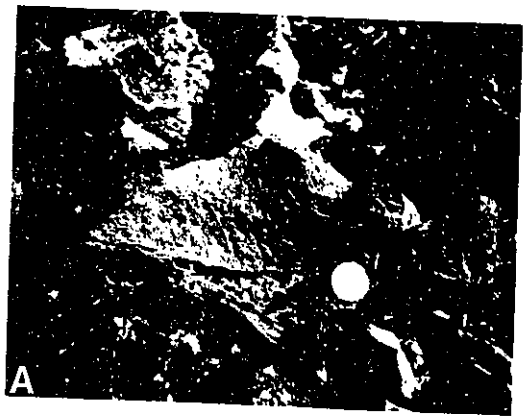
A


B

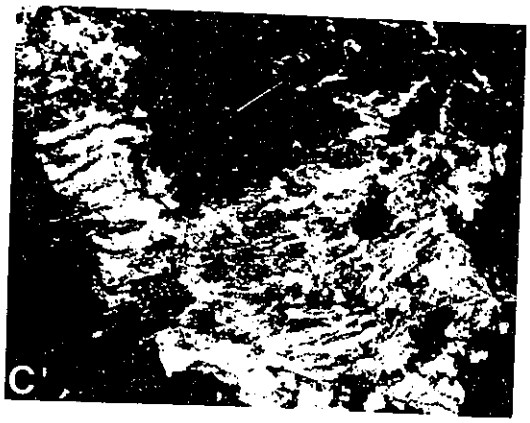
C


D

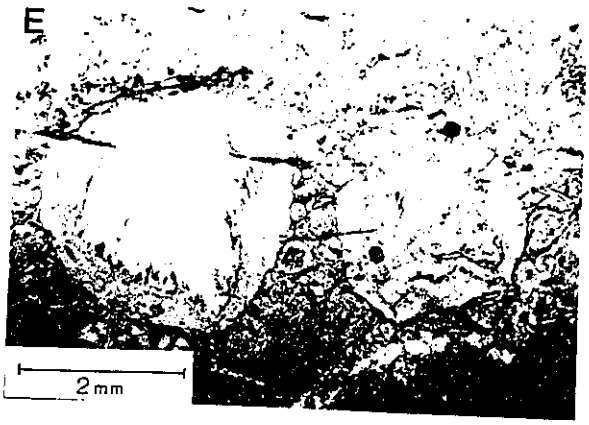
E
2 mm

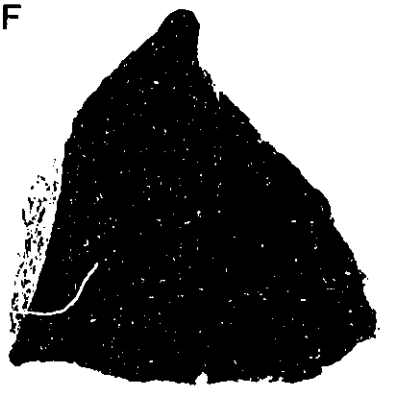
F

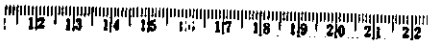

where there is an abundance of quartz and a lack of K-feldspar in the groundmass. Groundmass quartz and K-feldspar also show little variation in grain size, the groundmass being virtually equigranular. Rare massive crystal tuff occurs in the Central Trench as large (2m x 3m) weakly silicified and chloritised blocks.

Banded crystal tuff (Plate 1C) is the most common variety of tuff and is best exposed in the Central Trench where it makes up the bulk of the breccia fragments. It is also present in the North and East trenches where (in the North Trench) the banding is more weakly developed (possibly due to the intensity of alteration). In the East Trench the tuff is interlayered with brecciated units of similar composition as well as siltstone. While banded crystal tuff is the primary component of breccia fragments in the Central Trench, in the North Trench it occurs as unbrecciated layers interlayered with massive crystal tuff (units 2m and 2b, Figure 6). It is well-banded and moderately silicified at the western end of the trench varying to moderately banded and silicified to the east of the fault (Figure 4). Banding in this sub-unit consists of alternating light and dark layers which consist of alternating quartz-rich, K-feldspar poor and chlorite altered K-feldspar rich layers. The overprinting of the alteration in this trench makes the banding less prominent than in the Central and East Trenches.

In the Central Trench the banded crystal tuff is compositionally similar to the massive crystal tuffs in the North Trench with the exception of being more strongly chloritised, especially the darker bands. Other than the relative chlorite abundance light and dark layers have similar compositions in that they both consist of fine-grained quartz and K-feldspar in the groundmass and as crystals. In the darker bands chlorite occurs as a partial to complete replacement of the groundmass K-feldspar and partial replacement of K-feldspar crystals, while in the lighter bands K-feldspar crystals are either weakly chloritised or unaltered. While there is a high percentage of K-feldspar in these rocks, there is also an equally large amount of quartz present as groundmass and as crystals. Also in the Central Trench are large (2m x 3m) blocks of banded crystal tuff, similar in colour to the smaller (20cm to 50cm) breccia fragments making up the bulk of the breccia and consisting of light (quartz-rich) and dark (chloritised, K-feldspar rich) bands. In the Central Trench, rare banded crystal tuff blocks show distorted and convoluted banding similar to the flow-banded rhyolites.

A variety of tuff present only in the South Trench is nodular tuff (Plate 1D) (sub-units 4,5, Figure 7). Sub-unit #4 (MC-87-27) is characterised by distinctive nodules that consist of a subangular core of fine-grained highly strained quartz enveloped by a rounded shell of amorphous, fine-grained K-feldspar that has grown perpendicular to the quartz grain boundaries (Plate 1E). Where several nodules occur close together they commonly coalesce, the outer K-feldspar rich rim enveloping the nodule cores. The nodules average 0.25cm to 0.5cm in size but larger varieties, up to 0.75cm, were also observed. The groundmass surrounding the nodules consists of microcrystalline quartz and K-feldspar that supports rounded aggregates of extensively corroded quartz crystals full of mineral inclusions. Individual K-feldspar crystals with mantles of graphically intergrown quartz and K-feldspar are commonly incorporated into the nodules

and enveloped by the K-feldspar rim. The nodules are only locally developed in sub-unit #4a. The presence of the concentric, nodular, shell-like cavities filled with quartz or K-feldspar suggests a similarity to the lithophysae observed in rhyolites along the road north-east of Mount Costigan.

A significant characteristic of both massive and banded crystal tuffs is the presence of graphic overgrowths surrounding the K-feldspar in the crystal tuffs. Good examples of this occur in the South Trench, North Trench and the Central Trench. Graphic overgrowths indicate that conditions favouring vapour-phase crystallisation existed in these rocks at some point during their history. Since these K-feldspar crystals pre-date the crystal tuff it is likely that the overgrowths indicate the presence of vapour-phase conditions in the original magma or the later hydrothermal fluids responsible for the extensive alteration. Graphic texture is not unique to the crystal tuffs, as excellent examples are found in the perlite (MC-86-2S, see below) of the South Trench and the flow-banded rhyolites in the Central Trench.

2. Lapilli Tuff

Lapilli tuff is exposed in only two locations at Mount Costigan, the southern 15m of the South Trench (Figure 7) and the two Western trenches (Figure 8) where it represents stratigraphic unit D and is relatively unaltered. Here it consists of chlorite altered, fine-grained, dark grey rhyolite and massive crystal tuff (with K-feldspar crystals) lapilli in a chloritic, quartzofeldspathic groundmass (Plate 1F). Quartz and K-feldspar rich lapilli vary in shape from subrounded to lenticular to cuspate (Plate 2A) which is possibly an indication of cooling during air-fall. Staining of these rocks with sodium cobaltinitrate for K-feldspar shows that the lapilli are dominantly K-rich, typically showing silica-rich rims and K-feldspar cores. Many lapilli are foliated consisting of alternating K-rich and Si-rich layers, while others are either entirely K-rich or Si-rich. This staining clearly identifies a preferred orientation in the lapilli that has been interpreted in the field as bedding.

3. Rhyolite

Four varieties of rhyolite have been identified at Mount Costigan: 1. Massive; 2. Flow-banded; 3. Massive spherulitic; and 4. Flow-banded spherulitic. Massive and flow-banded rhyolites are most common in the Central Trench whereas massive and flow-banded spherulitic rhyolite is typically found in the South and Southwest Trenches. Rhyolite is absent in the North, West and East Trenches.

The massive rhyolite in the Central and South Trenches consists of a groundmass of fine-grained to microcrystalline quartz and K-feldspar that supports subhedral to euhedral quartz and weakly to moderately sericitised K-feldspar phenocrysts (1-3mm). These phenocrysts are similar to those in the crystal tuffs and graphic overgrowths around the K-feldspars are present in minor amounts. Groundmass quartz in the massive rhyolites, in thin section, typically displays fine-grained "dusty" inclusions.

Massive rhyolite occurs in two types, grey angular breccia fragments (1 to 5cm) (Plate 2B) and larger (0.5 x 1m) pink subangular blocks that commonly show incorporated pumice fragments replaced by

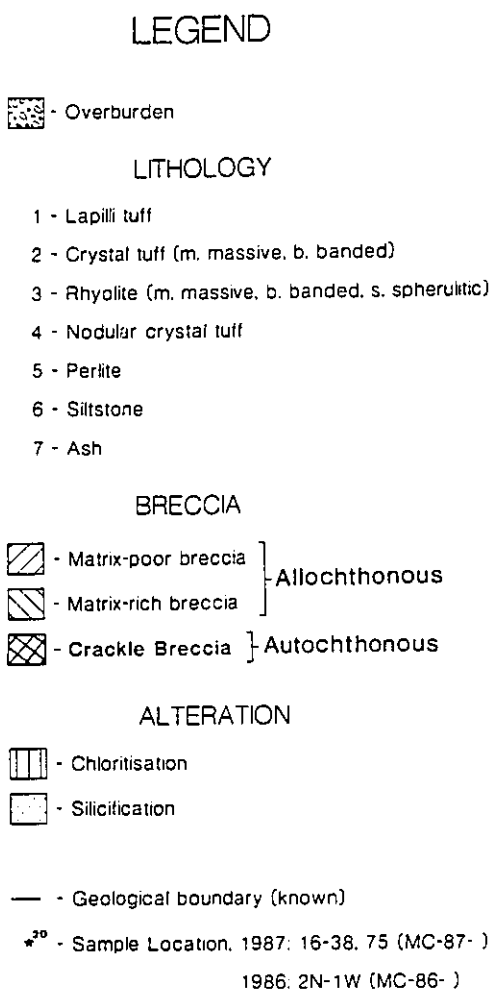

Figure 6: North Trench Geology, breccia distribution and alteration. Note the sharp contact between brecciated and unbrecciated crystal tuff.

Figure 7: South Trench Geology, breccia distribution and alteration. Note the unusual orientation of the geological contacts in the southern half of the trench, possibly indicating the presence of a fold.

Figure 8: Geology and alteration of the West Trenches. Note the change in type and intensity of alteration from west to east across the trenches. Relatively fresh (weakly chloritised) lapilli tuff to the west and moderate to intensely silicified lapilli tuff to the east.

North Trench

6

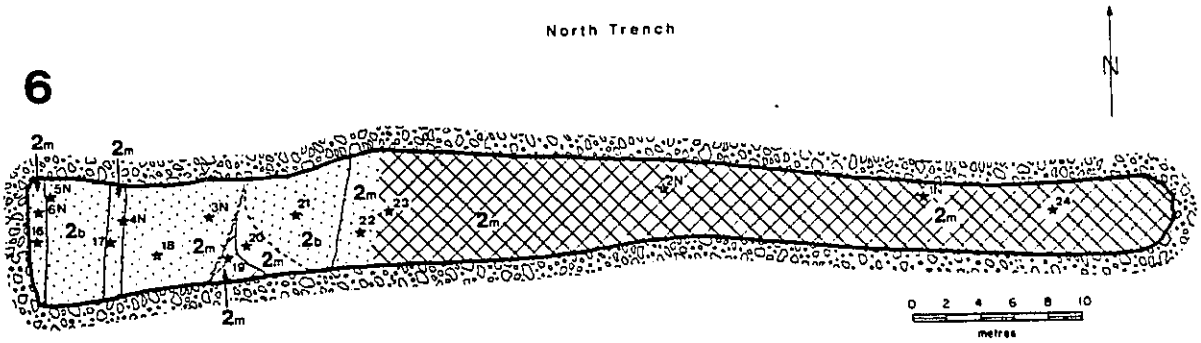

South Trench

7

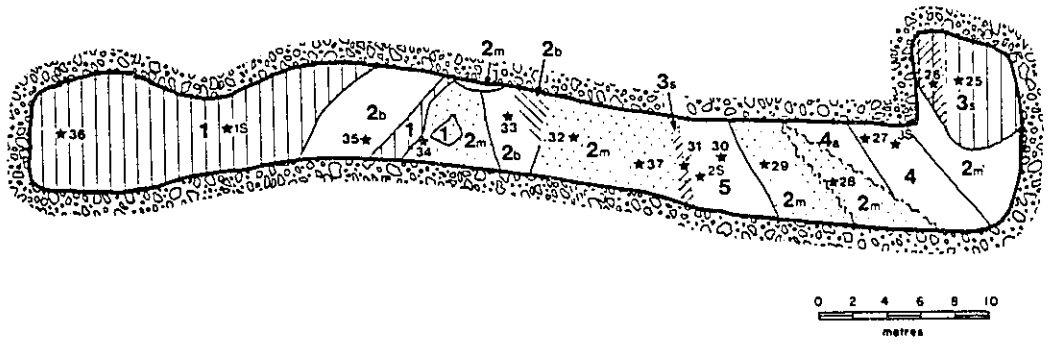

West Trenches

8

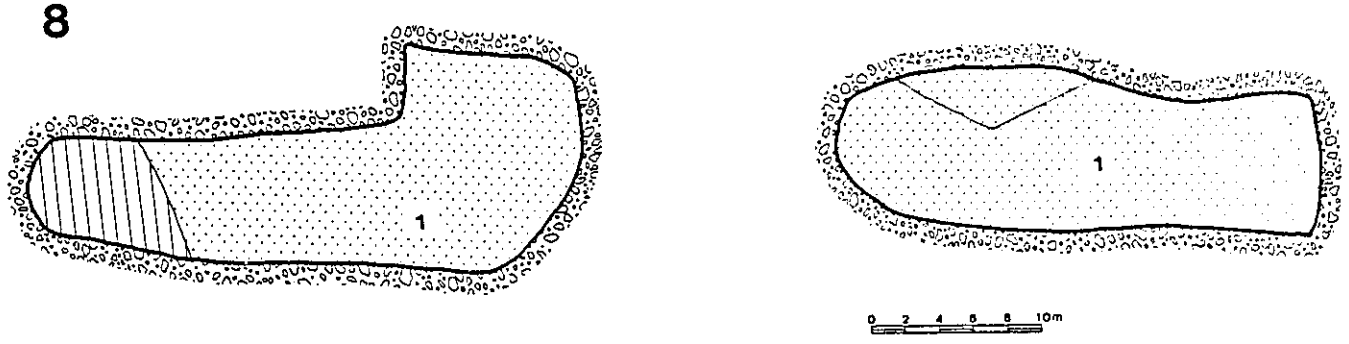

sulphides (Plate 2C). The smaller, grey rhyolite fragments are closely associated with the banded crystal tuff fragments and are commonly supported by a matrix of massive crystal tuff. In some parts of the breccia where there is a high abundance of crystal tuff and grey rhyolite, it is often difficult to distinguish whether the rhyolite or crystal tuff represent fragments or matrix. The massive rhyolite is more uniform in texture and contains large subhedral to euhedral quartz and K-feldspar phenocrysts along with rare, broken plagioclase phenocrysts (Plate 2D). In thin section, this rhyolite consists of a matrix of fine-grained K-feldspar, quartz (full of mineral inclusions) phenocrysts and spherulites. Chlorite occurs either as discrete grains within the matrix, or as an alteration of K-feldspar phenocrysts.

Flow-banded rhyolite in the Central Trench occurs primarily as large blocks 0.5 to 2m in size and is concentrated mainly to the east of the base-line (Figure 9). The blocks display a regular (light and dark) banding which show many similarities to the banding in the crystal tuff in that they consist of alternating layers fine-grained, chlorite-altered K-feldspar and coarser quartz and K-feldspar phenocrysts (commonly showing graphic textured overgrowths). Rounded to subangular pumice fragments (Plate 2E) were incorporated into the rhyolite while it was still cooling as indicated by distortion of the flow-bands around the pumice fragments.

Massive and flow-banded spherulitic rhyolite are best exposed in the South and Southwest Trenches. In the Southwest Trench there is a subtle, irregular gradation between flow-banded and massive rhyolite. The rhyolites here are dark pink in colour and the flow-banding, consisting of partially coalesced, chloritised spherulites (≈1mm) is more distinct. K-feldspar rich bands are also prominent in these flow-banded rhyolites and alternate with the spherulitic layers. Sodium cobaltinitrate staining, which mostly affects groundmass and the spherulites, shows that the groundmass consists primarily of fine-grained to medium-grained aggregates of quartz and K-feldspar and that the spherulites are bimodal in composition. The most abundant type of spherulite is quartz-rich but with a K-feldspar rich core. A second type of spherulite has a K-feldspar rich rim with an altered greenish (chloritic?) core. This type is rare but can vary widely in size, as can the altered core. A third rare type of spherulite has a K-feldspar rich core and a distinctive whitish rim with a cross-shaped internal structure.In the South Trench two varieties of spherulitic rhyolite (sub-unit 3) are present (Figure 7). Both are brecciated, however one, the southern-most, does not have an unbrecciated equivalent. The most significant difference between these two breccias is that in the southern-most breccia the angular fragments contain large (up to 3mm), grey-white, fractured spherulitic masses (Plate 2F) supported by a beige to cream coloured matrix which support smaller interstitial fragments (1.5 to 2.0cm).

The northern-most spherulitic, flow-banded rhyolite (sub-unit 3sb, Figure 7) shows distinct banding which consists of darker interlayered bands of partially to non-coalesced K-feldspar spherulites set in a fine-grained quartzofeldspathic groundmass and interlayered with coalesced K-feldspar spherulites containing interstitial chlorite (Plate 3A). Lighter bands result from individual spherulites (locally, poorly coalesced) in a quartzofeldspathic groundmass. The brecciated equivalent of this unit occurs to the south

Plate 2

A: Photomicrograph of typical lapilli tuff (ppl) showing randomly oriented chloritised lapilli in a fine-grained chloritised groundmass. West Trenches.

B: Massive grey, featureless rhyolite characteristic of rhyolite breccia fragments in the Central Trench. DDH LCO-5 (210m).

C: Block of massive rhyolite showing replacement by sphalerite and galena of an incorporated pumice fragment. Central Trench.

D: Photomicrograph of massive, non-spherulitic rhyolite, from the South-west Trench. Note the presence of rare, broken, plagioclase crystals (arrow).

E: Unbrecciated block of flow-banded rhyolite (Central Trench). The rounded pumice fragment distorting the bands indicates that it was incorporated into the rhyolite while the flow was still fluid.

F: Brecciated spherulitic rhyolite (South Trench). White structures in the breccia fragments are spherulites. Scale in centimetres.

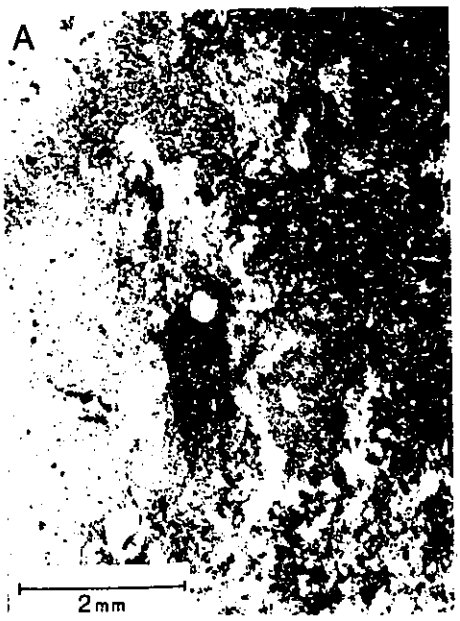
A
2mm


CENTIMETRES
B


C


D

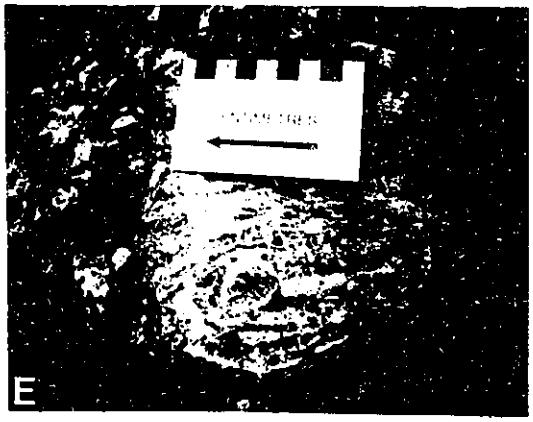
E

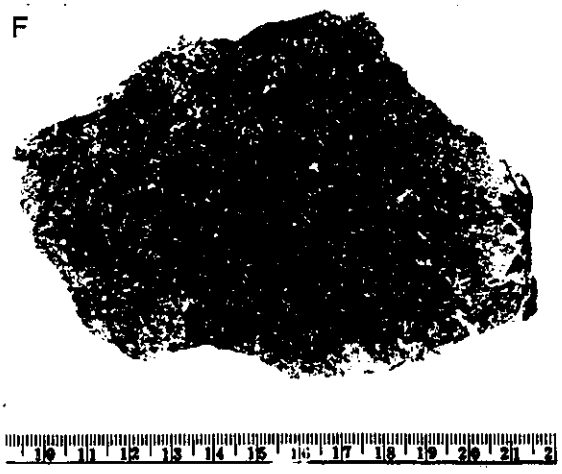
F

Figure 9: Central Trench Geology, breccia distribution and alteration. Note the sharp contact between unbrecciated crystal tuff and matrix-poor breccia in the west end of the trench. This is similar to the contact in the North Trench (see Figure 6). Note also, the apparent concentration of large blocks of flow-banded rhyolite and massive crystal tuff in the eastern part of the trench. The majority of breccia exposed in this trench is matrix-poor breccia with matrix-rich breccia only occurring in isolated pockets. Intense chlorite alteration in the eastern-most part of the trench is probably fault-related.

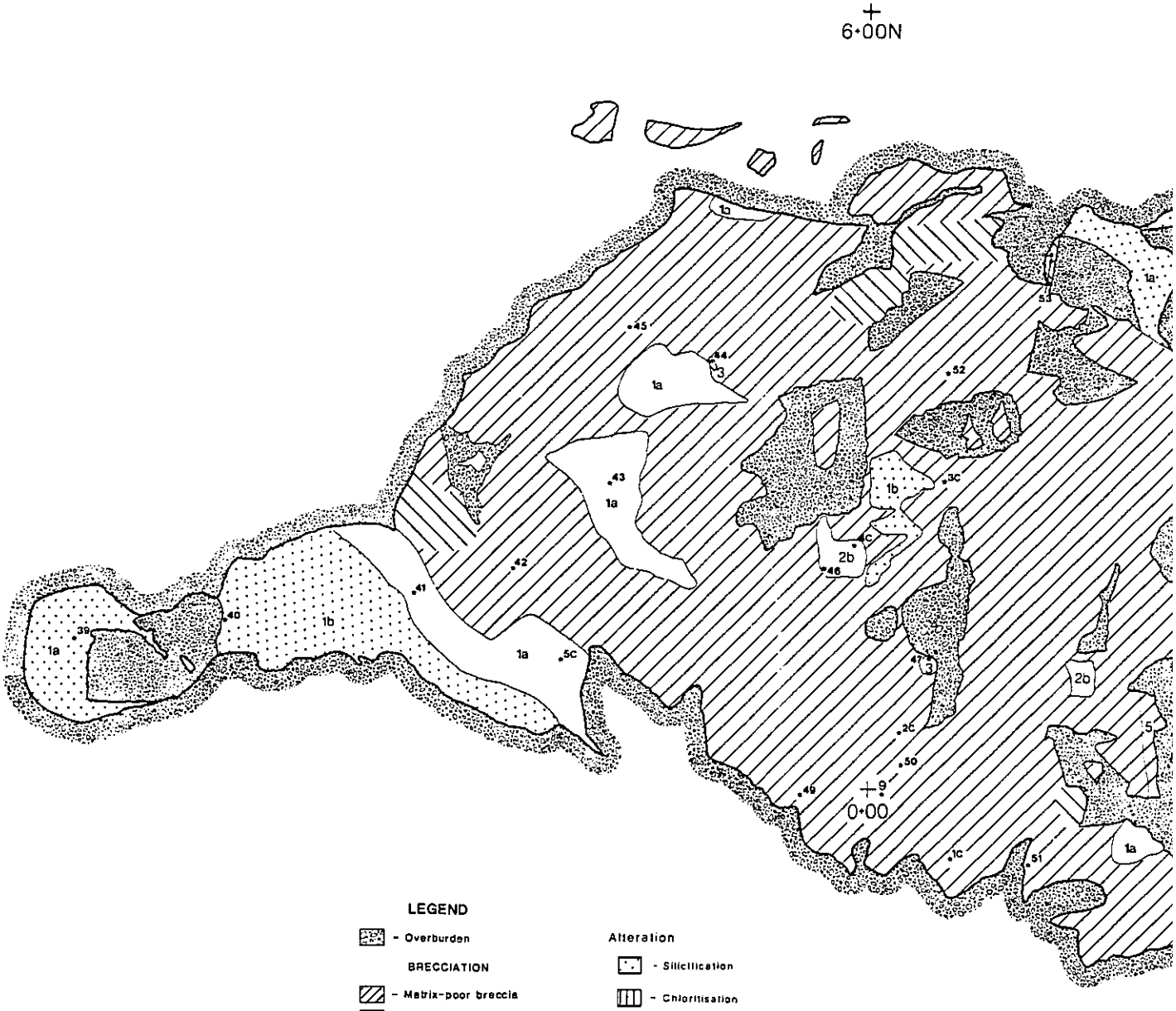

LEGEND

- Overburden

BRECCIATION

- Matrix-poor breccia
- Matrix-rich breccia

Alteration

- Silicification
- Chloritisation

LITHOLOGY

1 - Crystal tuff (a. massive, b. banded)

2 - Rhyolite (a. massive, b. banded)

3 - Agglomerate

4 - Mafic dyke

5 - Pumice

- Geological boundary (known)
- Fault (assumed)
- Grid station & number
- Diamond drill hole & number (vertical, inclined)

39• - Sample location; 1987, 39-72 (MC-87-)
1986, 1C-12C (MC-86-)

Geology, Brecciation & Alteration

CENTRAL TRE

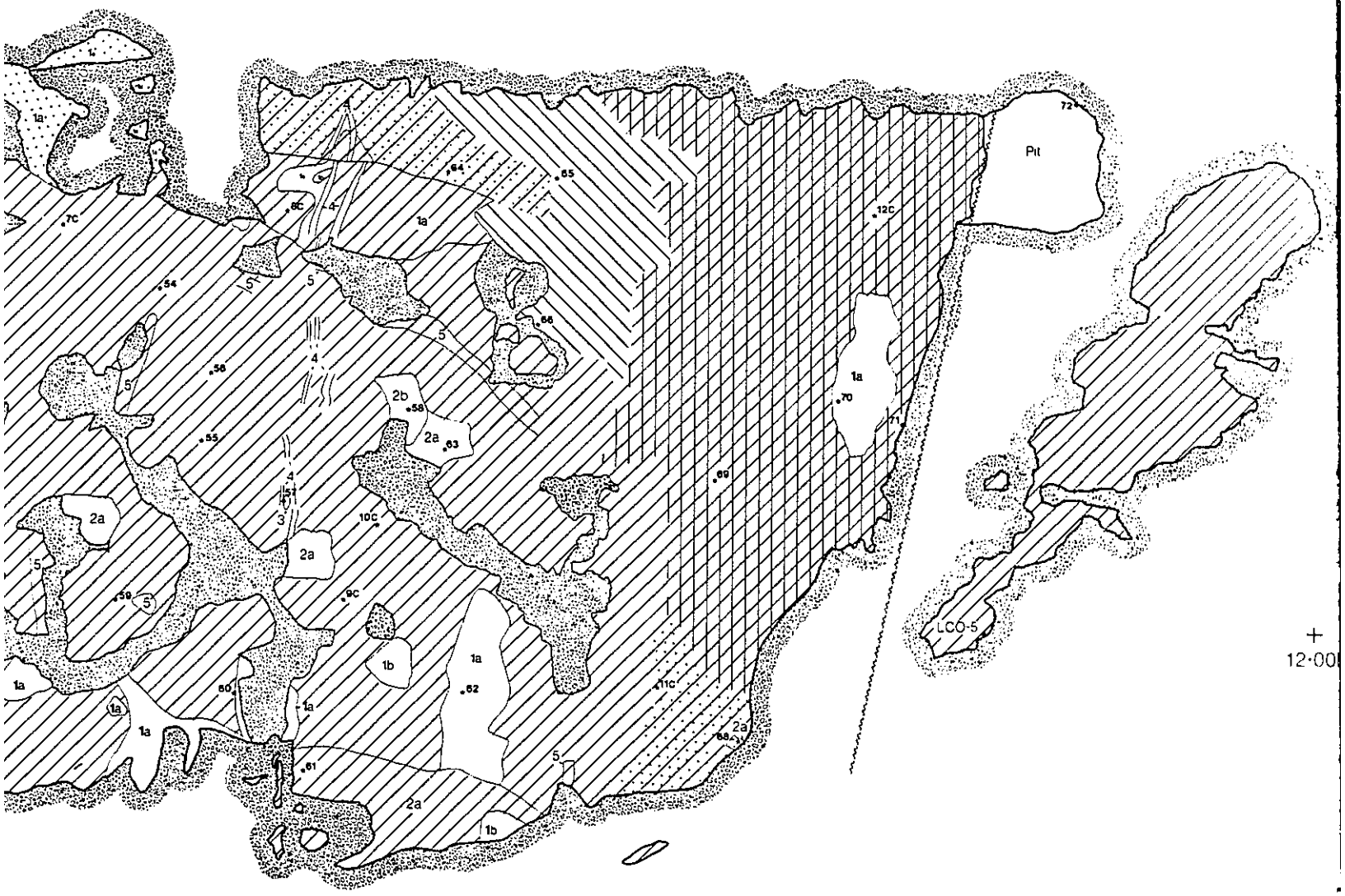

L TRENCH, MOUNT COSTIGAN LEAD-ZINC DEPOSIT

and consists of small (up to 10cm but averaging 3 to 5cm), angular, banded breccia fragments supported by a grey-white matrix of silicified, massive crystal tuff with a low percentage of interstitial fragments.

4. Perlite

This rock type is unique to the South Trench and occurs as a thin layer about one metre thick between a spherulitic rhyolite breccia and a massive, weakly mineralised, crystal tuff (Figure 7). The perlite is dark grey to green in colour and shows abundant dark yellowish bands (Plate 3B) that parallel the contacts with the surrounding rock units. These bands are representative of more highly altered zones in the perlite due to their lighter colour and since, compositionally, they appear to be identical to the darker material. In thin section, the highly fractured nature of the perlite [showing the characteristic concentric perlitic fractures (Plate 3C)] is clearly visible and best observed in the lighter bands. Discrete quartz and K-feldspar crystals are common in both layers of this rock, although there is a predominance of quartz in the lighter bands. Large K-feldspar crystals in the dark layers show excellent graphic textured overgrowths, which are interpreted to represent crystallisation during vapour phase conditions (Plate 3D). The presence of this perlite and the lithophysae in the nodular crystal tuff is good evidence for devitrification of the rocks in the South Trench.

5. Siltstone

Siltstone is exposed mainly in drill core east and west of the trenched area (DDH's LCO-4, LCO-84-4). Two varieties of siltstone are present at Mount Costigan and are found at opposite ends of the stratigraphy. The oldest siltstone (sub-unit #6, Figure 10) is fine-grained, dark brown to black and featureless. It is very friable due to the presence of two intersecting fracture sets (000°, and 320°) and is visible as minor outcrops in the East Trench where it is interlayered with, locally brecciated, banded crystal tuff. In drill core, fractures cutting the siltstone locally contain calcite (DDH LCO-84-1,2). Bedding within this sub-unit typically varies between 120° and 145° northwest (DDH LCO-84-4). Within the exposure of the siltstone in the East Trench are two small (0.5m) blocks of massive crystal tuff, which reflect in outcrop, what is visible on a hand sample (≈20cm) scale, that is, smaller, angular fragments of massive crystal tuff incorporated into the siltstone (Plate 3E). In thin section the groundmass is fine-grained and quartzofeldspathic in composition but contains abundant, thin, fine-grained muscovite laths. The interlayering of brecciated and unbrecciated crystal tuff and siltstone in the East Trench also reflects on a small scale what is apparent in drill core.

The younger siltstone occurring at the top of the stratigraphy is black, fine-grained and initially interlayered with the massive crystal tuff of stratigraphic unit F. It commonly grades into a fine- to coarse-grained silty tuff that contains moderate to strongly silicified polymictic lapilli tuff fragments. While brecciation commonly is only locally present, strong fracturing has produced carbonate-filled fractures. Overlying this is a dominantly siltstone-rich unit consisting primarily of fine-grained grey to

Plate 3

A: Photomicrograph of flow-banded spherulitic rhyolite from the South Trench (MC-87-25). Banding is represented by quartz and spherulites interlayered with spherulites and interstitial chlorite. Spherulites in the chlorite-rich zones are more coalesced than those in the quartz-rich zones.

B: Well banded K-feldspar-rich perlite from the South Trench.

C: Photomicrograph of B, showing excellent development of characteristic circular and semi-circular perlitic fractures.

D: Photomicrograph of graphic rim around K-feldspar in the perlite, indicating that vapour phase conditions existed during its crystallisation. Graphic rims are present not only in the perlite but are also common in all varieties of rhyolite and some banded crystal tuffs.

E: Siltstone from the East Trench. Note the incorporated fragment of massive crystal tuff that is representative of similar features on the thin section scale. Scale in centimetres.

F: Typical coarse matrix-poor breccia. Note the angular to subangular banded and massive crystal tuff fragments supported by a white quartzofeldspathic matrix that replacing the original matrix.


A


B


C
2mm


D


19 20 21
E

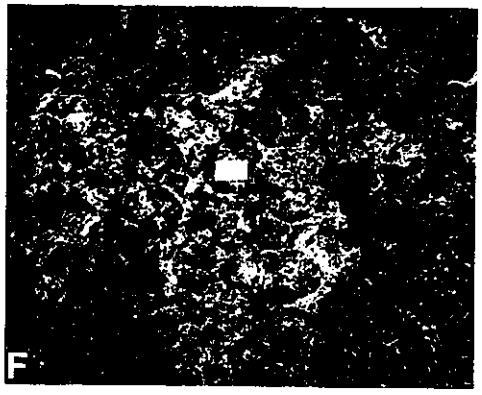
F

Figure 10: East Trench Geology, breccia distribution and alteration. Note the interlayering of brecciated and unbrecciated crystal tuff and siltstone sub-units. The presence of siltstone in this trench indicates that this trench is located near the base of stratigraphic unit C (see Figure 4).

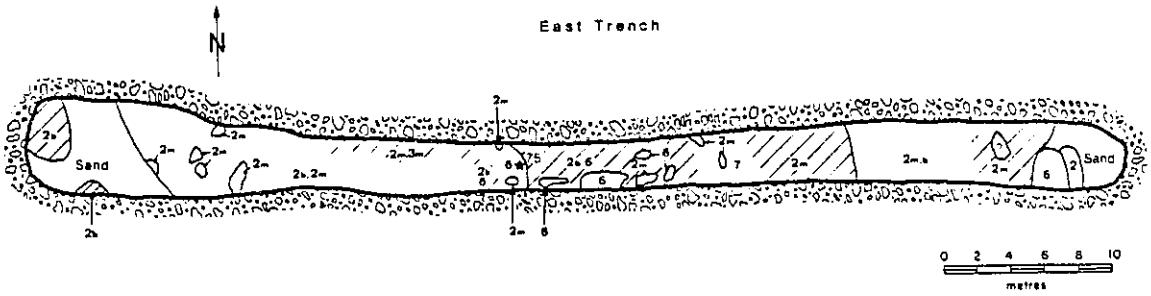
East Trench
N
Sand
Sand
0 2 4 6 8 10
metres

black, impure siltstone (containing minor subrounded to angular fragments of crystal and lapilli tuff). Fracturing is also quite strong in this unit as the siltstone is commonly very friable.

6. Conglomerate

The conglomerate does not outcrop on the property (Figure 2) and is only visible at the base of DDH LCO-84-5, although its thickness is unknown as this drill hole ends in the unit. It is grey in colour and interlayered with fine- to coarse-grained lithic arenite. Rock fragments in the conglomerate are polymictic, subrounded, up to 2cm in size and, consist primarily of volcanic glass (rhyolite?) with minor amounts of siltstone (Crevier, 1984).

c. Structure

i. Fracture Orientations

Three dominant fracture orientations (Figure 11a) are visible in the North Trench; the main trend being between 075° and 095° with dips commonly ranging from 75° to 85° southeast. The second most common orientation varies from 010° to 175° with steep southwest and northeast dips. A third fracture set trends between 130° and 160° with moderate (50° to 65°) dips to the southwest. Contacts between sub-units in the North Trench parallel the north-south trending fractures as is evident by their consistent trend between 004° and 012°.

Within the South Trench, structural measurements of fracture orientations reveal three major directions (Figure 11b). The primary direction is 135° to 165° with steep (60° to 75°) to near vertical (75° to 85°) dips trending southwest (locally northeast). A weak fracture set with near vertical dips occurs from 165° to 175°. A second major fracture set occurs commonly at 85° to 110° with moderate (35° to 55°) to steep (75° to 85°) dips trending dominantly to the south (also rarely to the north). The last main fracture set occurs at approximately 045° with moderate to steep southeast dips and locally northwest.

Stereographic plots (Figure 11c) of fracture orientations in the East Trench show the presence of three main trends which vary in orientation between 160° and 080°. The predominant fracture set here is oriented approximately north-northwest with steep (75° to 85°) dips to the southwest. It is best represented in the siltstone of sub-unit #6 and correlates with the northwest to southeast trending fracture sets observed in the North and South Trenches. The next prominent fracture set here trends north-south with steep (75° to 85°) dips to the east, which correlate closely to a similar set in the North and South trenches (with slightly shallower dips). The last major fracture set is oriented at approximately 080° with steep dips to the southeast. Although this fracture set is weakly defined here, it does appear to correspond to east-west trending fractures in the North and South Trenches. Lastly, there is a weak occurrence of shallow to moderate, north-east to south-east dipping fractures which appear unrelated to any of major structural trends discussed above since they are not obvious in the other trenches and probably just represent local re-adjustment of the rocks.

Figure 11a: Stereographic projection of fracture orientations in the North Trench. Note the steep dips of all the fracture sets. Note also the presence of three major groups of fracture orientations: a. 075° to 095°, dips to southeast; b. 175° to 010°, dips to the southwest and northeast; c. 130° to 160°, dips to the southwest.

Figure 11b: Stereographic projection of fracture orientation in the South Trench. Note the presence of three dominant structural trends: a. 135° to 165°, steep southwest dips; b. 85° to 110°, steep southerly dips; c. Southeast, dips to the southwest.

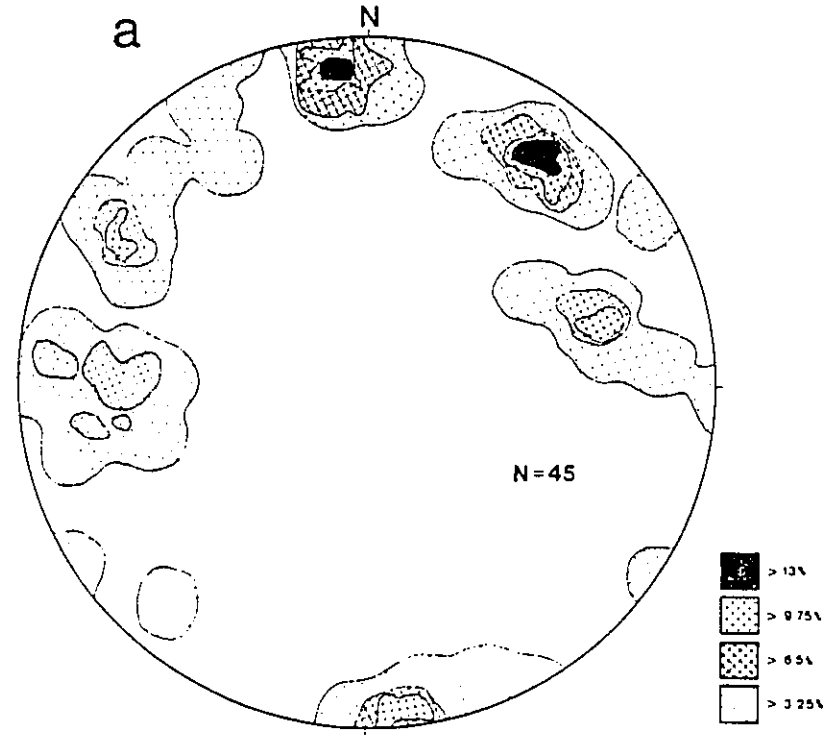

NORTH TRENCH

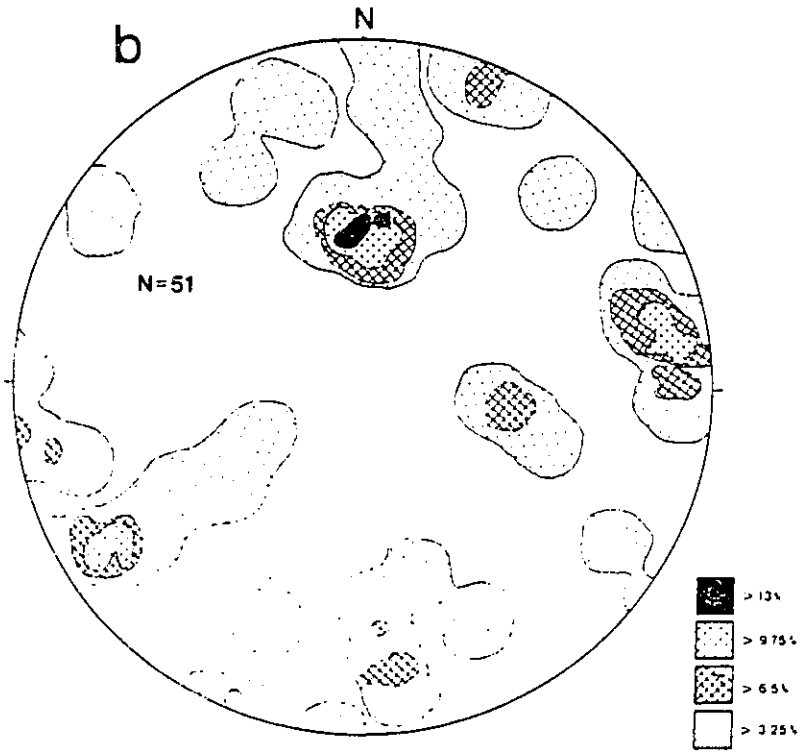

SOUTH TRENCH

Figure 11c: Stereographic projection of fracture orientations in the East Trench. Three major fracture sets are present here: a. 080° to 160°, steep southwest dips; b. 080°, steep southeast dips; c. northwest-southeast, moderate southwest dips.

Figure 11d: Stereographic projection of fracture and bedding orientations in the West Trenches. Excluding the bedding parallel fractures three fracture sets are present: a. 140° to 165°, steep northeast dips; b. East-west, steep dips north, c. northeast to southwest trends, steep dips to the northwest and southeast. Bedding fractures trend between 135° and 165° with shallow (20° to 30°) southwest dips.

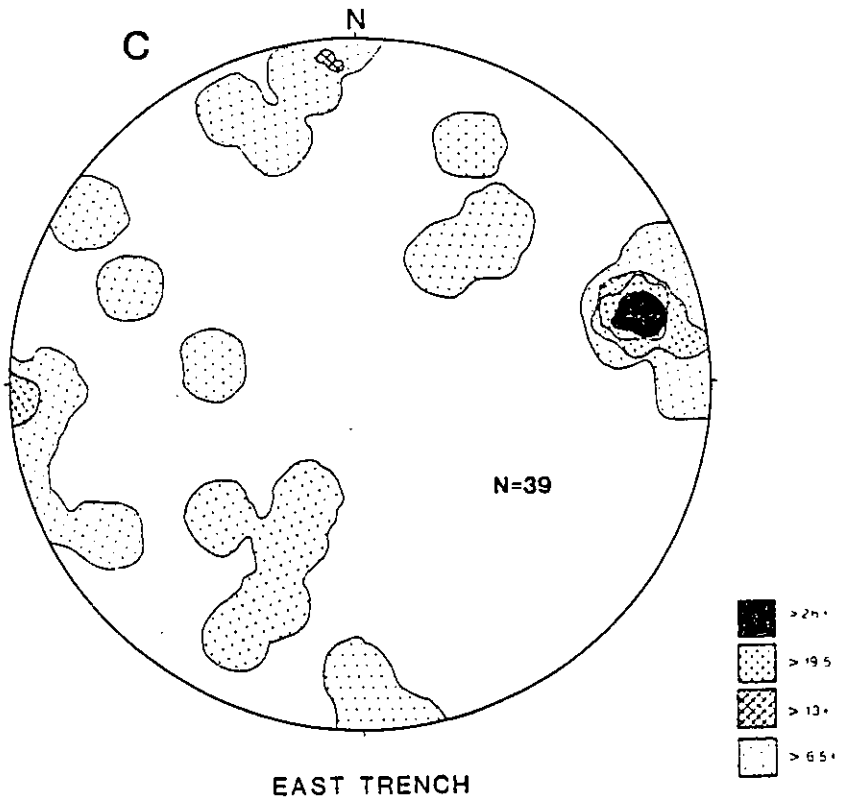
c
N
N=39
EAST TRENCH

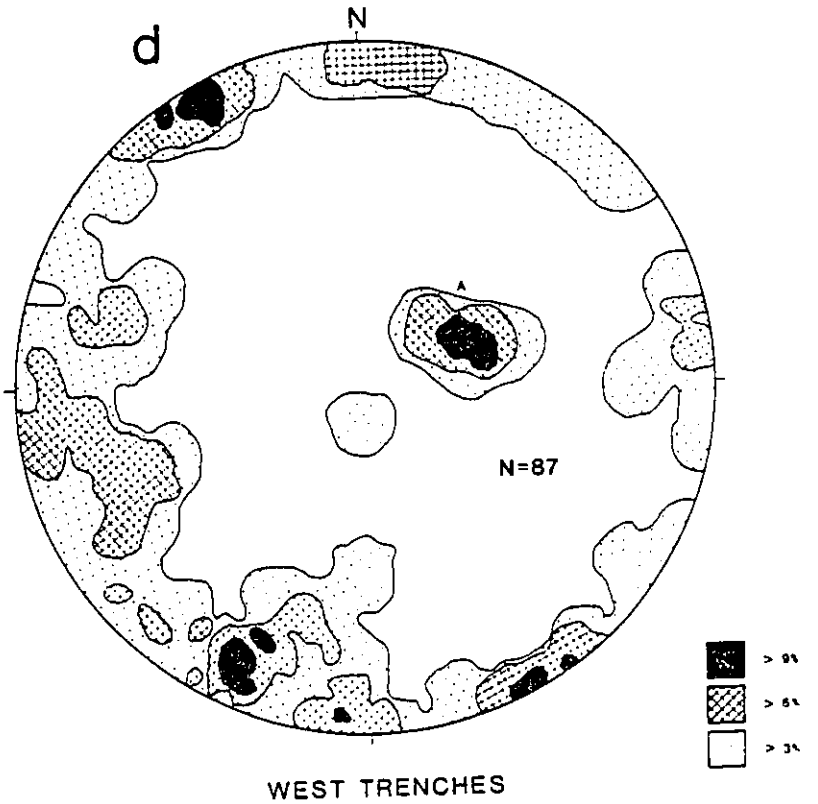
d
N
A
N=87
WEST TRENCHES

Figure 11e: Stereographic projection of fracture orientation in the Central Trench. Four major trends are visible: a. northeast to east-northeast, steep southeast dips; b. southeast, steep northeast dips; c. east-west, steep dips north; d. Southeast, steep dips to the southwest.

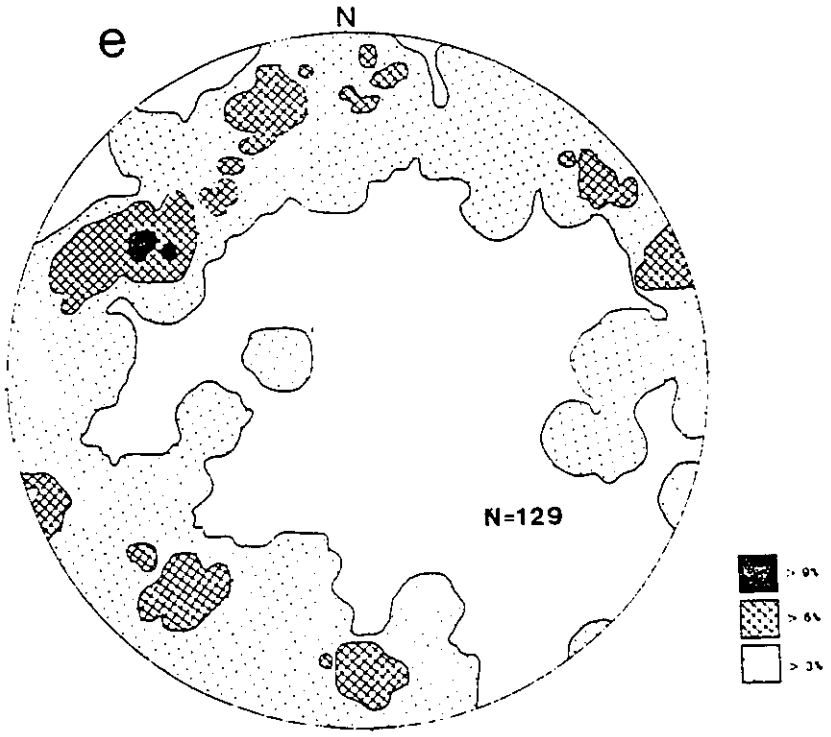

CENTRAL TRENCH

Stereographic plots of fractures in the West Trenches (Figure 11d) reveal the presence of four fracture sets which may be subdivided into two groups, a shallow set parallel to bedding and three steeply dipping sets that may be related to the regional tectonics. The bedding parallel fractures are the most prominent fracture set and trend between 135° and 165° with shallow dips from 20° to 30°. The three other fracture orientations are similar to those observed in the East and North Trenches occur at: 1. 020° to 045° with steep dips (75° to 90°) to the northwest and southeast; 2. 090° with steep dips to the north and 3. 140° to 165° with steep dips to the northeast.

Although fracture orientations in the Central Trench occur in all directions, they can be grouped into four major orientations (Figure 11e). The major direction is northeast to east-northeast with steep dips to the southeast. The second most prominent fracture set is that trending north-west with steep dips to the northeast. The third major group trends east to west and has steep dips toward the north. Lastly, the weakest fracture set is that trending north-west with dips to the southwest. These results show several prominent fractures cutting the trenches in an east-west direction. Those in the northern part of the trench are generally convex toward the north, while those in the south are convex toward the south.

It is clear from these stereographic projections that the majority of fractures in the Central Trench have steep dips and only 2% have shallow to moderate dips. The circumferential distribution of the fracture orientations does suggest that the breccia may be a pipe-shaped body, although there is one orientation where no fractures are developed (north-east to south-west with dips to the northwest). Furthermore, since several of the fracture sets are traceable through and beyond the breccia from north to south and east to west they may have resulted from another mechanism unrelated to the formation of the breccia.

Another possible explanation for these fracture orientations is the fact that these rocks were affected by the Acadian Orogeny. Since the dominant stress direction during this orogeny was north-west to south-east any conjugate fracture sets should be oriented at approximately 45° to this direction. This would suggest that the east-west and north-south fractures are unrelated to the process responsible for creating the breccia but are more closely associated with regional deformation. North-east to south-west trending fractures would be related to local readjustment of the regional structure during or slightly after deformation.

ii. Trench Structural Features

In the North Trench, the most significant structural feature is the white bleached zone at the eastern contact of sub-unit #2m. Although this zone was mapped as a fault by Lac Minerals Ltd. the lithologies on either side are broadly the same, the only difference being the degree of alteration, indicated by the sugary texture in the crystal tuff to the west. This structure may represent a right lateral fault as indicated by fractures in sub-unit 2m (southern 1.5m only) which turn into the plane of the structure (Figure 6). Other evidence is the proximity of the breccia in sub-unit #2m (separate from the

main breccia (Figure 11a)) which probably represents a fault breccia. The trend on the fault is 020°, and is approximately parallel to the major north-south trending fracture set and lithologic contacts.

Apart from fracture orientations, the structure in the South Trench appears quite complex, which complicates the interpretation of the geology (Figure 7). Firstly, in the lapilli tuff sub-unit (#1) no obvious bedding parallel fractures like those in the West Trenches are present and the contact with sub-unit #2b curves northward, varying from 137° at the east side of the trench to 165° at the west side. Secondly, in the northern 25 metres of the trench the lithologic contacts trend between 55° and 80°, while in the southern half of the trench (with the exception of the contact between silicified sub-unit 2m and sub-unit 2b) the contacts trend between 140° and 165°. Although this large variation in strike direction of the contacts between northern and southern parts of the trench may indicate the presence of a fold, it more likely represents a minor flexure in the contact.

Notwithstanding the variation in fracture and contact orientations in the South Trench the most significant structural features are the presence of two diverging bleached zones which form the northern contact of one of the repetitions of sub-unit #2m and were mapped as faults by Lac Minerals Ltd (Figure 7). This is a valid assumption since they have the same surface expression as the fault in the North Trench, although here there is no obvious evidence of any movement. They represent either two cross-cutting faults or one divergent fault zone since two bleached zones trending at N77°E (south branch) and N57°E (north branch) are clearly visible.

In the Central Trench, the most significant structural feature is the fault across the eastern end of the trench. The fault is oriented at 170° and since the associated intense chloritic alteration is only present on the west side, vertical or horizontal movement may be represented.

d. Breccia

The breccia at Mount Costigan is developed in only four of the six trenches on the property. The East and South Trenches contain the least, while the Central and North Trenches have the most breccia. Rocks in the West and South-west Trenches are unbrecciated.

i. Classification

This classification is an attempt to define the various kinds of breccia at Mount Costigan. There are two main breccia types present: **1.** an allochthonous breccia which is coarse- to fine-grained, polymictic (commonly containing large blocks of rhyolite and massive and banded crystal tuff) and is restricted primarily to the Central Trench; and **2.** an autochthonous crackle breccia which is coarse-grained, monomictic (consisting of angular crystal tuff fragments) and is found mostly in the North Trench.

Breccia Types

1. **Allochthonous Breccia**
   - a polymictic breccia which displays large degrees of fragment rotation.
   - can be divided into two sub-types as follows:

a. Matrix-poor
This variety of allochthonous breccia is characterised by a high fragment-to-matrix ratio. Fragments in this breccia commonly vary between 30 and 60cm, although smaller "rock chips" characteristically occur between the larger fragments. This polymictic breccia commonly contains fragments of crystal tuff, lapilli tuff and massive and flow-banded rhyolite. The material supporting the fragments is fine-grained and quartzofeldspathic in composition and likely represents a replacement of an earlier matrix.

b. Matrix-rich
This variety of allochthonous breccia is characterised by a high matrix-to-fragment ratio. Fragments in this breccia are commonly smaller than the matrix-poor breccia, ranging between 10 and 20cm. The smaller rock chips characteristic of the matrix-poor breccia are rare to absent here. While the matrix-poor breccia is characteristically polymictic the matrix-rich breccia appears to consist primarily of massive crystal tuff fragments.

2. **Crackle Breccia**
This breccia is unique to the North Trench. It is monomictic in lithology, consisting only of small (≤10cm) to large (10-20cm) fragments of massive crystal tuff that commonly display only slight degrees of rotation since many exhibit matching walls. This breccia may be considered autochthonous, since it appears to represent *in situ* brecciation. As in the allochthonous breccia the original matrix appears to have been replaced by fine-grained quartzofeldspathic material.

ii. Allochthonous Breccia

1. Morphology

a. Matrix-poor breccia

This variety of breccia is the most common of all the breccias at Mount Costigan and is best exposed in the Central Trench. It is polymictic in lithology and is characterised by banded crystal tuff with lesser amounts of massive and flow-banded rhyolite and massive crystal tuff (Plate 3F). The fragments are typically 50 to 70cm in size and display no obvious size or lithologic distribution. Interstitial to these fragments are smaller "chips" of massive crystal tuff and grey, massive rhyolite which, along with the main fragments are now supported by a white, microcrystalline quartzofeldspathic material that appears to have replaced the original matrix. The massive grey rhyolite fragments occur as small (3.0 to 5.0 cm) angular fragments supported by crystal tuff matrix and are found dominantly in the eastern portion of the trench.

There is commonly a higher proportion of banded crystal tuff to rhyolite fragments, however in the eastern part of the Central Trench there are pockets of breccia where there is a near equal proportion of banded crystal tuff, flow-banded rhyolite and massive rhyolite making determination of the matrix virtually impossible (Plate 4A).

Matrix-poor breccia in the South Trench is characterised by angular to subangular fragments of massive and flow-banded, spherulitic rhyolite characterised by large, white spherulites and supported by a similar quartzofeldspathic groundmass to the breccia in the Central Trench (see Plate 3A). Matrix-poor banded crystal tuff breccia is uncommon in the South Trench.

b. Matrix-rich breccia

This variety of allochthonous breccia is the least common and surface exposures are restricted mostly to pockets along the periphery of the Central Trench. It is monomictic in lithology, consisting of fine- to coarse- fragments of massive crystal tuff 10 to 20cm in size that display excellent white K-feldspar and quartz phenocrysts (Plate 4B). This breccia is also supported by the same white quartzo-feldspathic material as the matrix-poor breccia.

2. Distribution

The allochthonous breccia is exposed in the Central Trench and to a lesser extent in the South Trench. Since it is impossible to determine the exact nature of its surface distribution by the outcrop exposed in the trenches, its approximate shape was determined on the basis of breccia distribution in the boulder fields surrounding the trenches.

Due to low percentage of outcrop and the poor quality of that observed, mapping of the surface distribution of the breccia was not as successful as had been anticipated. Similarly, boulder fields used as a supplement that met the criteria for use in mapping were few and of very poor quality, the majority containing two to three lithologies, with individual boulders less than 1 square metre in size. While boulder size was a useful criterion in determining reliability of boulder fields, consistency of lithology was the determining factor. Despite these limitations the outcrop and boulder fields did provide useful data for determining the distribution of the breccia.

Observations showed that the breccia has a relatively large areal extent (Figure 12), best indicated by a large boulder field 25 x 20m in size (BF #1) containing abundant boulders of brecciated, silicified crystal tuff. These boulders are greater than $1m^2$ in area and probably represent frost-heaved outcrop. A boulder field similar in size, BF #2, contains distinctly smaller boulders of unaltered and strongly silicified, fine-grained lapilli tuff along with boulders of K-feldspar rich, massive crystal tuff breccia.

Boulder field #3 (Figure 12) is made up of two small boulder fields which consist of about 90% lapilli tuff boulders and rare boulders of crystal tuff breccia. Boulder field #4 and associated outcrop near DDH #23, however, consist of fine- to medium-grained, lapilli tuff breccia. The boulder field at BF #5

Plate 4

A: Coarse matrix-poor rhyolite and crystal tuff breccia. While fragments here consist of flow-banded rhyolite and banded crystal tuff, note how, due to the low proportion of quartzofeldspathic matrix, the crystal tuff appears to be supporting the rhyolite.

B: Typical matrix-rich breccia from the Central Trench. Note the higher proportion of matrix to fragments than in the matrix-poor breccia.

C: Unique thin disrupted, aphanitic, mafic dyke cutting the breccia in the eastern part of the trench (see Figure 26 for location). Note the white (bleached) chill margins (arrow) between the dyke and the agglomerate it cuts. Refer to D, for detail of the contact zone.

D: Photomicrograph of the contact zone between the mafic dyke (right) and the agglomerate (left). The chill margin is represented by the thin quartz veinlet near the right side of the photo. Note also the similarity between the composition of the dyke and the groundmass of the agglomerate.

E: Typical crackle breccia from the North Trench. While this breccia could be considered to be matrix-poor the fragments commonly show matching walls, an indication of minor amounts of movement.

F: Coarse-grained sphalerite and galena (arrow) filling voids between breccia fragments in a coarse-grained, matrix-poor, massive crystal tuff breccia. DDH LCO-8 (95.0m). Scale in centimetres.

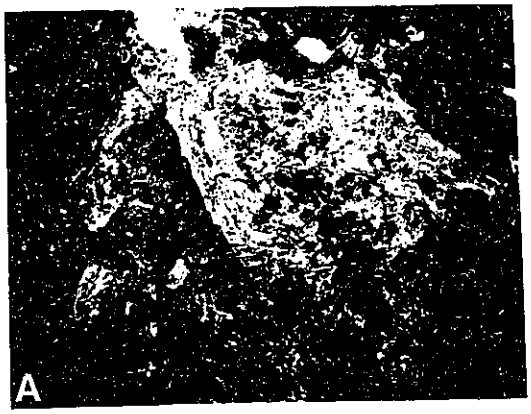
A

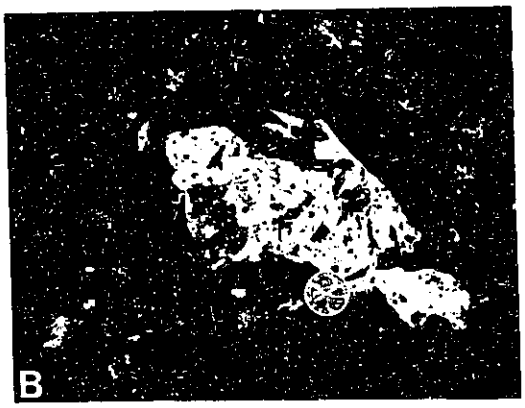
B

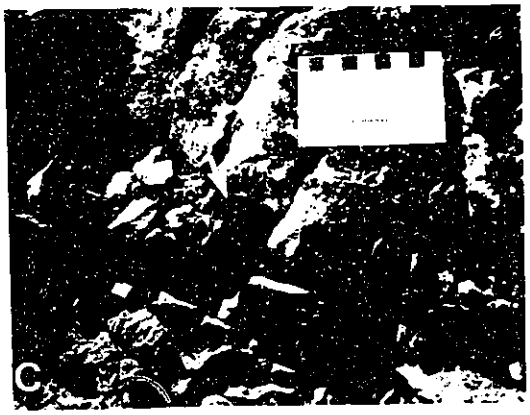
C


D

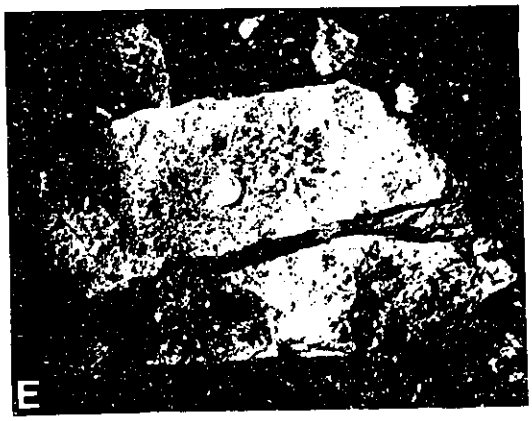
E


19 20 21 22 23
F

Figure 12: Boulder Field Location Map - not all drill holes are shown on this map and the horizontal projections have been omitted for clarity. Holes marked with no prefix (eg. 9) were drilled by Amoco while holes marked "LCO-" or "84-" were drilled by Lac Minerals Ltd. Dot-dashed line represents the breccia boundary as defined by Lac Minerals Ltd. Dashed line represents the extent of the deposit defined by this study. Note also that boulder fields within the breccia contain unbrecciated boulders and vice versa. (After Crevier, 1984).

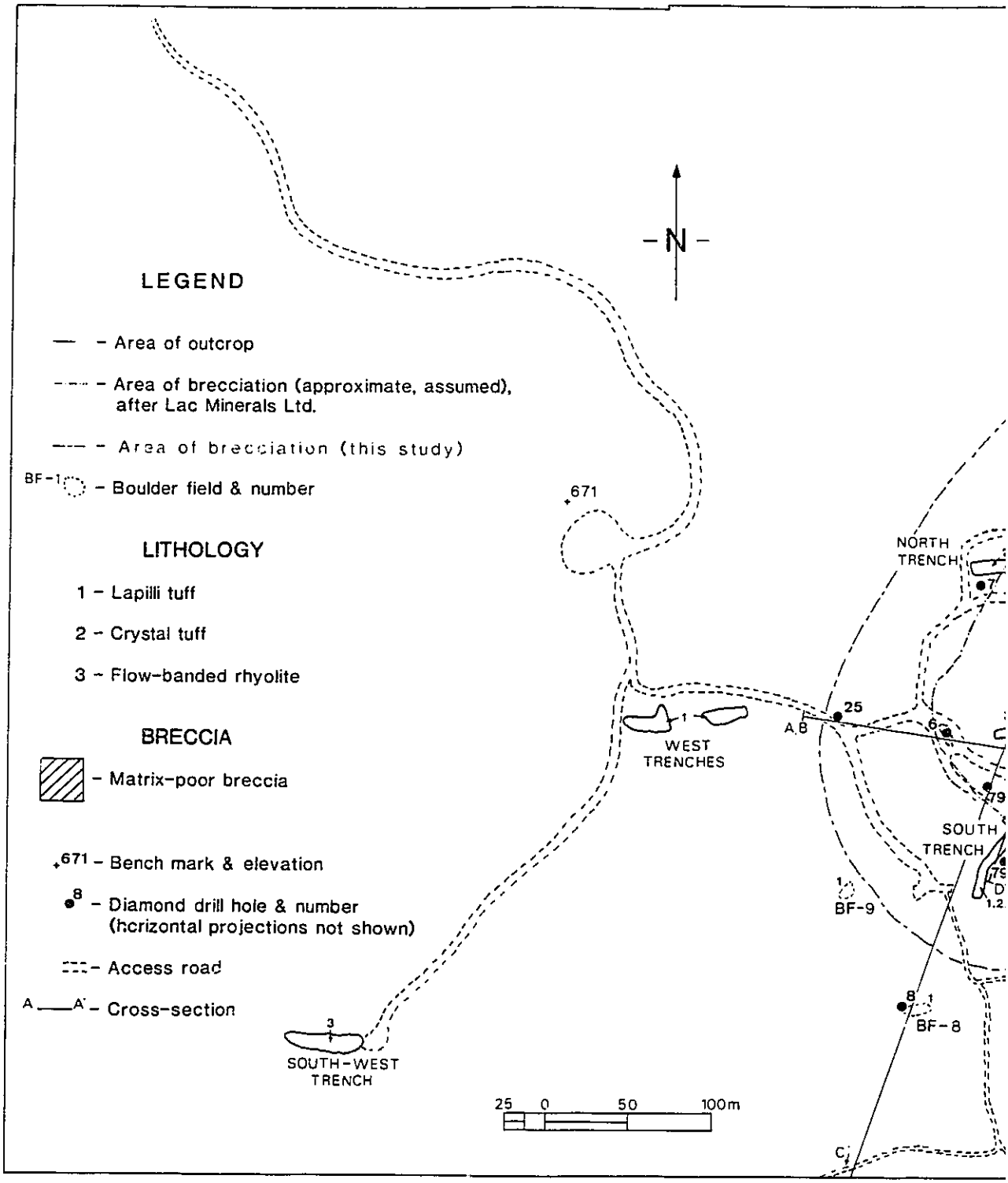
LEGEND
— – Area of outcrop
– – – – Area of brecciation (approximate, assumed), after Lac Minerals Ltd.
– – – Area of brecciation (this study)
BF-1 – Boulder field & number
LITHOLOGY
1 – Lapilli tuff
2 – Crystal tuff
3 – Flow-banded rhyolite
BRECCIA
– Matrix-poor breccia
671 – Bench mark & elevation
8 – Diamond drill hole & number (horizontal projections not shown)
– – – Access road
A — A' – Cross-section
N
671
NORTH TRENCH
WEST TRENCHES
SOUTH TRENCH
SOUTH-WEST TRENCH
BF-9
BF-8
A,B
C
25 0 50 100m

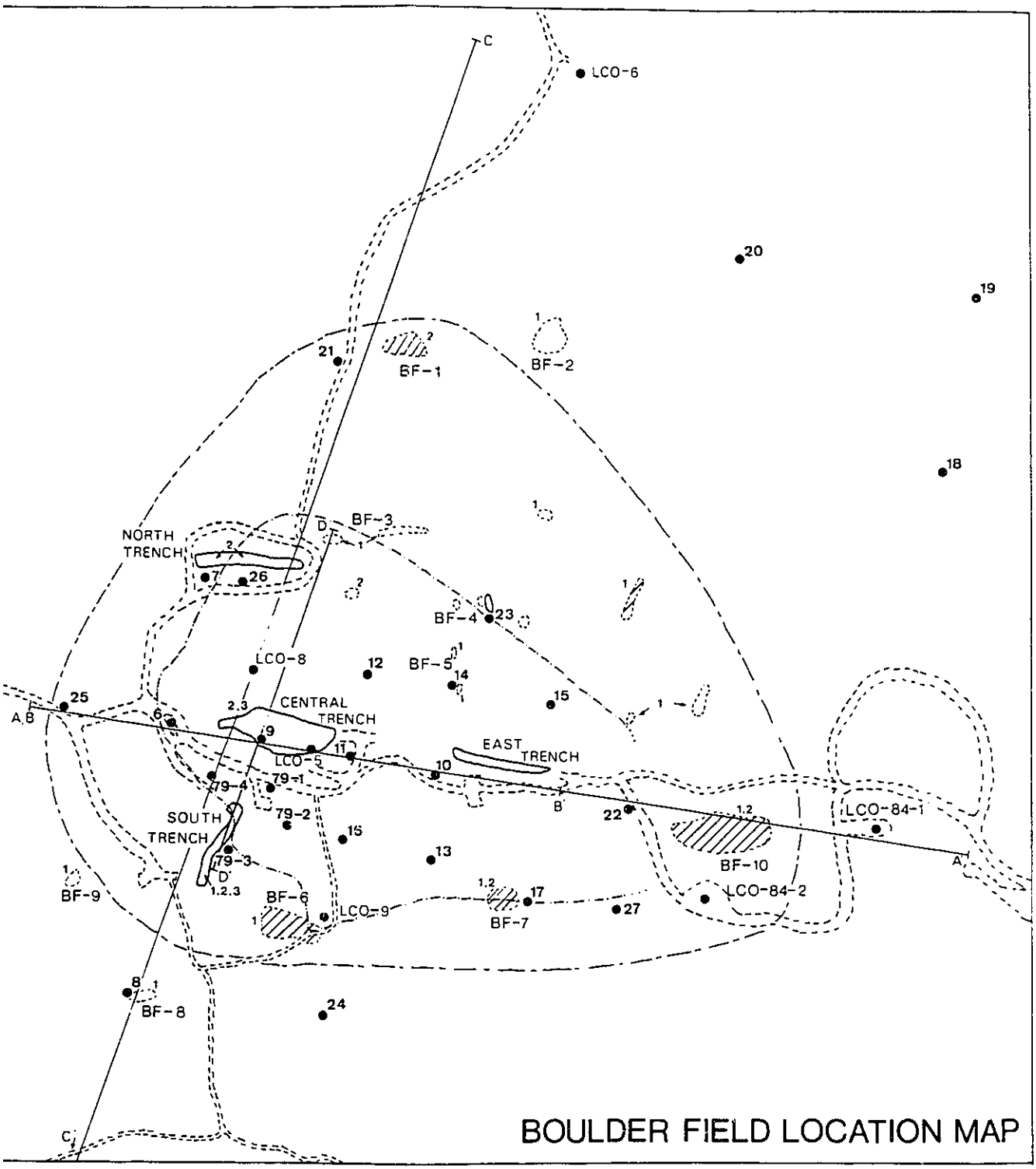
C
LCO-6
20
19
21
BF-1
BF-2
18
NORTH TRENCH
D
BF-3
7
26
BF-4
23
LCO-8
12
BF-5
14
25
A,B
6
2,3
CENTRAL TRENCH
15
9
11
LCO-5
EAST TRENCH
10
79-4
79-1
B
22
LCO-84-1
SOUTH TRENCH
79-2
16
13
79-3
D
1,2,3
BF-10
A
BF-9
BF-6
LCO-9
17
BF-7
LCO-84-2
27
8
BF-8
24
C
BOULDER FIELD LOCATION MAP

(near DDH #14) consists of massive and banded crystal tuff breccia with fine-grained pyrite in the matrix. To the south is a large boulder field around DDH #LCO-9 (BF #6) which contains boulders of massive, locally silicified, unbrecciated, fine-grained lapilli tuff and lapilli tuff breccia. Here, the matrix in the breccia is cream-coloured and silica-rich, which is similar to that observed in the Central Trench. In contrast, a boulder field occurring near DDH #17 (BF #7) consists of fine-grained, unbrecciated lapilli tuff boulders, similar to the rocks in the South Trench. Boulder fields to the south of the South Trench (BF #8,9) contain fine-grained silicified lapilli tuff and correspond to stratigraphic unit D, which incorporates the West Trenches and the southern 15m of the South Trench.

To the east of the trenched area boulder fields and outcrop are rare, with the exception of the boulder field at BF #10. This boulder field was found to contain angular to subrounded boulders of both unbrecciated crystal and lapilli tuff and crystal tuff breccia. The eastern extent of the breccia was left undefined by Lac Minerals Ltd., presumably due to the lack of conclusive drill hole data confirming the termination of the breccia. However, as can be seen here, it extends farther to the east than originally interpreted.

Although mapping conducted during this project did not identify any boulder fields west of the trenched area, mapping by Lac Minerals Ltd. indicates that boulder fields containing crystal tuff breccia occur to the north, south and east of the trenched area. While the breccia exposed in the Central, South and East Trenches is confined to stratigraphic unit C, boulder fields containing crystal tuff breccia occur stratigraphically above and below this unit, within units D and B4, indicating that the breccia may not be restricted to the one unit.

The presence of a thin, disrupted, aphanitic mafic dyke (Plate 4C,D) cutting the eastern half of the Central Trench (Figure 9) indicates that minor intrusive activity occurred during the late stages of development of the allochthonous breccia. This dyke runs approximately North-South and shows distinct chill margins where it cuts agglomerate of crystal tuff breccia fragments. It is commonly offset by Northwest-Southeast trending fractures and also frequently diverges to contain breccia fragments suggesting that it intruded the breccia prior to completion of brecciation and prior to development of the fractures. The significance of the dyke is unknown since it is the only observed intrusion within the trenched area.

3. Internal Structure

a. Surface

As exposed in the Central Trench the internal structure of the allochthonous breccia can be described as follows: 1. There is no apparent order to the brecciation; it is very chaotic since massive and banded crystal tuff and rhyolite fragments display evidence of a high degree of rotation and angularity. 2. At the west end of the Central Trench unbrecciated massive and banded crystal tuff sub-units overlie the breccia. It is possible that these two sub-units represent large blocks, similar to those in the eastern part

of the trench but due to the overburden cover their exact nature is unclear. 3. There is no distribution pattern to the large unbrecciated blocks of massive crystal tuff, except that they are more common in the eastern part of the trench, larger (2.0 to 4.0m) and more silicified than those the western part, which are smaller, more angular and chloritised. 4. Large (1.0 to 2m) flow-banded rhyolite fragments show a weak preferential concentration in the eastern portion of the trench. Rare occurrences of rhyolite, however, do occur in the western portion of the Trench.

b. Subsurface

The internal distribution of breccia as shown by cross-sections C and A [Figure 13, 14 (back pocket)] clearly indicates that the breccia is concordant with the stratigraphy and is underlain by the siltstone and pyroclastic units (units B2 to B4). The distribution of breccia in DDH's LCO-5, 79-3, LCO-8, LCO-9 and 17 [Figure 13, 14 (back pocket)] also shows the presence of a series of brecciated zones up to 128m thick which are separated by massive, unbrecciated layers of crystal and/or lapilli tuff. These zones vary from 6.0m thick in DDH LCO-9 (Figure 15, back pocket) to 73m thick in DDH LCO-8 (Figure 16, back pocket) and are common to all drill holes. Although the narrow, unbrecciated intervals in DDH LCO-9 could represent large breccia fragments, similar to those observed in the Central Trench, the same is not true for those unbrecciated horizons up to 73m thick. This evidence clearly indicates that the breccia body is intrinsic to the stratigraphy.

Breccia zones occur to the north of the trenched area as indicated by the breccia in DDH LCO-6 and DDH #21 (Figure 13) as well as to the south in DDH's #8 and #24. From this drill hole data it is clear that there are several layers of allochthonous breccia within the stratigraphy. Breccia overlying that in the Central Trench occurs to the west in DDH #25 and to the south in DDH #28, while the underlying breccia occurs to the east in DDH LCO-84-5.

iii. Crackle Breccia

1. Morphology and Distribution

The crackle breccia is confined primarily to the North Trench and is not found in the northern portion of the Central Trench. It is monomictic in lithology and consists of angular to subangular fragments of equigranular massive crystal tuff with minor, small, subrounded fragments of grey, massive rhyolite (Plate 4E) all supported by a microcrystalline quartzofeldspathic material that replaces the original matrix. This breccia most probably represents the products of *in situ* or autochthonous brecciation, since many of the breccia fragments display matching walls.

No boulder fields occur west of the trench so the distribution of the breccia in this direction is unknown, while those to the north consist mainly of massive brecciated crystal tuff. To the east and

Figure 13: Computer-generated north-south cross-section (C), looking east (see Figure 12 for location). Note the presence of breccia units both stratigraphically above and below the main breccia exposed in the Central Trench (eg. DDH's LCO-5,8).

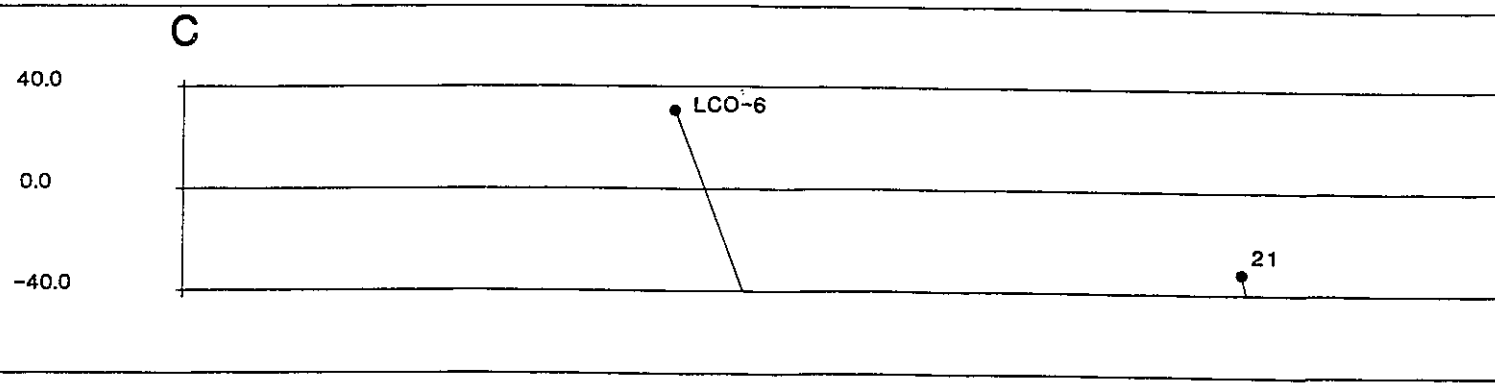
C
40.0
0.0
-40.0
LCO-6
21

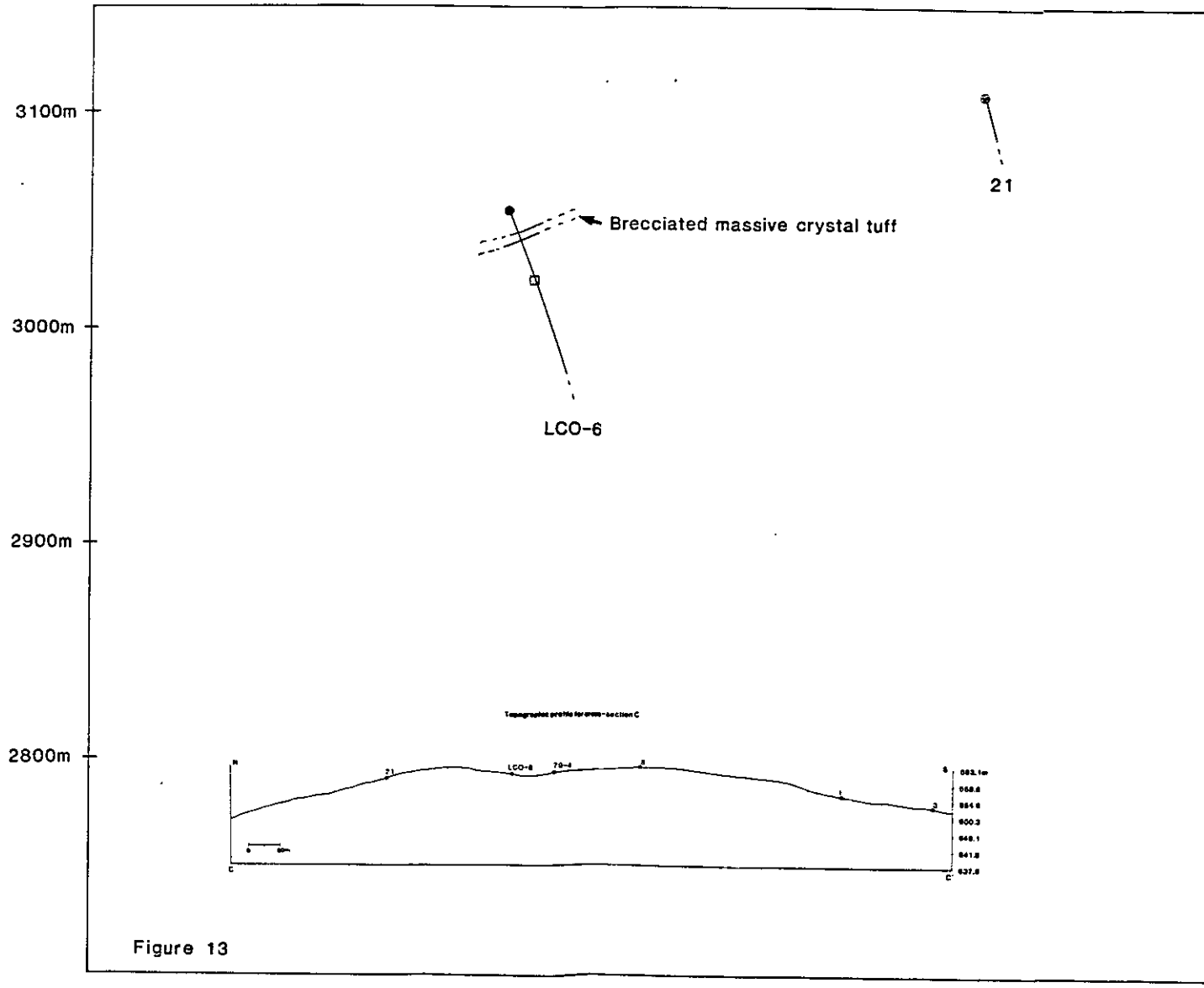
3100m
3000m
2900m
2800m
21
Brecciated massive crystal tuff
LCO-6

Figure 13

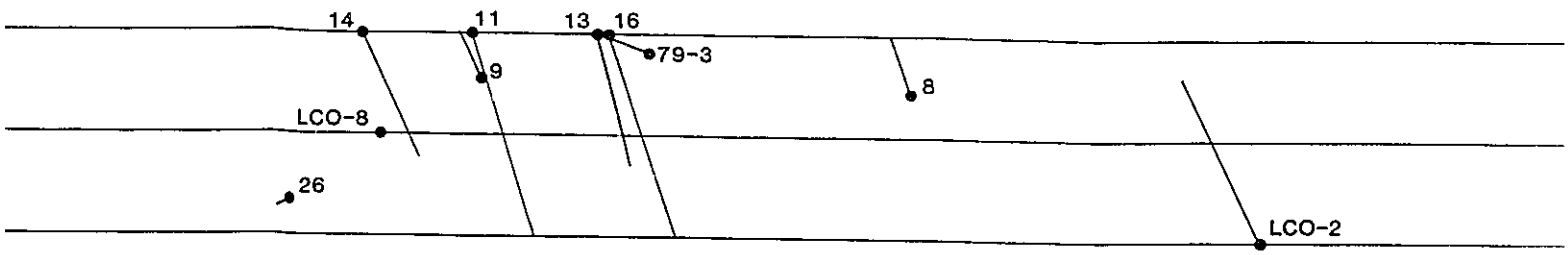

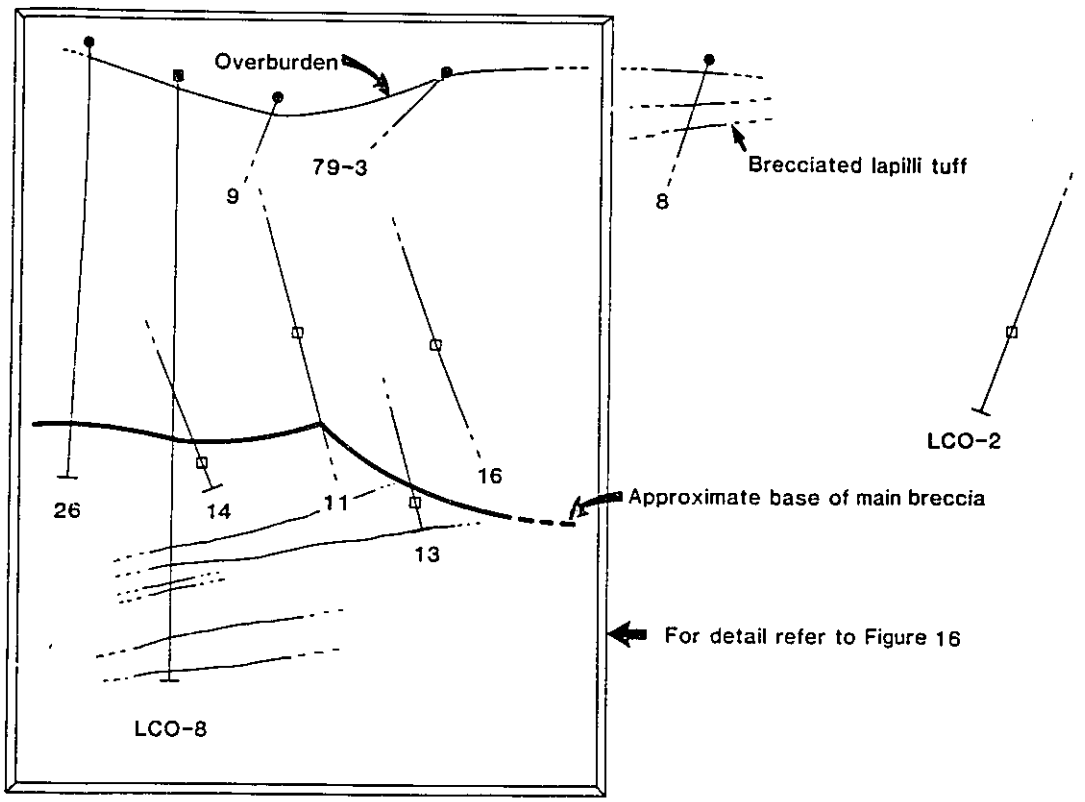

MOUNT COSTIGAN Pb–Zn DEPOSIT

Geology, long N–S section (N020E,90)

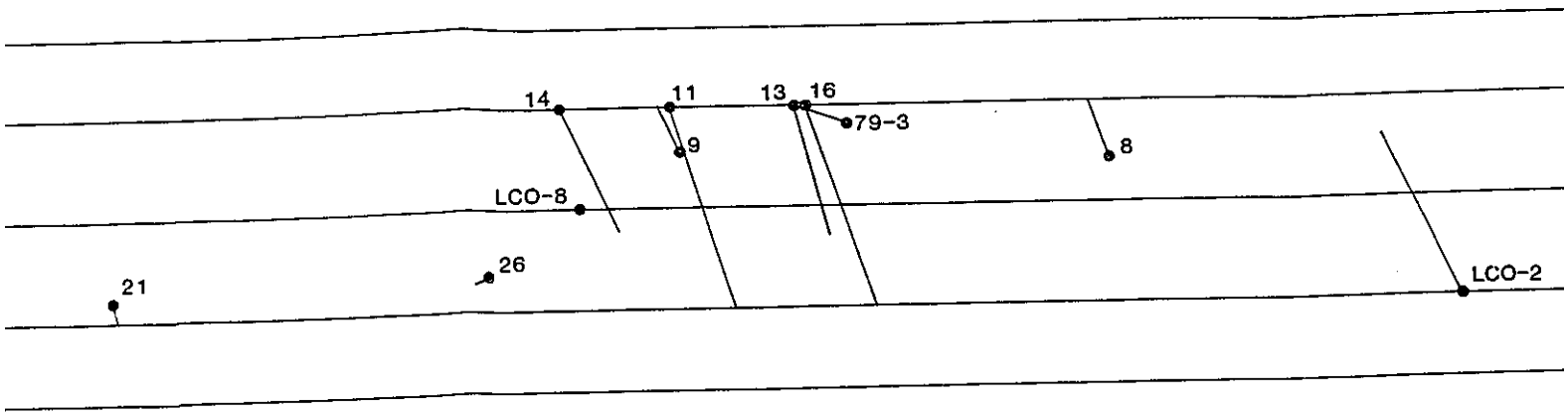

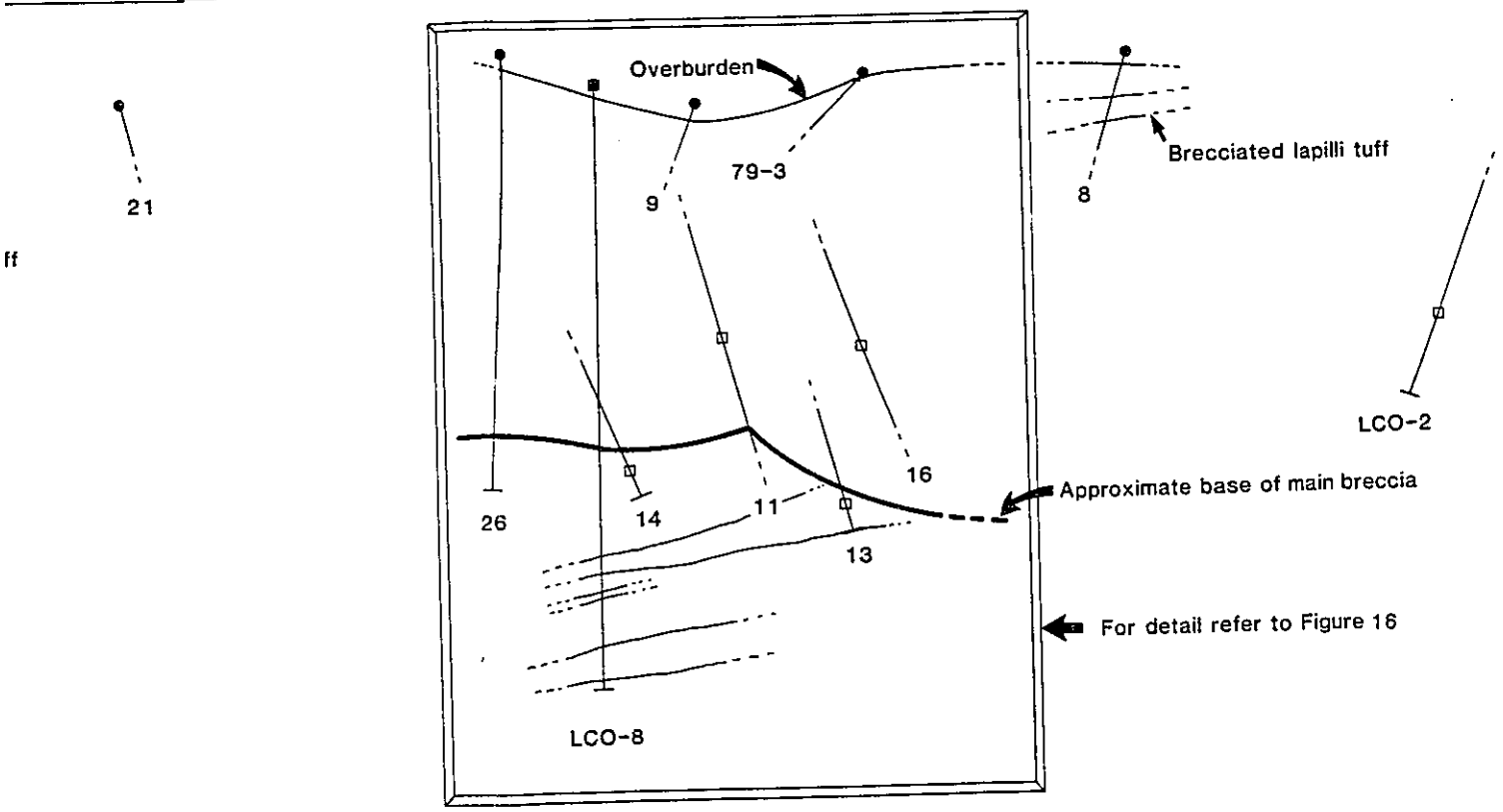

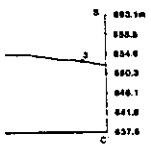

MOUNT COSTIGAN Pb-Zn DEPOS

Geology, long N-S section (N020E,90)

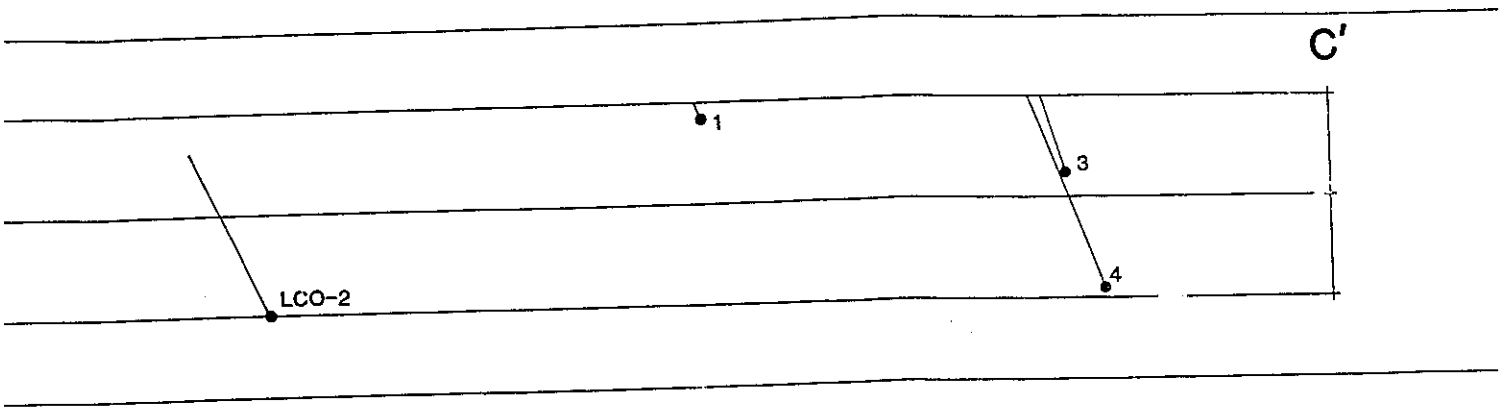

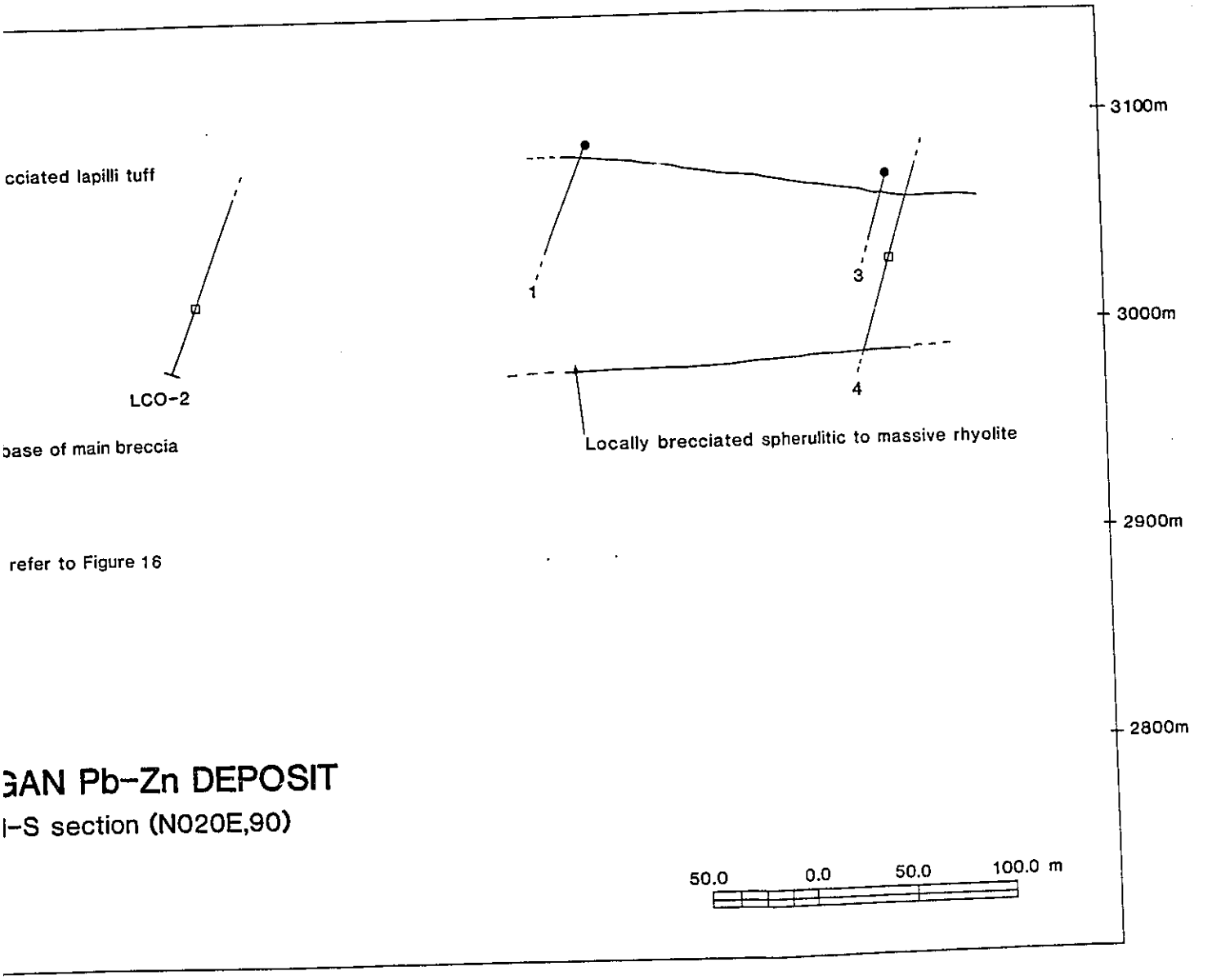

GAN Pb-Zn DEPOSIT

I-S section (N020E,90)

northeast boulder fields contain dominantly brecciated and unbrecciated banded crystal tuff and lapilli tuff which is more similar to the allochthonous breccia.

2. Internal Structure

a. Surface

As exposed in the North Trench the internal structure of the crackle breccia can be described as follows: **1.** The breccia fragments commonly show matching walls, which is good evidence for only minor degrees of movement. **2.** It is overlain to the west by unbrecciated, massive and banded crystal tuff that may be equivalent to a similar subunit exposed at the west end of the Central Trench and overlies the allochthonous breccia.

b. Subsurface

Crackle breccia occurs in the upper 50m of DDH #7 where it is interlayered with 5 to 10m of weakly, silicified, massive, (equigranular) crystal tuff. In DDH #26 the upper 24m also contain autochthonous breccia similar to that exposed in DDH #7, although here it appears to grade into locally brecciated, weakly silicified massive crystal tuff. DDH LCO-8 shows a similar relationship to that in DDH #7; the crackle breccia comprises the upper 47m and is underlain by massive, unbrecciated, equigranular, weakly silicified crystal tuff. These relationships would also suggest that the autochthonous breccia is separate from the allochthonous breccia, due to the presence of a thick interval of massive (locally brecciated) crystal tuff underlying it and the fact that it appears to grade into more incipient brecciation at depth.

The relationship between the allochthonous and autochthonous breccias at depth suggests that the autochthonous breccia overlies the allochthonous breccia and is therefore younger.

iv. Origin of the Breccias

To summarise, the breccia at Mount Costigan occurs in two main types. These are the allochthonous breccia, subdivided into matrix-poor and matrix-rich varieties found dominantly in the Central Trench, and the crackle breccia (autochthonous), confined to the North Trench. The allochthonous, matrix-poor breccia is polymictic and commonly consists of large angular fragments of banded crystal tuff and flow-banded rhyolite, with lesser amounts of massive crystal tuff and rhyolite. The matrix-rich breccia, conversely, is monomictic and consists mainly of massive crystal tuff fragments.

In their discussion of the pyroclastic flows of the 1902 eruption of Mt. Pelée, Martinique, Fisher (1979), Fisher et al. (1980) and Fisher and Heiken (1982) observed that the central portion of these flows commonly consists of coarse-grained, poorly sorted block and ash flow deposits, characterised by lapilli and crystal tuff breccia and lithic debris, overlain by fine-grained laminated ash. Blocks in these flows can be polymictic and vary up to several metres in size.

The allochthonous breccias in the Central Trench are atypical of pyroclastic flows (cf. Sheridan, 1979), in the sense that they have not travelled long distances from their source (e.g., the volcanic vent) as indicated by the angular nature of the breccia fragments, the relatively low proportion of matrix and the similarities of fragment lithologies to outcrop in the area. Accordingly, they are clearly pyroclastic in origin since the matrix-poor breccia (dominant breccia type) is typically polymictic and unsorted, consisting mainly of banded crystal tuff and rhyolite (massive and flow-banded). Thus these breccias most likely represent a volcanic breccia (e.g., a breccia formed by an explosive eruption), similar to the hydrothermal eruption breccias described by Nelson and Giles (1985), that filled in a lenticular topographic depression on the flanks of, or in proximity to, the vent. This interpretation is influenced by the similarity between the fabric of the allochthonous breccias and the breccias described by Nelson and Giles (op cit) as well as explosion breccias in northern British Columbia. The fragments in explosion breccias commonly have sharp to gradational contacts with the wall rocks while the angular to subangular nature of the fragments also indicates local transport. Explosion breccias from northern British Columbia, however, consist of small to large polymictic angular fragments commonly supported either by a drusy crystalline quartz cement or a fine-grained quartzofeldspathic matrix (Panteleyev, 1986) that could be equivalent to the quartzofeldspathic material replacing the original matrix at Mount Costigan.

The fine-grained crystal tuff that overlies the breccia in the North and Central Trench may represent air-fall ash or tuff that formed after the deposition of the breccia. This is interpreted as these sub-units (2m and 2b, Figures 6 and 9) contain no lithic fragments and their thickness is unknown, the upper contact being covered with overburden.

Other evidence suggesting that these breccias are the result of a volcanic eruption is the fact that the breccia has a relatively large surface extent as indicated by the distribution of boulder fields (Figure 12) containing crystal tuff and lapilli tuff breccia. Such boulders fields were encountered to the south of the trenched areas in BF #6, and to the east (BF #10). Also, in the vicinity of DDH's LCO-9 and 17 boulder fields containing both massive crystal tuff and lapilli tuff straddle the southern boundary of the breccia body as defined by Lac Minerals Ltd., indicating that the breccia body is larger than originally interpreted. This evidence, coupled with the fact that cross-sections show the regional stratigraphy continuing underneath the breccia (Figures 13,14) and that multiple breccia zones (best seen in section C) occur at depth, indicates that the breccia at Mount Costigan is a tabular or lenticular body and not pipe-shaped as has been previously suggested (Crevier, 1984).

Other possible origins for the allochthonous breccia are a lag breccia proximal to the volcanic vent, or, due to the presence of a large volume of rhyolite in the stratigraphy, a series of talus breccia on the flanks of a rhyolite dome (Sillitoe and Bonham, 1984). An origin as a lag breccia may be suggested because they are coarse-grained, occur in distinct layers, contain dense material too heavy to be transported very far and commonly are found closely associated with ignimbrites (Walker, 1985). However, because lag breccias are typically stratified and contain incorporated ignimbrite, the observed

absence of these characteristics precludes the allochthonous breccia from being a lag breccia, despite the fact that several layers of breccia occur within the stratigraphy and ignimbrites are common in the Costigan Mountain Formation south of the study area (St. Peter, 1978). The concordant nature of the allochthonous breccias at Mount Costigan could permit them to be interpreted as a talus breccia associated with a rhyolite dome, since a breccia formed in this manner would be lenticular or tabular in shape, while being approximately concordant to the stratigraphy. In addition, breccias associated with rhyolite domes are commonly autoclastic and supported by a rhyolitic matrix while the dominant lithology is massive to flow-banded rhyolite, although pumiceous material is commonly present (Laznicka, 1988). However, despite this it is unlikely that the breccias at Mount Costigan are associated with a rhyolite dome since such domes do not result from explosive activity, but rather form by a continuous brittle fragmentation that includes spalling and disintegration of the cooling crust on the surface of the lava dome (Laznicka, 1988). Rhyolite can also occur in dykes radiating outward from the dome.

Evidence for a breccia-pipe origin of the allochthonous breccia has been discussed previously. The evidence, however, is inconclusive because the relationship between fractures and the breccia is unclear. Moreover, since the same northwest-southeast fractures can be traced from the North Trench through the Central Trench and into the South Trench, they may be a result of regional deformation and not emplacement of the breccia.

e. Mineralisation

The Mount Costigan deposit (Figure 17) exposed mainly in the Central Trench where it defines an irregular-shaped body that contains approximately 600,000 to 800,000 tonnes of 2.5% combined Pb+Zn (Crevier and Gravel, 1984) and is roughly coincident with distribution of the breccia. From Lac Minerals Ltd. and Amoco drill hole data, the average assay values in the deposit are: 0.66% Pb, 1.24% Zn, 2.05g/t Ag. The highest values occur in DDH 79-3 from 64.50m to 66.00m where an intersection of 7.87% Pb, 14.40% Zn and 32.57g/t Ag was recorded.

i. Surface Sulphide distribution (Trenches)

The surface distribution of sulphide mineralisation at Mount Costigan (Figure 18) consists of fine- to coarse-grained sphalerite, galena and fine-grained pyrite and commonly defines four main habits:

1. Filling: (a) fractures cutting breccia matrix and/ or fragments; (b) voids between breccia fragments.
2. Replacement of: (a) pumice fragments in both massive and banded crystal tuffs and rhyolite; (b) banding in banded crystal tuff fragments; or (c) crystal tuff matrix.
3. Pods and veinlets in: (a) matrix; (b) breccia fragments; (c) cutting (a) and (b).
4. Disseminated: Fine- to medium-grained sulphides dominantly in massive crystal tuff but also rarely in banded crystal tuff and rhyolite.

Although the main zone of exposed sulphide mineralisation is restricted to the Central Trench (Figure 18), disseminated mineralisation also occurs in the peripheral trenches. In the North Trench, the only mineralisation observed occurs in the fault breccia of sub-unit #2m (Figure 6) as fine-grained pyrite, sphalerite and galena disseminated in both matrix and fragments of the crystal tuff breccia. No mineralisation was observed in any of the other sub-units in the trench, including the brecciated eastern exposure of sub-unit #2m.

In the South Trench, the only mineralisation observed occurs in the central-most exposure of sub-unit #2m (Figure 7) and consists of fine-grained, disseminated pyrite, galena and sphalerite and rare thin cross-cutting fractures. Mineralisation in the East Trench is rare and only found in the massive crystal tuff fragments of sub-unit #2b,6 where it occurs as disseminated sphalerite, galena and pyrite with minor fracture filling. The mineralisation is not continuous throughout this sub-unit, occurring only in small pockets in the tuff.

Disseminated sphalerite and galena occur in the silicified lapilli tuff of the West Trenches indicating that the sulphides were probably introduced with the silicification since the unaltered lapilli tuff at the west end of the western-most trench is barren of sulphides.

While trace to disseminated sulphide content (sphalerite, galena, pyrite) may be found in most of the allochthonous breccia, with the exception of the large blocks of unbrecciated massive crystal tuff, twenty distinct areas of noticeably higher sulphide mineralisation were observed and grouped into regions of disseminated, medium-sulphide and high-sulphide content. These areas can contain, within them, several smaller zones of high, medium or disseminated sulphide mineralisation, hence the repetition of some of the areas listed below.

In figure 18, areas A, C, F, I, M, N, P and T represent disseminated sulphide content while medium-sulphide content is characteristic of Areas B, D, E, G, H, J, L, N, Q, R, S and U. High-sulphide content is typical of Areas H, K and O.

Figure 17: Deposit location map - note that the bulk of the mineralisation is contained within the main breccia zone (after Crevier, 1984).

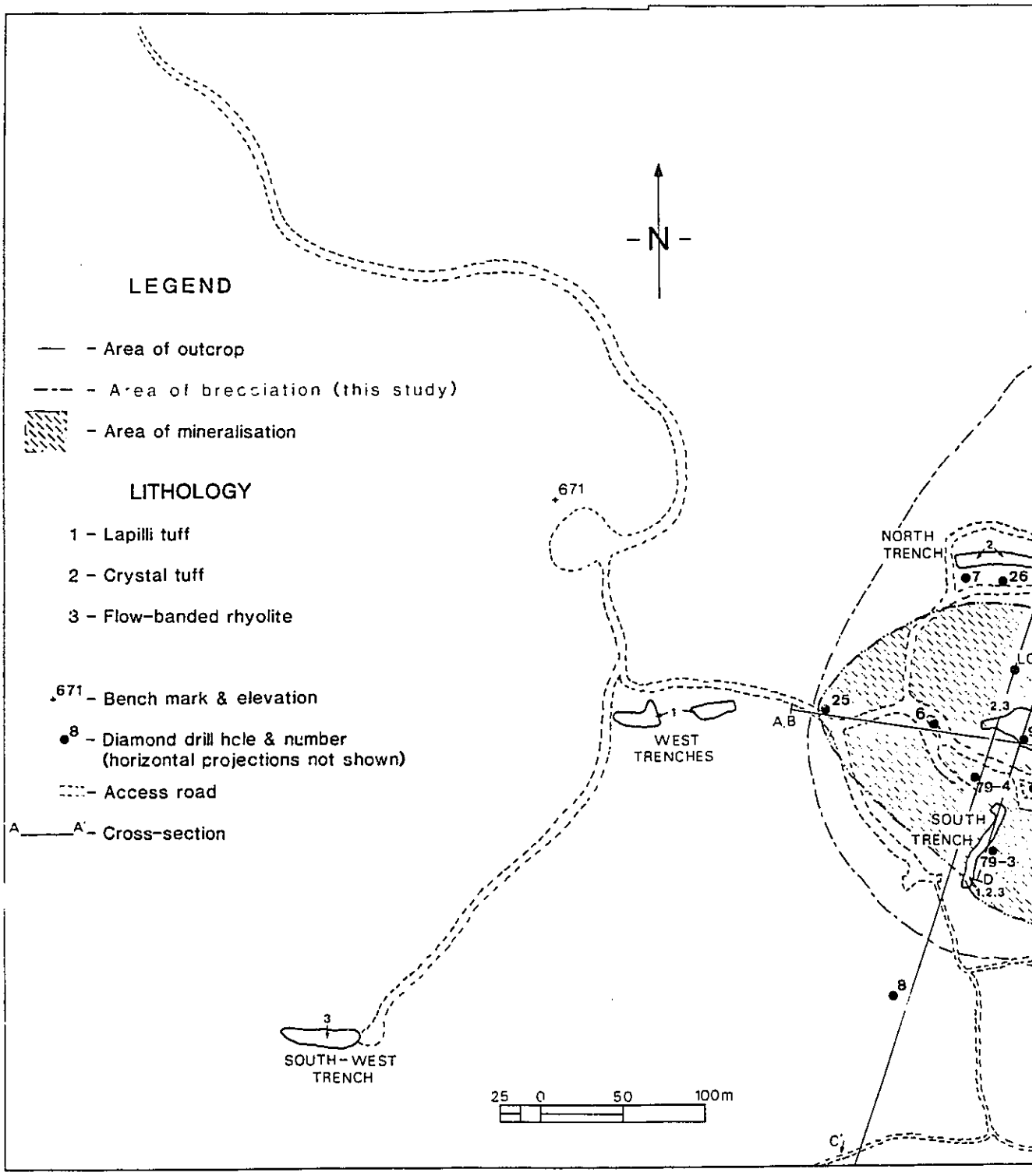
LEGEND
– Area of outcrop
– Area of brecciation (this study)
– Area of mineralisation
LITHOLOGY
1 – Lapilli tuff
2 – Crystal tuff
3 – Flow-banded rhyolite
671 – Bench mark & elevation
8 – Diamond drill hole & number (horizontal projections not shown)
– Access road
A A' – Cross-section
N
671
NORTH TRENCH
WEST TRENCHES
SOUTH TRENCH
SOUTH-WEST TRENCH
A,B
C
C'
25
6
7
26
2.3
79-4
79-3
8
3
1
2
25 0 50 100m

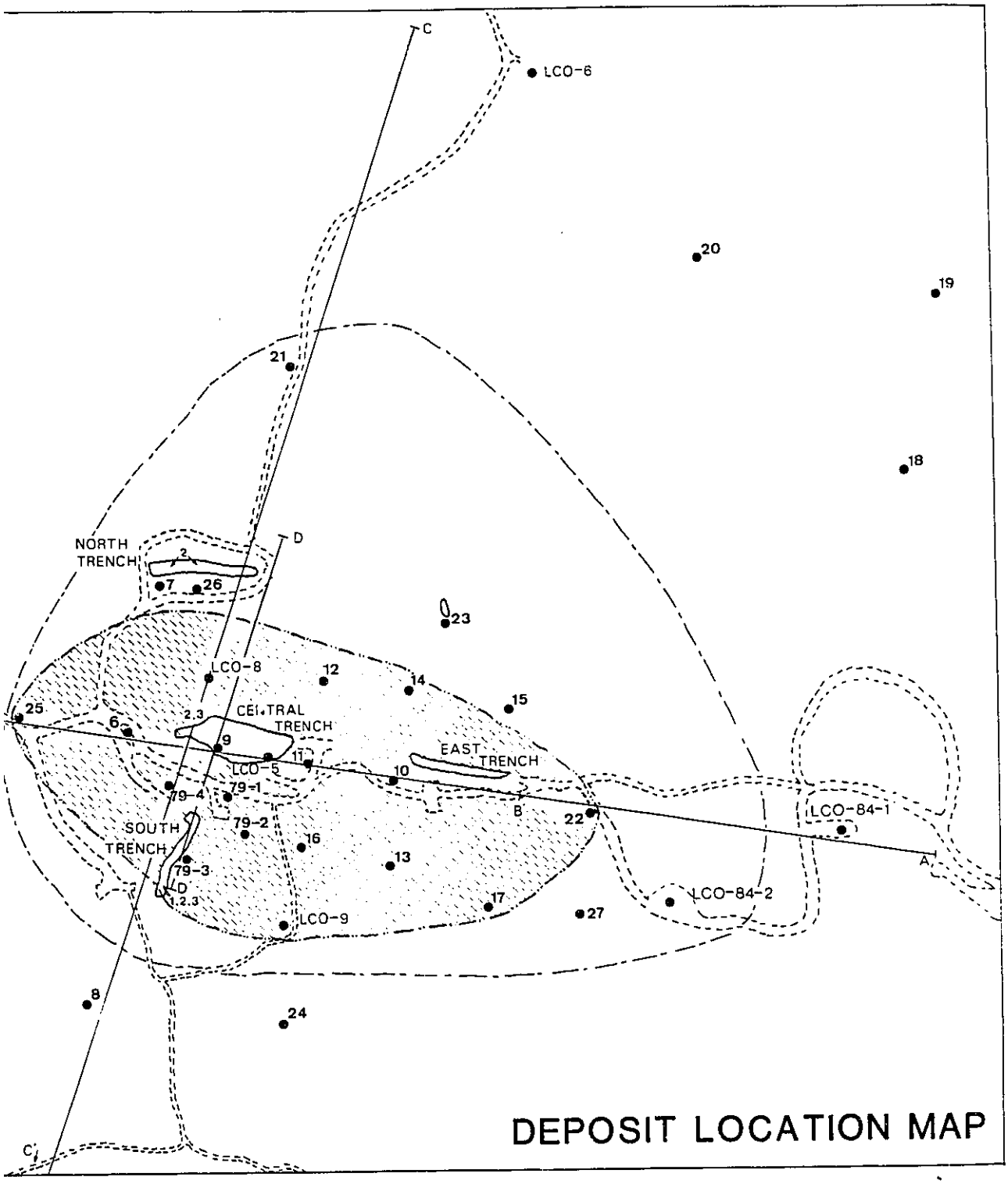

DEPOSIT LOCATION MAP

Disseminated sulphide mineralisation is characterised by: fine-grained disseminated sphalerite and galena in banded crystal tuff breccia fragments (Areas A, I, M, P and T); replacement of pumice fragments in crystal tuff or rhyolite fragments (Area A); disseminations in matrix (Areas A, C, F); replacement of massive crystal tuff fragments (Area I); fine-grained rims of galena around sphalerite (Area T); fine-grained sphalerite and galena veinlets cutting crystal tuff fragments and matrix (Area F); fine-grained sphalerite rims around massive rhyolite breccia fragments and fine-grained sphalerite and galena veinlets in crystal tuff (Area N).

Medium sulphide mineralisation occurs primarily as: coarse-grained sphalerite and galena filling voids (Plate 4F) between banded and massive crystal tuff fragments (Areas D, E, U); disseminations, thin veinlets and small coarse-grained pods (0.5 to 1.0cm) in massive and banded crystal tuff fragments (Plate 5A) (Areas G, J, L, U); sphalerite and galena veinlets cutting crystal tuff matrix and fragments (Areas N and Q); thin sphalerite rims (Plate 5B) around massive rhyolite fragments (Area Q) and as a replacement of pumice fragments (see Plate 2C) by sphalerite and galena (Area U).

High sulphide mineralisation is best found in Area K where coarse-grained sphalerite and galena occur as a space-filling between breccia fragments and in fractures cutting the matrix and fragments (Plate 5C). Also characteristic of this area is preferential replacement of banding in banded crystal tuff by fine- to medium-grained sphalerite and galena (Plate 5C). Along the periphery of Area K the high-sulphide mineralisation grades into disseminated sphalerite and galena in the crystal tuff and matrix. Coarse-grained sphalerite and galena completely replacing pumice is also characteristic of Area K, but the best example of this type of mineralisation is found in Area H and is very distinct from unmineralised pumice fragments (Plate 5D). Coarse- to fine-grained sphalerite and galena in the matrix material of a matrix-poor massive rhyolite breccia characterise Area O.

ii. Sulphide Mineralogy and Textures

The main sulphide minerals at Mt. Costigan are sphalerite and galena, accompanied by pyrite, with accessory chalcopyrite. Sulphide mineralisation is concentrated in the Central Trench but disseminated sphalerite, galena and pyrite occur in the North, South and East Trenches. Areas of most abundant sphalerite and galena in the Central Trench occur between breccia fragments or as veinlets cutting breccia fragments and matrix, while medium- to low-sulphide mineralisation is represented by more disseminated grains.

Sphalerite is the dominant sulphide mineral and most commonly occurs as individual grains within massive and banded crystal tuff fragments and massive crystal tuff matrix. When sphalerite is found as an open space filling it occurs as massive crystals and crystal aggregates, typically in conjunction with galena as a replacement of crystal tuff matrix. As individual grains in the tuffs (and rarely in the rhyolites) sphalerite frequently displays strongly corroded, grain boundaries which suggest a reaction with the quartz and K-feldspar in the groundmass (Plate 5E). In contrast, in quartz-rich breccia fragments,

Plate 5

A: Small pod of sphalerite and galena in a massive crystal tuff fragment. Central Trench (Area K).

B: Massive rhyolite breccia fragment showing development of a thin rim of fine-grained sphalerite and galena (arrow). The fragment is supported by a matrix of massive crystal tuff. Central Trench.

C: Sample MC-87-54 from high sulphide zone (K) showing excellent replacement of banding in crystal tuff by sphalerite and galena (a). Note also the coarse-grained fracture-filling sphalerite and galena (b). Scale in centimetres.

D: Unmineralised pumice fragment in the Central Trench showing development of characteristic pumice texture.

E: Coarse-grained sphalerite in massive crystal tuff showing development of irregular or corroded grain boundaries, an indication of a reaction between the sulphide and the quartzofeldspathic groundmass.

F: Photomicrograph of a typical paragenetic sequence for the sulphide mineralogy. Pyrite (P) was the first phase to crystallise followed by near simultaneous crystallisation of sphalerite (S) and galena (G) as indicated by their interpenetrating (I) and regular (R) contacts. Chalcopyrite (C) is the last phase.


A


B

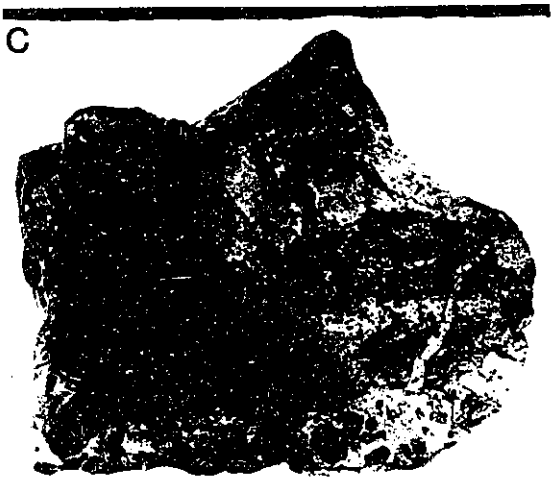
C


D

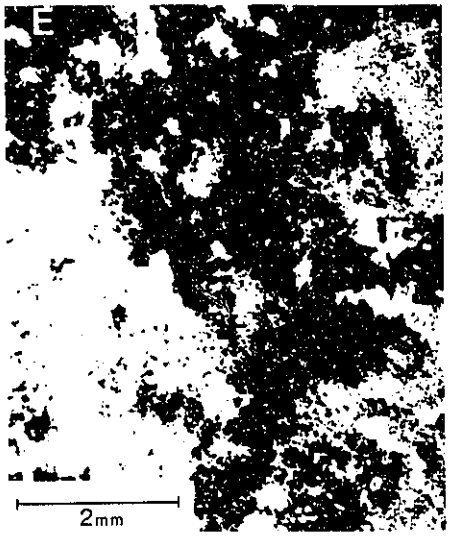
E
2mm


F
I
G
C
P
G
R
0.5mm

Figure 18: Mineralisation map of the Central Trench. Areas marked with "plus signs" are low sulphide content, areas with dots are medium sulphide content and areas marked with vertical lines are high sulphide content.

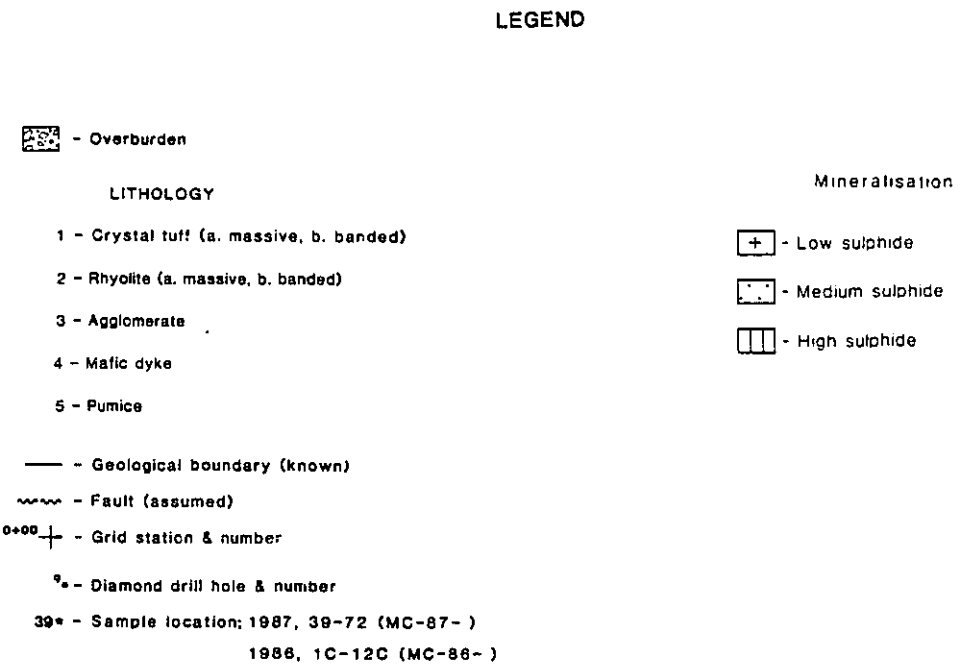

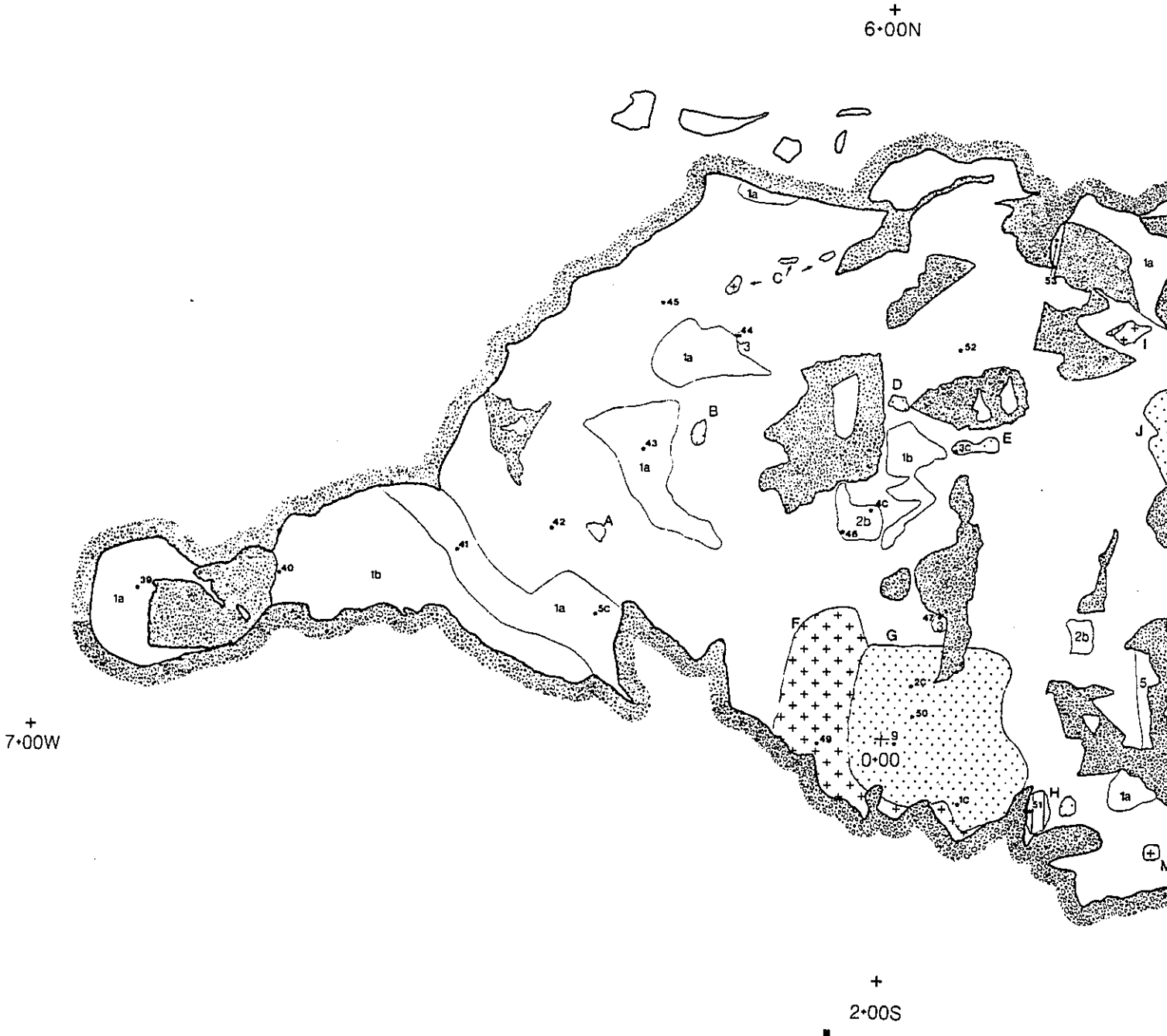
6·00N
7·00W
0·00
2·00S
1a
1b
2b
2c
3
3c
5
5c
A
B
C
D
E
F
G
H
I
J
39
40
41
42
43
44
45
46
47
48
49
50
51
52
53

TRENCH, MOUNT COSTIGAN LEAD-ZINC DEPOSIT

sphalerite exhibits rare smooth, regular grain boundaries. It also typically shows abundant, small (0.25 to 0.5mm) quartz inclusions. As space filling, where sphalerite is in contact with galena it also shows smooth regular grains boundaries (Plate 5F). Sphalerite regularly contains inclusions of euhedral pyrite, galena and blebs of chalcopyrite. Pyrite inclusions are usually unoriented suggesting they are earlier than the sphalerite. Conversely, crystallographically oriented blebs of chalcopyrite (Plate 6A) result from the exsolution of chalcopyrite in sphalerite. While the chalcopyrite is typically small (<0.25m), rare blebs up to 2.0mm can occur. Although sphalerite often contains inclusions of pyrite, it also forms thin rims around individual pyrite grains and aggregates and in rare cases it appears to be replacing the pyrite.

Some coarse-grained, space-filling sphalerite grains display an interpenetrating contact with galena suggesting the two minerals crystallised simultaneously. In LCO-9(2) sphalerite has a distinct lighter core (best visible in transmitted light) which, in reflected light, is emphasised by a fine-grained, circular train of quartz inclusions, indicating that the sphalerites are zoned. Other examples (LCO-9(3)) show a central core rimmed by fine-grained pyrite. In the spherulitic rhyolites of the South Trench sphalerite is a minor constituent, but occurs interstitially to the spherulites. Sphalerite grains in some of the brecciated samples are broken and show strongly corroded grain boundaries. This suggests that the mineralisation occurred during the late stages of brecciation and is supported by the presence of broken pyrite in the same sample. Individual sphalerite grains are cut by thin veinlets of galena (Plate 6B). These veinlets also (rarely) cut blebs of exsolved chalcopyrite, indicating that they are the later phase.

Sphalerite and galena typically occur together in veinlets and as space fillings, but galena rarely occurs as individual coarse-grained crystals the same size as sphalerite. Instead, galena normally replaces sphalerite (Plate 6B), occurring as rims around, or as veinlets cutting, individual sphalerite grains. In fractures filled with sphalerite and galena, galena replaces the margins of the sphalerite (Plate 6C) along the edges of the fracture where it is in contact with the gangue minerals (LCO-8(2)). In these veinlets replacement of sphalerite by galena occurs most commonly along the vein walls, where the galena is full of fine-grained quartz or sericite inclusions. Branching offshoots of these veinlets usually terminate in galena (LCO-8(2)) which has replaced earlier sphalerite. Here, the contacts between the galena and the quartz/K-feldspar groundmass are serrate indicating that there may have been a reaction between the galena and groundmass, contrasting with the contact between the sphalerite and groundmass, in the same veinlet that is commonly more regular (Plate 6D). Sphalerite also contains rare inclusions of pyrite.

Galena also contains rare inclusions of euhedral, fine-grained pyrite. Where galena occurs as individual grains in the groundmass of brecciated or unbrecciated, massive or banded crystal tuff it commonly occurs as small (0.5 to 1.0mm), euhedral grains which give the host a dusty texture. Coarse-grained, space-filling galena normally shows a slight degree of strain, evident by the minor flexures in the cleavage planes (reflected in the pitting), however the presence of non-pitted galena in some samples may indicated the presence of differential degrees of strain across the deposit.

Pyrite is the third most abundant sulphide present and normally occurs as small (1.0 to 1.5mm) euhedral grains in the groundmass of the crystal tuffs and as inclusions in both sphalerite and galena. Pyrite shows some interesting relationships with vein sphalerite and galena, most notably in LCO-9(1)a, where it is found along the contact between sphalerite and the gangue, being developed exclusively in the gangue within 0.5mm of the vein wall. Where pyrite occurs as inclusions in galena it is always found in association with inclusions of quartz. Where broken pyrite grains are found they show rare, late interstitial sphalerite enveloping the fragments. In Plate 6E pyrite occurs as fine-grained euhedral crystals which rim the breccia fragments in a matrix-poor crystal tuff. It rarely occurs in contact with sphalerite and galena but where it does there is commonly a bluish (reaction?) rim developed.

Pyrite inclusions are common in all non-sulphide minerals (crystals as well as groundmass). The largest inclusions are found in quartz grains. Pyrite is also not restricted to one particular rock type and occurs ubiquitously in brecciated and unbrecciated massive and banded crystal tuff (both fragments and matrix), lapilli tuff, agglomerate and massive and banded rhyolite; although it appears to concentrate preferentially in the massive rhyolite.

iii. Metal Distribution in the Subsurface (Drill core)

The subsurface distribution of the deposit is based entirely on assay data obtained from Amoco Canada Petroleum Ltd. and Lac Minerals Ltd. drill logs. These data were used to construct cross-sections A to D (Figures 13-16) across the deposit into the hanging wall and footwall rocks to identify its shape, the relationship between mineralisation and brecciation at depth as well as any relationship between Pb, Zn and Ag (and to a lesser extent Cu and Au). Zinc ratios (100*Zn/(Zn+Pb) after Huston and Large (1987) and the correlation coefficients between Pb and Zn, Pb and Ag, and Zn and Ag were calculated for the footwall, hanging wall and the main deposit. Of the 47 diamond drill holes drilled on the property the assay data from 22 holes cutting the deposit and peripheral rocks were used to determine these values.

In considering the average distribution of Pb, Zn, Ag, Au, Cu and Pb+Zn along cross-sections C and A the following observations can be made. Firstly, when using all of the available assay data for the holes along section C (Figure 19a) there is a southerly increase in Pb, Zn and Ag in the footwall from DDH #21 toward the deposit in DDH's LCO-8 and #26. Secondly, within the deposit, there is a sharp drop in the Ag values accompanied by a lesser decrease in Pb and Zn from LCO-8 to DDH #6, followed by a regular increase in Pb, Zn and Ag toward the centre of the deposit with a corresponding decrease to the hanging wall. Although the highest average Ag values (6.5g/t) along this section line occur in DDH LCO-3, in the hanging wall lapilli tuff unit, it does not represent elevated Ag in the hanging wall due the low number of assayed intervals (10) in this hole. This drop in Ag is also noticeable in section A (Figure 19a) since the silver values drop from 3.5 g/t in DDH #25 to ≈1.8g/t in DDH #6. Thirdly, through the centre of the deposit there is a steady increase in Ag values, although there is no corresponding increase

Plate 6

Note: These are photomicrographs in plane-polarised incident light

A: Sphalerite being cut by and replaced by secondary galena along grain boundaries.

B: Unusual replacement of sphalerite (S) by galena (G) at the margin of a veinlet cutting a massive crystal tuff fragment.

C: Typical replacement of sphalerite (S) by galena (G) at the terminations of sulphide veinlets.

D: Typical pyrite (P) occurring as inclusions in galena (G) and sphalerite (S). Note the abundance of pyrite in the gangue along the contact with the sulphides.

E: Unusual texture of pyrite space filling between massive crystal tuff breccia fragments in a matrix-poor breccia.

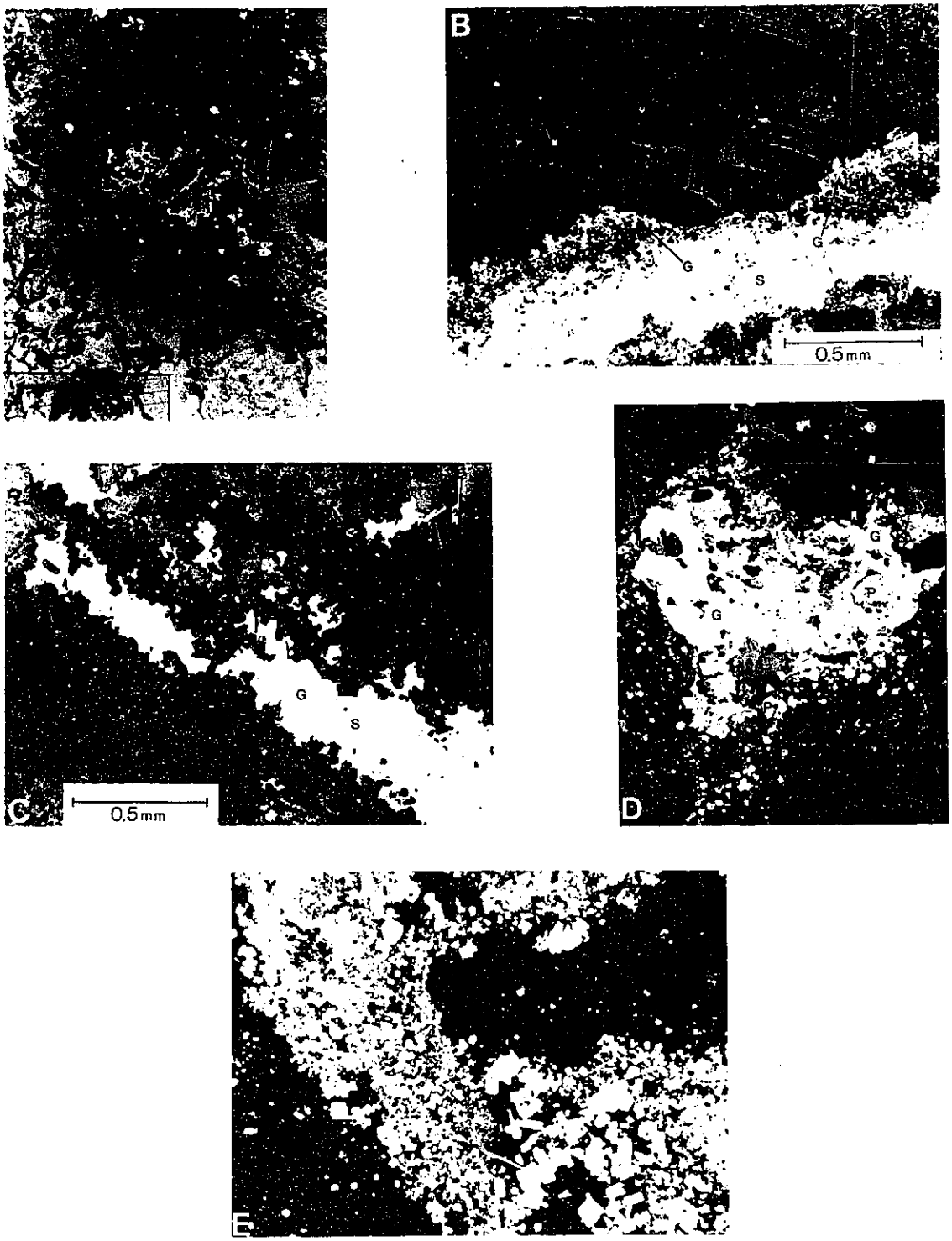
B
G
G
S
0.5mm
G
S
0.5mm
G
P
G
D
E

Figure 19a: Graphical depiction of the variation in average Pb, Zn, Ag, Au and Cu for all the drill hole data along sections A and C. Note that more holes are represented here than in Figures 13-16 to present a more complete representation of the variation in metal values across the deposit.

North–South variation in average Pb, Zn, Ag and Au

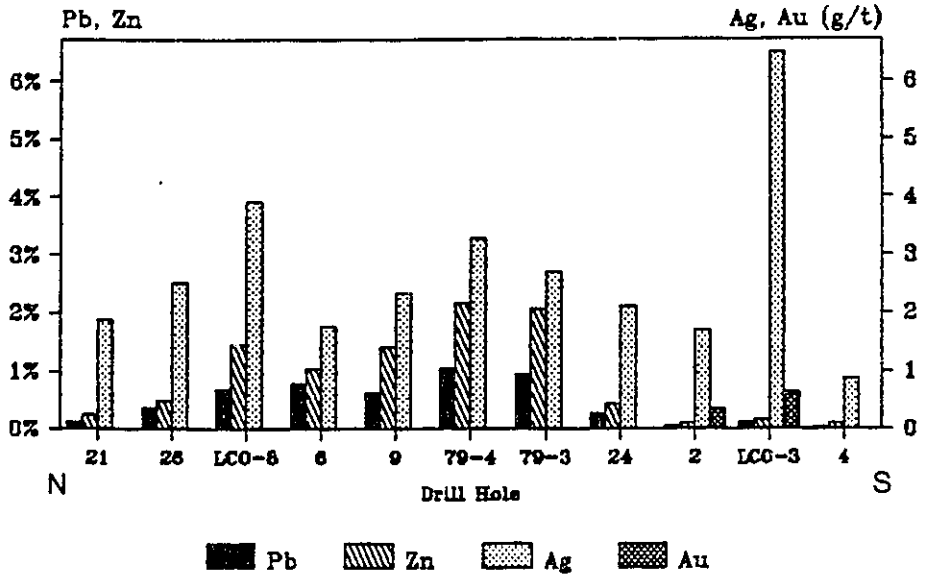

East–West variation in average Pb, Zn, Ag, Au & Cu

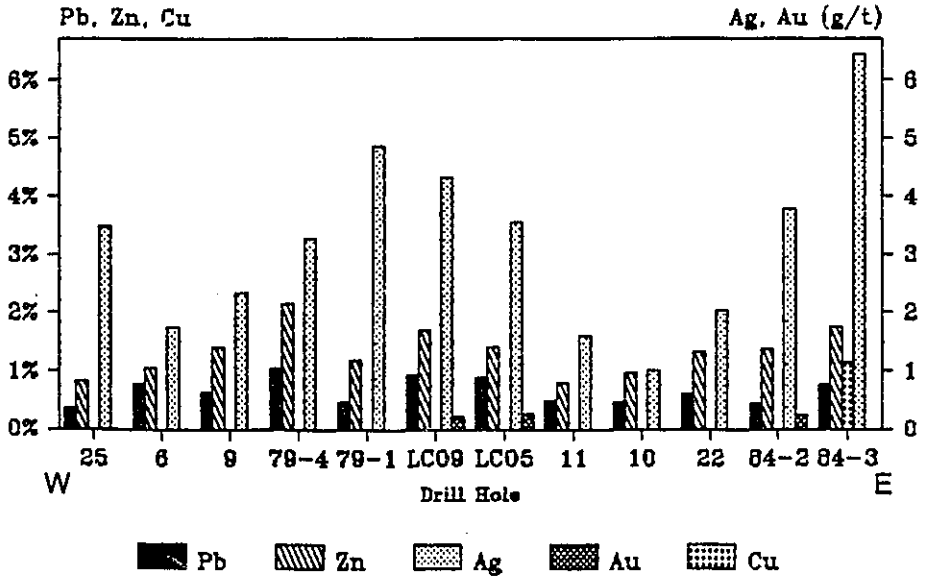

in Pb and Zn as is observed in section C. Like section C, in section A there is also a drop in Ag toward the periphery of the deposit, followed by a secondary increase in the footwall rocks.

The overall low proportion in metal assay values in these plots (Figure 19a) is due in part to the fact that a large percentage of the data consists of Pb+Zn values less than 2%. In order to offset this effect, a second set of plots was constructed using only the higher grade peaks for the holes along the section lines. Both standard assay values and mining widths (assay value * assayed interval) were used to confirm the reliability of the zoning discussed above.

The most significant difference between the two sets of data is that in the modified section C (Figure 19b), there is not as sharp a drop in Ag between LCO-8 and DDH #6 as previously seen and two zones of elevated Ag values are clearly apparent, one surrounding LCO-8 and the other between DDH #9 and DDH 79-3. What is also visible here that was not discernible in Figure 19a is the sharp drop in metal values between the deposit and the hanging wall and while high silver values exist in some of the holes, Pb and Zn values are commonly less than 1%.

The modified section A (Figure 19b) clearly does not show the drop in Ag between DDH #25 and DDH #6 as the Pb, Zn and Ag data are relatively constant (with minor fluctuations) along the entire section. Only one zone of elevated Ag occurs along this section, between DDH #9 and DDH LCO-5 and is correlatable with a similar zone in section C. This zone differs in that it is not accompanied by elevated Pb+Zn values. Another difference between the original and modified section A is that there is not the noticeable drop in metal values toward the footwall as the values in DDH's LCO-84-2 and LCO-84-3 are relatively consistent with those in the deposit.

1. Footwall

The footwall rocks are represented by the interlayered siltstone and pyroclastic rocks (units B1 to B4) and the lower part of unit C. These rocks are massive with only local brecciation occurring at depth (e.g., DDH LCO-84-5). They are poorly mineralised (Appendix 2a) and contain an average of 0.05% Pb, 0.1% Zn, 2.1g/t Ag, 0.006% Cu and 0.5g/t Au. Despite their low grade these rocks show some interesting trends in sulphide distribution. Firstly, in section C (Figure 19a) there is an increase in the average silver content (and to a lesser extent Pb+Zn) of the footwall rocks as the deposit is approached; and secondly, a similar increase in section A (Figure 19a) is also present where DDH LCO-84-3 contains the highest average Ag and Cu values. These elevated Ag, Cu and Au values may represent extensions to the deposit at depth since Crevier (1984) reports an increased abundance of chalcopyrite in the eastern part of the property (e.g., footwall rocks).

Within the footwall rocks there is a better correlation between Zn and Ag (Figure 20a), (0.86), than that for Pb and Ag (0.78). Similarly, there is also an excellent correlation between Pb and Zn (0.81) a fact supported by the sulphide petrology. The zinc ratio for the footwall rocks (Figure 21a) is similar to that for the main deposit in that it has a mean value of 66.25 with a mode of

Figure 19b: Graphical depiction of the variation in average Pb, Zn, Ag, Au and Cu for selected drill hole data along sections A and C. Data were selected to emphasize the higher Pb, Zn and Ag values.

North–South variation in average Pb, Zn, Ag & Au

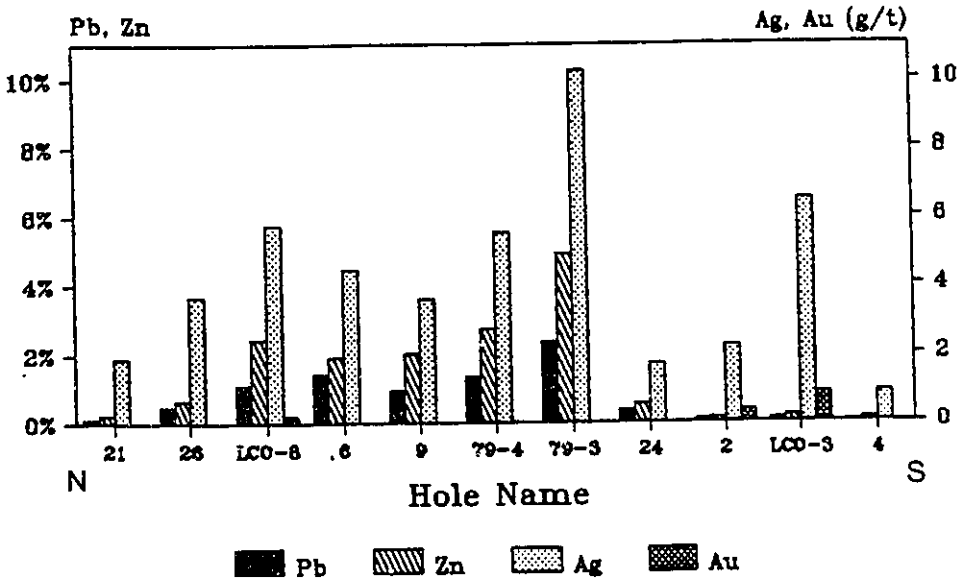

East–West variation in average Pb, Zn, Cu, Au & Ag

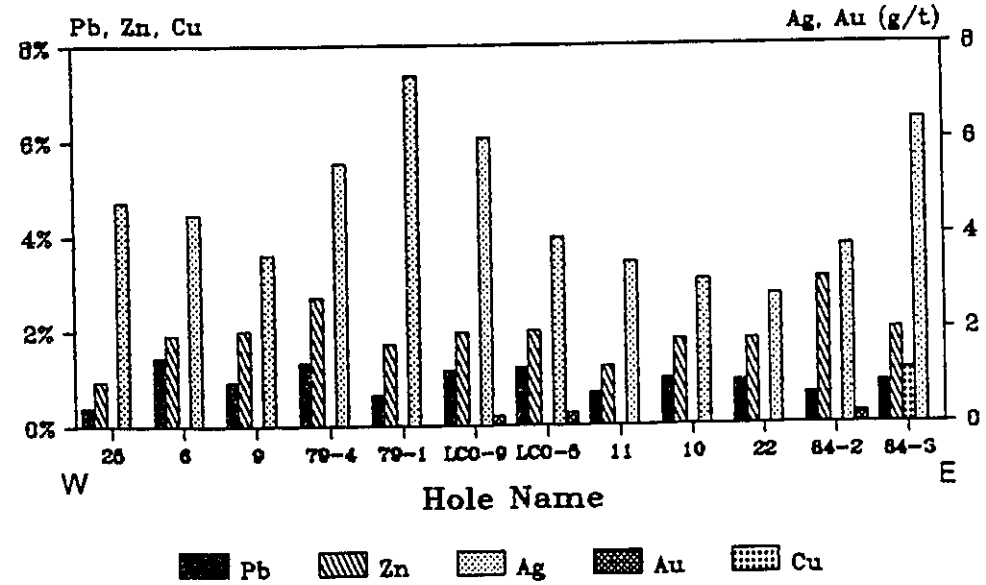

66.67 and a low standard deviation of 13.8.

2. Main Deposit

The main deposit (as exposed in the Central Trench) appears [Figures 22,23 (back pocket)], to have an irregular saddle or elliptical shape underground that extends east from approximately DDH #25 to LCO-84-2 at which point the grade of mineralisation decreases to less than 1% Pb+Zn. The lack of assay data west of DDH #25 precludes any definition of the sulphide body beyond this point. The deposit extends south from approximately DDH's #7 and #26 to DDH #8 where the Pb+Zn values diminish to less than 1% and unlikely extends any farther to the north since Pb and Zn values in DDH #21 are below 0.6% and the Ag content is below 1.0 g/t.

The deposit [Figure 22a,b; 23a,b (back pocket)] consists of an outer low grade shell of less than 4% Pb+Zn that contains numerous higher grade pockets of between 4 to 8% Pb+Zn. The central part of the deposit consists of a series of unevenly distributed zones of high grade mineralisation that vary between 8% and 18% Pb+Zn. One peak in this zone (DDH #10) contains approximately 20% Pb+Zn. Other high grade zones in the upper part of the deposit occur in DDH's 79-4 and #6 where values vary from 6 to 14% Pb+Zn. Medium-grade mineralisation of 4 to 8% Pb+Zn occur in the west end of the deposit in DDH's #6 and 9 and in the upper section of DDH LCO-5 (see Figure 22a,b). Underlying the main deposit are two thin tabular, westerly dipping minor orebodies characterised by low Pb and Zn values but unusually high Ag values. They consist roughly of 2 to 4% (Pb+Zn); 14-20g/t (Ag) and 4 to 5% (Pb+Zn); 6-8g/t (Ag) respectively.

The distribution of Pb and Zn mineralisation at depth is, in general, most closely associated with the brecciated zones, seen by comparing the variation in Pb+Zn [Figures 22a,b; 23a (back pocket)] in DDH's LCO-5,8,9 and #25 with the distribution of breccia. An excellent example of this occurs in DDH LCO-8 at approximately 195m where a 2m thick breccia zone has Pb and Zn values elevated well above those in the overlying and underlying unbrecciated wallrock. However, not all the highest values are associated with zones of breccia, since in DDH LCO-5 (Figure 24) the high peaks of 10 to 18% and 12% (Pb+Zn) occurring approximately at 54.5m and 150m respectively occur in unbrecciated, silicified lapilli tuff and banded crystal tuff. This is in contrast to what is observed in the surface, but clearly demonstrates the direct relationship between silicification and the sulphide mineralisation (discussed below). Zinc and lead show a fairly strong relationship as demonstrated by the regression curve in Figure 20b and by the correlation coefficient of 0.75.

High silver values most commonly correlate with high Pb and Zn values [Figures 22c, 23b (back pocket)], although this is not always the case, as extremely high Ag (e.g., 20.5g/t from 213.0 to 214.5m) can occur where there is a much higher Pb than Zn (commonly 2 to 3 times greater). More commonly, high Ag peaks appear to be associated with zones where there is a higher proportion of Zn to Pb (e.g., DDH LCO-5: 96.0-97.5m, Pb: 2.79%, Zn: 5.05%, Ag: 9.0g/t; LCO-5: 205.9-207.0m, Pb: 1.22%, Zn,

1.55%, Ag: 15.0g/t and DDH 79-3, Figure 25). Although Crevier (1984) reported that the Ag at Mount Costigan is most commonly found as argentiferous galena analysis of the relationship, in drill holes cutting the main deposit, between Pb and Zn peaks and high Ag values indicates that the Ag is not associated solely with the Pb. This is best observed in the similarity of the weak correlation between Pb and Ag (0.45) (Figure 20c) and Zn and Ag (0.33) (Figure 20d) and the fact that high Ag values are commonly associated with high Zn levels. Thus, despite the good correlation between Pb and Zn (0.75) it is possible that the high Ag values are associated with another sulphide phase.

Graphical analysis of the drill hole data from Mount Costigan shows that the deposit has a mean zinc ratio (Figure 21b) of 63.24 with a low standard deviation of 15.29; a plot of %Zn vs. zinc ratio also reflects this trend. Although Mount Costigan is not a massive sulphide deposit the zinc ratio and Pb vs. Zn plots exhibit similarities to the Phanerozoic deposits discussed by Huston and Large (1987), which commonly have zinc ratios ranging between 64 and 77 and standard deviations of less than 15. Huston and Large (1987) observed that for massive sulphide deposits a nearly constant zinc ratio is an indication that the metals in the deposit were precipitated from a saturated solution and transported dominantly as chloride complexes. While no salinity or temperature data are currently available for Mount Costigan, zinc ratios representing all available assay data for sections C and A (Figure 26a) are largely constant, although minor fluctuations exist in section C. Minor oscillations are also visible when using the modified data set (Figure 26b), although there is slightly more fluctuation in the zinc ratio along section A than previously observed. This would suggest that the temperature and salinity of the hydrothermal fluids responsible for precipitating metals at Mount Costigan were relatively constant. Despite the dissimilarities between Mount Costigan and massive sulphide deposits, provided the above zinc ratio data can be compared then, by considering Figure 11 of Huston and Large (1987), the temperature of the hydrothermal fluids responsible for sulphide precipitation at Mount Costigan should fall, approximately, between 200°C and 250°C.

3. Hanging wall

The hanging wall rocks consist of the upper part of unit C as well as units D to H. As with the footwall rocks the hanging wall rocks are locally brecciated and contain fine-grained, disseminated mineralisation. No assays were reported from DDH's LCO-1 to LCO-4 but Pb+Zn values in DDH's #1 to #4 are generally less than 1% indicating that here there is disseminated mineralisation peripheral to the deposit. There is a similarity to the footwall rocks in that there is an apparent increase in the Ag values as the deposit is approached from the west along section A (Figure 26a), although the corresponding increase in Ag outside the deposit along section C (DDH LCO-3, Figure 26a) is due to several high assay values in a low number of analyses. In the hanging wall there is also a much better correlation between Pb and Zn (Figure 20e) than in the footwall as the correlation coefficient is 0.59, compared to

Figure 20a: Regression analysis of Pb and Zn for footwall drill holes. Solid line represents line of best fit, dashed lines represent 99% confidence interval; r=correlation coefficient, m=slope, b=y-intercept. N=269; r=0.72; m=1.59; b=0.07

Figure 20b: Regression analysis of Pb and Zn for main deposit drill holes. N=1696; r=0.81; m=1.52; b=0.24

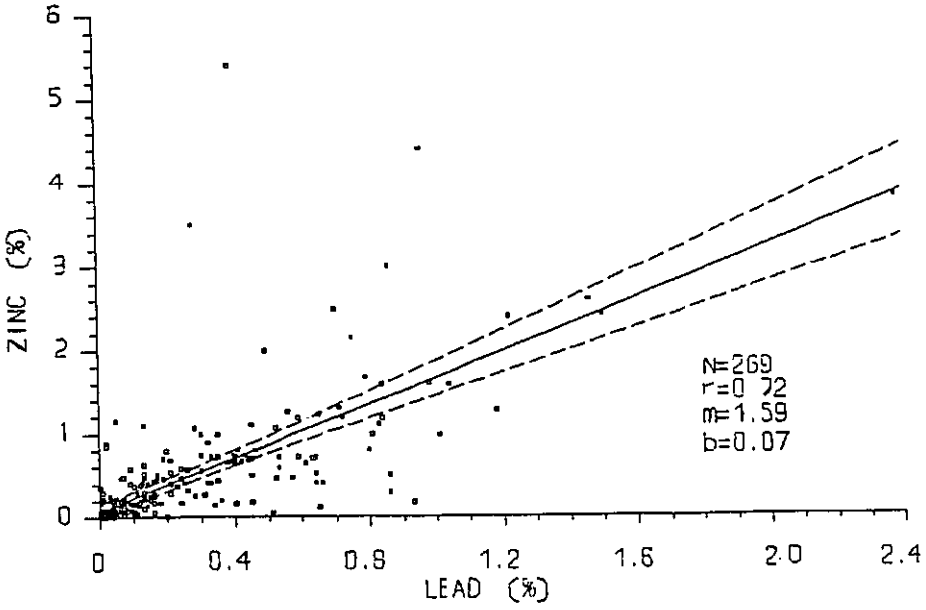
ZINC (%)
LEAD (%)
N=269
r=0.72
m=1.59
b=0.07
0
1
2
3
4
5
6
0.4
0.8
1.2
1.6
2.0
2.4

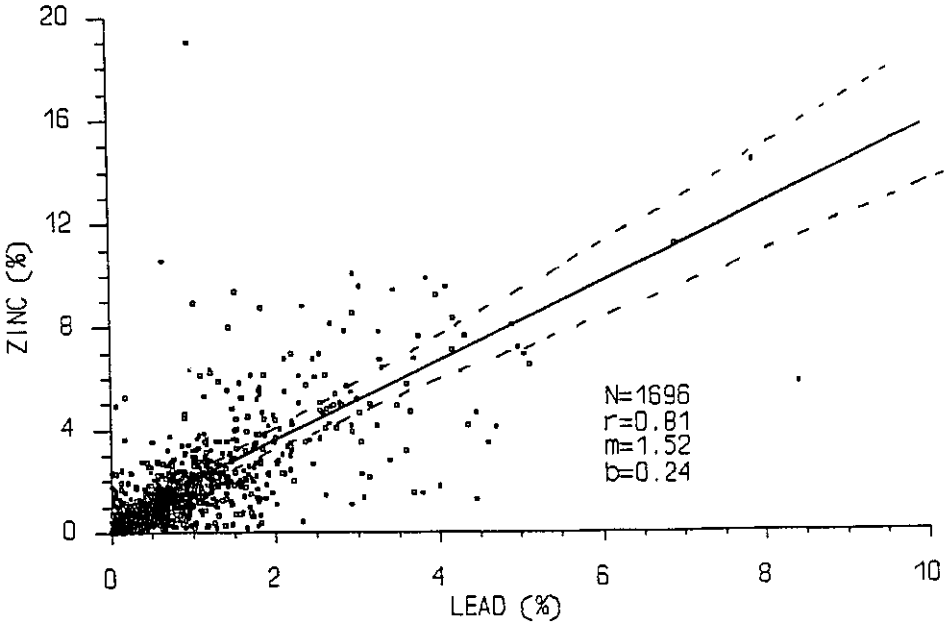
ZINC (%)
LEAD (%)
N=1696
r=0.81
m=1.52
b=0.24
0
4
8
12
16
20
2
6
10

Figure 20c: Regression analysis of Pb and Ag for main deposit drill holes. N=1696; r=0.75; m=2.45; b=0.53

Figure 20d: Regression analysis of Zn and Ag for main deposit drill holes. N=1696; r=0.33; m=1.08; b=0.81.

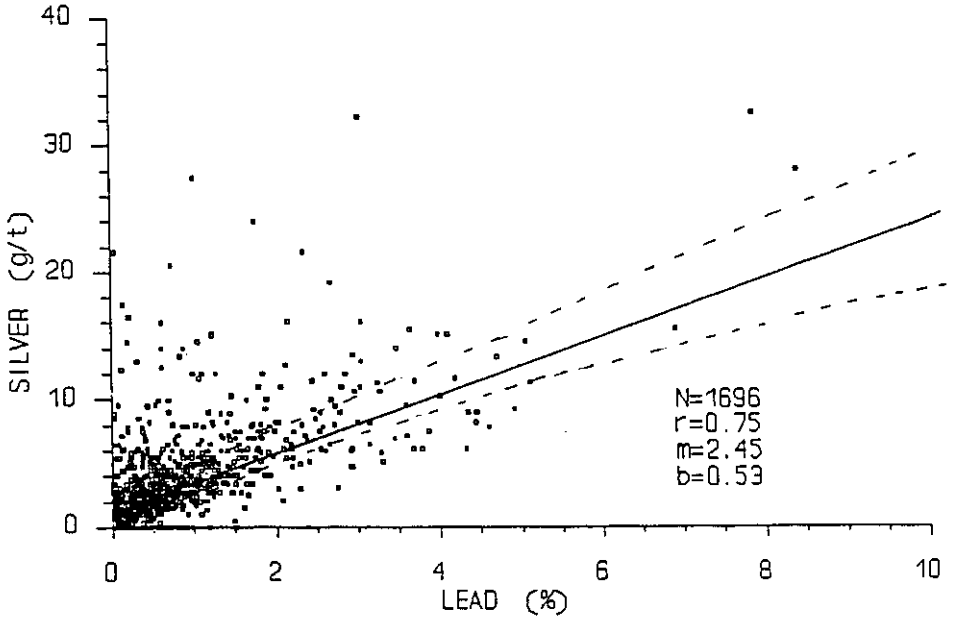
SILVER (g/t)
LEAD (%)
N=1696
r=0.75
m=2.45
b=0.53

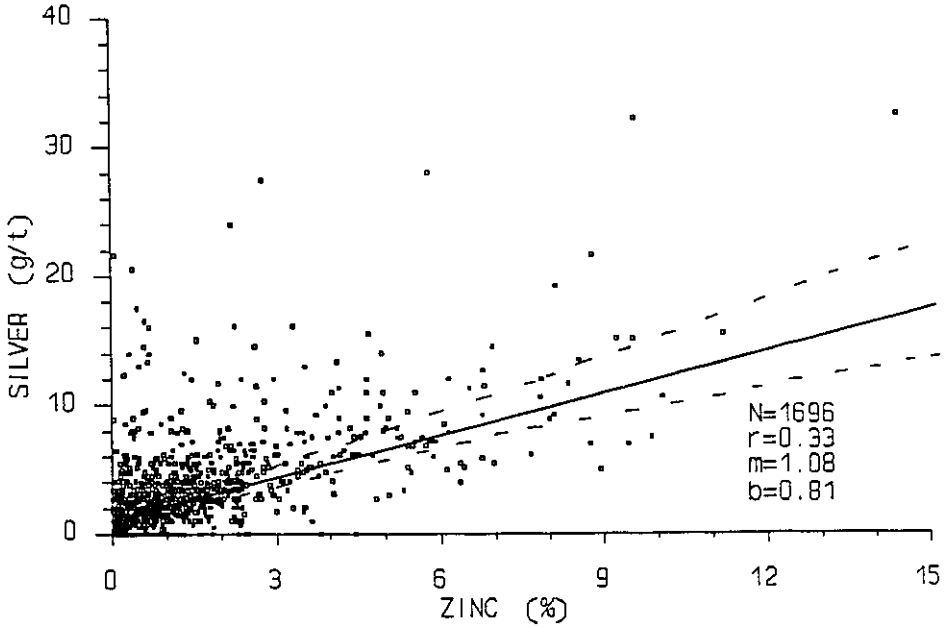
SILVER (g/t)
ZINC (%)
N=1696
r=0.33
m=1.08
b=0.81

Figure 20e: Regression analysis of Pb and Zn for hanging wall drill holes. N=171; r=0.88; m=1.52; b=0.03

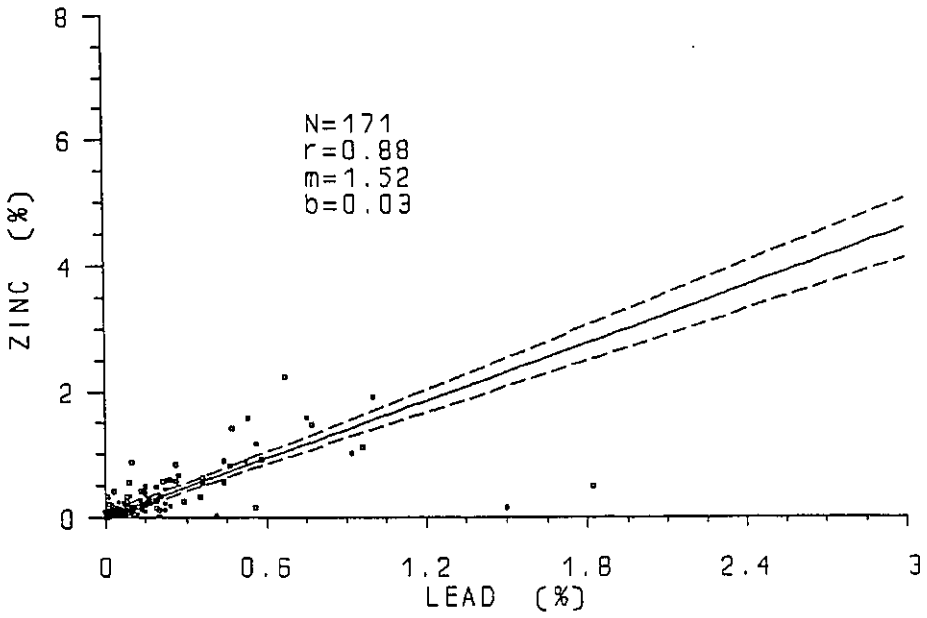
N=171
r=0.88
m=1.52
b=0.03
ZINC (%)
LEAD (%)
0
2
4
6
8
0
0.6
1.2
1.8
2.4
3

Figure 21a: Plot of Zinc ratio for footwall drill holes. N=269; Mean=65.43; S.D.=16.89

Figure 21b: Plot of Zinc ratio for the main deposit. N=1696; Mean=63.24; S.D.=15.29

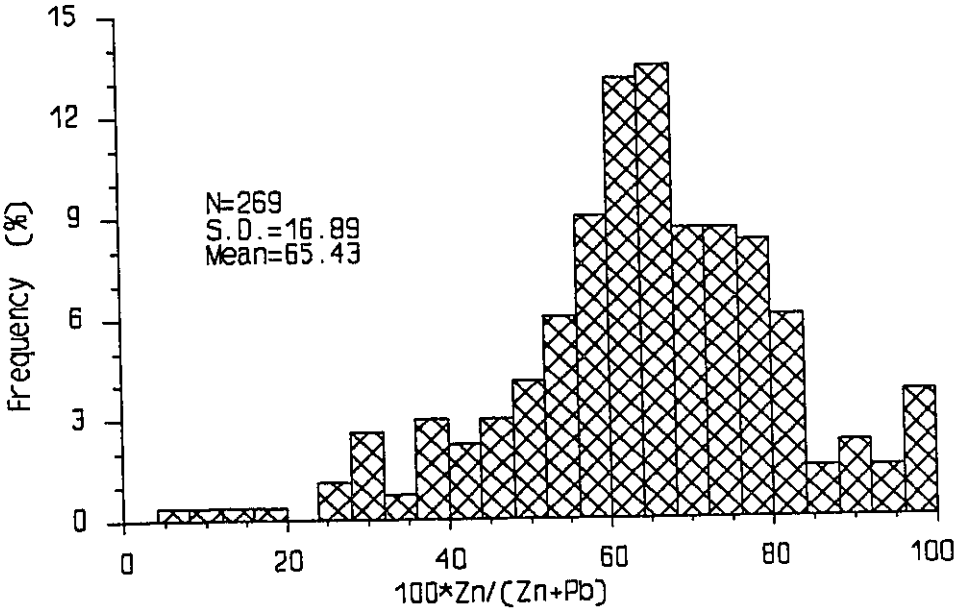
15
12
9
6
3
0
Frequency (%)
N=269
S.D.=16.89
Mean=65.43
0
20
40
60
80
100
100*Zn/(Zn+Pb)

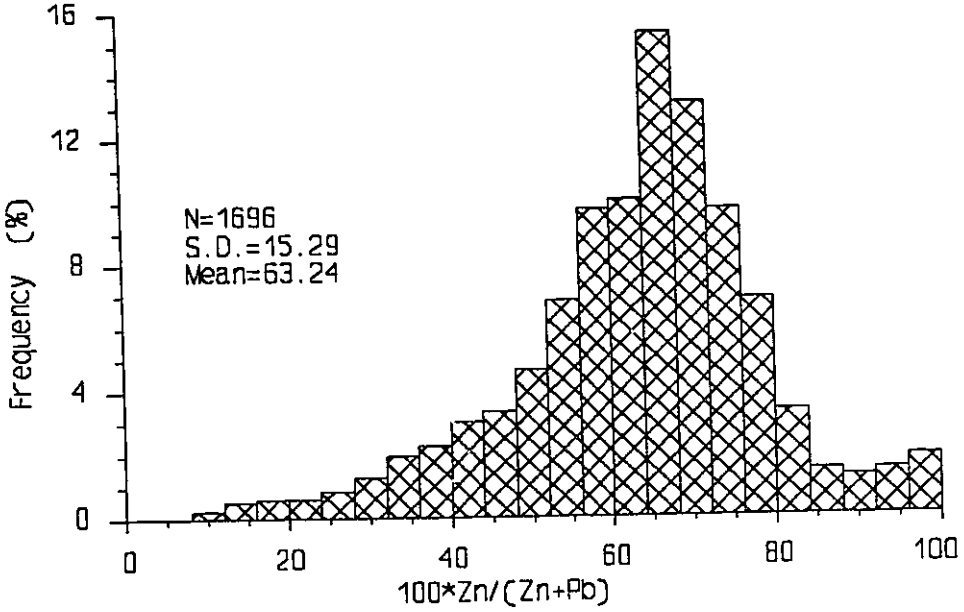
16
12
8
4
0
Frequency (%)
N=1696
S.D.=15.29
Mean=63.24
0
20
40
60
80
100
100*Zn/(Zn+Pb)

Figure 21c: Plot of Zinc ratio for hanging wall drill holes. N=171; Mean=65.07; S.D.=17.61

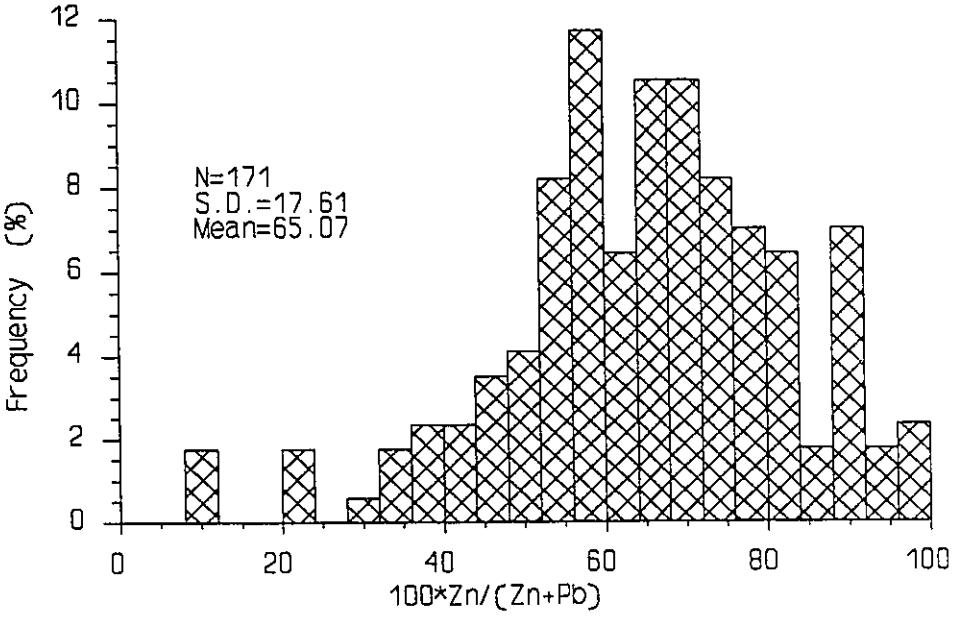
N=171
S.D.=17.61
Mean=65.07
Frequency (%)
0
2
4
6
8
10
12
0
20
40
60
80
100
100*Zn/(Zn+Pb)

0.81. An interesting trend is the similarity in the correlation between Pb and Ag and Zn and Ag (0.43 and 0.44 respectively) which reflects the association of zinc with high Ag observed in the Central Trench (Figures 22b,c).

In summary, based on the relative similarity of the zinc ratio data in Figure 26, the deposit is not markedly zoned. However, the deposit does show a variation in metal grades, that consists of a central, main irregular shaped body containing numerous high-grade (up to 20% Pb+Zn, 32g/t Ag, 0.86g/t Au) pockets enveloped by a low to medium-grade shell (2-8% Pb+Zn, 2-10g/t Ag). This variation in grade extends partially into the host rocks [Figure 27a,b (back pocket)] where there is locally elevated Ag (11g/t) and Au (1.88g/t) in the hanging wall (DDH LCO-3). Elevated Ag (10.29g/t) and Pb+Zn (5.36%) and Cu (1.15%) also occurs in the footwall rocks (DDH LCO-84-3) indicating that there is local concentrations of Cu in the east and Au to the west of the deposit, both of which are accompanied by higher Ag. Underlying the main deposit are two smaller minor orebodies that appear to be concordant with the regional stratigraphy and contain high Ag (up to 20g/t) (Figure 27c, back pocket) but relatively low corresponding Pb and Zn (2 to 5%).

f. Alteration

Alteration at Mt. Costigan has occurred in at least three phases in the following order: 1. chlorite, 2. potassic and 3. silica. Chlorite is interpreted to be the initial alteration phase because it is commonly overprinted by the other phases. It is unclear, however, whether or not the chlorite is associated with the regional greenschist facies metamorphism or with the brecciation, since such areally extensive chlorite alteration outside of the property is rare (G.P. Watson, pers. comm.). Also, in the Central Trench and in boulder fields surrounding the trenched area, the freshest crystal and lapilli tuffs are usually moderately chloritised. Although hand sample staining for calcite and plagioclase produced negative results, rare calcite was observed in thin section.

Chlorite alteration occurs as interstitial chlorite in the spherulitic, flow-banded rhyolites of the South Trench, chloritisation of fine-grained groundmass K-feldspar and minor alteration of K-feldspar phenocrysts in the crystal and lapilli tuffs. The chloritised lapilli tuff in the South Trench (sub-unit #1) further indicates that, of the three types of alteration, chlorite is the initial phase, since it appears to be overprinted by the potassic and silica alteration. In the North Trench, chlorite alteration is relatively minor, but is best observed in sub-unit 2b, where chlorite-altered K-feldspar rich layers alternate with quartz-rich, K-feldspar poor layers. In the East Trench, chlorite is the dominant form of alteration and is clearly visible in massive and banded, brecciated and unbrecciated crystal tuffs. Fault-related chlorite alteration (Figure 9), unassociated with the more widespread chloritisation seen elsewhere on the property, is developed at the east end of the Central Trench.

In the Central Trench (Figure 9) chlorite is the dominant alteration mineral, and is expressed by the characteristic dark (nearly black) colour and the softness of the breccia fragments. Thin sections reveal

OVB - Overburden
LC - Lost Core
MLNG - Melange
BCT - Banded Crystal Tuff
MCT - Massive Crystal Tuff
LT - Lapilli Tuff
PLT - Polymictic Lapilli Tuff
BRHY - Flow-banded Rhyolite
MRHY - Massive Rhyolite
SRHY - Spherulitic Rhyolite
SBRHY - Spherulitic, Flow-banded Rhyolite
SL - Siltstone
SLTF - Silty Tuff
SLLT - Silty Lapilli Tuff
TFSL - Tuffaceous Siltstone

Note: The prefix "BX" denotes brecciated varieties of the above lithologies

Figure 22a: Pb assay values for the main deposit along section B. Note the presence of two lower grade minor mineralised zones underlying the main breccia that appear to correspond to the underlying siltstone dominated stratigraphy. Note also that the deposit consists of irregularly distributed mineralised zones of high, medium and low sulphide and that no distinct grade zoning is visible. Fine lines on the section represents areas of low-, medium- and high-grade mineralisation. The solid bars on DDH 79-4 represent narrow assay widths.

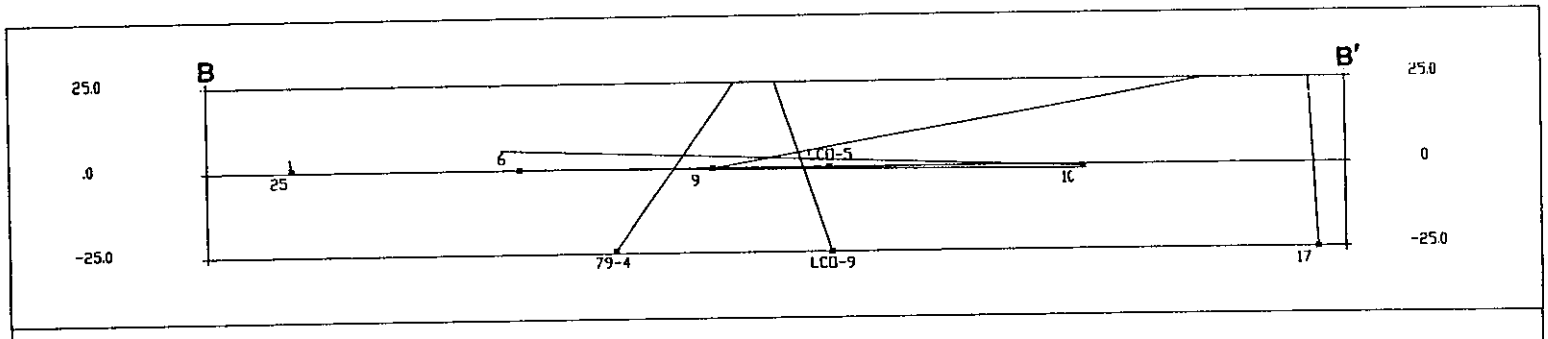
B
B'
25.0
0
-25.0
25
6
9
10
LCD-5
79-4
LCD-9
17

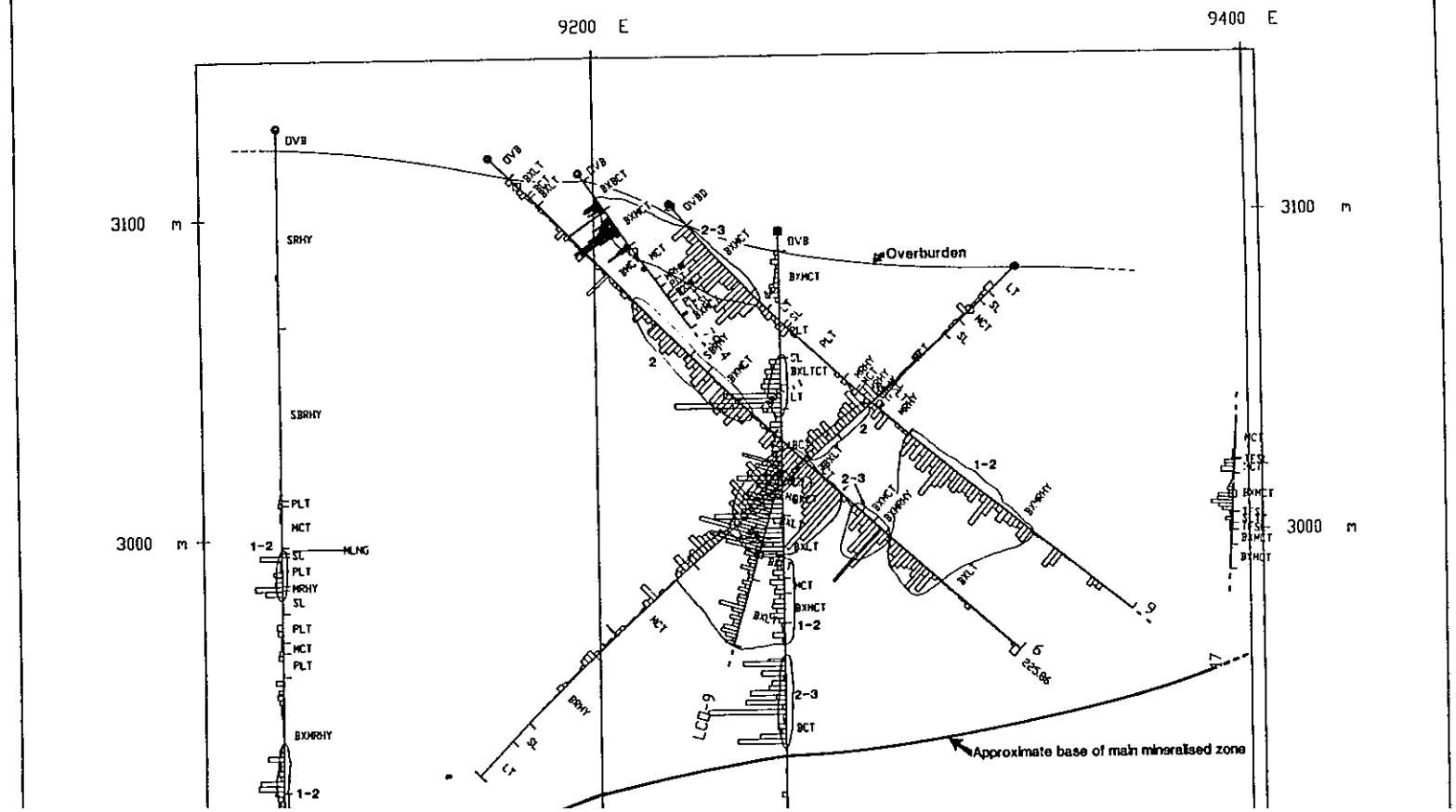
9200 E
9400 E
3100 m
3000 m
OVB
SRHY
SBRHY
PLT
MCT
SL
MRHY
BXHRHY
1-2
2-3
2
4
6
9
17
BXMCT
BXLT
BXLTCT
LT
NLNG
LCD-9
Overburden
Approximate base of main mineralised zone

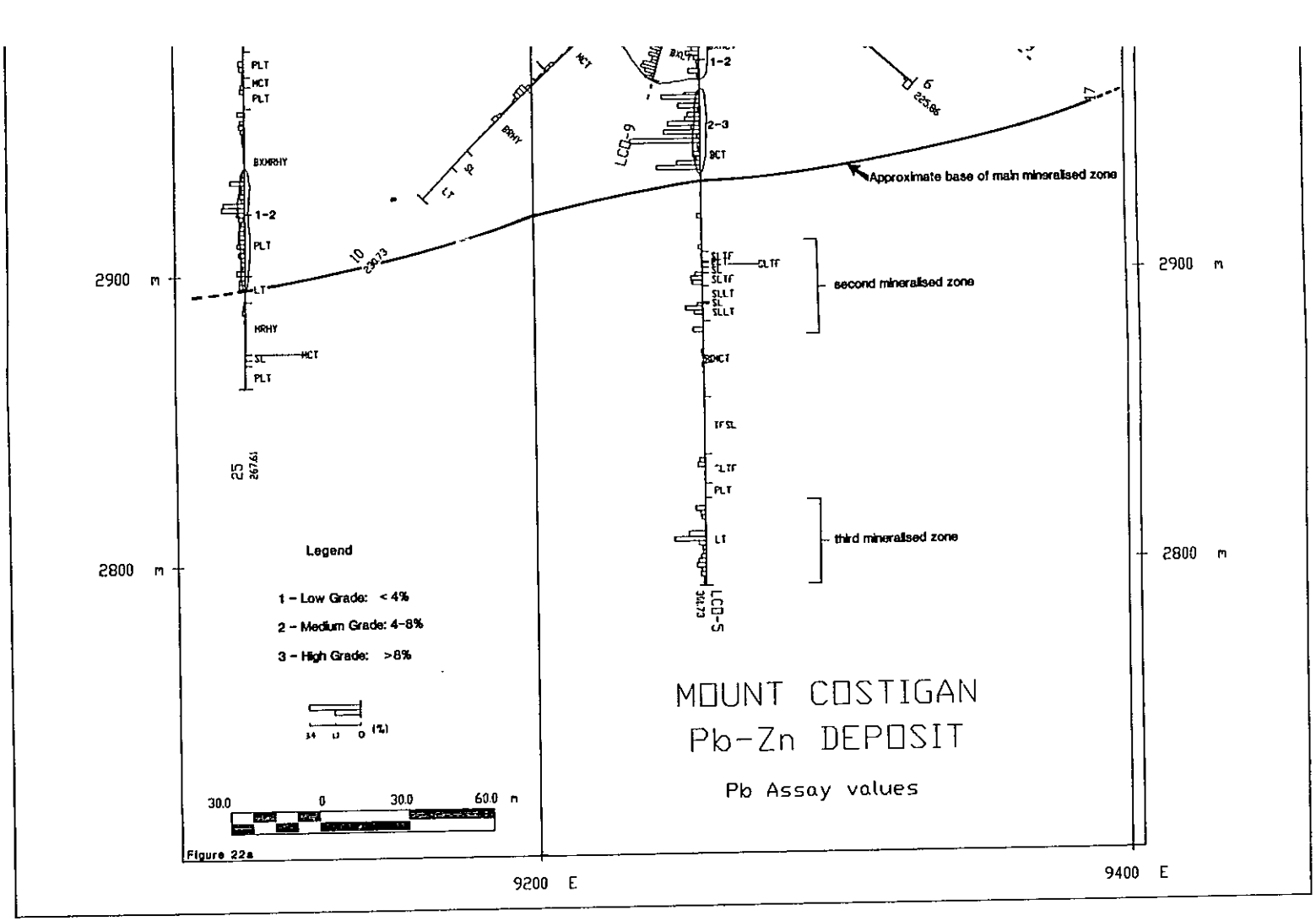
Approximate base of main mineralised zone
second mineralised zone
third mineralised zone
2900 m
2800 m
Legend
1 - Low Grade: < 4%
2 - Medium Grade: 4-8%
3 - High Grade: >8%
MOUNT COSTIGAN
Pb-Zn DEPOSIT
Pb Assay values
30.0 0 30.0 60.0 m
9200 E
9400 E

Figure 22a

OVB - Overburden
LC - Lost Core
MLNG - Melange
BCT - Banded Crystal Tuff
MCT - Massive Crystal Tuff
LT - Lapilli Tuff
PLT - Polymictic Lapilli Tuff
BRHY - Flow-banded Rhyolite
MRHY - Massive Rhyolite
SRHY - Spherulitic Rhyolite
SBRHY - Spherulitic, Flow-banded Rhyolite
SL - Siltstone
SLTF - Silty Tuff
SLLT - Silty Lapilli Tuff
TFSL - Tuffaceous Siltstone

Note: The prefix "BX" denotes brecciated varieties of the above lithologies

Figure 22b: Zn assay data for the main deposit along section B. Fine lines on the section represents areas of low-, medium- and high-grade mineralisation. The solid bars on DDH 79-4 represent narrow assay widths.

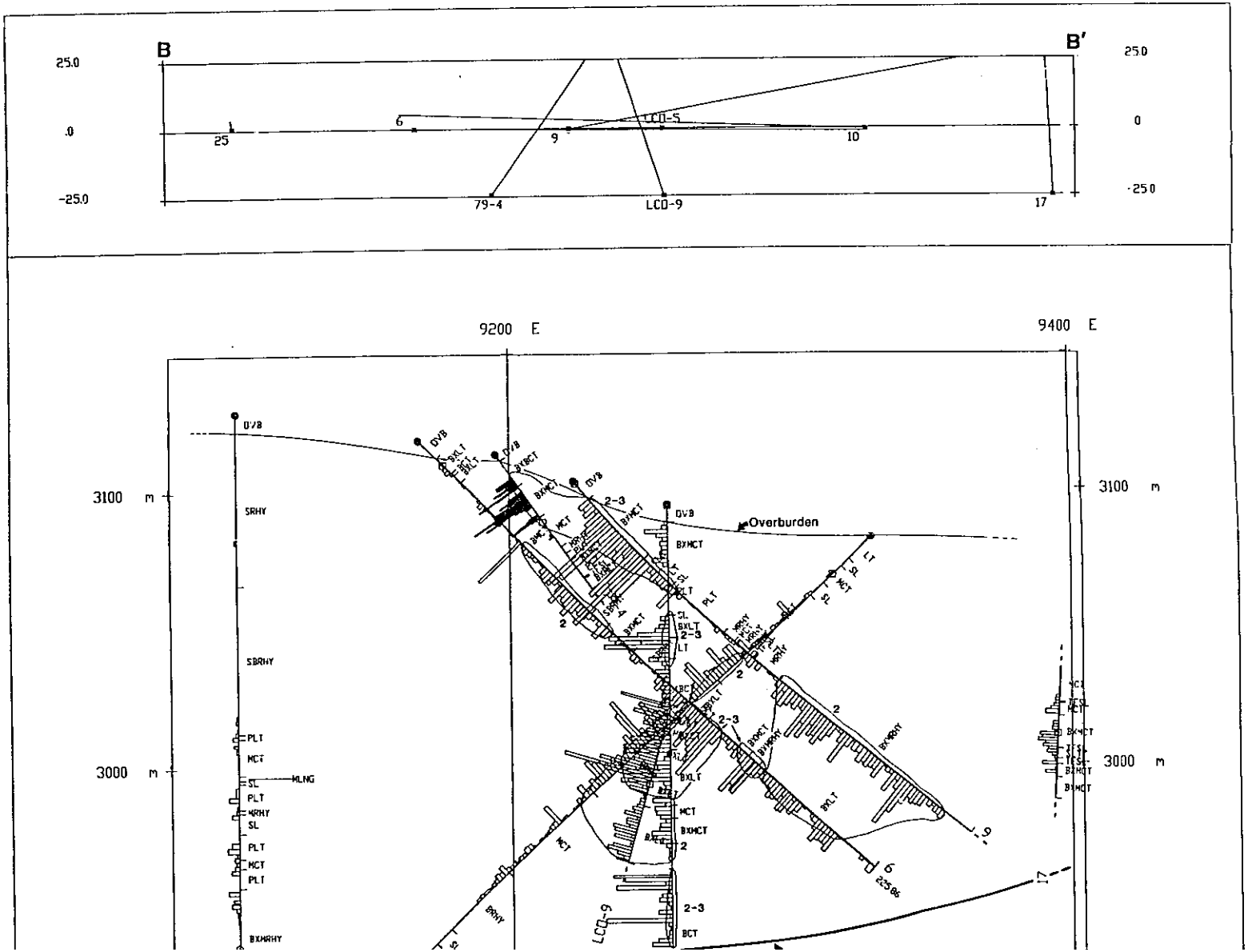
B
B'
25.0
.0
-25.0
25
6
9
LCD-5
10
79-4
LCD-9
17
9200 E
9400 E
3100 m
3000 m
Overburden
DVB
SRHY
SBRHY
PLT
MCT
SL
MLNG
BXMRHY
BXMCT
BXLT
BCT
LT
2-3
2
LCD-9

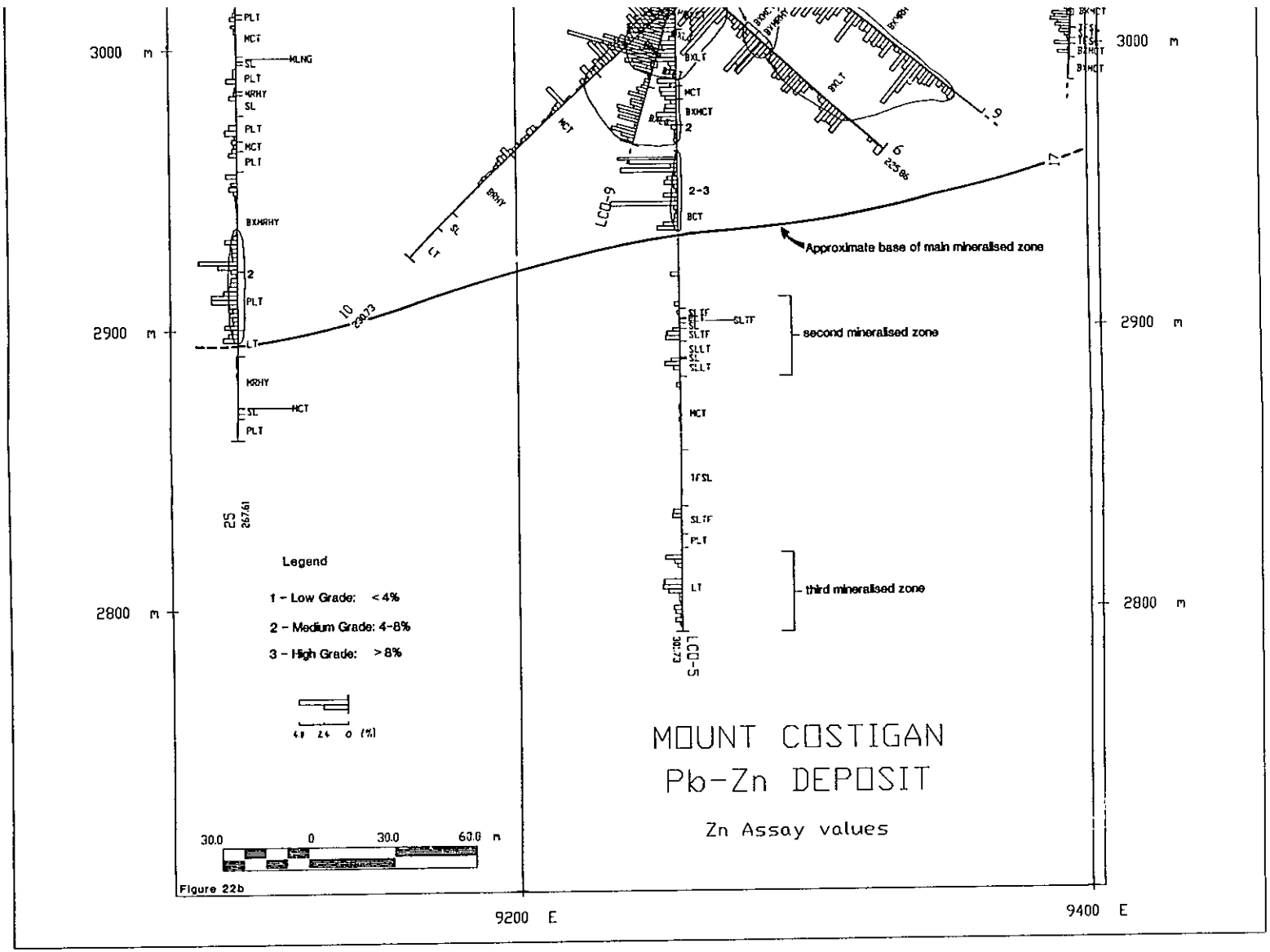
3000 m
2900 m
2800 m
9200 E
9400 E
Approximate base of main mineralised zone
second mineralised zone
third mineralised zone
Legend
1 – Low Grade: <4%
2 – Medium Grade: 4-8%
3 – High Grade: >8%
30.0 0 30.0 60.0 m
MOUNT COSTIGAN
Pb-Zn DEPOSIT
Zn Assay values

Figure 22b

OVB - Overburden
LC - Lost Core
MLNG - Melange
BCT - Banded Crystal Tuff
MCT - Massive Crystal Tuff
LT - Lapilli Tuff
PLT - Polymictic Lapilli Tuff
BRHY - Flow-banded Rhyolite
MRHY - Massive Rhyolite
SRHY - Spherulitic Rhyolite
SBRHY - Spherulitic, Flow-banded Rhyolite
SL - Siltstone
SLTF - Silty Tuff
SLLT - Silty Lapilli Tuff
TFSL - Tuffaceous Siltstone

Note: The prefix "BX" denotes brecciated varieties of the above lithologies

Figure 22c: Ag assay data for the main deposit along section B. Note that some of the highest Ag values are within the minor mineralised zones. Fine lines on the section represents areas of low-, medium- and high-grade mineralisation. The solid bars on DDH 79-4 represent narrow assay widths.

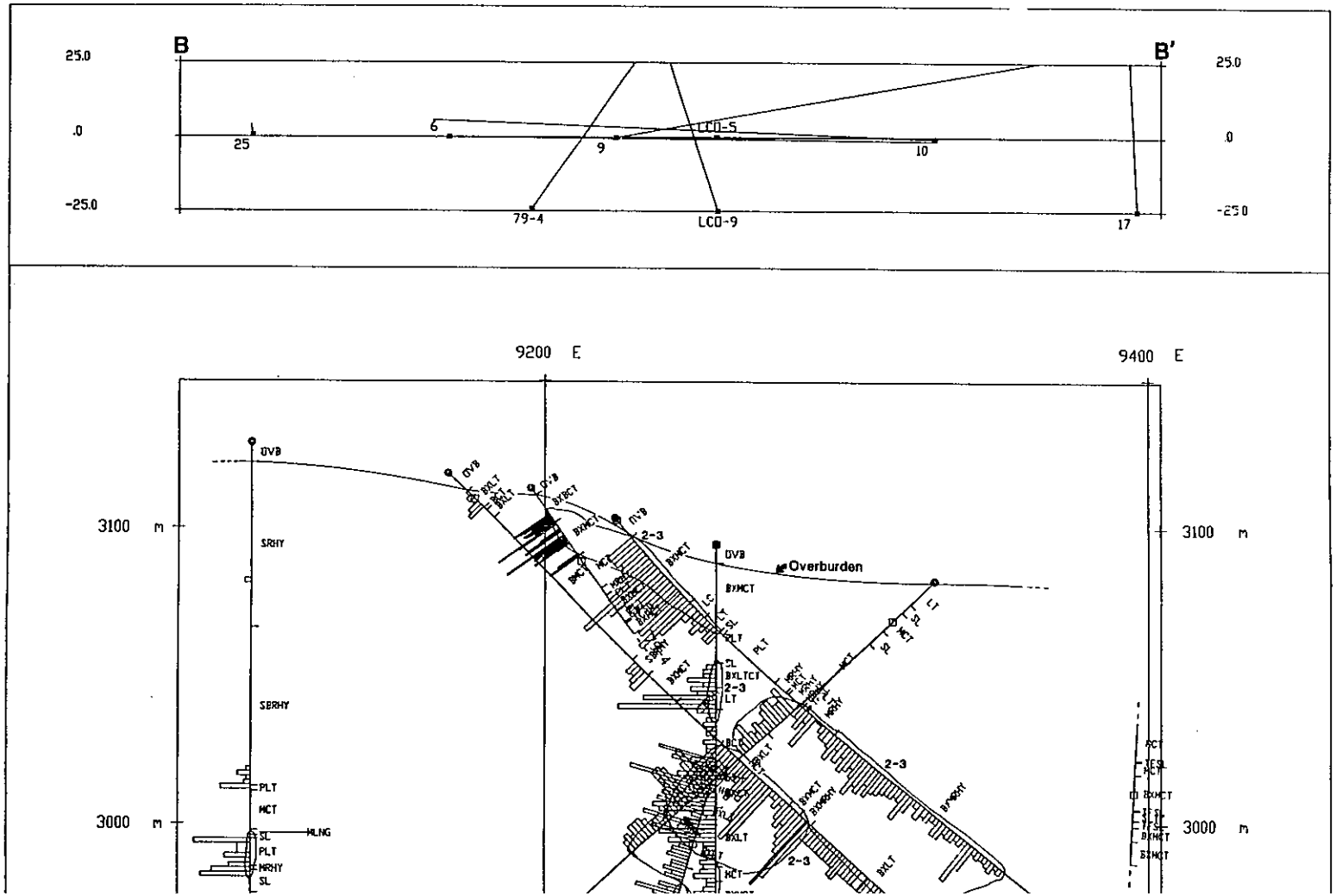
B
B'
25.0
.0
-25.0
6
25
9
LCO-5
10
79-4
LCO-9
17
9200 E
9400 E
3100 m
3000 m
OVB
Overburden
SRHY
SBRHY
PLT
MCT
SL
MRHY
2-3
LT
BXMCT
BXLT

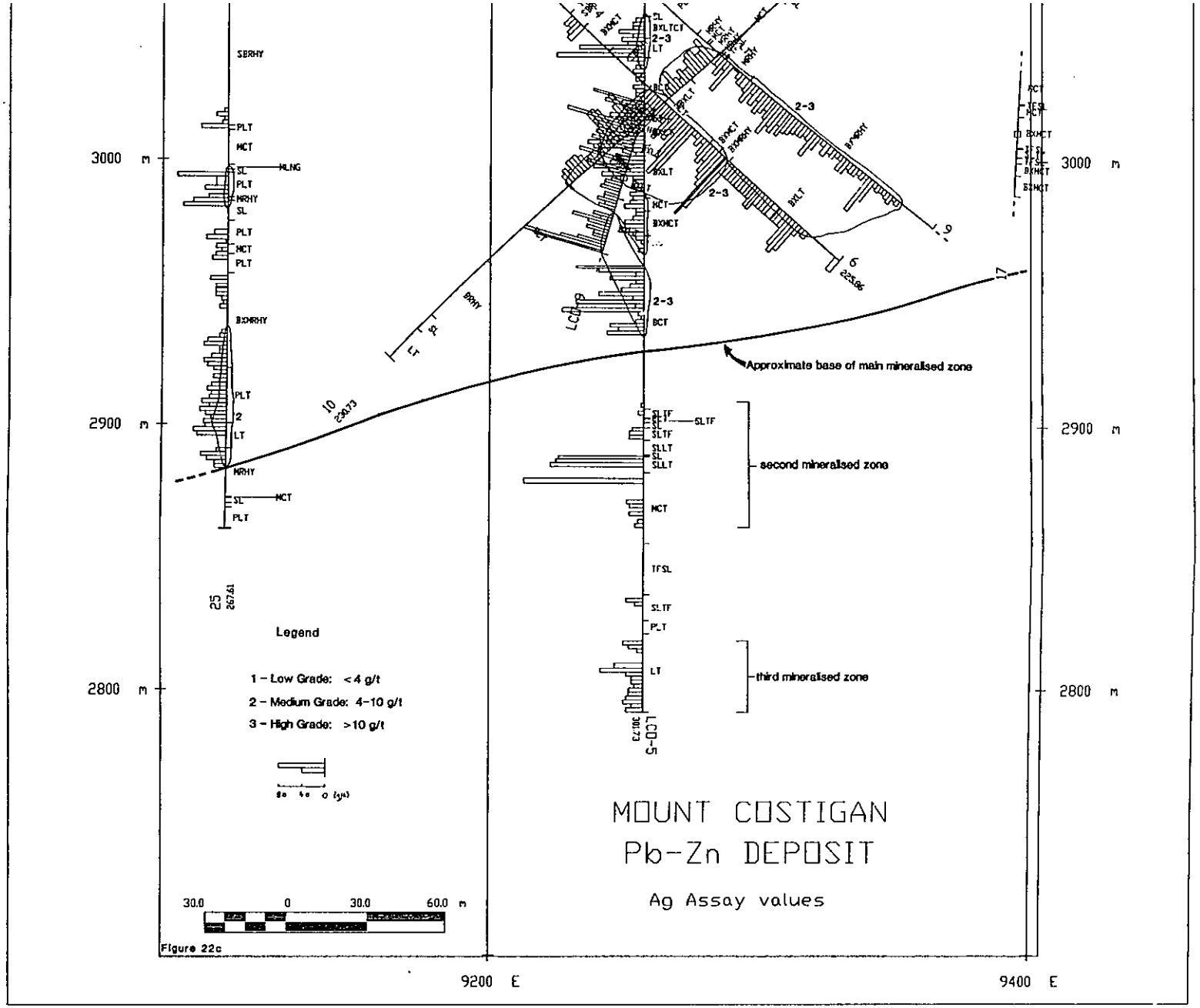
3000 m
2900 m
2800 m
Approximate base of main mineralised zone
second mineralised zone
third mineralised zone
Legend
1 – Low Grade: < 4 g/t
2 – Medium Grade: 4–10 g/t
3 – High Grade: >10 g/t
30.0 0 30.0 60.0 m
MOUNT COSTIGAN
Pb–Zn DEPOSIT
Ag Assay values
9200 E
9400 E

Figure 22c

Figure 24: Graphical representation of the variation in Pb and Zn values in DDH LCO-5. Note that, in general, the highest values are associated with zones of breccia. Note also that the highest Ag grades occur outside of the main mineralised zone in the second mineralised zone. Refer to Figure 16 for geology.

Pb, Zn & Ag values for DDH LCO-5

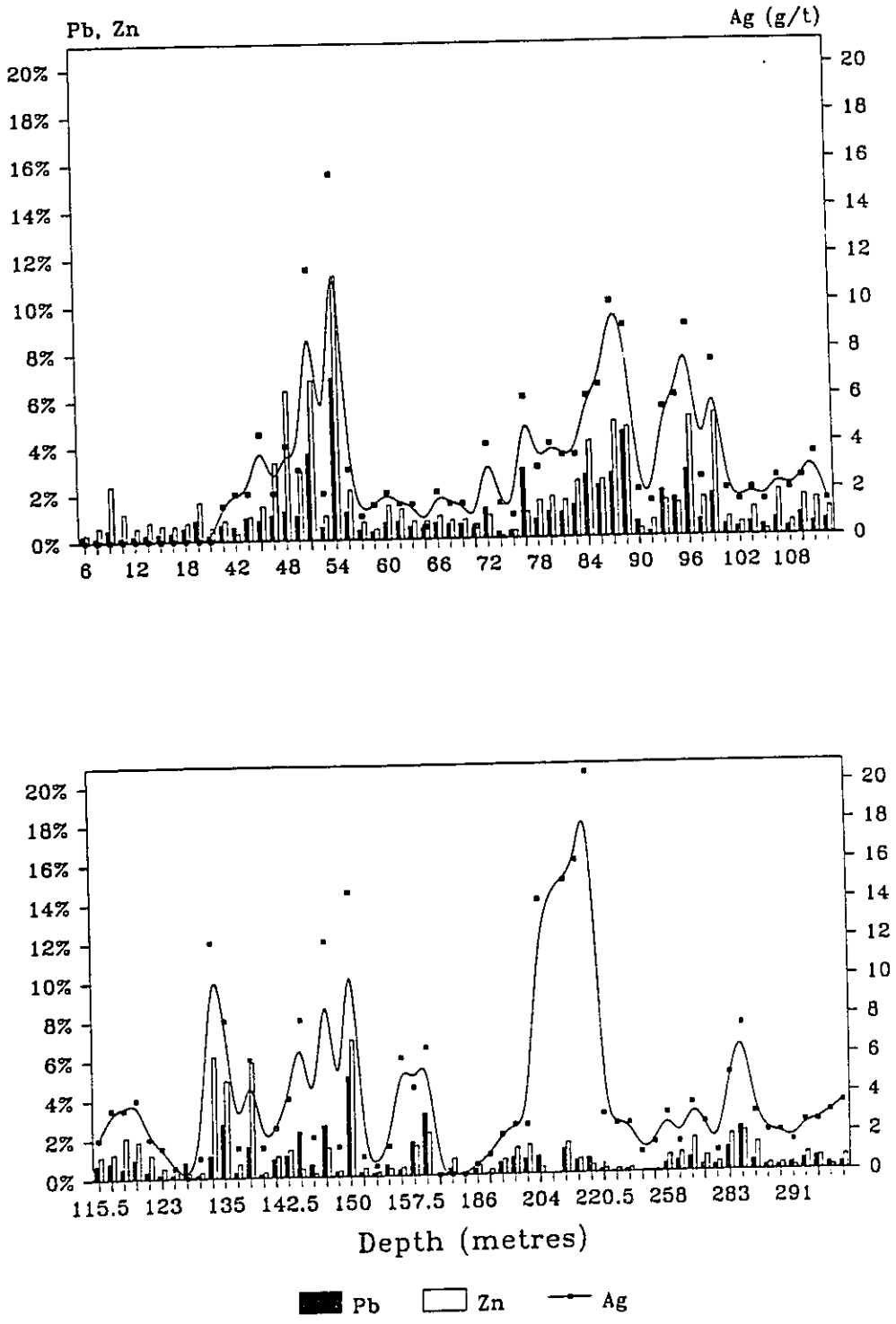

Figure 25: Graphical representation of Pb, Zn and Ag data for DDH 79-3. Note that the highest Ag values do not always correspond to high Pb peaks suggesting that the Ag may not be entirely associated with galena but may have some association with sphalerite as well.

Pb, Zn & Ag values for DDH 79-3

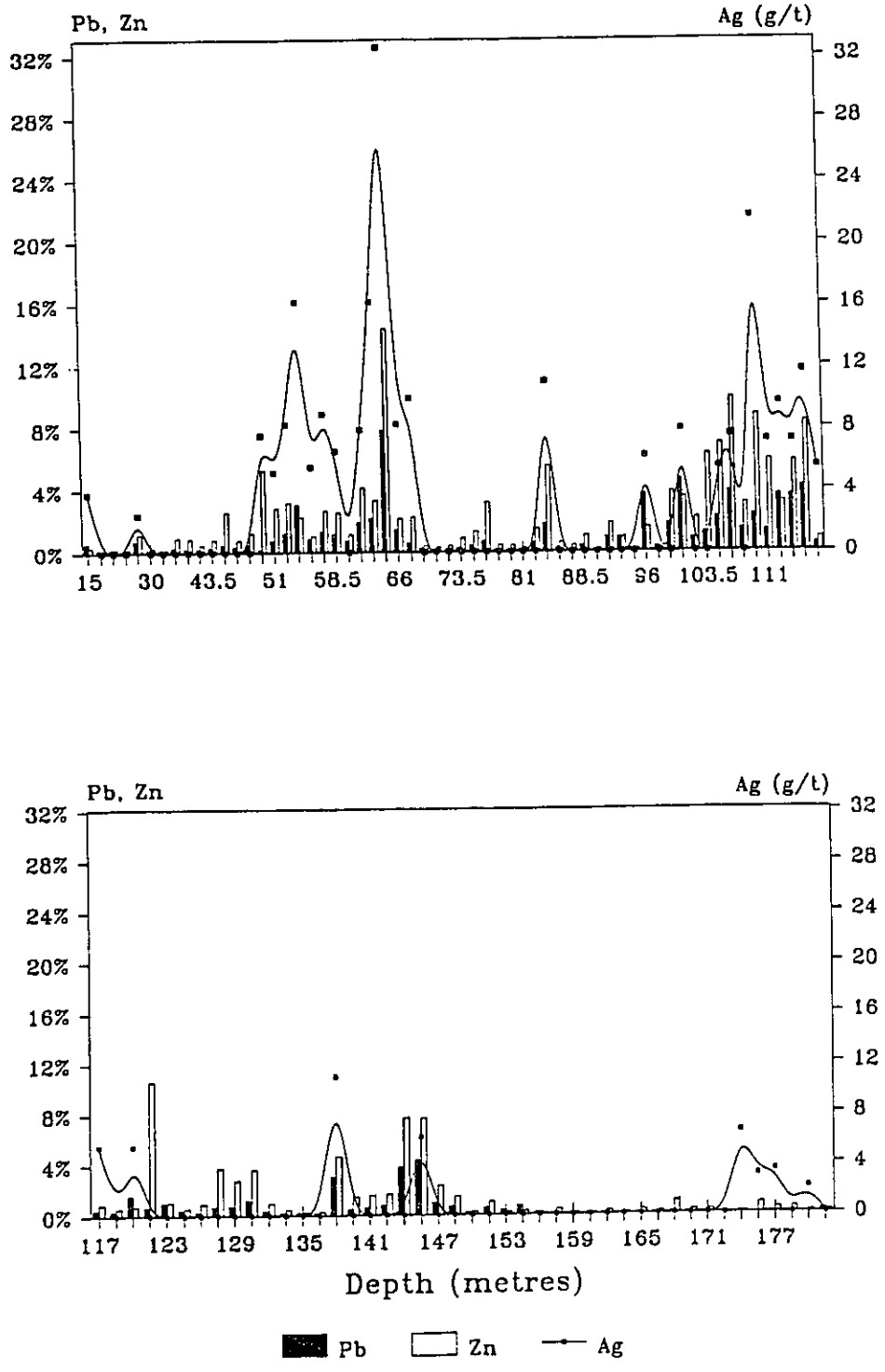

Figure 26a: Graphical depiction of the variation in average Pb+Zn and zinc ratio for all the drill hole data along sections A and C. Note that more holes are represented here than in figures 13-16 to present a more complete representation of the variation in metal values across the deposit.

North–South variation in average Pb+Zn and Zinc ratio

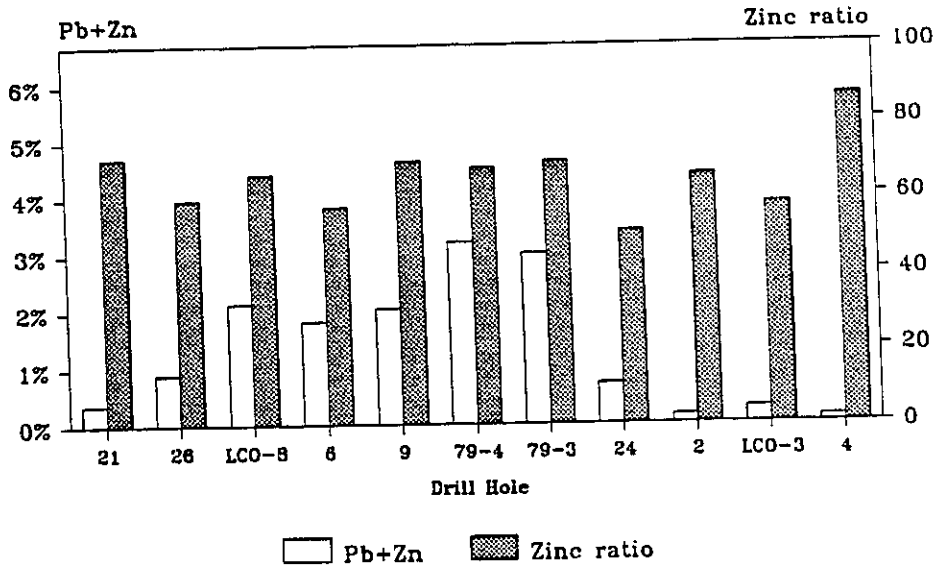

East–West variation in average Pb+Zn and Zinc ratio

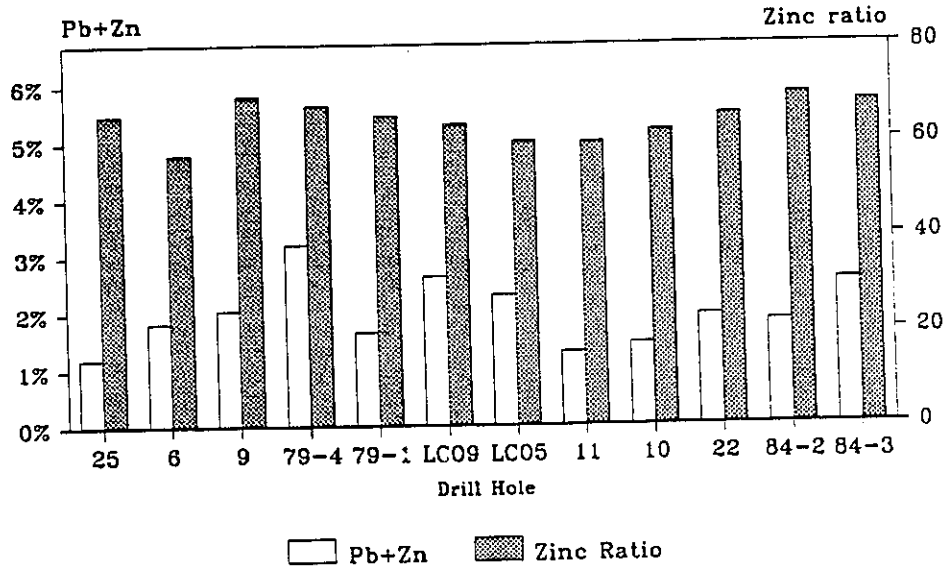

Figure 26b: Graphical depiction of the variation in average Pb+Zn and Zinc ratio for selected drill hole data along sections A and C. Data were selected to emphasize the higher Pb+Zn and zinc ratio data.

North–South variation in average Pb+Zn and zinc ratio

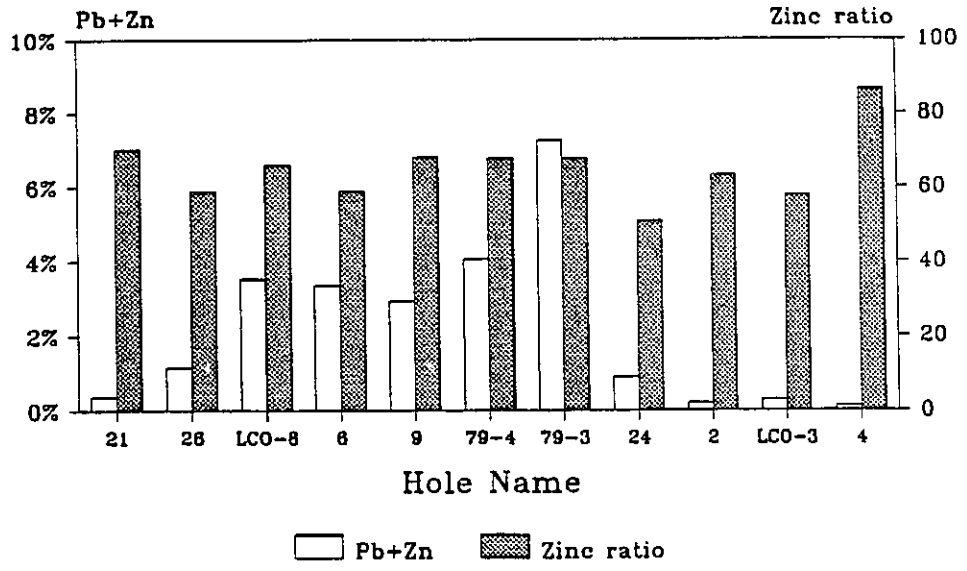

East–West variation in average Pb+Zn & zinc ratio

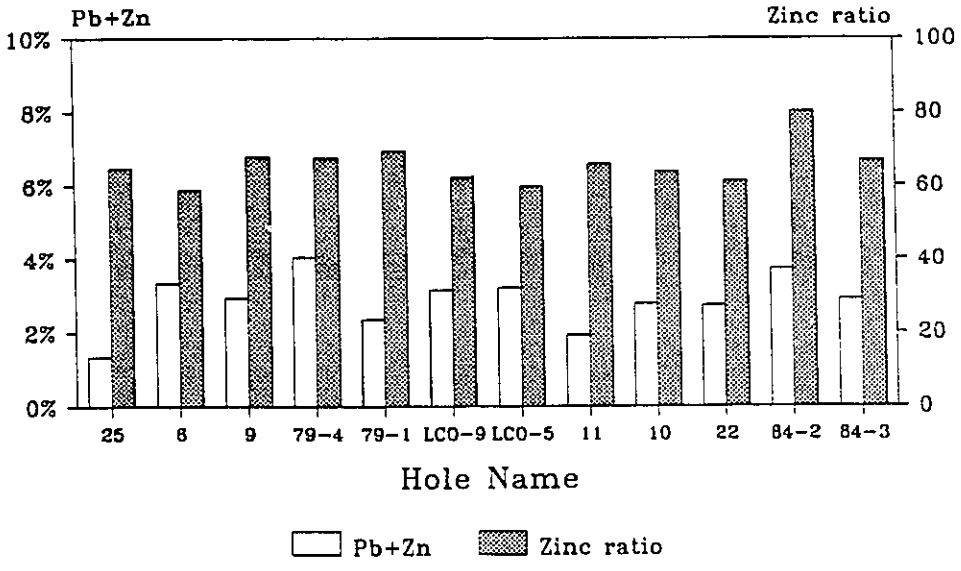

that the fine-grained, quartzofeldspathic groundmass has undergone the most complete alteration, whereas the K-feldspar phenocrysts show varying degrees of alteration from none to near complete chloritisation. Within this trench a distinct zone of moderate to intense chloritisation occurs at the eastern end roughly from 6+2.0E to 9+00E, and is unrelated to the more regional chloritisation seen in the South, West and East Trenches. Chlorite alteration in this area is probably related to fluid activity along the fault at the eastern end of the trench (Figure 9). This alteration has nearly obliterated all original textures in the massive crystal tuff breccia fragments, although in banded fragments intensely chloritised bands separated by lighter, quartz-rich bands are still distinguishable.

Potassic alteration is interpreted to be the second alteration phase and although its presence is difficult to identify but based on analysis of thin sections is probably represented in the crystal and lapilli tuffs by sericitisation of K-feldspar crystals and fine-grained K-feldspar in the breccia matrix. The rhyolites best show the extent of potassic alteration, since they can contain up to 12% K_2O, which confirmed in thin section by the presence potassic alteration of the groundmass K-feldspar.

In order to determine the degree of potassic alteration in the rocks at Mount Costigan the 1986 samples were stained for potassium by using sodium cobaltinitrate. This staining revealed that all of the rocks at Mount Costigan (even the most highly silicified ones) have been affected by a pervasive potassic alteration. Because of this, staining only really showed that banding in the flow-banded rhyolites of the South-East Trench is dominantly K-rich. Also, nodules in the nodular tuff of the South Trench commonly have K-feldspar rich cores, although some nodules display quartz-rich cores and K-feldspar rich rims. Rare spherulites in the South Trench also have K-feldspar rich cores but mostly they are entirely potassic in composition.

Silicification is interpreted to be the latest phase of alteration because it appears to overprint both the potassic and chloritic alteration. The intensity of silicification in the deposit area appears to increase from west to east beginning 15m from the end of the western-most of the two West Trenches (Figure 8) to the banded and massive, unbrecciated crystal tuff at the west end of the Central Trench. The same pattern is also present in the North Trench where the unbrecciated crystal tuffs west of the breccia are the most strongly silicified, while the brecciated massive crystal tuff is relatively fresh. Intense silicification is associated with the faults in the North and South Trenches.

In the North Trench, silicification is the dominant type of alteration where it commonly varies from weak to intense. The intense silicification is recognised in the massive and banded crystal tuffs by their greater hardness and characteristic sugary texture (best observed in sub-unit 2m, Figure 6). This texture is commonly formed by the weathering out of fine-grained K-feldspar in the groundmass which causes the rounded to subangular quartz crystals to become pronounced. Silicification is characteristically more intense in the banded tuffs of the western part of the trench.

In the South Trench, like the North Trench, because silicification varies across the length of the trench there is no zoning to the alteration, and silicification appears to have only affected particular sub-

units. An example of this is sub-unit 2m. Here, moderate silicification occurs in the most southerly exposure of sub-unit #2m and strong to intense alteration in the exposure of sub-unit #2m between the two bleached zones (see Figure 7). Furthermore, strong to intense silicification of sub-unit #2m occurs in the central part of the trench where it is in contact with moderately silicified rhyolite breccia (sub-unit #3sm) and unsilicified perlite (sub-unit #5). A similar example is the thin, chloritised and weakly silicified, exposure of sub-unit #1 sandwiched between the moderately silicified banded crystal tuff of sub-unit #2b and the strongly silicified massive crystal tuff exposed in sub-unit #2b. Thus, it can be seen that while silicification has affected the bulk of the South Trench rocks, several subunits (in particular units #1, 2b, 5 and 3sb) are relatively unaffected.

Lapilli tuff exposed in the West Trenches shows a very distinctive alteration zoning toward the breccia in the Central Trench. In the western-most of the two trenches (Figure 8) the western 15m are chloritised and unsilicified as indicated by the dark colour of the outcrop and relatively fresh lapilli. There is a progressive, but erratic, increase in silicification from weak to intense as the breccia is approached. This is clearly observed by the change in colour of the outcrop from pale yellowish-green near the chlorite altered zone to buff-white at the east end of the eastern-most of the two trenches. This is also visible by the development of "sugary" texture in the more strongly silicified rocks as previously noted in the North Trench. Although there is a general increase in alteration intensity from west to east, the most intense silicification is commonly associated with northeast to southwest trending fractures.

In the Central Trench, although silicification is less extensive than chloritisation, strong silicification occurs at the western end of the trench while weak to moderate silicification occurs in the large, un-brecciated blocks of massive crystal tuff (Figure 9) in the eastern part of the trench (at 5+2.0E). The strongly silicified massive and banded crystal tuff at the west end of the trench are the only visible remnants of the intense silicification seen in the West Trenches, since they are juxtaposed against chloritised, matrix-poor breccia to the east. The lack of evidence for any chlorite alteration in these rocks suggests that the silicification has either been introduced as an overprint on the chlorite or they were originally only silicified.

The genetic relationship between mineralisation and alteration at Mount Costigan is unclear, although the mineralisation appears to have a close association with silicification and possibly chloritisation. A genetic relationship may be inferred by the presence of coarse-grained sphalerite and galena in Area K (Figure 9) which replaces banding in banded crystal tuff, while occurring within a distinctly silicified zone. Outside this silicified zone mineralisation is minimal occurring as medium- to fine-grained sphalerite and galena. The presence of zones of disseminated and medium-sulphide mineralisation within the chlorite alteration envelope associated with the fault at the east end of the Central Trench (Figure 9), suggests that the mineralisation may have also been associated with hydrothermal fluids that moved along the fault.

g. Whole Rock Geochemistry

Ten rock samples from this study were analysed by XRF to determine their chemical composition and test the reliability of the field identification. Thirty-eight additional samples from Mount Costigan and surrounding areas, collected by Dr. G.P. Watson (Geological Survey of Canada) were used for comparison. Data from fourteen unaltered rhyolites were taken from the literature in an attempt to define a "fresh" rhyolite field, so as to ascertain the degree of alteration of the Mount Costigan rhyolites. Two samples of Silurian and Devonian rhyolites from Gates and Moench (1981) were also used in an attempt to correlate the Mount Costigan and regional rhyolites with rocks of similar age and lithology.

The pervasive nature of the alteration at Mount Costigan has made determination of the protoliths of these rocks extremely difficult, if not impossible in most cases. Standard Harker variation diagrams (Figure 28) commonly show a random distribution pattern, with the only clear trends occurring in the SiO_2 vs K_2O and SiO_2 vs Na_2O diagrams. Here the majority of the Mount Costigan and regional volcanic rocks are clearly depleted in sodium relative to the fresh rhyolites as reported in the literature, with the exception of the flow-banded rhyolite from the South Trench. Those regional rocks enriched in sodium (samples WZ-87-033, 040) are from the Gulquac River area, approximately 3 to 4 kilometres from Mount Costigan and may represent relatively fresh rhyolite. In contrast to this the SiO_2 vs K_2O plot shows that all of the rhyolites are strongly enriched in K_2O, relative to the rhyolite field, defined by the data from the literature, and shows the degree of potassium metasomatism in the area. Rhyolites from Mount Costigan show a large variation in K_2O content, the highest being from the Central Trench and the South Trench. Tuffaceous rocks from Mount Costigan are also characteristically enriched in K_2O.

Despite the random nature of the data one weak trend visible is that the Mount Costigan rhyolites and tuffs are commonly more altered than the regional rocks in the sense that they consistently (with the exception of K_2O and total alkalis) plot above or below the regional rhyolitic rocks. The regional rhyolites generally plot closer to the rhyolite "field" than the rhyolites and tuffs from Mount Costigan, suggesting they are less altered.

Analysis of the trace element data (Figure 28) also displays the same random distribution as observed for the major elements. The separation of Mount Costigan and regional rocks discussed above is present, but less visible since both rhyolites, tuffs and sedimentary rocks plot near or within the fresh rhyolite field.

When Harker variation diagrams are normalised against TiO_2 and Al_2O_3 (Figure 29a,b) it readily becomes apparent that the rhyolites and tuffs from Mount Costigan can be sub-divided into two major groups. Firstly, with respect to the tuffs, there is a group has relatively high abundances of TiO_2 and low SiO_2. Secondly there is a group which has significantly higher SiO_2 and lower TiO_2. Regional and Mount Costigan rhyolites commonly overlap or plot adjacent to both groups of tuffs, and give further support to the interpretation that those rhyolites higher in SiO_2 are probably the least altered.

Figure 28: Geochemical variation diagrams for samples taken from Mount Costigan and the surrounding area. Note the lack of any distribution pattern, with the exception of K_2O and Na_2O which are typical of potassium metasomatism. Mt. Costigan rhyolites = open circles; Mt. Costigan tuffs = 'x'; Regional rhyolites = open square; Regional basalts = filled square; Mt. Costigan siltstones = vertical line; Perlite (S. Trench) = 'plus sign'; Mafic dyke (Central Trench) = forward slash. Circled area represents an approximate region for "fresh" rhyolites as defined by the following samples: Rhyolites from Carmichael et al. (1974) = back slash; Daly (1968) = filled hexagon; Le Maitre (1976) = filled star; Grove and Donnelly-Nolan (1986), >72% SiO_2 = inverted open triangle; Grove and Donnelly-Nolan (1986), >70%<72% SiO_2 = filled diamond; Silurian rhyolite from Gates and Moench (1981) = open diamond; Devonian rhyolite from Gates and Moench (1981) = filled circle.

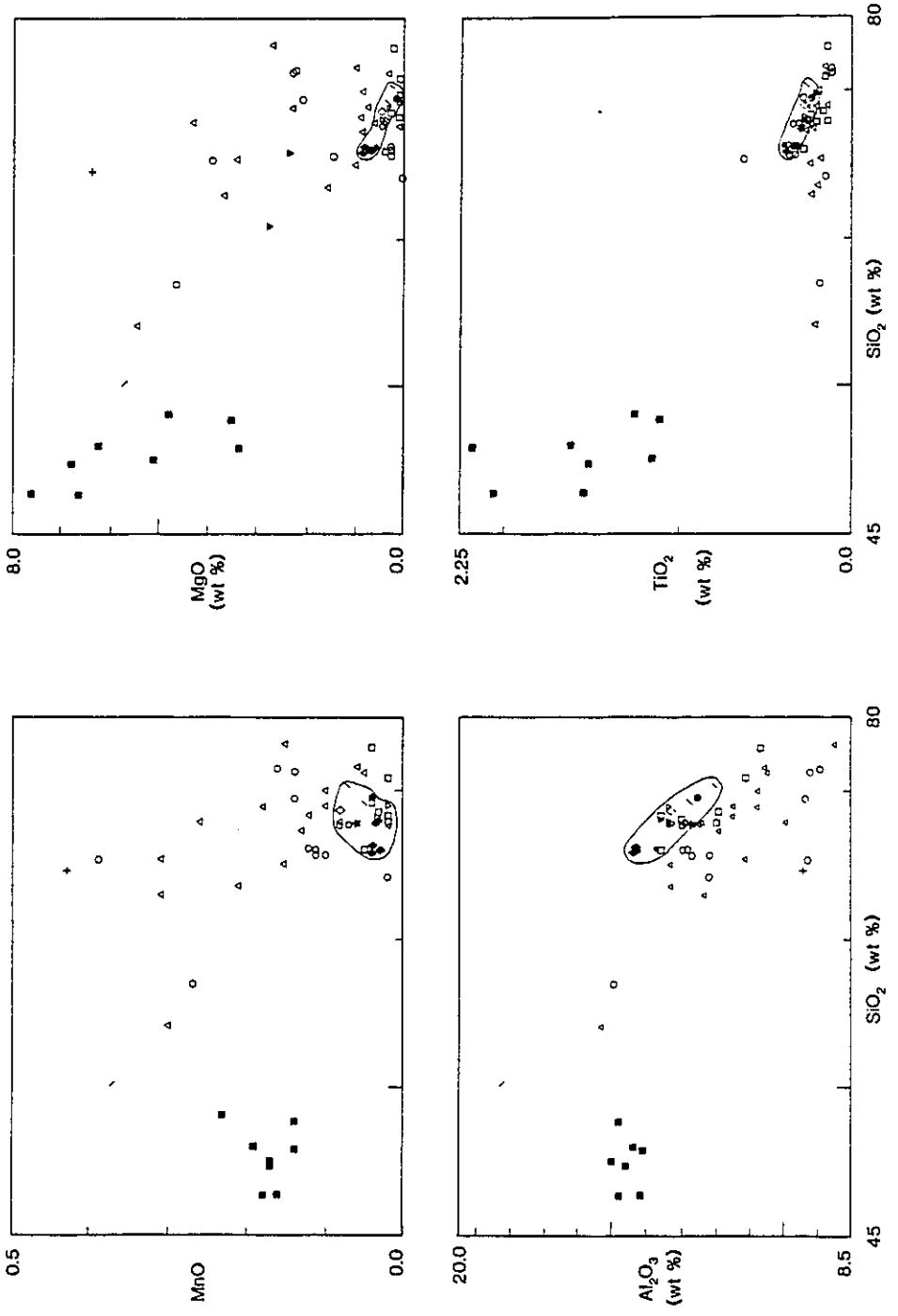
8.0
0.0
MgO
(wt %)
2.25
0.0
TiO2
(wt %)
45
80
SiO2 (wt %)
0.5
0.0
MnO
20.0
8.5
Al2O3
(wt %)
45
80
SiO2 (wt %)

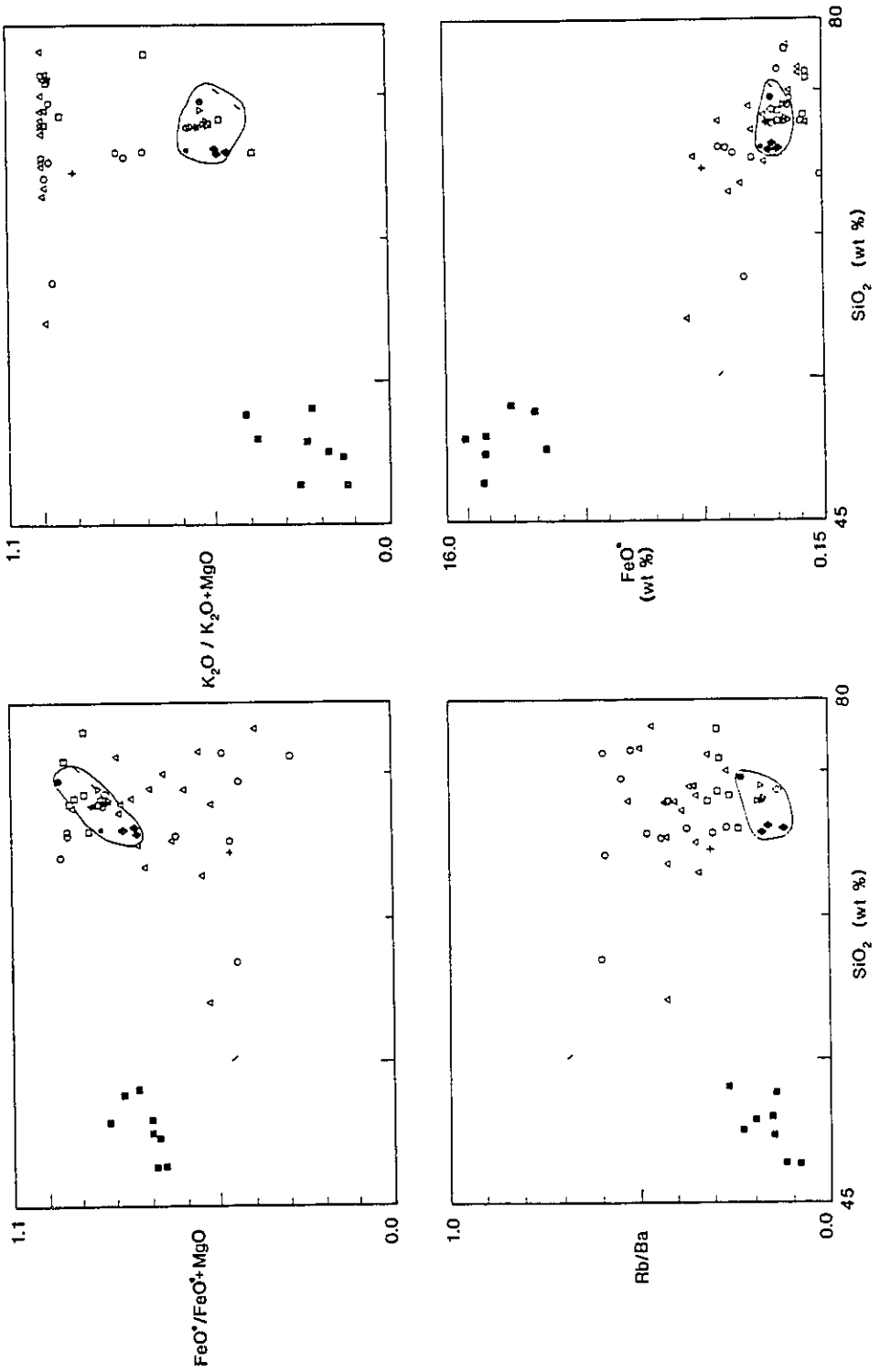
1.1
0.0
K_2O / K_2O+MgO
16.0
0.15
FeO*
(wt %)
45
80
SiO_2 (wt %)
1.1
0.0
FeO*/FeO*+MgO
1.0
0.0
Rb/Ba
45
80
SiO_2 (wt %)

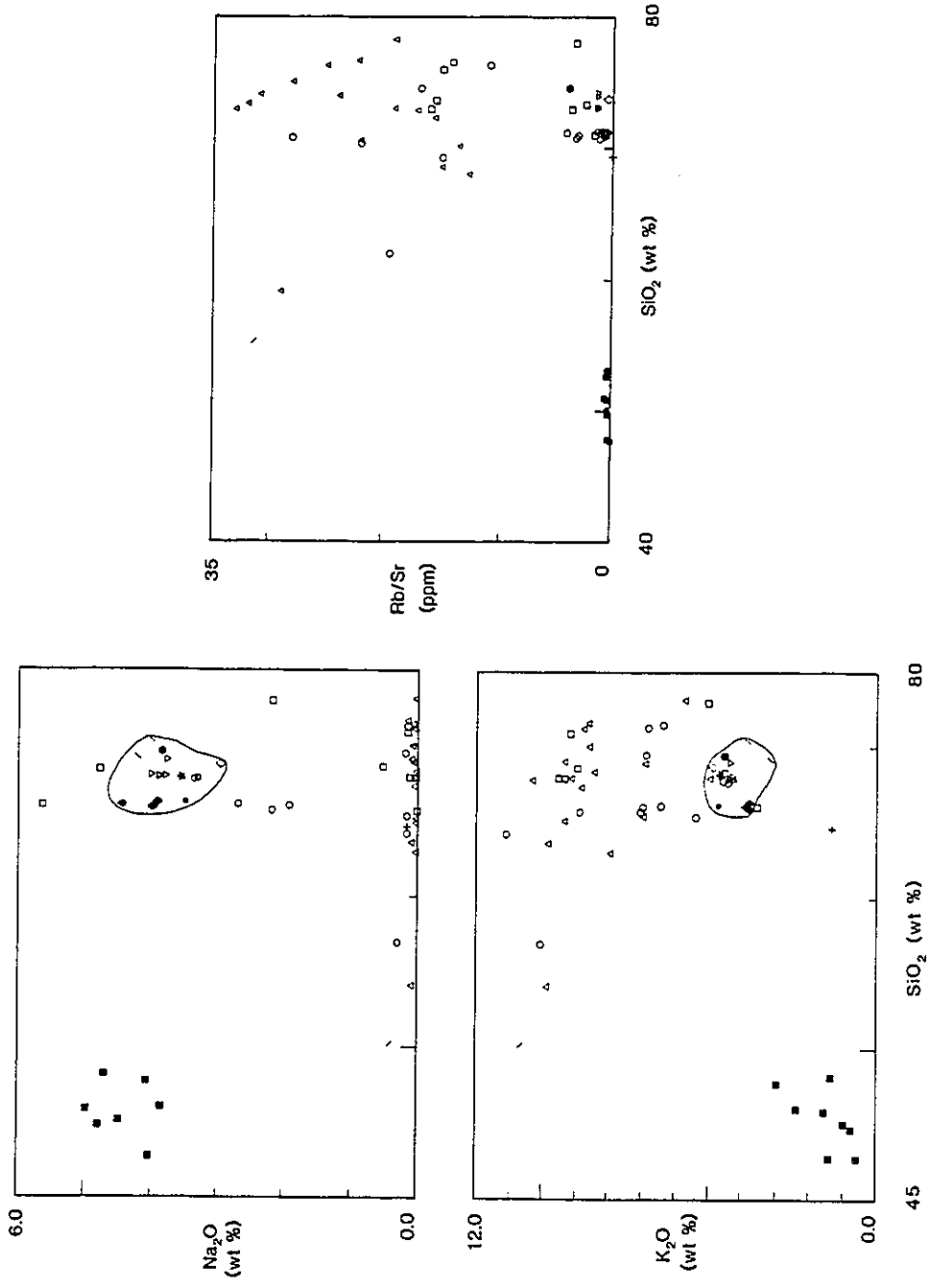
35
Rb/Sr (ppm)
0
40
80
SiO2 (wt %)
6.0
Na2O (wt %)
0.0
12.0
K2O (wt %)
0.0
45
80
SiO2 (wt %)

Normalising Harker diagrams against Al_2O_3 (Figure 29b) confirms the above observations that the rhyolites on Mount Costigan fall into two groups and that there is a close similarity between the tuffs on Mount Costigan and the rhyolites. The Mount Costigan rhyolites fall into two main groups represented by one group that is high in SiO_2 and low in Al_2O_3, while the other group is relatively high in SiO_2 and Al_2O_3. This second group commonly has similar proportions of Na_2O, K_2O, MnO and TiO_2 to the regional rhyolites while the former commonly have more elevated values.

Also of note in these diagrams is the fact that the regional rhyolites and the rhyolites from Mount Costigan commonly plot within the field defining Mount Costigan tuffs. This suggests either that the tuffs were derived from rhyolitic magma or that the rhyolites have been altered and now plot in the tuffaceous field. Since the regional rhyolites plot almost consistently overlapping or adjacent to the tuffs it would appear that the tuffs were derived from the rhyolites since several of these rhyolites appear relatively fresh. This is observation is strengthened also by considering the plot of K_2O/total alkalis vs. SiO_2 (Figure 28). Here the field of tuffaceous rocks is overlapped by that of the regional and Mount Costigan rhyolites.

A plot of log $Zr/(TiO_2*10{,}000)$ vs. SiO_2 (Figure 30) shows that while most of the rhyolites from Mount Costigan are within the rhyolite field some are slightly altered and plot within the rhyodacite-dacite field. However since the "fresh" rhyolite field overlaps the rhyolite and rhyodacite-dacite fields of Winchester and Floyd (1977) there is apparently a discrepancy in the literature as to where the rhyolite field ends. This discrepancy appears to exist between the rhyolite field boundary from Winchester and Floyd (1977) and the rhyolite samples between 70 and 72% SiO_2 from Grove and Donnelly-Nolan (1986). One rhyolite sample from Mount Costigan plots within the trachyte field and probably represents the highest degree of alteration in the rhyolites. All the tuffaceous rocks from Mount Costigan plot within the rhyolite and rhyodacite-dacite fields, indicating they were probably derived from a rhyolitic magma. The fact that the siltstones from DDH LCO-84-3 plot within the andesite field suggests that they may represent water-lain volcanic ash.

In summary, although the number of samples from this investigation was small and thus may not be representative of the entire suite of rocks at Mount Costigan, the analyses did provide the following results (Appendix 1). Firstly, the rhyolite mapped at the north end of the South Trench, while displaying good banded spherulitic texture in thin section has only 61.93% SiO_2, but also has 4.66% MgO and 10.04% K_2O, suggesting that it represents a strongly potassic and chlorite altered spherulitic rhyolite. Secondly, sample MC-87-68, mapped and identified in thin section as a silicified siltstone is strongly altered since its SiO_2 and Al_2O_3 values plot in the rhyolite field. Thirdly, the siltstone sample from the East Trench is too high in SiO_2 to represent a sedimentary siltstone and thus likely represents water-lain volcanic ash, due to the similarity between its chemistry and that of the crystal tuffs.

Figure 29a: Geochemical variation diagrams normalised against TiO_2, symbols as in Figure 28. Note that here the Mount Costigan rhyolites (open circles) and regional rhyolites (open squares) fall into two groups, the more silicic of which may be representative of fresher rhyolite.

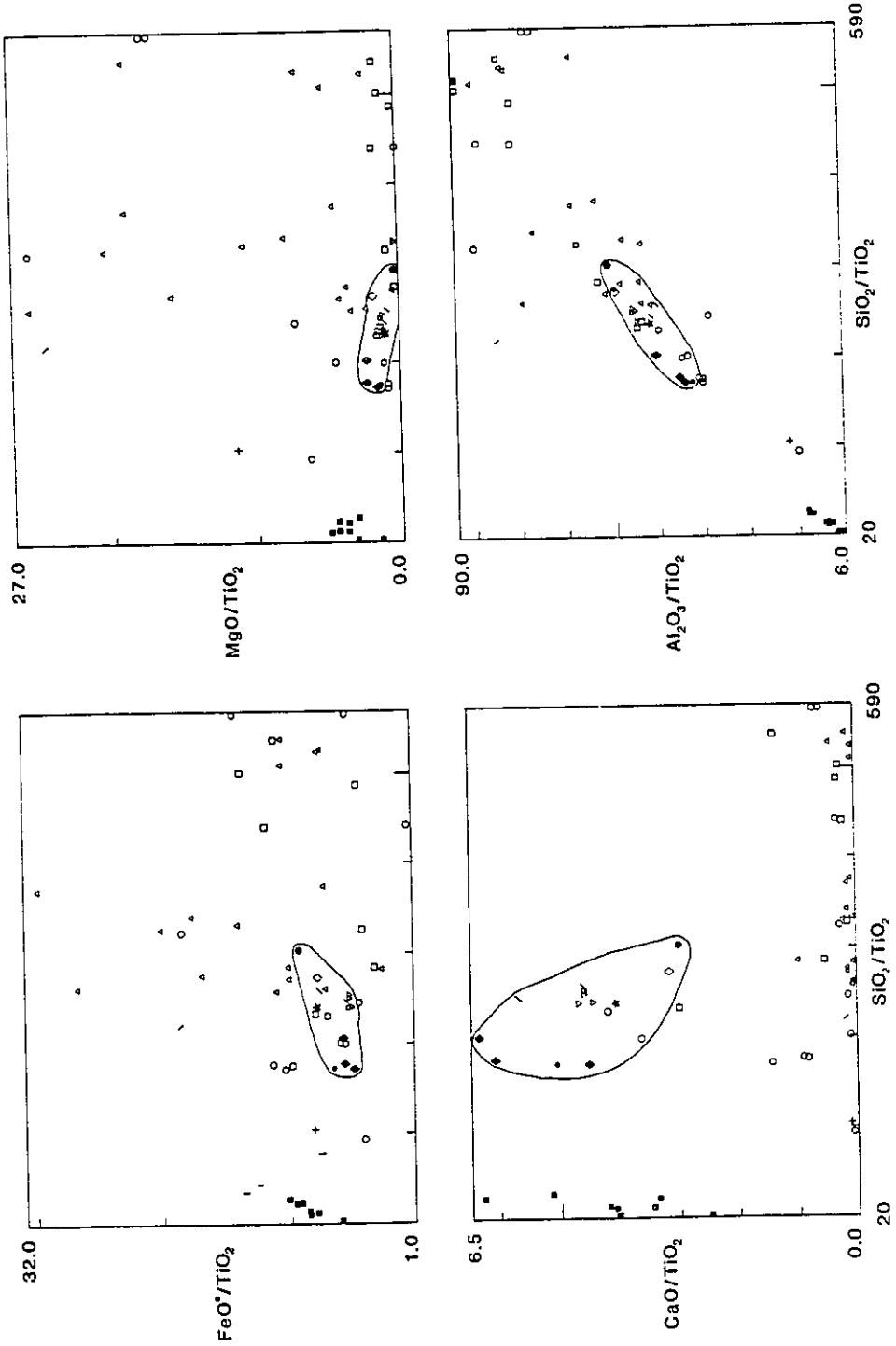
27.0
0.0
MgO/TiO2
90.0
6.0
Al2O3/TiO2
20
590
SiO2/TiO2
32.0
1.0
FeO*/TiO2
6.5
0.0
CaO/TiO2
20
590
SiO2/TiO2

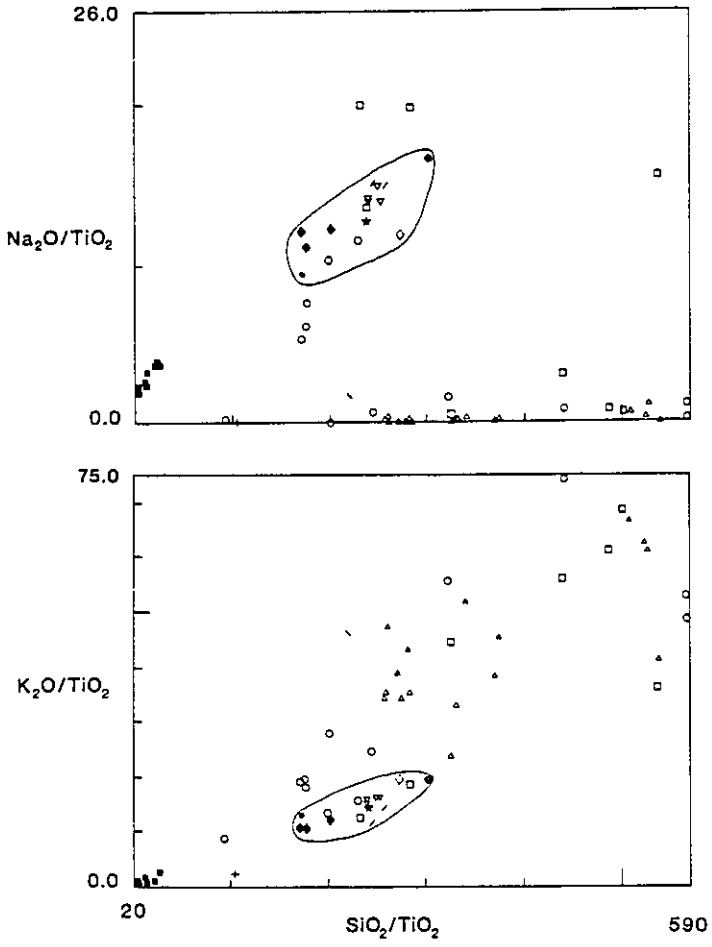
26.0
Na_2O/TiO_2
0.0
75.0
K_2O/TiO_2
0.0
20
SiO_2/TiO_2
590

Figure 29b: Geochemical variation diagrams normalised against Al_2O_3, symbols as in Figure 28.

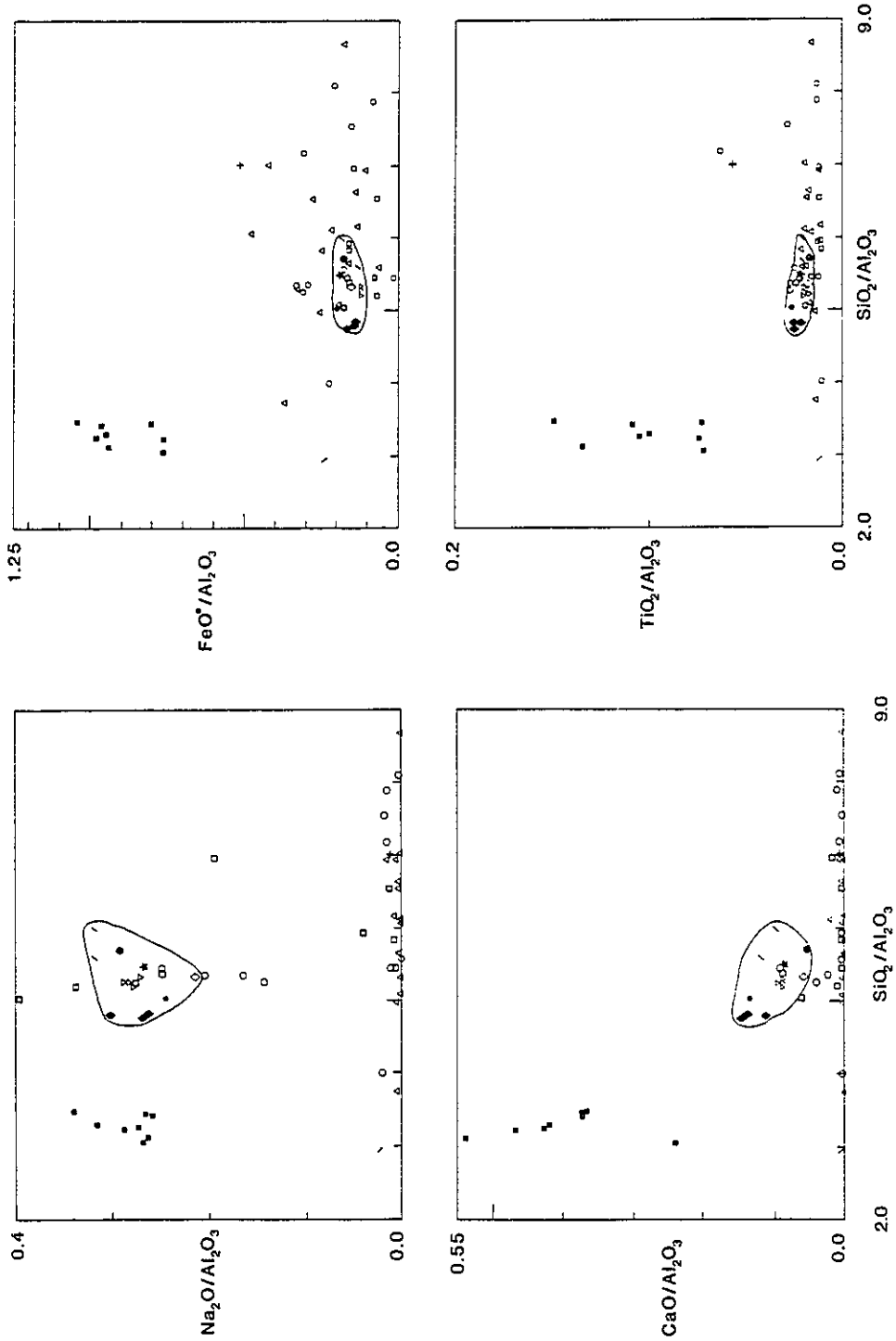
1.25
0.0
FeO*/Al2O3
0.2
0.0
TiO2/Al2O3
0.4
0.0
Na2O/Al2O3
0.55
0.0
CaO/Al2O3
2.0
9.0
SiO2/Al2O3
2.0
9.0
SiO2/Al2O3

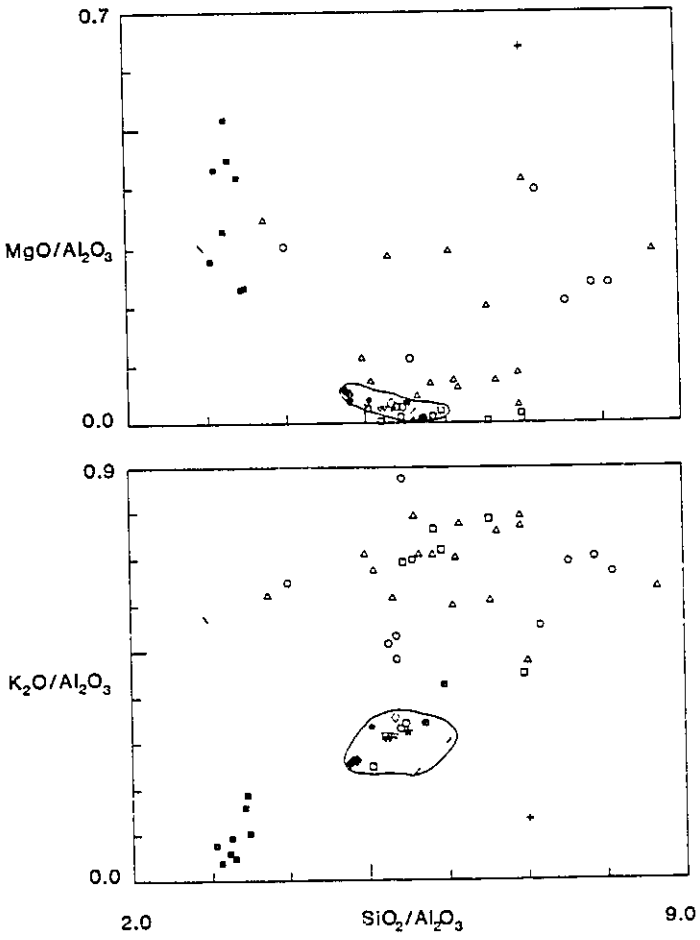
0.7
MgO/Al_2O_3
0.0
0.9
K_2O/Al_2O_3
0.0
2.0
SiO_2/Al_2O_3
9.0

Figure 30: Log $Zr/(TiO_2 \times 10{,}000)$ vs. SiO_2 plot (after Winchester and Floyd, 1977). Note the concentration of Mt. Costigan tuffs (x) within the rhyolite field, suggesting a rhyolitic origin.

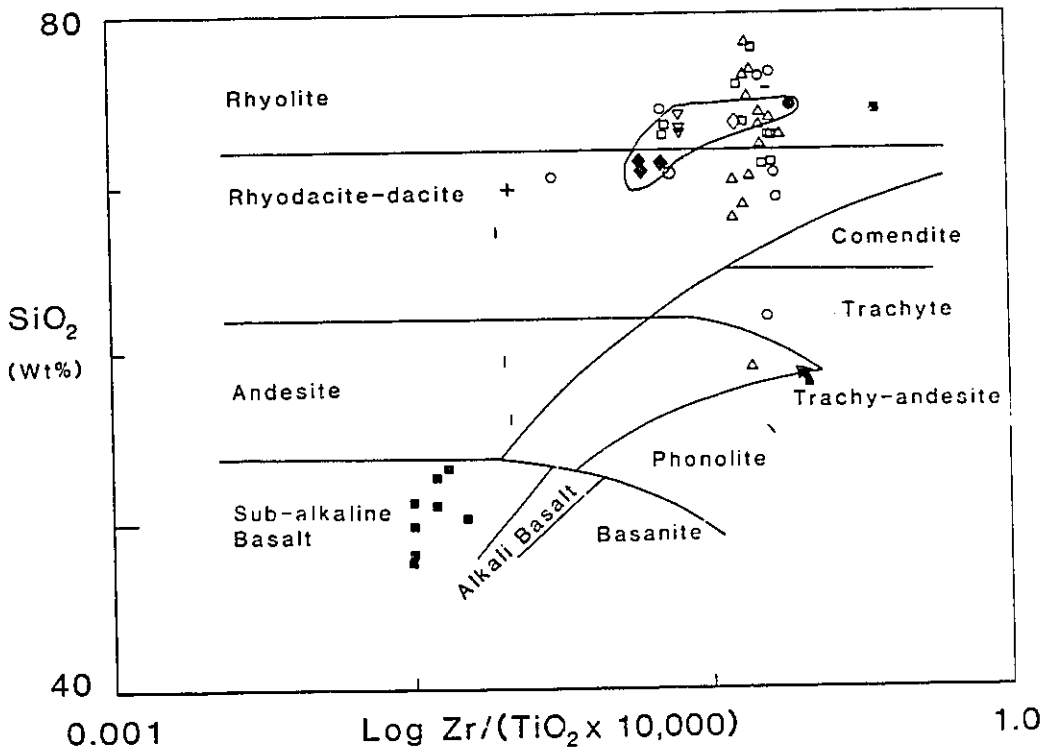
80
40
SiO_2
(Wt%)
0.001
Log $Zr/(TiO_2 \times 10{,}000)$
1.0
Rhyolite
Rhyodacite-dacite
Andesite
Sub-alkaline Basalt
Alkali Basalt
Basanite
Phonolite
Trachy-andesite
Trachyte
Comendite

CHAPTER 4

DISCUSSION

a. Geological Setting

i. Depositional Conditions

The stratigraphy at Mt. Costigan consists of a mafic basal sequence of dominantly basalts and siltstones which grade up into a more felsic sequence of intercalated siltstone, conglomerate and pyroclastic rocks overlain by a thick sequence of interbedded crystal and lapilli tuffs and flow-banded, spherulitic to massive rhyolite flows. The top of the stratigraphy is another sequence of siltstones similar to that at the base of the section.

The basal sequence of basalts and siltstones represents a near-shore marine environment as suggested by graptolites and brachiopods in equivalent siltstones outside the property area (Fyffe and Pronk, 1985; St. Peter, 1978). The conglomerate and pyroclastic rocks, intercalated with the siltstones above the basalt, suggest water depth was shallowing to the west. The thick overlying sequence of pyroclastic and felsic volcanic rocks represent subaerial volcanism as indicated by welded tuffs in equivalent rocks south of Mt. Costigan (St. Peter, 1978). A return to submarine deposition is indicated by the re-appearance of siltstones at the top of the section.

b. Genetic Models

i. Classification

The Mount Costigan Pb-Zn deposit represents a small, low- to medium-grade, low tonnage deposit hosted in brecciated subaerial pyroclastic and volcanic rocks adjacent to a nearshore (shallow) marine environment. The deposit consists of an irregular shaped central (high grade) Pb-Zn body enveloped by a lower grade shell. It shows no metal zonation but does show weak sulphide zoning as represented by the increase of chalcopyrite in the footwall. Thus, based on the discussion of mineral deposit types by Sawkins (1984) the only deposit type that satisfies most of the characteristics of Mount Costigan is the epithermal Ag deposit type. The diagnostic features of this deposit type (Panteleyev, 1986) are as follows: 1. near surface mineralisation (no greater than 1000m); 2. Vein ore hosts, but also breccias, stockworks and replacement zones; 3. Mineralisation in volcanic terranes in well-differentiated subaerial pyroclastic rocks and small sub-volcanic intrusions; 4. Ore minerals deposited as an open space filling. Evidence of cycles of ore deposition; 5. Main ore minerals are native gold and silver, electrum, silver-bearing sulphosalts, tellurides. Galena and sphalerite are common; 6. Gangue minerals are quartz and calcite with minor fluorite, barite and pyrite; 7. Hydrothermal alteration consists of silicification flanked by illite-sericite alteration, all within a larger zone of propylitic alteration.

1. Discussion

Based on the presence of coarse-grained, space-filling sphalerite and galena hosted in a breccia, higher silver than gold values, fine-grained hydrothermal quartz and K-feldspar replacing an earlier matrix and subaerially deposited host rocks enriched in K_2O and depleted in Na_2O Mount Costigan may be interpreted to represent a type of epithermal deposit.

Because it does not, however, possess enough similarities to Au-Ag epithermal deposits in the Canadian Cordillera as described by Panteleyev (1986) it may actually represent a base-metal variety of epithermal deposit. Firstly, although sphalerite and galena are an integral part of silver-rich epithermal deposits these minerals are not as abundant as the main gold and silver-bearing minerals in epithermal deposits. Secondly, within silver-rich epithermal deposits the base-metal "zone" is found (Table 1) normally 150 to 200m below the silver- and gold-rich zones (Berger, 1985 - Figure 36). Henley and Hedenquist (1986) report sphalerite and galena in the New Zealand epithermal systems to occur at depths of 200 to 2000m below the present erosion level as disseminated sulphides in veins and vugs, typically closely associated with adularia and calcite. These authors also report the presence of crude metalliferous zoning with gold and tellurides occurring near the surface and lead, zinc, silver and copper at depth. Although there is no indication at Mount Costigan that the Ag-rich zone occurs stratigraphically above the Pb and Zn, it is conceivable that there has been a significant degree of erosion (enough to expose the base metal zone). However, with Mount Costigan being a base metal dominated epithermal deposit, it is more likely that the base metal zone occurs near the surface and very little unroofing has occurred. Thirdly, although base-metal mineralisation occurs at depth it rarely exceeds that of the original concentration in unaltered rocks, as at the Okahuri epithermal field in New Zealand (Henneberger, 1986). Laznicka (1985) also notes the common low base metal contents of epithermal deposits. Mount Costigan, in contrast, averages 0.66% Pb, 1.24% Zn and 2.05g/t Ag compared to 0.01% Zn and 0.002% Pb for fresh felsic volcanic rocks (Johnson and Lipman, 1988). Fourthly, although mineralisation in silver-rich epithermal deposits is characterised by gold and silver-bearing tellurides, acanthite, electrum and sulphosalts, none of these are present at Mount Costigan (Table 1). The precious metal mineralisation at Mount Costigan is, however, associated with the sphalerite and galena. Fifthly, the open spaces in silver-rich epithermal breccias appear to have been much longer-lived, or re-opened several times as shown by the common banded, crustiform or colloform textures. Multiple periods of deposition (Table 1) are commonly indicated in silver-rich epithermal deposits by the presence of coarse-grained, well crystallised quartz and amethyst overgrowths on breccia fragments. Also, mineralisation in these deposits appears to have occurred during brecciation and is a result of the same fluids responsible for the formation of the breccia. Although two stages of mineralisation characterise the Mount Costigan deposit they do not represent multiple re-openings of the inter-fragment spaces in the breccia. The principal mineralising event occurred in close association with the development of the allochthonous breccia and was a single event as there is no indication of a third mineralising period.

While there is a broad similarity between the non-sulphide mineralogy of silver-rich epithermal deposits and Mount Costigan (quartz and minor fluorite being present in both) the quartz at Mt. Costigan is dominantly fine-grained, occurring as a major constituent of the matrix. It is only coarse-grained when found as phenocrysts in the crystal tuffs and rhyolites and rarely as coarse, isolated crystals in the breccia. The amorphous silica (chalcedony and opal) common to silver-rich epithermal deposits is unknown at Mount Costigan, but probably occurs in a slightly different form (see discussion on genesis, below). Fluorite is only found as rare, isolated, coarse crystals in the massive crystal tuffs at Mount Costigan and is not as abundant as in these deposits.

In some silver-rich epithermal deposits, Au:Ag ratios (Table 1) can range from 3:1 (Goldfield District; 32g/t Au, 10.6g/t Ag) (Ashley, 1974) to 1:111.5 (Tonopah District; 10.9g/t Au, 2288g/t Ag) (Bonham and Garside, 1974, 1979), while Au:Ag ratios at Mount Costigan vary from 1:6 (DDH LCO-3) to 1:38 (DDH LCO-5) with the average about 1:15. However, the silver (up to 32 g/t) and gold (up to 0.18 g/t) values at Mount Costigan are considerably lower than most silver-rich epithermal deposits which are identified by silver and gold grades up to 14080-18560g/t (Ashley, 1974).

Breccias in silver-rich epithermal deposits are thought to result from hydraulic fracturing produced by the episodic boiling of hydrothermal fluids (de Ronde and Blattner, 1988); and are generated by the sudden release of fluid overpressures. As a result of this, the breccias (Table 1) typically occur, at depth, as dyke-like bodies, low-angle brecciated veins and discordant, upwardly-flaring pipes (Berger, 1985). Multiple periods of brecciation and uncemented breccias are thought to be characteristic of these precious-metal epithermal deposits (Berger, 1985), and while only two main periods of brecciation are present at Mount Costigan (autochthonous breccia in the North Trench and the allochthonous breccia in the Central Trench) breccia occurs stratigraphically above and below the deposit in units E and B. The breccias at Mount Costigan is clearly concordant with the stratigraphy (Figures 13,14) and is characterised by a large zone of polymictic allochthonous breccia (≈200m thick) which would not be expected to occur in a silver-rich epithermal system since most of the energy is dissipated at depth, little fall-back would be expected. Only the thinner (≈ 100m thick), monomictic crackle breccia could possibly be produced by hydraulic fracturing resulting from fluid overpressure release, since the fragments commonly show matching walls or only minor degrees of rotation (Nelson and Giles, 1985). While extrusive breccias are reported by (Henneberger, 1986) to occur in the Okahuri hydrothermal field, in the Taupo volcanic zone, New Zealand none, however, are base-metal mineralised.

Hydrothermal alteration around silver-rich epithermal deposits (Table 1) is normally characterised by a central quartz-alunite (Panteleyev, 1986) or quartz-adularia (Henneberger and Browne, 1988) core surrounded by successive zones of mordenite, smectite, illite-sericite, kaolinite and propylitic alteration, which occur with increasing distance and depth (Figure 31) from the centre of the deposit. Kaolinite may also occur as an overprint on the previous phases of alteration (de Ronde and Blattner, 1988). Alteration zoning of this nature is one of the distinguishing characteristics of these deposits and is similar to that

FEATURE	Panteleyev (1986)	Borealis (Nevada)	Mt. Costigan
Breccia	As pipes, stockworks and fine-grained bedding replacement zones	Externally is broadly lenticular in shape, quartz dominates. Has a sharp contact with underlying lithologies. Matrix is mainly fine-grained quartz-sulphide. Formed by explosive volcanism. Bounded by a major fault.	A large lenticular, stratiform body over and underlain by thinner (similar) zones of breccia.
Au:Ag Ratios	Varies between 1:128 (109g/t Ag, 0.85g/t) for Equity Silver, to 1:4 (110g/t Ag, 27g/t Au) for Blackdome	Unavailable	Varies from 1:6 to 1:38 (32g/t Ag, 0.18g/t Au).
Alteration -mineralogy -zoning	Quartz, sericite, illite, adularia, alunite, kaolinite. Zoning in general consists of a central silicified core flanked by illite-sericite and propylitic zones. At depth some veins may contain adularia. Alunite found in veins near surface.	Quartz, chaledony, opal, montmorillonite, kaolinite, jarosite, alunite. Zoning in general consists of high level silicification grading into argillisation at depth.	Microcrystalline quartz and K-feldspar; sericite, chlorite. Zoning consists of a central chloritic core surrounded by a wide zone of silicification. Potassic alteration is pervasive throughout.
(Ore) sulphide mineralogy	Native gold and silver, electrum, acanthite, tellurides, galena, sphalerite, chalcopyrite arsenic-antimony sulphosalts, enargite, cinnabar, tetrahedrite and selenides.	Native gold (micron to submicron sized). pyrite, chalcopyrite, bravoite, cobaltite.	Sphalerite, galena, chalcopyrite and pyrite.
Gangue minerals	Quartz (as amethyst, opal, chalcedony or cristobalite), calcite, ± fluorite, barite and pyrite.	Barite, haematite	Quartz, ±fluorite, calcite, K-feldpar
Depth of mineralisation	Average depth is 350m but can range up to 600m. Base metal zone commonly between 350 and 500m.	Not mentioned but appears to be between 0 and 50m from the surface.	Unknown
Host Rocks & age	In volcanic terranes associated with subaerial pyroclastic rocks & small subvolcanic intrusions. Commonly Cretaceous or Tertiary in age.	Tertiary hornblende andesite flows and laharic breccias, interbedded with tuffaceous sedimentary rocks.	Lower Devonian (possibly Lower Silurian) crystal and lapilli tuff, rhyolite flows; minor siltstone, conglomerate and greywacke.

Table 1: Comparison of the epithermal model discussed by Panteleyev (1986) with the Borealis epithermal deposit (Strachan, 1986) and Mount Costigan, New Brunswick.

around porphyry copper deposits (Sillitoe and Bonham, 1984). Alteration zoning at Mount Costigan consists of a central chloritic core (represented by the breccia in the Central Trench) overprinted by potassic alteration and enveloped by an outer silicified zone (represented by the western 6m of the Central Trench, the western half of the North Trench and the eastern two thirds of the West Trenches). Silicification increases in intensity from west to east in the West Trenches, toward the Central Trench and is sharply cut off by the breccia. Chlorite alteration in lapilli and crystal tuffs is repeated again west of the silicification. Kaolinite is also a characteristic alteration mineral in silver-rich epithermal deposits and although it has been reported at Mount Costigan (Riddell, 1971) its extent and distribution is unknown. Intensive alteration associated with epithermal deposits also includes pyritisation, but rarely carries any base-metal mineralisation. Thus although the alteration zoning at Mt. Costigan is more erratic and inconsistent than silver-rich epithermal deposits, implying that Mount Costigan is not a Cordilleran-type epithermal deposit, the overall similarity of the alteration mineralogy suggests that Mount Costigan is actually epithermal in nature. Geochemically, silver-rich epithermal deposits are characterised by low Na_2O and high K_2O (potassium metasomatism), also representative of the rocks at Mount Costigan.

Mature epithermal systems commonly develop in the waning stages of volcanic activity (Laznicka, 1985), prior to which has been a phase of explosive volcanism. This would suggest that Mount Costigan represents a primitive epithermal deposit in the sense that the breccia (host rocks) has formed during the initial stages of development of the system. However, since the nature and origin of the mineralising fluids are unknown, it is possible that they may be related to the same epithermal system as the fluid activity increased during the later stages of volcanism. Alternatively the mineralising fluids could be entirely unrelated to the volcanic activity but associated with Redstone Mountain Granite, since it intrudes the Costigan Mountain Formation and outcrops approximately 2km from the deposit. Thus, while the host rocks were formed by explosive volcanic activity the deposit could have formed during or, subsequent to, intrusion of the Redstone Mountain Granite.

Hydrothermal brecciation related to epithermal deposits (Nelson and Giles, 1985) is commonly followed by a progressive replacement of matrix by sulphidic microcrystalline silica commonly containing fine-grained pyrite or copper sulphides as well as elevated precious metal values. This is similar to that at Mount Costigan, since the breccia matrix has largely been replaced by microcrystalline quartz and K-feldspar. In areas of medium- to high-grade sulphide mineralisation this material contains fine- to medium-grained pyrite or is replaced by sphalerite and galena.

ii. Genesis of the Mount Costigan Deposit

At Mount Costigan mineralisation occurred firstly as a weak mineralising phase prior to emplacement of the allochthonous breccia, as indicated by the trace and disseminated sphalerite and galena present in the unbrecciated blocks of massive crystal tuff in the Central Trench, and massive crystal tuff boulders outside the trenched area. While the trace and disseminated mineralisation may be

Figure 31: General model for precious-metal epithermal deposits found in the North American Cordillera (Guilbert and Park, 1986). Note the depth at which base metal mineralisation occurs in this system and how the discordant breccia is restricted to the narrow vein system.

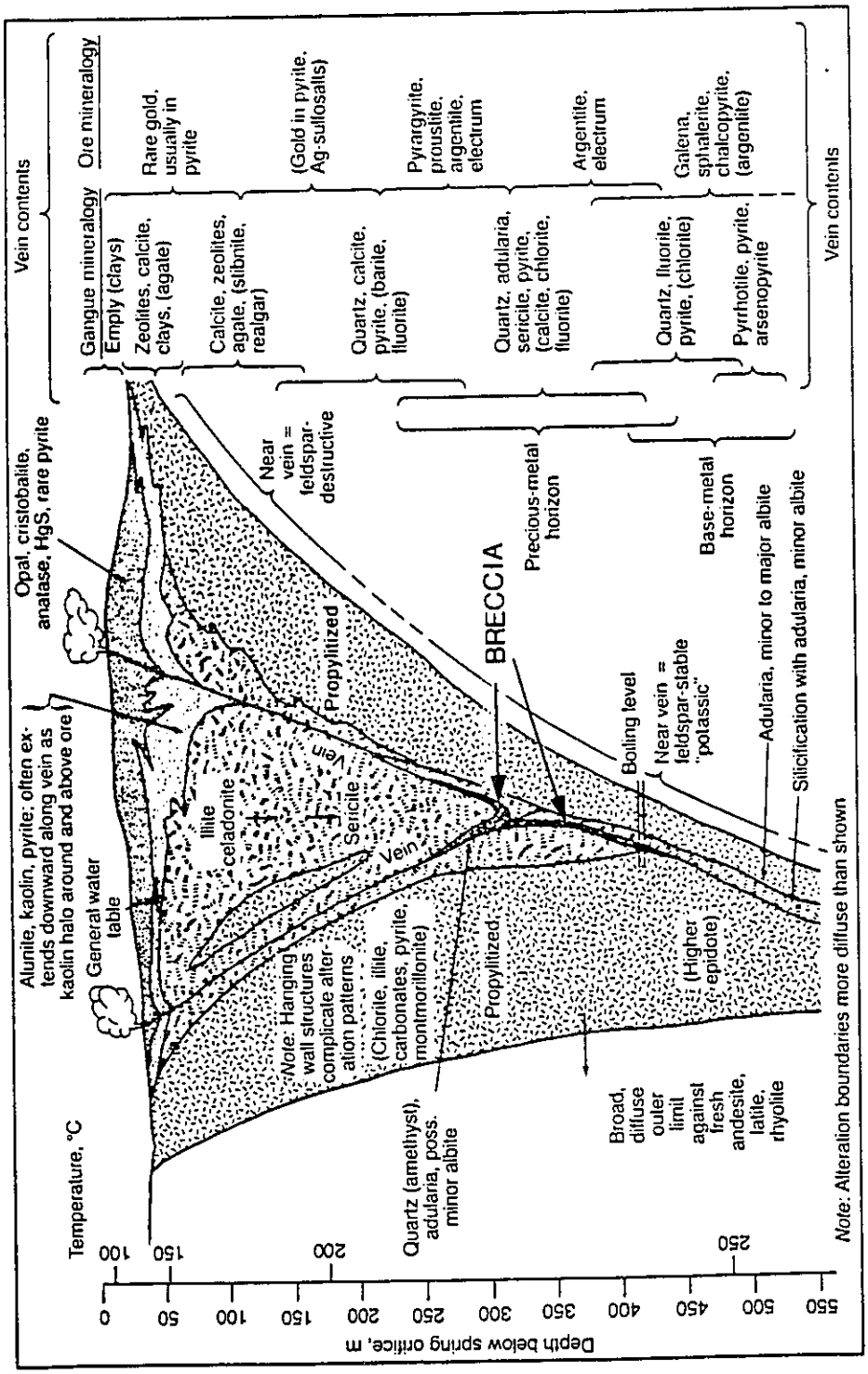
Vein contents
Ore mineralogy
Gangue mineralogy
Empty (clays)
Zeolites, calcite, clays, (agate)
Calcite, zeolites, agate, (stibnite, realgar)
Quartz, calcite, pyrite, (barite, fluorite)
Quartz, adularia, sericite, pyrite, (calcite, chlorite, fluorite)
Quartz, fluorite, pyrite, (chlorite)
Pyrrhotite, pyrite, arsenopyrite
Rare gold, usually in pyrite
(Gold in pyrite, Ag-sulfosalts)
Pyrargyrite, proustite, argentite, electrum
Argentite, electrum
Galena, sphalerite, chalcopyrite, (argentite)
Vein contents
Opal, cristobalite, anatase, HgS, rare pyrite
Alunite, kaolin, pyrite; often extends downward along vein as kaolin halo around and above ore
General water table
Illite
Celadonite
Sericite
Vein
Propylitized
Near vein = feldspar-destructive
BRECCIA
Precious-metal horizon
Base-metal horizon
Boiling level
Near vein = feldspar-stable "potassic"
Adularia, minor to major albite
Silicification with adularia, minor albite
Note: Hanging wall structures complicate alteration patterns
(Chlorite, illite, carbonates, pyrite, montmorillonite)
Propylitized
(Higher epidote)
Quartz (amethyst), adularia, poss. minor albite
Broad, diffuse outer limit against fresh andesite, latite, rhyolite
Temperature, °C
100
150
200
250
Depth below spring orifice, m
0
50
100
150
200
250
300
350
400
450
500
550
Note: Alteration boundaries more diffuse than shown

associated with hydrothermal activity it is also possible that it is intrinsic to the tuffs since all freshly deposited subaerial pyroclastic rocks contain small quantities of Cu, U, Pb and Zn (Laznicka, 1985). Secondly, an intense phase of mineralisation occurred after the emplacement of the breccia. It is represented by the presence of coarse-grained, space-filling sphalerite and galena in fractures cutting breccia fragments and matrix, in spaces between fragments and as a replacement of pumice fragments and banding in banded crystal tuff. The presence of successive mineralised breccia zones within the stratigraphy, separated by poorly mineralised to barren, unbrecciated, rhyolite, crystal and lapilli tuff suggests that the mineralising fluids moved along faults and fractures cutting the less permeable, unbrecciated horizons and into the breccia where the porosity was higher. Once in the porous breccia, the fluids would then be controlled by the distribution and permeability of the breccia. Evidence for fluid movement along fractures exists in the fact that several of the east-west trending fractures in the Central Trench have an envelope of bleached, highly altered rock (0.25 to 0.5m wide). Precipitation of sulphides from these fluids within the porous brecciated layers resulted in development of a weak Pb, Zn and Ag zoning within the deposit. This is indicated by the presence of two main anomalous areas in the deposit surrounded by a low- to medium-grade Pb, Zn, Ag and Cu shell in the footwall and hanging walls. The mineralisation of the breccia may have occurred relatively soon after deposition while it still retained a high degree of porosity, since reduction in the porosity due to compaction of the breccia would have produced finer-grained mineralisation.

An epithermal deposit which appears to have similar characteristics to those of Mount Costigan is the Borealis deposit in Nevada (Strachan, 1986) (Table 1). Although this is a disseminated gold deposit the ore is hosted, in part, by an altered lenticular quartz breccia (Figure 32) that is in sharp contact with the underlying units. Extremely fine-grained, disseminated sulphides make up to 10% of the breccia matrix and consist primarily of pyrite with minor chalcopyrite, bravoite and cobaltite. No sphalerite and galena are present. The breccia is cut by a sub-vertical fault which is believed to have been the conduit by which ascending hydrothermal fluids altered and mineralised the host rocks. This deposit is similar to Mount Costigan in that: **1.** the breccia is broadly concordant to the stratigraphy; **2.** the ore is hosted by the breccia and occurs at a relatively shallow level; **3.** the proximity of the breccia to a local fault; **4.** the presence of a hydrothermal overprint of sugary quartz.

The only features of the Borealis deposit which do not correlate with Mount Costigan are the alteration mineralogy and zoning and the sulphide mineralogy (Table 1), since the ore at Borealis contains no sphalerite and galena or silver and the associated minor sulphides (bravoite and cobaltite) at Borealis are unknown at Mount Costigan. Alteration at Borealis is characterised by silicification and argillisation. Silicification varies from opal to quartz with some chalcedony, while argillic alteration ranges from montmorillonite to kaolinite-alunite and shows very sharp contacts with the unaltered rocks. Silicification at Mount Costigan is characterised solely by fine-grained microcrystalline quartz which replaces tuff and breccia matrix. Neither chalcedony nor opaline varieties of quartz have been reported. Similarly, the only

Figure 32: Generalised geological cross-section of the Borealis deposit, Nevada (Strachan, 1986). Note how the breccia is lenticular in shape and is cut by a major fault.

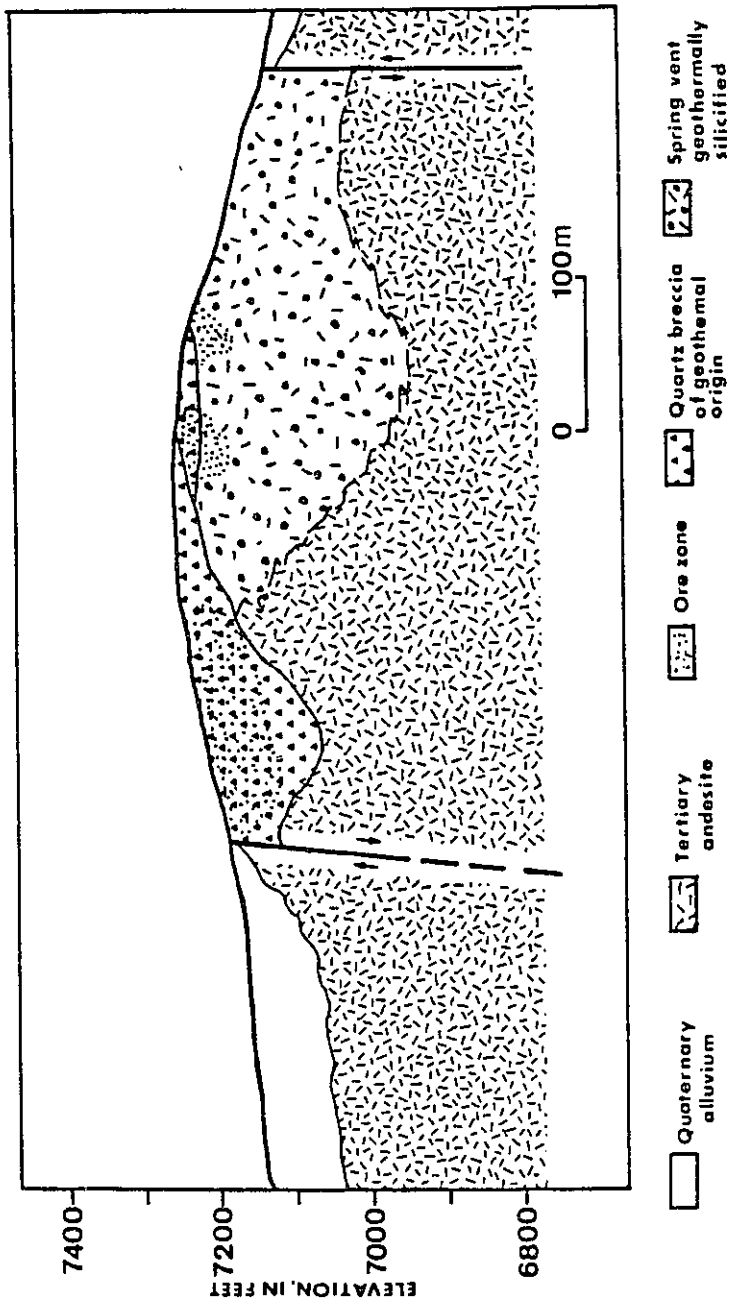
7400
7200
7000
6800
ELEVATION, IN FEET
0
100 m
Quaternary alluvium
Tertiary andesite
Ore zone
Quartz breccia of geothermal origin
Spring vent geothermally silicified

clay mineral reported at Mount Costigan is (rare) kaolinite; no alunite has ever been observed. However, the presence of siliceous and potassic alteration minerals at Mount Costigan which, while occurring in a different form (quartz and K-feldspar), may be analogous to the quartz, opal, chalcedony and adularia. Since there has been lower to middle greenschist facies metamorphism in the Mount Costigan area the microcrystalline quartz and K-feldspar present at Mount Costigan may represent the metamorphosed equivalent of the unstable varieties of quartz (opal and chalcedony) and K-feldspar (adularia) found at Borealis.

A volcanic origin for the Mount Costigan was first contemplated by Ruitenberg and Fyffe (1982) who considered it to represent the high-level
equivalent of a porphyry copper deposit. Thus considering all geological and geochemical evidence together from the above discussion, an epithermal origin for Mt. Costigan is regarded as being most plausible.

In conclusion, Mount Costigan is interpreted to represent a base metal variety of epithermal deposit hosted in a breccia, formed during the initial phase of the development of an epithermal system. Sulphide deposition occurred either during the mature, later, stages of the epithermal system or was associated with hydrothermal fluids related to intrusion of the Redstone Mountain Granite.

c. Tectonic History

As the epithermal deposits in New Zealand, the western U.S. and British Columbia are spatially associated with subduction zones then it is possible that Mount Costigan had a similar tectonic association. The current interpretation of the early Palaeozoic tectonic history of New Brunswick envisages development, during the Late Ordovician to Early Silurian, of a westerly dipping subduction zone (Van Staal, 1987) following the closure of the Iapetus Ocean. Since this subduction zone was active in the early Silurian (Van der Pluijm and Van Staal, 1988), then it may be possible that (provided the Costigan Mountain Formation is Silurian and not Devonian) the epithermal system responsible for the formation of the host rocks, alteration and sulphide mineralisation at Mount Costigan was associated with subduction-related volcanism. Similarly, it is possible that the intrusion of the Redstone Mountain Granite and any hydrothermal fluid activity (responsible deposition of sulphide mineralisation at Mount Costigan?) are also subduction-related, although Fyffe (1982) noted that faulting along the boundary of the Miramichi terrane and the Matapedia Cover Sequence has juxtaposed deep level Devonian granites against lower grade Devonian volcanic rocks.

CHAPTER 5

SUMMARY

To sum up, the conclusions reached about the geology of the Mt. Costigan deposit and immediate area are as follows:

1. The property stratigraphy represents a transition from near-shore marine mafic volcanics and sediments (basalt, siltstone and conglomerate) to sub-aerial felsic volcanism represented by the pyroclastic rocks and rhyolite flows (Costigan Mountain Formation). There is a return to near-shore sedimentation and volcanism with the re-appearance of the siltstones (Wapske Formation) at the top of the section. At both the top and bottom of the stratigraphy the transition from subaerial to submarine environment is marked by a series of intercalated siltstones and pyroclastic rocks.

2. The allochthonous breccia at Mount Costigan is best considered as having resulting from an episodic, explosive hydrothermal eruption since there are large unbrecciated rhyolite, crystal and lapilli tuff horizons up to 60m thick, separated by thinner brecciated zones. Thus, since several vertical drill holes in the Central Trench terminate in unbrecciated rock it is possible that another (mineralised ?) breccia zone exists at depth. The nature of the formation of the autochthonous breccia is unclear but it appears to have formed *in situ*, contemporaneous with or later than the allochthonous breccia.

3. Although the presence of circumferentially oriented fractures around the breccia exposed on the surface in the Central Trench may suggest a discordant, cylindrical structure to the breccia, distribution of the breccia as revealed in drill core shows that it is, in fact, concordant with the stratigraphy.

4. Alteration at Mt. Costigan has occurred in at least three phases, an early chlorite phase followed by later potassic and silicic phases. The chloritic and potassic phases are the most pervasive. The surface expression of silicification is best exposed in the Western Trenches and, locally, in the Central Trench.

5. The close association of silicification and chlorite alteration with the deposit indicates that the hydrothermal fluids responsible for producing the mineralisation also resulted in the alteration of the host rocks.

6. The presence of low to very low sulphide mineralisation in massive unbrecciated crystal tuff and medium- to high- sulphide mineralisation in the brecciated zones, indicates that there has probably been two periods of mineralising activity. The first (low-sulphide) period likely occurred prior to emplacement of the breccia and was relatively short lived whereas the second, higher sulphide, phase occurred after formation of the breccia and was a much longer lived event.

7. The hydrothermal activity at Mount Costigan resulted in the development of a weak Cu, Ag, Au zoning in the footwall and hanging wall of the deposit. The main deposit consists of two main anomalous areas of Pb, Zn and Ag around DDH's LCO-8 and LCO-5, 79-4, and 79-3 enveloped by a low- to

medium- grade shell. Underlying the main deposit are two minor disseminated mineralised zones that contain up to 20g/t Ag and appear to be parallel to the stratigraphy.

8. Due to the similarity between the geologic and geochemical characteristics of Mount Costigan and epithermal deposits in New Zealand, the western U.S. and British Columbia, Mount Costigan is interpreted to have had a similar genesis but instead represents a base-metal rich deposit. Although the best explanation for the mineralisation at Mount Costigan is an epithermal model, it is also possible that it resulted from metal-rich fluids associated with the intrusion of the nearby Redstone Mountain Granite.

9. The strong probability of the existence of a northeast to southwest trending subduction zone during the time the Mount Costigan deposit formed suggests that volcanic activity responsible for the development of the mineralising epithermal system was subduction-related. Similarly the intrusion of the Redstone Mountain Granite and related fluid activity would also be subduction-related.

REFERENCES

Ashley, R.P., 1974. Goldfield mining district. Nevada Bureau of Mines Geology report. v.19, p.49-66.

Berger, B.R., 1985. Geologic-geochemical features of hot-spring precious-metal deposits in Geologic characteristics of sediment- and volcanic-hosted disseminated gold deposits - search for an occurrence model (E.W. Tooker, ed.); United States Geological Survey Bulletin 1646, pp.47-53.

Bevier, M.L. and Whalen, 1989. U-Pb geochronology of Silurian granites, Miramichi terrane, New Brunswick. in Radiogenic age and isotope studies: Report 3, Geological Survey of Canada, Paper 89-2, in press.

Bonham, H.F., Jr. and Garside, L.J., 1979. Geology of the Tonopah, Lone Mountain, Klondike and northern Mud Lake quadrangles, Nevada. Nevada Bureau of Mines Geology Bulletin. v.92, 142p.

Bonham, H.F., Jr. and Garside, L.J., 1974. Tonopah mining district and vicinity; in Guidebook to the geology of four Tertiary volcanic centres in central Nevada. Nevada Bureau of Mines and Geology Report 19, pp. 42-48.

Bjornson, B., 1975. Report of work on the Ogilvie (Mount Costigan) Group. Amoco Canada Petroleum Ltd.. New Brunswick Department of Natural Resources and Energy, Mineral Resources Division, Assessment Report #470298, 36p..

Carmichael, I.S.E., Turner, F.J. and Verhoogen, J., 1974. Igneous Petrology, McGraw-Hill, New York. 739p.

Crevier, M., 1983. Report of the works for the first year of the "initial exploration period" on the Mt. Costigan property, Victoria County, New Brunswick. Minerais Lac Limitée. New Brunswick Department of Natural Resources and Energy, Mineral Resources Division, Assessment Report #472943, 13p..

Crevier, M., 1984. Report of the works for the second year of the "initial exploration period" on the Mount Costigan property, Victoria County, New Brunswick. Minerais Lac Limitée. New Brunswick Department of Natural Resources and Energy, Mineral Resources Division, Assessment Report #473035, 52p..

Crevier, M. and Gravel, L., 1984. Geology of the Mount Costigan Breccia-pipe. Unpubl. paper presented in Bathurst, New Brunswick at a district CIM meeting.

Daly, R.A., 1968. Igneous rocks and the depths of the Earth. Hafner Publishing Company, London.

De Ronde, C.E.J. and Blattner, P., 1988. Hydrothermal alteration, stable isotopes and fluid inclusions of the Golden Cross epithermal gold-silver deposit, Waihi, New Zealand. Economic Geology, v.83, p.895-917.

Fisher, R.V., 1979. Models for pyroclastic flows and pyroclastic surges. Jour. of Volc. and Geoth. Res., v.8, pp.305-318.

Fisher, R.V. and Heiken, G., 1982. Mont Pelée, Martinique: May 8 and 20, 1902, pyroclastic flows and surges. Jour. of Volc. and Geoth. Res., v.13, pp.339-371.

Fisher, R.V., Smith, A.L. and Roobol, M.J., 1980. Destruction of St. Pierre, Martinique, by ash cloud surges, May 8 and 20, 1902. Geology, v.8, pp.472-476.

Fyffe, L.R., 1982. Taconian and Acadian structural trends in central and northern New Brunswick. in Major Structural Zones and Faults of the Northern Appalachians (P. St. Julien and S. Béland, eds.). Geological Association of Canada Special Paper Number 24. p.117-130.

Fyffe, L.R. and Fricker, A., 1987. Tectonostratigraphic terrane analysis of New Brunswick. Maritime sediments and Atlantic Geology, v.23, pp.113-122.

Fyffe, L.R. and Pronk, A.G., 1985. Bedrock and surficial geology - Rock and till geochemistry in the Trousers Lake area, Victoria County, New Brunswick. Mineral Resources Division, Department of Natural Resources, New Brunswick, R.I. No. 20, 74p..

Gates, O. and Moench, R.H., 1981. Bimodal Silurian and Lower Devonian volcanic rock assemblages in the Mathias-Eastport area, Maine. United States Geological Survey Professional Paper 1184, 32p.

Grove, T.L. and Donnelly-Nolan, J.M., 1986. The evolution of young silicic lavas at Medicine Lake Volcano, California: Implications for the origin of compositional gaps in calc-alkaline series lavas. Contrib. Mineral. Petrol. v.92, pp.281-302.

Guilbert, J.M. and Park, C.F., 1986. The Geology of Ore Deposits. W.H. Freeman and Company. New York. 985p.

Heiken, G., 1979. Pyroclastic flow deposits. American Scientist, v.67, pp.564-571.

Henley, R.W. and Hedenquist, J.W., 1986. Introduction to the geochemistry of active and fossil geothermal systems. Mineralium Deposita Monograph Series on Mineral Deposits, No. 26; Guide to the active epithermal (geothermal) systems and precious metal deposits of New Zealand (Henley, R.W. and Hedenquist, J.W., eds.), pp.1-22.

Henneberger, R.C., 1986. Ohakuri fossil epithermal field. Mineralium Deposita Monograph Series on Mineral Deposits, No. 26; Guide to the active epithermal (geothermal) systems and precious metal deposits of New Zealand (Henley, R.W. and Hedenquist, J.W., eds.), pp.121-128.

Henneberger, R.C. and Browne, P.R.L., 1988. Hydrothermal alteration and evolution of the Okahuri hydrothermal system, Taupo Volcanic Zone New Zealand. Journal of Volcanology and Geothermal Research, v.34, p.211-231.

Huston, D.L. and Large, R.R., 1987. Genetic and exploration significance of the Zinc Ratio (100*Zn/(Zn + Pb)) in massive sulphides. Economic Geology, v.82, pp.1521-1539.

Johnson, C.M. and Lipman, P.W., 1988. Origin of metaluminous and alkaline volcanic rocks of the Latir volcanic field, northern Rio Grande rift, New Mexico. Contrib. Mineral. Petrol. v.100, p.107-128.

Laznicka, P., 1985. Empirical Metallogeny. Developments in economic geology #19, v.1. Elsevier Science Publishers B.V., Amsterdam. 1002p.

Laznicka, P., 1988. Breccias and coarse fragmentites: petrology, environments, associations, ores. Developments in economic geology #25. Elsevier Science Publishers B.V., Amsterdam. 832p.

Le Maitre, R.W., 1976. The chemical variability of some common igneous rocks. Journal of Petrology, v.17, pp.589-637.

Lock, T.B., 1956. Report on assessment work performed on the Costigan Mountain Claims, Victoria County, Western New Brunswick. New Brunswick Department of Natural Resources and Energy, Mineral Resources Division, Assessment Report #470300, 3p..

MacLean, W.H., 1963. Report on the Mount Costigan Claim Group. Mount Costigan Mines Ltd.. New Brunswick Department of Natural Resources and Energy, Mineral Resources Division, Assessment Report #470302, 11p..

Maingot, P.J., 1974. Report on Ogilvie (Costigan Mountain) Group, Tobique follow-up Project. New Brunswick Department of Natural Resources and Energy, Mineral Resources Division, Assessment Report #470297, 12p..

Nelson, C.E. and Giles, D.L., 1985. Hydrothermal Eruption Mechanisms and Hot Spring Gold Deposits. Economic Geology v.80, pp.1633-1639.

Nockolds, S.R., Knox, O'B. and Chinner, G.A., 1978. Petrology for students. Cambridge University Press, London. 435p.

Norton, D.L. and Cathles, L.M., 1973. Breccia pipes - products of exsolved vapour from magmas. Economic Geology, v.68, pp.540-546.

Panteleyev, A., 1986. Ore Deposits #10. A Canadian cordilleran model for epithermal Gold-Silver deposits. Geoscience Canada, v.13, no.2, pp.101-111.

Riddell, J.E., 1971. Summary report on the properties in the Gulquac River - Costigan Mountain area. Silcan Mines Ltd.. New Brunswick Department of Natural Resources and Energy, Mineral Resources Division, Assessment Report #470303, 18p..

Ruitenberg, A.A. and Fyffe, L.R., 1982. Mineral deposits associated with granitoid intrusions and related subvolcanic stocks in New Brunswick and their relationship to Appalachian tectonic evolution. CIM Bulletin, v.75, pp.83-97.

Sawkins, F.J., 1984. Metal deposits in relation to plate tectonics. Springer-Verlag, Heidelberg, West Germany. 325p.

Sheridan, M.F., 1979. Emplacement of pyroclastic flows: A review. Geological Society of America Special Paper 180, p.125-136.

Sillitoe, R.H. and Bonham, H.F., Jr., 1984. Volcanic Landforms and Ore Deposits. Economic Geology, v.79, pp.1286-1298.

Skinner, R., 1982. Geology of the Plaster Rock (east half) map area, New Brunswick. Geological Survey of Canada, Paper 81-8, 16p..

Skinner, R., 1974. Geology of the Tuadook Lake map area, New Brunswick. Geological Survey of Canada, Paper 74-33, 9p..

St. Peter, C., 1978. Geology of the Head of the Wapske River map area J-13 (21 J/14). Mineral Resources Division, Department of Natural Resources, New Brunswick, M.R. 78-1, 24pp..

Strachan, D.G., 1985. Geologic discussion of the Borealis gold deposit, Mineral County, Nevada. in Geologic characteristics of sediment- and volcanic-hosted disseminated gold deposits - search for an occurrence model (E.W. Tooker, ed.); United States Geological Survey Bulletin 1646, pp.89-94.

Van der Pluijm, B.A. and Van Staal, C.R., 1988. Characteristics and evolution of the Central Mobile Belt, Canadian Appalachians. Journal of Geology, v. 96, p.535-547.

Van Staal, C.R., 1987. Tectonic setting of the Tetagouche Group in northern New Brunswick: implications for tectonic models of the northern Appalachians. Canadian Journal of Earth Sciences, v.24, no.7, p.1329-1351.

Walker, G.P.L., 1985. Origin of coarse lithic breccias near ignimbrite source vents. Jour. of Volc. and Geoth. Res., v.25, pp.157-171.

Winchester, J.A. and Floyd, P.A., 1977. Geochemical discrimination of different magma series and their differentiation products using immobile elements. Chemical Geology, v.20, p.352-343.

Appendix 1: Whole rock geochemistry

	5035[1]	5037	5039	5040	5041	5044	5045A	5046	5047	5048	5050	5051	5065	5066
SiO_2	73.90	78.20	75.00	74.00	76.20	71.00	70.70	71.10	73.30	72.30	72.90	72.80	59.60	56.00
TiO_2	0.21	0.14	0.19	0.14	0.14	0.37	0.36	0.36	0.24	0.26	0.26	0.24	0.95	1.03
Al_2O_3	11.30	9.02	11.30	12.00	11.00	13.50	13.20	13.30	12.00	12.40	12.90	13.00	15.60	16.90
Fe_2O_3	2.05	1.09	1.04	1.21	0.97	3.10	2.74	3.12	1.90	2.32	1.68	0.81	7.60	8.84
FeO	1.30	0.60	0.60	0.50	0.30	1.40	1.40	1.60	0.90	1.00	0.60	0.10	6.00	7.00
MNO	0.18	0.15	0.10	0.10	0.05	0.11	0.10	0.12	0.12	0.13	0.08	0.02	0.35	0.34
MGO	2.27	2.66	0.85	0.72	0.32	0.30	0.27	0.30	0.88	0.86	0.61	0.07	3.43	4.39
CAO	0.02	0.02	0.02	0.01	0.01	0.54	0.30	0.33	0.24	0.02	0.01	0.01	1.02	1.11
Na_2O	0.02	0.01	0.03	0.09	0.05	1.93	2.18	2.71	0.01	0.03	0.02	0.04	1.62	1.81
K_2O	6.88	5.74	8.59	9.36	8.72	6.95	7.04	6.44	8.45	8.85	9.14	10.30	4.86	4.85
H2O+	nd	nd	nd	nd	nd	nd	nd	nd	nd	nd	nd	nd	nd	nd
H2O-	nd	nd	nd	nd	nd	nd	nd	nd	nd	nd	nd	nd	nd	nd
P_2O_5	0.03	0.03	0.03	0.02	0.02	0.07	0.07	0.07	0.04	0.04	0.04	0.03	0.15	0.18
TOTAL	98.16	97.66	97.75	98.15	97.78	99.27	98.36	99.45	98.08	98.21	98.24	97.42	101.18	102.45
CO_2	0.01	0.01	0.01	0.01	0.01	0.16	0.01	0.03	0.2	0.01	0.01	0.01	0.01	0.01
Ba[2]	670	410	1050	880	800	760	860	900	930	810	630	800	580	540
Co[2]	4.00	3.00	3.00	3.00	4.00	7.00	7.00	7.00	7.00	7.00	5.00	5.00	35.00	38.00
Cu[2]	2.00	7.00	8.50	3.50	14.00	8.00	5.50	6.00	39.00	6.00	4.00	2.50	2.50	23.00
Ni[2]	3.00	2.00	2.00	2.00	3.00	3.00	3.00	3.00	8.00	7.00	4.00	3.00	93.00	110.00
Rb[2]	240	190	280	310	250	280	260	240	320	310	330	340	180	200
Sr[2]	10.00	10.00	10.00	10.00	10.00	90.00	80.00	60.00	10.00	20.00	10.00	20.00	40.00	70.00
Y[2]	70.00	10.00	70.00	60.00	30.00	90.00	60.00	70.00	150.00	70.00	50.00	80.00	10.00	30.00
Zr[2]	340	190	260	210	190	600	600	590	360	390	400	410	190	220
V[2]	6.00	2.00	6.00	4.00	4.00	8.00	6.00	8.00	10.00	16.00	8.00	8.00	170.00	170.00
K_2O+Na_2O	6.90	5.75	8.62	9.45	8.77	8.88	9.22	9.15	8.46	8.88	9.16	10.34	6.48	6.66
Alk_T	0.99	0.99	0.99	0.99	0.99	0.78	0.76	0.70	0.99	0.99	0.99	0.99	0.75	0.73
Rb/Sr	24.00	19.00	28.00	31.00	25.00	3.11	3.25	4.00	32.00	15.50	33.00	17.00	4.50	2.86
Zr/TiO_2	0.16	0.14	0.14	0.15	0.14	0.16	0.17	0.16	0.15	0.15	0.15	0.17	0.02	0.02

5035 - Mineralised crystal tuff breccia, Central Trench
5037 - ibid
5039 - Massive crystal tuff, crackle breccia, North Trench
5040 - Banded crystal tuff, North Trench
5041 - Silicified massive crystal tuff, Central Trench
5044 - Flow-banded rhyolite, South-west Trench
5045A - ibid
5046 - ibid
5047 - Massive crystal tuff, East Trench
5048 - Banded crystal tuff, East Trench
5050 - Massive crystal tuff, East Trench
5051 - ibid
5065 - Siltstone, DDH LCO-84-5 (221.5m)
5066 - Siltstone, DDH LCO-84-3 (227.0m)

[1] Short form for samples collected by G.P. Watson, G.S.C.. First digit refers to the year (i.e. '85). Remaining digits represent the sample number. E.g. 85-085.

[2] Values in parts per million

Appendix 1 (con't)

	6265	6266	6267	6268	6269	6270	6271	6272	6273	6274	6275	7010	7013
SiO_2	75.90	73.60	72.90	78.00	70.10	68.60	68.00	70.40	59.10	72.90	70.70	70.90	52.70
TiO_2	0.15	0.16	0.14	0.14	0.24	0.19	0.23	0.18	0.21	0.21	0.32	0.72	1.11
Al_2O_3	11.60	12.40	12.50	11.20	13.80	13.80	12.80	11.60	15.80	10.40	12.70	11.10	15.30
Fe_2O_3	0.56	1.48	1.50	1.08	1.91	2.38	2.79	3.74	3.91	2.90	1.71	5.00	7.41
FeO	0.30	0.70	0.70	0.70	0.90	1.40	1.60	2.20	2.30	1.80	0.70	3.20	5.60
MnO	0.02	0.03	0.03	0.04	0.15	0.21	0.31	0.31	0.30	0.26	0.11	0.08	0.14
MgO	0.05	0.26	0.16	0.21	1.01	1.53	3.64	3.43	5.44	4.32	1.43	2.33	3.52
CaO	0.05	0.04	0.04	0.19	0.04	0.03	0.04	0.03	0.01	0.04	0.04	1.46	5.73
Na_2O	0.13	0.50	0.09	2.18	0.01	0.07	0.01	0.01	0.07	0.01	0.01	2.47	4.09
K_2O	9.17	8.96	9.59	5.04	9.34	9.82	7.91	6.94	9.87	4.99	8.86	1.94	2.93
H_2O+	0.30	0.60	0.50	0.70	1.40	1.10	2.00	2.10	2.80	2.20	1.20	2.30	2.80
H2O-	nd	nd	nd	nd	nd	nd	nd	nd	nd	nd	nd	nd	nd
P_2O_5	0.02	0.02	0.02	0.02	0.04	0.02	0.03	0.03	0.02	0.03	0.03	0.12	0.18
TOTAL	98.25	98.75	98.17	99.50	98.94	99.15	99.36	100.97	99.83	100.06	97.81	101.62	101.51
CO_2	0.01	0.01	0.01	0.02	0.06	0.01	0.01	0.01	0.01	0.01	0.01	0.62	3.80
Ba	1060	1070	1020	660	780	720	730	520	680	470	590	510	690
Co	1.00	1.00	1.00	1.00	1.00	1.00	1.00	1.00	1.00	1.00	1.00	23.00	27.00
Cu	3.00	2.00	2.00	2.00	21.00	6.00	21.00	39.00	29.00	3.00	31.00	12.00	39.00
Ni	2.00	2.00	1.00	1.00	2.00	1.00	3.00	2.00	1.00	1.00	2.00	58.00	24.00
Rb	300	310	320	190	270	300	250	220	290	190	280	90.00	100.00
Sr	20.00	20.00	20.00	60.00	20.00	20.00	20.00	10.00	10.00	10.00	10.00	92.00	219
Y	60.00	90.00	60.00	60.00	70.00	70.00	60.00	30.00	70.00	20.00	60.00	24.00	27.00
Zr	190	210	230	200	290	250	280	250	290	340	240	250	136
V	6.00	6.00	4.00	6.00	10.00	8.00	12.00	10.00	8.00	6.00	24.00	nd	nd
K_2O+Na_2O	9.30	9.46	9.68	7.22	9.35	9.89	7.92	6.95	9.94	5.00	8.87	4.41	7.02
Alk_T	0.98	0.95	0.99	0.69	0.99	0.99	0.99	0.99	0.99	0.99	0.99	0.44	0.42
Rb/Sr	15.00	15.50	16.00	3.17	13.50	15.00	12.50	22.00	29.00	19.00	28.00	0.99	0.46
Zr/TiO_2	0.13	0.13	0.16	0.14	0.12	0.13	0.12	0.14	0.14	0.16	0.07	0.03	0.01

6267 - Altered flow-banded rhyolite, Costigan Mountain Formation
6268 - Flow-banded rhyolite with lithophysal concretions, Costigan Mountain Formation
6269 - Silicified banded crystal tuff, North Trench (West end), Mount Costigan deposit
6270 - Silicified banded crystal tuff, North Trench (West end), Mount Costigan deposit
6271 - Silicified banded crystal tuff, North Trench (West end), Mount Costigan deposit
6272 - Banded crystal tuff, Central Trench (west of DDH #9), Mount Costigan deposit
6273 - Altered lapilli tuff, South Trench (centre)
6274 - Altered lapilli tuff, South Trench (south end)
6275 - Flow-banded rhyolite, South Trench, (north end)
7010 - Massive to well-bedded quartz-rich sandstone
7013 - Layered, mafic tuffs and vesicular flows

Appendix 1 (con't)

	7014	7018	7020	7026	7027	7028	7031	7032	7033	7039	7040	58[3]
SiO_2	50.80	47.80	47.70	53.10	74.40	50.10	49.70	51.00	71.00	72.90	73.30	76.48
TiO_2	2.18	1.54	2.05	1.25	0.14	1.15	1.51	1.61	0.28	0.21	0.24	0.13
Al_2O_3	14.60	14.70	15.30	17.40	12.50	15.50	15.10	14.90	14.10	13.40	14.10	9.45
Fe_2O_3	9.72	8.82	10.00	7.85	1.83	7.09	8.93	8.53	1.78	1.07	0.95	2.18
FeO	6.50	6.50	5.40	6.20	1.30	5.40	6.30	6.70	0.90	0.10	0.10	nd
MnO	0.14	0.16	0.18	0.23	0.04	0.17	0.17	0.19	0.05	0.02	0.02	0.16
MgO	3.37	7.61	6.63	4.81	0.05	5.10	6.76	6.23	0.36	0.19	0.09	2.24
CaO	5.40	6.30	8.27	4.21	0.53	7.25	6.35	5.57	0.84	0.03	0.13	0.08
Na_2O	4.98	4.02	4.04	4.70	3.15	4.49	4.77	3.85	5.62	0.10	4.77	0.03
K_2O	1.55	1.39	0.56	1.35	5.38	0.97	0.77	2.36	3.55	9.34	4.49	6.34
H_2O+	1.90	1.90	2.00	1.30	0.60	2.60	1.90	1.20	0.50	1.30	0.80	nd
H_2O-	nd	nd	nd	nd	nd	nd	nd	nd	nd	nd	nd	nd
P_2O_5	0.35	0.25	0.38	0.21	0.02	0.23	0.25	0.26	0.06	0.03	0.04	0.03
TOTAL	101.49	100.99	102.51	102.61	99.94	100.05	102.51	102.40	99.04	98.69	99.03	97.12
CO_2	2.61	2.30	0.01	0.98	0.25	4.51	0.76	1.35	1.37	nd	nd	nd
Ba	260	360	240	190	180	210	210	530	570	830	770	433
Co	33.00	45.00	40.00	40.00	2.00	33.00	38.00	36.00	3.00	2.00	2.00	nd
Cu	54.00	18.00	38.00	14.00	12.00	4.00	29.00	34.00	4.00	2.00	7.00	nd
Ni	19.00	76.00	70.00	42.00	6.00	32.00	66.00	50.00	7.00	6.00	9.00	nd
Rb	52.00	43.00	19.00	51.00	200	48.00	31.00	81.00	134	350	200	224
Sr	258	230	235	270	154	200	280	223	94.00	98.00	87.00	16.00
Y	57.00	36.00	32.00	28.00	110.00	30.00	38.00	36.00	50.00	34.00	38.00	38.00
Zr	252	150	209	163	498	172	157	168	433	150	172	211
V	nd	nd	nd	nd	nd	nd	nd	nd	nd	nd	nd	nd
K_2O+Na_2O	6.53	5.41	4.60	6.05	8.53	5.46	5.54	6.21	9.17	9.44	9.26	6.37
Alk_T	0.24	0.26	0.12	0.22	0.63	0.18	0.14	0.38	0.39	0.99	0.48	0.01
Rb/Sr	0.20	0.19	0.08	0.19	1.30	0.24	0.11	0.36	1.43	3.57	2.30	14.00
Zr/TiO_2	0.01	0.01	0.01	0.01	0.36	0.01	0.01	0.01	0.15	0.07	0.07	0.16

7014 - Medium-grained brown basalt with calcite, quartz and epidote filling rubble top
7018 - Basalt in contact with bedded sedimentary rocks
7020 - Basalt
7026 - Well laminated to dark-grey sandstone/siltstone with cross-beds and graded bedding
7027 - Altered, vesicular basalt
7028 - Basalt
7031 - Basalt
7032 - Basalt in contact with siltstone
7033 - Massive rhyolite
7039 - Rhyolite, massive, flow-banded and minor porphyritic
7040 - massive brecciated rhyolite
58 - Flow-banded rhyolite (Central Trench)

[3] Short form for sample numbers from this study. Prefix is MC-87-

Appendix 1 (con't)

	75	57	25	30	39	46	65	68	63	PNG	NZ	R1	R2	R3
SiO_2	67.08	69.58	61.93	55.20	76.60	74.44	76.26	69.22	70.32	75.33	74.22	71.10	72.77	72.80
TiO_2	0.68	0.56	0.18	0.23	0.14	0.28	0.13	0.15	0.62	0.27	0.28	0.37	0.29	0.33
Al_2O_3	12.56	9.92	15.48	18.71	11.05	9.88	9.68	12.70	9.80	12.58	13.27	14.15	13.33	13.49
Fe_2O_3	6.42	5.68	3.87	5.00	1.28	1.67	0.90	0.23	3.40	1.58	0.88	1.56	1.40	1.45
FeO	nd	nd	nd	nd	nd	nd	nd	nd	nd	0.88	0.92	1.33	1.02	0.88
MnO	0.43	0.43	0.27	0.37	0.06	0.14	0.14	0.02	0.39	0.07	0.05	0.05	0.07	0.08
MgO	3.65	6.36	4.66	5.69	0.97	2.07	2.29	0.01	3.88	0.24	0.28	0.55	0.38	0.38
CaO	0.06	0.06	0.05	0.05	0.06	0.05	0.09	0.05	0.05	1.25	1.59	1.87	1.22	1.20
Na_2O	0.12	0.13	0.30	0.41	0.16	0.17	0.14	0.13	0.14	4.02	4.24	3.47	3.34	3.38
K_2O	4.20	1.31	10.04	10.69	8.56	6.87	6.84	11.12	5.43	3.82	3.18	4.73	4.58	4.46
H_2O+	nd	nd	nd	nd	nd	nd	nd	nd	nd	0.31	0.80	0.71	nd	nd
H_2O-	nd	nd	nd	nd	nd	nd	nd	nd	nd	nd	nd	nd	nd	nd
P_2O_5	0.11	0.15	0.02	0.02	0.02	0.04	0.01	0.03	0.12	0.02	0.05	0.11	0.10	0.08
TOTAL	95.31	94.18	96.80	96.37	98.90	95.61	96.48	93.66	94.15	100.37	99.76	100.00	98.50	98.53
CO_2	nd	nd	nd	nd	nd	nd	nd	nd	nd	nd	nd	nd	nd	nd
Ba	408	166	552	505	495	431	417	660	401	nd	nd	nd	nd	nd
Co	nd	nd	nd	nd	nd	nd	nd	nd	nd	nd	nd	nd	nd	nd
Cu	nd	nd	nd	nd	nd	nd	nd	nd	nd	nd	nd	nd	nd	nd
Ni	47.00	33.00	nd	nd	nd	nd	nd	nd	nd	nd	nd	nd	nd	nd
Rb	158	51.00	330	345	245	235	247	386	176	nd	nd	nd	nd	nd
Sr	19.00	nd	17.00	11.00	11.00	15.00	23.00	27.00	8.00	nd	nd	nd	nd	nd
Y	42.00	51.00	73.00	75.00	49.00	61.00	39.00	47.00	41.00	nd	nd	nd	nd	nd
Zr	133	118	281	359	200	200	192	252	193	nd	nd	nd	nd	nd
V	100.00	61.00	nd	8.00	4.00	nd	nd	nd	29.00	nd	nd	nd	nd	nd
K_2O+Na_2O	4.32	1.44	10.34	11.10	8.72	7.04	6.98	11.25	5.57	7.84	7.42	8.20	7.92	7.84
Alk_T	0.01	0.01	0.01	0.01	0.01	0.9	0.97	0.98	0.99	0.97	0.49	0.43	0.58	0.58
Rb/Sr	8.31	nd	19.41	31.36	22.27	16.75	10.75	14.86	22.00	nd	nd	nd	nd	nd
Zr/TiO_2	0.02	0.02	0.16	0.16	0.14	0.07	0.15	0.17	0.03	nd	nd	nd	nd	nd

75 - Brown (tuffaceous) siltstone from East Trench
57 - Aphanitic mafic dyke (Central Trench)
25 - Spherulitic, flow-banded rhyolite (South Trench)
30 - Perlite (South Trench)
39 - Silicified massive crystal tuff (Central Trench)
46 - Flow-banded Rhyolite (Central Trench)
65 - Flow-banded rhyolite (Central Trench)
68 - Silicified siltstone (Central Trench)
63 - Massive pink rhyolite (Central Trench)
PNG - Rhyolite from Papua New Guinea (Carmichael, Turner and Verhoogen, 1974)
NZ - Rhyolite from New Zealand (Taupo Volcanic Zone) (ibid)
R1 - Rhyolite from Nockolds, Knox and Chinner (1978), average of 80
R2 - Rhyolite from Daly (1968), average of 102
R3 - ibid, average of 126

Appendix 1 (con't)

	R4	R5	R6	R7	R8	R9	R10	R11	R12	R13	R14
SiO_2	72.82	74.00	73.10	73.00	73.00	72.90	71.20	70.90	71.00	73.63	74.50
TiO_2	0.28	0.27	0.28	0.28	0.27	0.28	0.32	0.36	0.37	0.25	0.23
Al_2O_3	13.27	13.90	14.10	13.90	13.90	13.90	14.80	14.90	14.80	13.83	13.05
Fe_2O_3	1.48	1.87	1.91	1.85	1.87	1.95	2.42	2.62	2.39	1.07	1.50
FeO	1.11	nd	nd	nd	nd	nd	nd	nd	nd	1.21	0.99
MnO	0.06	0.02	0.03	0.03	0.03	0.03	0.04	0.04	0.03	0.08	0.04
MgO	0.39	0.30	0.38	0.35	0.35	0.34	0.77	0.85	0.63	0.46	0.09
CaO	1.14	1.25	1.25	1.25	1.25	1.31	2.04	2.19	1.68	0.79	0.69
Na_2O	3.55	3.78	3.94	3.92	4.01	3.83	3.92	4.01	4.44	2.96	3.85
K_2O	4.30	4.37	4.35	4.34	4.33	4.30	3.87	3.81	3.86	4.90	4.50
H_2O+	1.10	nd	nd	nd	nd	nd	nd	nd	nd	0.68	0.84
H_2O-	0.31	nd	nd	nd	nd	nd	nd	nd	nd	0.09	0.08
P_2O_5	0.07	0.05	0.05	0.05	0.05	0.04	0.08	0.09	0.04	0.03	0.05
TOTAL	99.88	99.81	99.39	98.97	99.06	98.88	99.46	99.77	99.24	99.98	100.41
CO_2	0.08	nd	nd	nd	nd	nd	nd	nd	nd	0.04	0.02
Ba	nd	820	858	863	865	845	747	790	942	554	636
Co	nd	1.80	2.20	2.00	2.00	2.10	4.10	4.30	3.10	2.42	1.01
Cu	nd	nd	nd	nd	nd	nd	nd	nd	nd	nd	nd
Ni	nd	nd	nd	nd	nd	nd	nd	nd	nd	6.10	13.00
Rb	nd	146	150	152	154	157	122	136	112	74.00	144
Sr	nd	113	118	113	115	132	154	186	135	140	38.00
Y	nd	27.00	23.00	26.00	23.00	27.00	20.00	24.00	32.00	57.00	100.00
Zr	nd	217	223	229	230	239	184	212	267	325	443
V	nd	nd	nd	nd	nd	nd	nd	nd	nd	12.30	15.00
K_2O+Na_2O	7.85	8.15	3.94	8.26	8.34	8.13	7.79	7.82	8.30	7.86	8.35
Alk_T	0.55	0.54	1.10	0.53	0.52	0.53	0.49	0.49	0.47	0.62	0.54
Rb/Sr	nd	1.29	1.27	1.35	1.34	nd	0.79	0.73	0.83	0.53	3.79
Zr/TiO_2	nd	0.08	0.08	0.08	0.08	0.08	0.06	0.06	0.07	0.13	0.19

R4 - Rhyolite from Le Maitre (1976), average of 670
R5 - Rhyolite from Grove and Donnelly-Nolan (1986)
R6 - ibid
R7 - ibid
R8 - ibid
R9 - ibid
R10 - ibid, less than 72% SiO_2
R11 - ibid
R12 - ibid
R13 - Silurian rhyolite (average of 3) from Gates and Moench (1981)
R14 - Early Devonian rhyolite (average of 2), ibid

Appendix 2a: Assay data from drill holes cutting the footwall

HOLE	FROM[1]	TO[1]	LEAD[2]	ZINC[2]	SILVER[3]	COPPER[2]	GOLD[3]	Pb+Zn[2]	Zn ratio
18[4]	5.25	6.89	0.016	0.01	2.06			0.03	38.46
	6.89	8.53	0.039	0.016	2.06			0.06	29.09
	8.53	10.17	0.022	0.096	1.37			0.12	81.36
	10.17	11.81	0.033	0.083	0.69			0.12	71.55
	11.81	13.45	0.014	0.067	2.74			0.08	82.72
	13.45	15.09	0.009	0.05	0.69			0.06	84.75
	15.09	16.73	0.009	0.047	1.37			0.06	83.93
	16.73	18.37	0.01	0.035	0.69			0.05	77.78
	18.37	20.01	0.016	0.039	2.06			0.06	70.91
	20.01	21.65	0.019	0.044	0.69			0.06	69.84
	21.65	23.29	0.019	0.048	2.06			0.07	71.64
	23.29	24.93	0.005	0.047	0.69			0.05	90.38
	24.93	26.57	0.044	0.062	3.43			0.11	58.49
	26.57	28.22	0.022	0.048	2.06			0.07	68.57
	28.22	29.86	0.022	0.061	0.69			0.08	73.49
	29.86	31.50	0.009	0.084	1.37			0.09	90.32
	31.50	33.14	0.043	0.163	2.06			0.21	79.13
	33.14	34.78	0.037	0.096	2.06			0.13	72.18
	34.78	36.42	0.039	0.163	0.69			0.20	80.69
	36.42	38.06	0.027	0.057	0.69			0.08	67.86
	38.06	39.70	0.046	0.069	0.69			0.12	60.00
	39.70	41.34	0.016	0.037	2.06			0.05	69.81
	41.34	42.98	0.02	0.04	0.69			0.06	66.67
	42.98	44.62	0.031	0.051	2.06			0.08	62.20
	44.62	46.26	0.08	0.073	0.69			0.15	47.71
	46.26	47.90	0.01	0.021	0.69			0.03	67.74
	47.90	49.54	0.02	0.033	2.06			0.05	62.26
	49.54	51.18	0.008	0.018	1.37			0.03	69.23
	51.18	52.82	0.015	0.024	1.37			0.04	61.54
	52.82	54.46	0.009	0.021	0.69			0.03	70.00
	54.46	56.10	0.008	0.014	2.06			0.02	63.64
	56.10	57.74	0.008	0.021	1.37			0.03	72.41
	57.74	59.38	0.034	0.099	0.69			0.13	74.44
	59.38	61.02	0.01	0.016	0.69			0.03	61.54
	61.02	62.66	0.016	0.019	2.06			0.04	54.29
	62.66	64.30	0.012	0.019	2.06			0.03	61.29
	64.30	65.94	0.014	0.026	0.69			0.04	65.00
	65.94	67.59	0.036	0.027	0.34			0.06	42.86
	67.59	69.23	0.012	0.018	2.06			0.03	60.00
	69.23	70.87	0.044	0.076	0.69			0.12	63.33
	70.87	72.51	0.017	0.025	2.06			0.04	59.52
	72.51	74.15	0.105	0.159	0.69			0.26	60.23
	74.15	75.79	0.022	0.027	0.69			0.05	55.10
	75.79	77.43	0.024	0.035	2.06			0.06	59.32
	77.43	79.07	0.005	0.01	1.37			0.02	66.67
	79.07	80.71	0.009	0.015	0.69			0.02	62.50
	80.71	82.35	0.008	0.014				0.02	63.64
	82.35	83.99	0.012	0.02	1.37			0.03	62.50
	83.99	85.63	0.045	0.043	1.37			0.09	48.86
	85.63	87.27	0.03	0.051	1.37			0.08	62.96
	87.27	88.91	0.03	0.251	0.69			0.28	89.32

HOLE	FROM	TO	LEAD	ZINC	SILVER	COPPER	GOLD	Pb+Zn	Zn ratio
18	88.91	90.55	0.046	0.032	2.06			0.08	41.03
	90.55	92.19	0.033	0.046	0.69			0.08	58.23
	92.19	93.83	0.109	0.156	0.69			0.27	58.87
	93.83	95.47	0.118	0.149	0.69			0.27	55.81
	95.47	97.11	0.03	0.017	0.69			0.05	36.17
	97.11	98.75	0.125	0.418	1.37			0.54	76.98
	98.75	100.39	0.404	0.159	0.69			0.56	28.24
	100.39	102.03	0.067	0.08	2.06			0.15	54.42
	102.03	103.67	0.016	0.023	0.69			0.04	58.97
	103.67	105.31	0.031	0.03				0.06	49.18
	105.31	106.96	0.006	0.012	1.37			0.02	66.67
	106.96	108.60	0.013	0.027	1.37			0.04	67.50
	108.60	110.24	0.006	0.021	0.69			0.03	77.78
	110.24	111.88	0.01	0.23	0.34			0.24	95.83
	111.88	113.52	0.006	0.01	0.69			0.02	62.50
	113.52	115.16	0.013	0.011	0.69			0.02	45.83
	115.16	116.80	0.012	0.016	0.69			0.03	57.14
	116.80	118.44	0.011	0.023	0.69			0.03	67.65
	118.44	120.08	0.014	0.021	0.69			0.04	60.00
	120.08	121.72	0.009	0.013	0.69			0.02	59.09
	121.72	123.36	0.006	0.015	1.37			0.02	71.43
	123.36	125.00	0.006	0.011	1.03			0.02	64.71
	125.00	126.64	0.004	0.008	0.69			0.01	66.67
	126.64	128.28	0.003	0.008	0.69			0.01	72.73
	128.28	129.92	0.003	0.013	2.06			0.02	81.25
	129.92	131.56	0.005	0.012	0.69			0.02	70.59
	131.56	133.20	0.003	0.007	0.34			0.01	70.00
	133.20	134.84	0.009	0.012	0.69			0.02	57.14
	134.84	136.48	0.004	0.012	1.37			0.02	75.00
	136.48	138.12	0.004	0.016	0.69			0.02	80.00
	138.12	139.76	0.002	0.008	2.06			0.01	80.00
	139.76	141.40	0.003	0.009	1.37			0.01	75.00
	141.40	143.04	0.006	0.009	0.69			0.02	60.00
	143.04	144.69	0.005	0.01	1.37			0.02	66.67
	144.69	146.33	0.004	0.008	1.37			0.01	66.67
	146.33	147.97	0.003	0.008	0.69			0.01	72.73
	147.97	149.61	0.009	0.015	1.37			0.02	62.50
	149.61	151.25	0.011	0.022	0.69			0.03	66.67
	151.25	152.89	0.004	0.008	0.69			0.01	66.67
	152.89	154.53	0.003	0.01	1.37			0.01	76.92
	154.53	156.17	0.007	0.014	0.69			0.02	66.67
	156.17	157.81	0.003	0.008	0.69			0.01	72.73
	157.81	159.45	0.002	0.009	1.37			0.01	81.82
	159.45	161.09	0.009	0.011	0.69			0.02	55.00
	161.09	162.73	0.006	0.009	1.37			0.02	60.00
	162.73	164.37	0.003	0.009				0.01	75.00
	164.37	166.01	0.015	0.009	0.07			0.02	37.50
	166.01	167.65	0.003	0.008	0.69			0.01	72.73
	167.65	169.29	0.005	0.008	0.69			0.01	61.54
	169.29	170.93	0.027	0.036				0.06	57.14
	170.93	172.57	0.003	0.008	0.69			0.01	72.73
	172.57	174.21	0.002	0.008	0.69			0.01	80.00
	174.21	175.85	0.005	0.009	1.37			0.01	64.29
	175.85	177.49	0.931	0.18	0.69			1.11	16.20
	177.49	179.13	0.013	0.027	1.37			0.04	67.50

HOLE	FROM	TO	LEAD	ZINC	SILVER	COPPER	GOLD	Pb+Zn	Zn ratio
18	179.13	180.77	0.01	0.007	0.34			0.02	41.18
	180.77	182.09	0.005	0.01	0.34			0.02	66.67
84-2[5]	64.50	66.00	0.13	0.47				0.60	78.33
	66.00	67.50	0.65	0.12				0.77	15.58
	69.00	70.50	0.64	0.52				1.16	44.83
	70.50	72.00	0.44	0.69				1.13	61.06
	83.00	84.00	0.02	0.85				0.87	97.70
	84.00	85.50	0.02	0.89				0.91	97.80
	87.00	88.50	0.72	1.20				1.92	62.50
	88.50	90.00	0.06	0.47				0.53	88.68
	90.00	91.50	0.51	0.05				0.56	8.93
	94.75	96.00	0.28	3.50	1.71		0.20	3.78	92.59
	96.00	97.50	0.40	5.40	6.86		0.30	5.80	93.10
	97.50	99.00	0.45	1.10	3.43			1.55	70.97
	99.00	100.50	1.22	2.40	5.14			3.62	66.30
	100.50	102.00	0.86	3.00	1.71			3.86	77.72
	102.00	103.50	0.84	1.18				2.02	58.42
	103.50	105.00	0.00	0.17				0.17	97.70
84-3	171.92	172.36	0.52	1.06				1.58	67.09
	203.45	204.00	0.53	0.72	3.43	0.86		1.25	57.60
	205.95	207.00	0.79	1.67	6.86	0.84		2.46	67.89
	207.00	208.50	1.04	1.58	8.57	1.98		2.62	60.31
	208.50	210.00	1.01	0.98	5.14	1.60		1.99	49.25
	210.00	211.50	1.46	2.60	6.86	1.40		4.06	64.04
	215.20	216.00	0.75	2.15	5.14	0.91		2.90	74.14
	216.00	217.50	0.49	1.99	5.14	1.15		2.48	80.24
	217.50	219.00	0.96	4.40	10.29	0.42		5.36	82.09
	219.00	220.50	0.17	0.51				0.68	75.00
84-4	22.50	24.00	0.00	0.36				0.36	99.17
	66.00	67.50	0.16	0.44				0.60	73.33
	67.50	69.00	0.09	0.40				0.49	81.63
	70.30	71.40	0.10	0.37				0.47	78.72
	96.00	97.50	0.05	0.23				0.28	82.14
	98.50	99.25	0.05	1.15				1.20	95.83
15	7.87	9.51	0.40	0.65				1.05	61.90
	9.51	11.15	1.50	2.43				3.93	61.83
	11.15	12.79	0.26	0.32				0.58	55.17
	12.79	14.43	0.86	0.30				1.16	25.86
	14.43	16.07	0.04	0.21				0.25	84.00
	16.07	17.71	0.53	0.59				1.12	52.68
	17.71	19.35	0.13	0.63				0.76	82.89
	19.35	20.99	0.28	1.06				1.34	79.10
	20.99	22.63	0.86	0.51				1.37	37.23
	22.63	24.27	0.04	0.17				0.21	80.95
	24.27	25.91	0.05	0.02				0.07	28.57
	25.91	27.55	0.05	0.03				0.08	37.50
	27.56	29.20	0.03	0.05				0.08	62.50
	29.20	30.84	0.56	1.26				1.82	69.23
	30.84	32.48	0.35	0.99				1.34	73.88
	32.48	34.12	0.01	0.08				0.09	88.89
	34.12	35.76	0.00	0.04				0.04	100.00
	35.76	37.40	0.06	0.19				0.25	76.00
	37.40	39.04	0.07	0.15				0.22	68.18
	39.04	40.68	0.04	0.17				0.21	80.95
	40.68	42.32	0.00	0.08				0.08	100.00

HOLE	FROM	TO	LEAD	ZINC	SILVER	COPPER	GOLD	Pb+Zn	Zn ratio
15	42.32	43.96	0.02	0.01				0.03	33.33
	43.96	45.60	0.07	0.23				0.30	76.67
	45.60	47.24	0.21	0.28				0.49	57.14
	47.24	48.88	0.11	0.15				0.26	57.69
	48.88	50.52	0.16	0.06				0.22	27.27
	50.52	52.16	0.09	0.17				0.26	65.38
	52.16	53.80	0.20	0.01				0.21	4.76
	53.80	55.44	0.24	0.17				0.41	41.46
	55.44	57.08	0.20	0.79				0.99	79.80
	57.08	58.72	0.46	0.80				1.26	63.49
	58.72	60.36	0.65	1.23				1.88	65.43
	60.36	62.00	0.59	1.18				1.77	66.67
	62.00	63.64	0.30	0.73				1.03	70.87
	63.64	65.28	0.07	0.18				0.25	72.00
	65.28	66.92	0.10	0.07				0.17	41.18
	66.93	68.57	0.13	0.22				0.35	62.86
	68.57	70.21	0.83	1.11				1.94	57.22
	70.21	71.85	2.38	3.82				6.20	61.61
	71.85	73.49	0.98	1.60				2.58	62.02
	73.49	75.13	0.42	0.67				1.09	61.47
	75.13	76.77	0.21	0.54				0.75	72.00
	76.77	78.41	0.04	0.12				0.16	75.00
	78.41	80.05	0.14	0.14				0.28	50.00
	80.05	81.69	0.38	0.65				1.03	63.11
	81.69	83.33	0.12	0.39				0.51	76.47
	83.33	84.97	0.15	0.21				0.36	58.33
	84.97	86.61	0.26	0.57				0.83	68.67
	86.61	88.25	0.30	0.99				1.29	76.74
	88.25	89.89	0.45	0.70				1.15	60.87
	89.89	91.53	0.40	0.68				1.08	62.96
	91.53	93.17	0.61	0.64				1.25	51.20
	93.17	94.81	1.18	1.27				2.45	51.84
	94.81	96.45	0.64	0.41				1.05	39.05
	96.45	98.09	0.28	0.25				0.53	47.17
	98.09	99.73	0.59	0.72				1.31	54.96
	99.73	101.37	0.80	0.80				1.60	50.00
	101.37	103.01	0.57	0.47				1.04	45.19
	103.01	104.65	0.18	0.17				0.35	48.57
	104.65	106.29	0.45	0.50				0.95	52.63
	106.30	107.94	0.66	0.41				1.07	38.32
	107.94	109.58	0.84	1.59				2.43	65.43
	109.58	111.22	0.52	0.46				0.98	46.94
	111.22	112.86	0.36	0.20				0.56	35.71
	112.86	114.50	0.81	0.99				1.80	55.00
	114.50	116.14	0.70	2.49				3.19	78.06
	116.14	117.78	0.63	0.70				1.33	52.63
	117.78	119.42	0.32	0.41				0.73	56.16
	119.42	121.06	0.33	0.41				0.74	55.41
	121.06	122.70	0.30	0.55				0.85	64.71
	122.70	124.34	0.35	0.43				0.78	55.13
	124.34	125.98	0.24	0.58				0.82	70.73
	125.98	127.62	0.33	0.72				1.05	68.57
	127.62	129.26	0.24	0.46				0.70	65.71
	129.26	130.90	0.16	0.25				0.41	60.98
	130.90	132.54	0.06	0.08				0.14	57.14

HOLE	FROM	TO	LEAD	ZINC	SILVER	COPPER	GOLD	Pb+Zn	Zn ratio
15	132.54	134.18	0.01	0.30				0.31	96.77
	134.18	135.82	0.11	0.04				0.15	26.67
	135.82	137.46	0.07	0.48				0.55	87.27
	137.46	139.10	0.17	0.47				0.64	73.44
	139.10	140.74	0.13	1.10				1.23	89.43
	140.74	142.38	0.10	0.04				0.14	28.57
	142.38	144.02	0.09	0.08				0.17	47.06
	144.02	145.66	0.03	0.04				0.07	57.14
	145.67	147.31	0.01	0.03				0.04	75.00
	147.31	148.95	0.07	0.03				0.10	30.00
	148.95	150.59	0.16	0.29				0.45	64.44
	150.59	152.23	0.10	0.06				0.16	37.50
	152.23	153.87	0.13	0.10				0.23	43.48
	153.87	155.51	0.12	0.20				0.32	62.50
	155.51	157.15	0.16	0.18				0.34	52.94
	157.15	158.79	0.21	0.68				0.89	76.40
	158.79	160.43	0.14	0.40				0.54	74.07
	160.43	162.07	0.04	0.15				0.19	78.95
	162.07	163.71	0.01	0.06				0.07	85.71
	163.71	165.35	0.01	0.04				0.05	80.00
	165.35	166.99	0.19	0.46				0.65	70.77
	166.99	168.63	0.40	0.74				1.14	64.91
	168.63	170.27	0.15	0.26				0.41	63.41
	170.27	171.91	0.19	0.70				0.89	78.65
	171.91	173.55	0.09	0.58				0.67	86.57
	173.55	175.19	0.11	0.28				0.39	71.79
	175.19	176.83	0.13	0.30				0.43	69.77
	176.83	178.47	0.13	0.25				0.38	65.79
	178.47	180.11	0.01	0.01				0.02	50.00
	180.11	181.75	0.02	0.02				0.04	50.00
	181.75	183.39	0.00	0.04				0.04	100.00
	183.39	185.03	0.00	0.01				0.01	100.00
	185.04	186.68	0.00	0.01				0.01	100.00
	186.68	188.32	0.01	0.03				0.04	75.00
	188.32	189.96	0.04	0.19				0.23	82.61
	189.96	191.60	0.13	0.52				0.65	80.00
	191.60	193.24	0.43	0.74				1.17	63.25
	193.24	194.88	0.64	0.72				1.36	52.94
	194.88	196.52	0.35	0.72				1.07	67.29
	196.52	198.16	0.32	0.89				1.21	73.55
	198.16	199.80	0.41	0.80				1.21	66.12
	199.80	201.44	0.23	0.37				0.60	61.67
	201.44	203.08	0.34	0.14				0.48	29.17
	203.08	204.72	0.21	0.40				0.61	65.57
	204.72	206.36	0.05	0.23				0.28	82.14
	206.36	208.00	0.03	0.03				0.06	51.61
	208.00	209.64	0.06	0.12				0.18	66.67
	209.64	211.28	0.45	0.18				0.63	28.57
	211.28	212.92	0.31	0.27				0.58	46.55
	212.92	214.56	0.71	1.31				2.02	64.85
	214.56	216.20	0.25	0.41				0.66	62.12
	216.20	220.47	0.04	0.05				0.09	55.56
21	11.81	13.45	0.32	0.56	3.43			0.88	63.64
	77.11	78.74	0.14	0.14	1.03			0.28	50.00
	137.79	139.43	0.01	0.03	0.68			0.04	75.00

HOLE	FROM	TO	LEAD	ZINC	SILVER	COPPER	GOLD	Pb+Zn	Zn ratio
21	175.52	177.17	0.02	0.24	2.39			0.26	92.31

Correlation Co-efficients

Pb on Zn	0.72
Pb on Ag	0.21
Zn on Ag	0.43

Appendix 2b: Assay data from drill holes cutting the deposit

HOLE	FROM	TO	LEAD	ZINC	SILVER	COPPER	GOLD	Pb+Zn	Zn ratio
LCO-5[6]	6.00	7.50	0.27	0.31	0.00			0.58	53.45
	7.50	9.00	0.19	0.62				0.81	76.54
	9.00	10.50	0.49	2.37				2.86	82.87
	10.50	12.00	0.19	1.18				1.37	86.13
	12.00	13.50	0.22	0.57				0.79	72.15
	13.50	15.00	0.27	0.81				1.08	75.00
	15.00	16.50	0.29	0.66				0.95	69.47
	16.50	18.00	0.35	0.63				0.98	64.29
	18.00	19.50	0.54	0.75				1.29	58.14
	19.50	21.00	0.87	1.63				2.50	65.20
	21.00	22.50	0.22	0.56				0.78	71.79
	40.50	42.00	0.69	0.87	1.50			1.56	55.77
	42.00	43.50	0.59	0.31	2.00			0.90	34.44
	43.50	45.00	0.98	1.02	2.00			2.00	51.00
	45.00	46.50	0.86	1.47	4.50			2.33	63.09
	46.50	48.00	1.07	3.30	2.00		0.17	4.37	75.51
	48.00	49.50	1.22	6.35	4.00		0.17	7.57	83.88
	49.50	51.00	1.03	2.95	3.00		0.17	3.98	74.12
	51.00	52.50	3.70	6.80	11.50		0.17	10.50	64.76
	52.50	54.00	0.57	1.03	2.00		0.17	1.60	64.38
	54.00	55.50	6.90	11.20	15.50		0.17	18.10	61.88
	55.50	57.00	1.18	2.12	3.00		0.17	3.30	64.24
	57.00	58.50	0.42	0.75	1.00			1.17	64.10
	58.50	60.00	0.34	0.45	1.50			0.79	56.96
	60.00	61.50	0.74	1.45	2.00			2.19	66.21
	61.50	63.00	0.75	1.29	1.50		0.34	2.04	63.24
	63.00	64.50	0.53	0.76	1.50			1.29	58.91
	64.50	66.00	0.47	0.75	0.50			1.22	61.48
	66.00	67.50	0.69	0.97	2.00			1.66	58.43
	67.50	69.00	0.61	0.77	1.50			1.38	55.80
	69.00	70.50	0.62	0.81	1.50			1.43	56.64
	70.50	72.00	0.42	0.59	0.50			1.01	58.42
	72.00	73.50	1.29	0.98	4.00		0.51	2.27	43.17
	73.50	75.00	0.25	0.09	1.50		0.51	0.34	26.47

HOLE	FROM	TO	LEAD	ZINC	SILVER	COPPER	GOLD	Pb+Zn	Zn ratio
LCO-5	75.00	76.50	0.31	0.29	1.00			0.60	48.33
	76.50	78.00	2.92	1.08	6.00		0.86	4.00	27.00
	78.00	79.50	0.77	1.56	3.00		0.69	2.33	66.95
	79.50	81.00	1.10	1.73	4.00			2.83	61.13
	81.00	82.50	1.06	1.57	3.50		0.17	2.63	59.70
	82.50	84.00	1.34	2.37	3.50		0.17	3.71	63.88
	84.00	85.50	2.61	4.05	6.00			6.66	60.81
	85.50	87.00	2.18	2.43	6.50			4.61	52.71
	87.00	88.50	2.68	4.90	10.00		0.17	7.58	64.64
	88.50	90.00	4.45	4.65	9.00		0.17	9.10	51.10
	90.00	91.50	0.63	0.32	2.00			0.95	33.68
	91.50	93.00	0.18	0.68	1.50			0.86	79.07
	93.00	94.50	1.96	1.52	5.50			3.48	43.68
	94.50	96.00	1.61	1.39	6.00			3.00	46.33
	96.00	97.50	2.79	5.05	9.00			7.84	64.41
	97.50	99.00	0.67	1.61	2.50		0.17	2.28	70.61
	99.00	100.50	1.78	5.20	7.50		0.17	6.98	74.50
	100.50	102.00	0.45	0.75	2.00			1.20	62.50
	102.00	103.50	0.33	0.53	1.50			0.86	61.63
	103.50	105.00	0.54	1.17	2.00			1.71	68.42
	105.00	106.50	0.43	0.23	1.50			0.66	34.85
	106.50	108.00	0.71	1.90	2.50			2.61	72.80
	108.00	109.50	0.35	0.59	2.00			0.94	62.77
	109.50	111.00	0.92	1.67	2.50			2.59	64.48
	111.00	112.50	0.52	1.55	3.50		0.17	2.07	74.88
	112.50	114.00	0.64	1.15	1.50		0.17	1.79	64.25
	114.00	115.50	0.31	0.57	1.50			0.88	64.77
	115.50	117.00	0.71	1.13	2.00			1.84	61.41
	117.00	118.50	0.81	1.26	3.50			2.07	60.87
	118.50	120.00	0.52	2.07	3.50			2.59	79.92
	120.00	121.50	0.95	1.86	4.00		0.51	2.81	66.19
	121.50	123.00	0.36	1.19	2.00			1.55	76.77
	123.00	124.50	0.17	0.52	1.50		0.17	0.69	75.36
	124.50	126.00	0.13	0.25	0.50			0.38	65.79
	126.00	127.50	0.78	0.22				1.00	22.00
	127.50	129.00	0.14	0.28	1.00		0.17	0.42	66.67
	134.20	135.00	1.10	6.14	12.00		0.17	7.24	84.81
	135.00	136.50	2.72	4.95	8.00			7.67	64.54
	136.50	138.00	0.27	0.68	1.50		0.51	0.95	71.58
	138.00	139.50	1.56	5.85	6.00		0.17	7.41	78.95
	139.50	141.00	0.14	0.25	1.50			0.39	64.10
	141.00	142.50	0.91	1.05	2.50			1.96	53.57
	142.50	144.00	1.09	1.37	4.00		0.51	2.46	55.69
	144.00	145.50	2.32	0.41	8.00		0.17	2.73	15.02
	145.50	147.00	0.62	0.18	2.00			0.80	22.50
	147.00	148.50	2.60	1.46	12.00			4.06	35.96
	148.50	150.00	0.23	0.28	1.50			0.51	54.90
	150.00	151.50	5.05	6.95	14.50		0.51	12.00	57.92
	151.50	153.00	0.18	0.42	1.00			0.60	70.00
	153.00	154.50	0.14	0.19	0.50			0.33	57.58
	154.50	156.00	0.54	0.34	1.50			0.88	38.64
	156.00	157.50	0.28	0.41	6.00			0.69	59.42
	157.50	159.00	1.69	1.50	4.50		0.17	3.19	47.02
	159.00	160.50	3.14	2.15	6.50		0.34	5.29	40.64
	168.00	169.50	0.03	0.07				0.10	70.00

HOLE	FROM	TO	LEAD	ZINC	SILVER	COPPER	GOLD	Pb+Zn	Zn ratio
LCO-5	175.50	177.00	0.32	0.82				1.14	71.93
	183.00	184.50	0.04	0.06				0.10	60.00
	186.00	187.50	0.26	0.47	0.50			0.73	64.38
	189.00	190.50	0.07	0.24	1.00			0.31	77.42
	195.30	196.50	0.55	0.74	2.00		0.17	1.29	57.36
	196.50	198.00	0.83	1.32	2.50		0.17	2.15	61.40
	198.00	199.50	0.72	1.45	2.50			2.17	66.82
	204.00	205.50	0.87	0.31	14.00			1.18	26.27
	205.90	207.00	1.22	1.55	15.00			2.77	55.96
	207.00	208.50	0.61	0.69	16.00		0.17	1.30	53.08
	207.00	208.50	0.61	0.69	14.00		0.17	1.30	53.08
	213.00	214.50	0.73	0.39	20.50			1.12	34.82
	220.50	222.00	0.13	0.19	3.00			0.32	59.38
	222.00	223.50	0.07	0.16	2.50			0.23	69.57
	225.00	226.50	0.12	0.19	2.50			0.31	61.29
	228.00	229.50	0.01	0.02	1.00			0.03	66.67
	229.50	231.00	0.02	0.06	1.50			0.08	75.00
	258.00	259.50	0.39	0.81	3.00			1.20	67.50
	259.50	261.00	0.52	0.92	1.50			1.44	63.89
	274.50	276.00	0.67	1.67	3.50			2.34	71.37
	276.00	277.50	0.33	0.75	2.50			1.08	69.44
	277.50	279.00	0.27	0.43	1.00			0.70	61.43
	283.00	285.00	1.18	1.83	5.00			3.01	60.80
	285.00	286.50	2.22	1.99	7.50			4.21	47.27
	286.50	288.00	0.49	1.41	3.00			1.90	74.21
	288.00	289.50	0.22	0.31	2.00			0.53	58.49
	289.50	291.00	0.19	0.31	2.00			0.50	62.00
	291.00	292.50	0.32	0.18	1.50		0.17	0.50	36.00
	292.50	294.00	0.51	0.84	2.50			1.35	62.22
	294.00	295.50	0.64	0.66	2.50			1.30	50.77
	295.50	297.00	0.31	0.17	3.00			0.48	35.42
	297.00	298.50	0.36	0.73	3.50			1.09	66.97
	298.50	300.00	0.11	0.21	2.00			0.32	65.63
	300.00	301.72	0.15	0.08	3.00			0.23	34.78
LCO-8	5.20	6.00	0.37	1.04	5.50		0.17	1.41	73.76
	6.00	7.50	2.85	7.85	12.00			10.70	73.36
	7.50	9.00	2.95	8.55	13.50		0.17	11.50	74.35
	9.00	10.50	2.55	5.05	9.00		0.17	7.60	66.45
	10.50	12.00	2.45	2.65	11.50		0.34	5.10	51.96
	12.00	13.50	0.84	1.85	3.50			2.69	68.77
	13.50	15.00	0.99	1.85	5.00			2.84	65.14
	15.00	16.50	0.55	0.73	3.50			1.28	57.03
	18.00	19.50	1.41	3.55	6.00			4.96	71.57
	19.50	21.00	0.59	1.66	3.50			2.25	73.78
	21.00	22.50	0.31	0.79	1.00			1.10	71.82
	22.50	24.00	1.76	2.20	24.00			3.96	55.56
	24.00	25.50	3.65	4.70	15.50			8.35	56.29
	25.50	27.00	3.05	3.53	13.00			6.58	53.65
	27.00	28.50	0.59	1.06	3.00			1.65	64.24
	28.50	30.00	0.42	0.64	2.50			1.06	60.38
	30.00	31.50	1.16	[illegible]	6.00			3.74	68.98
	31.50	33.00	0.14	0.57	4.50			0.71	80.28
	33.00	34.50	0.55	1.59	4.50		0.20	2.14	74.30
	34.50	36.00	1.03	8.95	5.00		0.30	9.98	89.68
	36.00	37.50	1.83	8.75	7.00			10.58	82.70

HOLE	FROM	TO	LEAD	ZINC	SILVER	COPPER	GOLD	Pb+Zn	Zn ratio
LCO-8	37.50	39.00	0.85	2.38	4.00			3.23	73.68
	39.00	40.50	0.09	0.27	2.00			0.36	75.00
	40.50	42.00	0.13	0.18	2.00			0.31	58.06
	42.00	43.50	0.39	0.19	3.00			0.58	32.76
	43.50	45.00	1.21	2.51	5.50			3.72	67.47
	45.00	46.50	2.49	6.05	8.50		0.20	8.54	70.84
	46.50	48.00	0.38	0.74	4.00			1.12	66.07
	48.00	49.50	0.08	0.12	2.00			0.20	60.00
	49.50	51.00	0.20	0.40	2.00			0.60	66.67
	51.00	52.50	0.21	0.39	2.00			0.60	65.00
	52.50	54.00	0.21	0.39	2.00			0.60	65.00
	54.00	55.50	0.13	0.16	2.00			0.29	55.17
	55.50	57.00	0.14	0.33	1.00			0.47	70.21
	57.00	58.50	0.25	0.54	2.00			0.79	68.35
	58.50	60.00	0.18	0.38	1.50			0.56	67.86
	60.00	61.50	0.12	0.13	1.50			0.25	52.00
	61.50	63.00	1.89	1.85	10.00		0.17	3.74	49.47
	63.00	64.50	1.09	2.31	5.50			3.40	67.94
	64.50	66.00	0.15	0.29	1.00			0.44	65.91
	71.50	73.50	1.77	1.68	6.00			3.45	48.70
	73.50	75.00	0.78	1.44	3.00			2.22	64.86
	78.00	79.50	1.22	2.41	5.50			3.63	66.39
	79.50	81.00	0.69	1.29	4.00			1.98	65.15
	81.00	82.50	0.71	1.73	2.50			2.44	70.90
	82.50	84.00	0.82	2.38	2.00			3.20	74.38
	84.00	84.7.	0.84	1.98	6.00			2.82	70.21
	85.50	87.00	0.49	0.96	3.00		0.17	1.45	66.21
	87.00	88.50	0.19	0.49	1.50			0.68	72.06
	88.50	90.00	0.15	0.17	1.00			0.32	53.13
	90.00	91.50	0.12	0.27	1.00			0.39	69.23
	91.50	93.00	0.19	0.54	1.50			0.73	73.97
	93.00	94.50	0.06	0.29	0.50			0.35	82.86
	94.50	96.00	0.12	0.37	1.00			0.49	75.51
	96.00	97.50	0.25	0.54	0.50			0.79	68.35
	97.50	99.00	0.14	0.35	1.00			0.49	71.43
	99.00	100.50	0.29	0.21	1.50		0.17	0.50	42.00
	100.50	102.00	0.24	0.44	1.00			0.68	64.71
	102.00	103.50	0.13	0.38	1.00			0.51	74.51
	103.50	105.00	0.26	0.29	0.50			0.55	52.73
	105.00	106.50	0.27	0.47				0.74	63.51
	106.50	108.00	0.31	0.46	3.50			0.77	59.74
	108.00	109.50	0.10	0.31	2.00			0.41	75.61
	109.50	111.00	0.12	0.32	1.50			0.44	72.73
	111.00	112.50	0.09	0.21	2.00			0.30	70.00
	112.50	114.00	0.06	0.10	2.00			0.16	62.50
	114.00	115.50	0.08	0.18	2.00			0.26	69.23
	115.50	117.00	0.09	0.35	2.00			0.44	79.55
	117.00	118.50	0.19	0.34	2.00			0.53	64.15
	118.50	120.00	0.22	0.65	2.00			0.87	74.71
	120.00	121.50	0.23	0.55	2.00			0.78	70.51
	121.50	123.00	0.11	0.37	2.50			0.48	77.08
	181.50	183.00	0.53	0.66	4.50		0.51	1.19	55.46
	184.50	186.00	0.05	0.13	2.00		0.20	0.18	72.22
	186.00	187.80	0.26	0.73	2.50			0.99	73.74
	190.80	192.00	0.13	0.66	2.00		0.20	0.79	83.54

HOLE	FROM	TO	LEAD	ZINC	SILVER	COPPER	GOLD	Pb+Zn	Zn ratio
LCO-8	192.00	193.50	0.17	0.15	2.00		0.20	0.32	46.88
	195.70	196.50	1.59	0.77	5.50			2.36	32.63
	196.50	198.00	1.07	1.17	3.50			2.24	52.23
	198.00	199.30	0.33	0.63	3.00			0.96	65.63
	204.00	205.50	0.12	0.22	2.50			0.34	64.71
	225.00	226.50	0.11	0.26	6.00		0.20	0.37	70.27
LCO-9	7.50	9.00	0.43	0.57	9.50			1.00	57.00
	9.00	10.50	0.19	0.12	3.00			0.31	38.71
	11.75	13.50	0.66	1.19	4.50		0.20	1.85	64.32
	13.50	14.50	1.18	1.09	9.00			2.27	48.02
	15.00	15.50	0.23	0.81	5.00			1.04	77.88
	16.50	18.00	0.69	0.39	9.00			1.08	36.11
	37.02	37.62	1.32	3.55	6.00			4.87	72.90
	39.43	40.50	0.68	1.01	4.00			1.69	59.76
	40.50	42.00	0.29	0.71	2.50			1.00	71.00
	42.00	43.50	0.31	0.76	2.50			1.07	71.03
	49.50	51.00	0.22	0.43	2.50			0.65	66.15
	51.00	52.50	0.25	2.31	3.50			2.56	90.23
	52.50	54.35	0.73	1.73	6.00		0.20	2.46	70.33
	55.50	57.00	1.23	1.09	8.00			2.32	46.98
	57.00	58.50	0.27	0.53	4.00			0.80	66.25
	58.50	59.25	0.23	0.48	5.50		0.20	0.71	67.61
	64.50	66.00	0.28	0.79	2.50			1.07	73.83
	68.00	69.00	1.02	1.39	8.00		0.20	2.41	57.68
	69.00	70.50	0.43	0.81	2.50		0.20	1.24	65.32
	72.00	73.50	1.05	2.62	14.50		0.20	3.67	71.39
	73.50	75.00	0.56	1.58	5.50			2.14	73.83
	75.00	76.50	1.73	2.54	7.00		0.20	4.27	59.48
	76.50	78.00	0.95	3.40	5.00		0.20	4.35	78.16
	78.00	79.50	0.61	1.45	4.00		0.20	2.06	70.39
	79.50	81.00	1.24	1.34	4.50		0.20	2.58	51.94
	82.50	84.00	0.58	2.09	4.00		0.30	2.67	78.28
	84.00	85.50	0.95	0.84	4.00		0.50	1.79	46.93
	85.50	87.00	1.82	0.36	8.00			2.18	16.51
	87.00	88.50	0.91	0.56	4.50			1.47	38.10
	92.50	93.00	0.35	1.01	3.50		0.30	1.36	74.26
	93.00	94.50	1.01	0.18	5.00			1.19	15.13
	94.50	96.00	1.50	3.95	7.50		0.20	5.45	72.48
	96.00	97.50	1.05	2.23	6.50			3.28	67.99
	97.50	99.00	1.29	3.55	5.00			4.84	73.35
	99.00	101.50	1.81	5.65	7.50			7.46	75.74
	101.50	101.15	0.49	1.44	5.00			1.93	74.61
	102.00	103.50	0.62	1.36	4.00			1.98	68.69
	103.50	105.00	0.82	1.76	5.00			2.58	68.22
	105.00	106.50	0.81	1.91	3.50			2.72	70.22
	106.50	108.00	2.73	5.40	9.50			8.13	66.42
	108.00	109.50	1.05	1.26	5.50			2.31	54.55
	109.50	111.00	1.72	3.25	7.00			4.97	65.39
	111.00	112.50	0.89	2.23	3.50			3.12	71.47
	112.50	114.00	0.17	3.65	1.00			3.82	95.55
	114.00	115.50	0.58	0.87	2.50			1.45	60.00
	115.50	117.00	0.78	1.99	2.50			2.77	71.84
	117.00	118.50	1.31	2.32	4.00			3.63	63.91
	118.50	120.00	0.31	0.51	13.00			0.82	62.20
	120.00	121.50	0.92	1.81	5.50			2.73	66.30

HOLE	FROM	TO	LEAD	ZINC	SILVER	COPPER	GOLD	Pb+Zn	Zn ratio
LCO-9	121.50	123.00	1.72	1.97	8.00			3.69	53.39
	123.00	124.50	1.51	2.34	7.00			3.85	60.78
	124.50	126.00	0.51	1.08	4.50			1.59	67.92
	126.00	127.50	1.35	1.27	7.00			2.62	48.47
	127.50	129.00	0.68	1.63	4.00		0.20	2.31	70.56
	129.00	130.50	1.57	2.04	7.50			3.61	56.51
	130.50	132.00	1.37	1.92	3.50		0.30	3.29	58.36
	132.00	133.50	1.61	2.42	1.50			4.03	60.05
	133.50	135.00	0.68	1.82				2.50	72.80
	135.00	136.50	1.66	2.27	2.50		0.20	3.93	57.76
	136.50	138.00	4.35	4.15	9.00			8.50	48.82
	138.00	139.50	8.40	5.80	28.00			14.20	40.85
	139.50	141.00	1.49	1.84	0.50			3.33	55.26
	141.00	142.50	3.45	9.45	7.00		0.20	12.90	73.26
	142.50	144.00	2.29	5.05	3.00			7.34	68.80
	145.50	147.00	0.51	0.66	2.00			1.17	56.41
	145.50	147.00	0.91	2.31				3.22	71.74
	147.00	148.50	0.57	1.99	3.00			2.56	77.73
	148.50	150.00	0.36	0.32	3.00			0.68	47.06
	150.00	151.50	0.89	0.17	3.50			1.06	16.04
	151.50	153.00	0.34	0.48				0.82	58.54
	153.00	154.50	0.26	0.48	2.50			0.74	64.86
	154.50	156.00	0.24	0.68	2.50			0.92	73.91
	156.00	157.50	0.55	1.04	3.50			1.59	65.41
	157.50	159.00	0.32	0.79	2.00			1.11	71.17
	159.00	160.50	0.69	1.74	3.00			2.43	71.60
	160.50	162.00	0.15	0.32				0.47	68.09
	162.00	163.50	0.59	1.32				1.91	69.11
	163.50	165.00	0.62	1.27	3.50			1.89	67.20
	165.00	166.50	0.48	0.89	2.00			1.37	64.96
	166.50	168.00	1.67	2.58	7.00		0.20	4.25	60.71
	168.00	169.50	0.75	2.31	4.00			3.06	75.49
	169.50	171.00	0.24	0.38				0.62	61.29
	171.00	172.50	0.75	2.16	4.00			2.91	74.23
	172.50	174.00	0.44	0.27	2.50			0.71	38.03
	174.00	175.50	0.44	0.27	2.50			0.71	38.03
	175.50	177.00	0.98	2.05				3.03	67.66
	177.00	178.50	1.08	2.55	5.00			3.63	70.25
	178.50	180.00	0.74	1.37	8.00			2.11	64.93
	180.00	181.50	0.19	0.59	14.50			0.78	75.64
	181.50	183.00	0.61	1.33	12.50		0.20	1.94	68.56
	183.00	184.50	0.49	1.33				1.82	73.08
	184.50	186.00	0.57	1.93				2.50	77.20
	186.00	187.50	0.54	0.99	1.50			1.53	64.71
	187.50	189.00	0.35	0.87	2.50			1.22	71.31
	189.00	190.50	0.36	0.82				1.18	69.49
	190.50	192.00	0.06	0.43	1.00			0.49	87.76
	192.00	193.50	0.45	0.49				0.94	52.13
	193.50	195.00	0.72	2.03				2.75	73.82
	195.00	196.50	0.92	0.67				1.59	42.14
	196.50	198.00	2.02	2.67	3.00			4.69	56.93
	198.00	199.50	2.29	6.10	5.00			8.39	72.71
	199.50	200.50	0.28	0.65				0.93	69.89
	208.50	209.50	0.86	2.71			0.20	3.57	75.91
	232.50	234.00	0.16	0.26				0.42	61.90

HOLE	FROM	TO	LEAD	ZINC	SILVER	COPPER	GOLD	Pb+Zn	Zn ratio
LCO-9	241.50	243.00	0.51	0.91				1.42	64.08
	243.00	244.50	0.49	0.95				1.44	65.97
	246.40	247.95	0.64	0.41				1.05	39.05
	250.50	251.85	0.41	0.95				1.36	69.85
79-1	13.50	15.00	0.79	1.12	6.51		1.91	1.91	58.64
	15.00	16.50	0.80	1.47	7.20		2.27	2.27	64.76
	16.50	18.00	0.91	1.96	7.89		2.87	2.87	68.29
	18.00	19.50	0.59	1.38	5.83		1.97	1.97	70.05
	19.50	21.00	0.41	1.12			1.53	2.20	74.55
	21.00	22.50	0.56	1.64	3.43		2.20	3.02	64.57
	22.50	24.00	1.07	1.95	11.66		3.02	3.29	79.33
	24.00	25.50	0.68	2.61	6.51		3.29	2.70	58.52
	25.50	27.00	1.12	1.58	3.09		2.70	2.79	70.25
	27.00	28.50	0.83	1.96	3.77		2.79	4.25	79.76
	28.50	30.00	0.86	3.39	7.89		4.25	7.32	86.75
	30.00	31.50	0.97	6.35	5.49		7.32	10.81	75.21
	31.50	33.00	2.68	8.13	19.20		10.81	12.63	75.93
	33.00	34.50	3.04	9.59	32.23		12.63	8.90	76.18
	34.50	36.00	2.12	6.78	12.69		8.90	6.50	71.69
	36.00	37.50	1.84	4.66	12.00		6.50	3.78	73.28
	37.50	39.00	1.01	2.77	27.43		3.78	5.57	70.38
	39.00	40.50	1.65	3.92	9.94		5.57	1.81	53.59
	40.50	42.00	0.84	0.97	2.06		1.81	2.07	65.70
	42.00	43.50	0.18	0.48			0.66	1.36	80.88
	43.50	45.00	0.04	0.10			0.14	0.91	71.43
	45.00	46.50	0.16	0.24			0.40	1.89	67.20
	46.50	48.00	0.71	1.36	4.50		2.07	1.36	69.12
	48.00	49.50	0.26	1.10	2.98		1.36	0.71	88.86
	49.50	51.00	0.26	0.65			0.91	0.31	83.07
	51.00	52.50	0.62	1.27	3.09		1.89	0.26	78.13
	52.50	54.00	0.42	0.94	6.17		1.36	0.18	74.29
	54.00	55.50	0.08	0.63	9.60		0.71	0.12	81.97
	55.50	57.00	0.05	0.26	5.49		0.31	0.07	72.97
	57.00	58.50	0.06	0.20	4.11		0.26	0.16	61.73
	58.50	60.00	0.05	0.13	2.64		0.18	0.07	59.70
	60.00	61.50	0.02	0.10	2.26		0.12	0.11	58.33
	61.50	63.00	0.02	0.05	4.11		0.07	0.27	92.59
	63.00	64.50	0.02	0.07			0.10	0.32	68.75
	64.50	66.00	0.02	0.04			0.06	0.10	42.00
	66.00	67.50	0.02	0.05			0.07	0.60	40.00
	67.50	69.00	0.06	0.10	4.11		0.16	1.50	44.67
	69.00	70.50	0.03	0.04	8.91		0.07	2.92	76.37
	70.50	72.00	0.05	0.06	21.60		0.11	0.85	57.65
	72.00	73.50	0.02	0.25	8.57		0.27	1.80	70.56
	73.50	75.00	0.10	0.22			0.32	1.30	82.31
	75.00	76.50	0.06	0.04	2.81		0.10	0.51	82.84
	76.50	78.00	0.36	0.24	4.80		0.60	0.53	64.15
	78.00	79.50	0.83	0.67	13.37		1.50	2.58	77.91
	79.50	81.00	0.69	2.23	9.94		2.92	2.05	84.88
	81.00	82.50	0.36	0.49	5.83		0.85	0.35	40.00
	82.50	84.00	0.53	1.27	9.60		1.80	0.69	60.87
	84.00	85.50	0.23	1.07	3.77		1.30	7.21	74.90
	85.50	87.00	0.09	0.42	3.12		0.51	4.25	65.65
	87.00	88.50	0.19	0.34	7.89		0.53	1.63	68.71
	88.50	90.00	0.57	2.01	2.23		2.58	0.68	47.06

HOLE	FROM	TO	LEAD	ZINC	SILVER	COPPER	GOLD	Pb+Zn	Zn ratio
79-1	90.00	91.50	0.31	1.74	3.77		2.05	2.52	63.89
	91.50	93.00	0.21	0.14	4.80		0.35	5.58	68.46
	93.00	94.50	0.27	0.42	1.71		0.69	2.77	75.81
	94.50	96.00	0.07	0.06	6.51		0.13	5.47	96.53
	96.00	97.50	0.63	1.49	4.46		2.12	3.62	79.01
	97.50	99.00	0.91	0.20	3.77		1.11	4.42	72.40
	99.00	100.50	0.23	0.28	5.83		0.51	5.31	42.56
	100.50	102.00	0.80	2.33	4.80		3.13	1.90	54.74
	102.00	103.50	0.46	1.85	4.80		2.31	3.97	66.75
	103.50	105.00	0.41	0.65	4.11		1.06	3.74	68.18
	105.00	106.50	0.52	1.36	5.49		1.88	6.06	68.32
	106.50	108.00	0.34	0.66	3.77		1.00	5.47	60.69
	108.00	109.50	0.41	1.50	2.85		1.91	22.27	64.66
	109.50	111.00	0.53	0.84	3.19		1.37	3.53	60.34
	111.00	112.50	0.56	0.46	5.14		1.02	2.81	79.72
	112.50	114.00	0.33	0.55	3.77		0.88	9.17	75.90
	114.00	115.50	0.58	1.92	3.77		2.50	13.75	71.93
	115.50	117.00	0.52	0.28	4.11		0.80	11.16	78.94
	117.00	118.50	0.20	0.13			0.33	7.21	81.69
	118.80	120.00	0.17	0.14			0.31	6.77	46.97
	120.00	121.50	0.08	0.07			0.15	9.40	61.70
	121.50	123.00	0.06	0.06			0.12	12.53	66.64
	123.00	124.50	0.05	0.07			0.12	1.38	64.49
	124.50	126.00	0.06	0.25			0.31	7.69	60.60
	126.00	127.50	0.06	0.14			0.20	11.97	63.91
	127.50	129.00	0.06	0.17			0.23	3.18	65.72
	129.00	130.50	0.14	0.13			0.27	1.69	49.70
	130.50	132.00	0.03	0.06			0.09	3.36	63.39
	132.00	133.50	0.02	0.05			0.07	2.91	65.98
	133.50	135.00	0.07	0.07			0.14	1.40	65.71
	135.00	136.50	0.33	0.06			0.39	1.63	70.55
	136.50	138.00	0.15	0.18			0.33	3.85	71.69
	138.00	139.50	0.61	0.96			1.57	3.18	72.01
	139.50	141.50	0.34	0.33			0.67	0.99	78.79
79-2	42.00	43.50	0.02	0.09			0.11	7.77	63.84
	43.50	45.00	0.16	0.14			0.30	3.15	87.62
	45.00	46.50	0.24	0.26			0.50	2.41	74.69
	46.50	48.00	1.81	5.40	5.14		7.21	2.07	70.05
	48.00	49.50	1.46	2.79	10.29		4.25	4.44	67.57
	49.50	51.00	0.51	1.12	4.80		1.63	6.08	66.12
	93.00	94.50	0.31	0.15			0.46	4.63	60.69
	94.50	96.00	0.36	0.32	5.14		0.68	10.03	67.30
	96.00	97.50	0.18	0.09			0.27	5.35	83.18
	97.50	99.00	0.39	0.58			0.97	7.09	58.67
	99.00	100.50	0.35	0.29			0.64	8.38	65.16
	100.50	102.00	0.09	0.37			0.46	3.49	55.59
	102.00	103.50	0.09	0.88			0.97	1.98	63.13
	103.50	105.00	0.67	1.20				1.87	64.17
	105.00	106.50	0.91	1.61	4.80			2.52	63.89
	106.50	108.00	1.76	3.82	5.49			5.58	68.46
	108.00	109.50	0.67	2.10	4.11			2.77	75.81
	109.50	111.00	0.84	1.50				2.34	64.10
	111.00	112.50	0.36	0.70	2.13			1.06	66.04
	112.50	114.00	0.95	0.70				1.65	42.42
	114.00	115.50	0.56	1.55				2.11	73.46

HOLE	FROM	TO	LEAD	ZINC	SILVER	COPPER	GOLD	Pb+Zn	Zn_ratio
79-2	115.50	117.00	0.61	1.66				2.27	73.13
	117.00	118.50	0.56	1.70				2.26	75.22
	118.50	120.00	1.63	3.16	5.49			4.79	65.97
	120.00	121.50	1.22	1.74				2.96	58.78
	121.50	123.00	1.74	3.41				5.15	66.21
	123.00	124.50	0.63	1.31				1.94	67.53
	124.50	126.00	1.16	2.85	5.49			4.01	71.07
	126.00	127.50	0.57	0.96				1.53	62.75
	127.50	129.00	0.71	2.32				3.03	76.57
	129.00	130.50	0.43	0.68				1.11	61.26
	130.50	132.00	0.19	0.97				1.16	83.62
79-3	15.00	16.50	0.59	0.31	3.77			0.90	34.44
	16.50	18.00	0.15	0.13				0.28	46.43
	18.00	19.50	0.20	0.25				0.45	55.56
	19.50	21.00	0.12	0.20				0.32	62.50
	28.50	30.00	0.74	1.16	2.39			1.90	61.05
	30.00	31.50	0.17	0.28				0.45	62.22
	31.50	33.00	0.16	0.16				0.32	50.00
	39.00	40.50	0.31	0.93				1.24	75.00
	40.50	42.00	0.26	0.86				1.12	76.79
	42.00	43.50	0.25	0.48				0.73	65.75
	43.50	45.00	0.29	0.80				1.09	73.39
	45.00	46.50	0.47	2.59				3.06	84.64
	46.50	48.00	0.37	0.76				1.13	67.26
	48.00	49.50	0.52	1.23				1.75	70.29
	49.50	51.00	0.19	5.28	7.54			5.47	96.53
	51.00	52.50	0.76	2.86	5.14			3.62	79.01
	52.50	54.00	1.22	3.20	8.23			4.42	72.40
	54.00	55.50	3.05	2.26	16.11			5.31	42.56
	55.50	57.00	0.86	1.04	5.48			1.90	54.74
	57.00	58.50	1.32	2.65	8.91			3.97	66.75
	58.50	60.00	1.19	2.55	6.51			3.74	68.18
	60.00	61.50	0.75	1.15				1.90	60.53
	61.50	63.00	1.92	4.14	7.89			6.06	68.32
	63.00	64.50	2.15	3.32	16.11			5.47	60.69
	64.50	66.00	7.87	14.40	32.57			22.27	64.66
	66.00	67.50	1.40	2.13	8.23			3.53	60.34
	67.50	69.00	0.57	2.24	9.94			2.81	79.72
	69.00	70.50	0.23	0.40				0.63	63.49
	70.50	72.00	0.12	0.29				0.41	70.73
	72.00	73.50	0.10	0.39				0.49	79.59
	73.50	75.00	0.25	0.87				1.12	77.68
	75.00	76.50	0.40	1.29				1.69	76.33
	76.50	78.00	0.69	3.20				3.89	82.26
	78.00	79.50	0.13	0.44				0.57	77.19
	79.50	81.00	0.10	0.38				0.48	79.17
	81.00	82.50	0.13	0.26				0.39	66.67
	82.50	84.00	0.57	1.47				2.04	72.06
	84.00	85.50	1.80	5.54	10.97			7.34	75.48
	85.50	87.00	0.26	0.58				0.84	69.05
	87.00	88.50	0.11	0.38				0.49	77.55
	88.50	90.00	0.40	1.04				1.44	72.22
	90.00	91.50	0.11	0.18				0.29	62.07
	91.50	93.00	0.94	1.82				2.76	65.94
	93.00	94.50	0.87	0.87				1.74	50.00

HOLE	FROM	TO	LEAD	ZINC	SILVER	COPPER	GOLD	Pb+Zn	Zn_ratio
79-3	94.50	96.00	0.14	0.18				0.32	56.25
	96.00	97.50	3.68	1.55	6.17			5.23	29.64
	97.50	99.00	0.31	0.22				0.53	41.51
	99.00	100.50	1.80	3.82				5.62	67.97
	100.50	102.00	4.60	3.50	7.89			8.10	43.21
	102.00	103.50	0.86	2.15				3.01	71.43
	103.50	105.00	1.23	6.24				7.47	83.53
	105.00	106.50	2.21	6.96	5.48			9.17	75.90
	106.50	108.00	3.86	9.89	7.54			13.75	71.93
	108.00	109.50	1.45	3.08				4.53	67.99
	109.50	111.00	2.35	8.81	21.59			11.16	78.94
	111.00	112.50	1.32	5.89	7.19			7.21	81.69
	112.50	114.00	3.59	3.18	9.59			6.77	46.97
	114.00	115.50	3.60	5.80	7.19			9.40	61.70
	115.50	117.00	4.18	8.35	11.65			12.53	66.64
	117.00	118.50	0.49	0.89	5.48			1.38	64.49
	118.50	120.00	0.33	0.58				0.91	63.74
	120.00	121.50	1.55	0.71	5.48			2.26	31.42
	121.50	123.00	0.65	10.58				11.23	94.21
	123.00	124.50	0.98	1.03				2.01	51.24
	124.50	126.00	0.42	0.58				1.00	58.00
	126.00	127.50	0.28	0.92				1.20	76.67
	127.50	129.00	0.72	3.75				4.47	83.89
	129.00	130.50	0.75	2.76				3.51	78.63
	130.50	132.00	1.17	3.64				4.81	75.68
	132.00	133.50	0.38	0.94				1.32	71.21
	133.50	135.00	0.20	0.44				0.64	68.75
	135.00	136.50	0.20	0.21				0.41	51.22
	136.50	138.00	0.13	0.27				0.40	67.50
	138.00	139.50	3.03	4.66	10.97			7.69	60.60
	139.50	141.00	0.45	1.45				1.90	76.32
	141.00	142.50	0.62	1.54				2.16	71.30
	142.50	144.00	0.73	1.63				2.36	69.07
	144.00	145.50	3.76	7.67				11.43	67.10
	145.50	147.00	4.32	7.65	6.17			11.97	63.91
	147.00	148.50	0.97	2.30				3.27	70.34
	148.50	150.00	0.64	1.45				2.09	69.38
	150.00	151.50	0.18	0.23				0.41	56.10
	151.50	153.00	0.57	1.05				1.62	64.81
	153.00	154.50	0.37	0.18				0.55	32.73
	154.50	156.00	0.70	0.29				0.99	29.29
	156.00	157.50	0.13	0.11				0.24	45.83
	157.50	159.00	0.02	0.38				0.40	95.00
	159.00	160.50	0.01	0.14				0.15	93.33
	160.50	162.00	0.04	0.10				0.14	71.43
	162.00	163.50	0.02	0.29				0.31	93.55
	163.50	165.00	0.02	0.06				0.08	75.00
	165.00	166.50	0.02	0.32				0.34	94.12
	166.50	168.00	0.04	0.20				0.24	83.33
	168.00	169.50	0.08	1.01				1.09	92.66
	169.50	171.00	0.03	0.28				0.31	90.32
	171.00	172.50	0.02	0.28				0.30	93.33
	172.50	174.00	0.02	0.01				0.03	33.33
	174.00	175.50	0.02	0.09	6.51			0.11	81.82
	175.50	177.00	0.01	0.78	3.08			0.79	98.73

HOLE	FROM	TO	LEAD	ZINC	SILVER	COPPER	GOLD	Pb+Zn	Zn ratio
79-3	177.00	178.50	0.01	0.39	3.43			0.40	97.50
	178.50	180.00	0.01	0.41				0.42	97.62
	180.00	181.50	0.01	0.12	2.06			0.13	92.31
	181.50	183.00	0.29	0.18				0.47	38.30
79-4	13.72	14.17	1.09	2.09	6.85			3.18	65.72
	14.17	14.63	0.85	0.84	5.83			1.69	49.70
	14.63	15.09	1.23	2.13	5.14			3.36	63.39
	15.09	15.55	0.99	1.92	3.77			2.91	65.98
	15.55	16.00	0.48	0.92	3.77			1.40	65.71
	16.00	16.46	0.48	1.15	5.48			1.63	70.55
	16.46	16.91	1.09	2.76	5.14			3.85	71.69
	16.91	17.37	0.89	2.29	4.45			3.18	72.01
	17.37	17.83	0.37	0.99				1.36	72.79
	17.83	18.29	0.21	0.78	3.77			0.99	78.79
	18.29	18.75	2.81	4.96	10.97			7.77	63.84
	18.75	19.20	0.39	2.76	7.19			3.15	87.62
	21.49	21.94	0.61	1.80	3.77			2.41	74.69
	21.94	22.40	0.62	1.45	6.17			2.07	70.05
	22.40	22.86	1.44	3.00	6.85			4.44	67.57
	22.86	23.32	0.94	2.11				3.05	69.18
	23.32	23.77	0.63	1.54				2.17	70.97
	23.77	24.23	1.05	3.64				4.69	77.61
	24.23	24.69	1.17	2.66				3.83	69.45
	24.69	25.17	2.06	4.02	10.97			6.08	66.12
	25.17	25.60	1.82	2.81	5.83			4.63	60.69
	25.60	26.06	3.28	6.75	5.83			10.03	67.30
	26.06	26.52	0.90	4.45				5.35	83.18
	26.52	26.98	2.93	4.16	6.17			7.09	58.67
	26.98	27.43	0.58	1.37				1.95	70.26
	27.43	27.91	2.92	5.46	4.79			8.38	65.16
	27.91	28.34	1.25	1.83				3.08	59.42
	28.34	28.80	1.55	1.94	6.51			3.49	55.59
	28.80	29.26	0.73	1.25	2.39			1.98	63.13
	29.26	29.72	0.18	0.86				1.04	82.69
	29.72	30.18	0.36	0.83				1.19	69.75
	34.29	34.74	0.25	1.05				1.30	80.77
	34.74	35.20	0.77	1.50	3.77			2.27	66.08
	35.23	35.66	1.01	2.57				3.58	71.79
	35.66	36.12	1.75	3.47	5.48			5.22	66.48
	36.12	36.58	0.80	1.06				1.86	56.99
	45.72	46.18	0.20	0.27				0.47	57.45
	46.18	46.63	0.23	0.32				0.55	58.18
	46.63	47.09	0.32	0.19				0.51	37.25
	47.09	47.55	0.22	0.57				0.79	72.15
6	9.14	10.67	0.37	0.06	0.34			0.43	13.95
	10.67	12.19	0.05	0.03	1.03			0.08	37.50
	12.19	13.77	0.04	0.15	0.68			0.19	78.95
	13.77	15.25	0.36	0.46	2.05			0.82	56.10
	15.25	16.45	0.42	0.58	2.74			1.00	58.00
	16.45	17.98	0.18	0.25				0.43	58.14
	17.98	19.51	0.17	0.07				0.24	29.17
	19.51	21.04	0.06	0.10				0.16	62.50
	21.04	22.57	0.14	0.14				0.28	50.00
	22.57	24.10	0.20	0.21				0.41	51.22
	24.10	25.63	0.11	0.07				0.18	38.89

HOLE	FROM	TO	LEAD	ZINC	SILVER	COPPER	GOLD	Pb+Zn	Zn ratio
6	25.63	27.16	0.07	0.03				0.10	30.00
	27.16	28.65	0.11	0.12				0.23	52.17
	28.65	30.48	0.09	0.07				0.16	43.75
	30.48	32.01	0.23	0.26				0.49	53.06
	32.01	33.22	0.66	0.65				1.31	49.62
	33.22	34.29	0.08	0.06				0.14	42.86
	34.29	35.35	0.34	0.40				0.74	54.05
	35.35	36.57	0.12	0.20				0.32	62.50
	36.57	38.10	0.07	0.12				0.19	63.16
	38.10	39.63	0.13	0.20				0.33	60.61
	39.63	41.16	0.14	0.17				0.31	54.84
	41.16	42.69	0.70	0.43				1.13	38.05
	42.69	44.22	0.09	0.08				0.17	47.06
	44.22	45.75	0.06	0.08				0.14	57.14
	45.75	47.28	0.07	0.15				0.22	68.18
	47.28	48.81	0.25	0.23				0.48	47.92
	48.81	50.34	0.09	0.10				0.19	52.63
	50.34	51.66	0.18	0.21				0.39	53.85
	51.66	52.57	1.86	6.14				8.00	76.75
	52.57	53.64	0.13	0.14				0.27	51.85
	53.64	55.17	0.23	0.39				0.62	62.90
	55.17	56.70	0.26	0.62				0.88	70.45
	56.70	58.23	0.23	0.47				0.70	67.14
	58.23	59.24	0.18	0.36				0.54	66.67
	59.24	61.26	0.33	0.38				0.71	53.52
	61.26	62.78	0.17	0.13				0.30	43.33
	62.78	64.31	0.12	0.18				0.30	60.00
	64.31	65.83	0.35	0.81				1.16	69.83
	65.83	67.36	0.29	1.07				1.36	78.68
	67.36	68.88	0.93	1.25				2.18	57.34
	68.88	70.41	0.36	0.68				1.04	65.38
	70.41	71.93	0.41	0.69				1.10	62.73
	71.93	73.45	0.22	0.32				0.54	59.26
	73.45	74.06	0.81	1.15				1.96	58.67
	74.06	75.59	0.91	2.24				3.15	71.11
	75.59	77.12	0.88	1.01				1.89	53.44
	77.12	78.65	0.63	1.39				2.02	68.81
	78.65	80.18	0.95	1.47				2.42	60.74
	80.18	81.71	1.21	2.33				3.54	65.82
	81.71	83.24	0.97	1.50				2.47	60.73
	83.24	84.77	0.56	0.98				1.54	53.64
	84.77	86.30	0.57	1.19				1.76	67.61
	87.30	87.83	0.50	1.04				1.54	67.53
	87.83	89.36	0.50	0.72				1.22	59.02
	89.36	90.89	0.70	0.50	2.06			1.20	41.67
	90.89	92.42	0.43	0.10	1.71			0.53	18.87
	92.42	93.95	0.94	0.58	2.74			1.52	38.16
	93.95	96.01	1.24	1.74	3.43			2.98	58.39
	96.01	97.54	0.52	1.06				1.58	67.09
	97.54	99.07	1.28	0.17				1.45	11.72
	99.07	100.60	0.12	0.03				0.15	20.00
	100.60	102.13	0.05	0.03				0.08	37.50
	102.13	103.63	1.30	0.66				1.96	33.67
	103.63	105.15	1.38	0.28				1.66	16.87
	105.15	106.67	1.64	0.16				1.80	8.89

HOLE	FROM	TO	LEAD	ZINC	SILVER	COPPER	GOLD	Pb+Zn	Zn ratio
6	106.67	108.20	1.18	0.27				1.45	18.62
	108.20	109.72	0.49	0.33				0.82	40.24
	109.72	111.25	1.69	0.77				2.46	31.30
	111.25	112.77	0.79	0.73				1.52	48.03
	112.77	114.29	0.96	0.29				1.25	23.20
	114.29	115.82	0.13	0.12				0.25	48.00
	115.82	117.34	0.11	0.10				0.21	47.62
	117.34	118.87	0.08	0.05				0.13	38.46
	118.87	120.39	0.25	0.19				0.44	43.18
	120.39	121.92	0.18	0.09				0.27	33.33
	121.92	123.44	1.09	0.88				1.97	44.67
	123.44	124.96	1.15	1.40				2.55	54.90
	124.96	126.49	0.58	0.54				1.12	48.21
	126.49	128.61	0.53	0.99				1.52	65.13
	128.61	129.53	1.59	1.99				3.58	55.59
	129.53	131.06	4.44	1.29	8.23			5.73	22.51
	131.06	132.58	3.79	1.53	6.17			5.32	28.76
	132.58	134.11	1.88	1.34	4.11			3.22	41.61
	134.11	135.63	0.45	0.48	8.23			0.93	51.61
	135.63	137.00	2.08	2.28	2.05			4.36	52.29
	137.00	138.07	3.00	5.20	8.23			8.20	63.41
	138.07	139.59	1.08	1.38	3.08			2.46	56.10
	139.59	140.81	0.68	1.35	3.08			2.03	66.50
	140.81	142.06	0.64	1.66	2.05			2.30	72.17
	142.06	143.56	1.66	4.50	6.17			6.16	73.05
	143.56	145.08	1.85	3.24	4.11			5.09	63.65
	145.08	146.61	2.41	3.59	5.14			6.00	59.83
	146.61	148.13	2.75	4.05	3.08			6.80	59.56
	148.13	149.65	3.15	5.00	8.23			8.15	61.35
	149.65	151.10	5.11	6.53	11.31			11.64	56.10
	151.18	152.70	4.00	1.79	10.28			5.79	30.92
	152.70	154.23	0.36	0.62	1.03			0.98	63.27
	154.23	155.75	0.15	0.57	1.03			0.72	79.17
	155.75	157.27	0.22	0.61	2.05			0.83	73.49
	157.27	158.80	0.47	1.02	1.03			1.49	68.46
	158.80	160.23	0.45	0.64	3.08			1.09	58.72
	160.32	161.84	1.40	1.31	4.11			2.71	48.34
	161.84	163.37	0.74	0.48	3.08			1.22	39.34
	163.37	164.89	1.10	1.28	5.14			2.38	53.78
	164.89	166.42	2.55	4.76	6.17			7.31	65.12
	166.42	167.94	2.36	3.52	7.19			5.88	59.86
	167.94	168.55	4.70	4.12	13.37			8.82	46.71
	168.44	169.77	3.24	4.15	11.31			7.39	56.16
	169.77	171.29	0.90	1.31	2.74			2.21	59.28
	171.29	172.81	0.38	0.76	2.74			1.14	66.67
	172.81	174.33	0.42	0.99	2.74			1.41	70.21
	174.33	175.86	0.93	1.17	2.74			2.10	55.71
	175.86	177.38	0.89	1.09	2.74			1.98	55.05
	177.38	178.91	1.46	1.10	2.74			2.56	42.97
	178.91	180.43	1.30	1.98	2.74			3.28	60.37
	180.43	181.95	1.03	1.81	2.74			2.84	63.73
	181.95	183.43	0.85	1.53	2.74			2.38	64.29
	183.48	184.70	0.73	0.83	2.74			1.56	53.21
	184.70	185.92	1.12	2.35	4.11			3.47	67.72
	185.92	187.15	1.92	2.24	4.11			4.16	53.85

HOLE	FROM	TO	LEAD	ZINC	SILVER	COPPER	GOLD	Pb+Zn	Zn ratio
6	187.15	188.67	0.56	0.43	2.74			0.99	43.43
	188.67	190.19	1.57	1.77	2.74			3.34	52.99
	190.19	191.72	0.27	1.06	2.74			1.33	79.70
	191.72	193.24	0.05	0.23	2.74			0.28	82.14
	193.24	195.77	0.06	0.03	2.74			0.09	33.33
	195.77	196.29	0.03	0.02	2.74			0.05	40.00
	196.29	197.28	0.11	0.50	2.74			0.61	81.97
	197.28	199.34	0.05	0.65	2.74			0.70	92.86
	199.34	200.86	0.02	1.28	2.74			1.30	98.46
	200.86	202.39	0.13	2.45	6.17			2.58	94.96
	202.39	203.91	0.12	1.95	7.19			2.07	94.20
	203.91	205.43	0.31	1.79	6.17			2.10	85.24
	205.43	206.95	0.01	1.78	2.06			1.79	99.44
	206.95	208.48	0.01	2.32	1.03			2.33	99.57
	208.48	210.31	0.01	0.20	1.37			0.21	95.24
	210.31	211.83	0.01	0.05				0.06	83.33
	211.83	213.36	0.02	0.04				0.06	66.67
	213.36	214.88	0.00	0.04				0.04	100.00
	214.88	216.41	0.00	0.02				0.02	100.00
	216.41	217.93	0.01	0.02				0.03	66.67
	217.93	219.45	0.00	0.02				0.02	100.00
	219.45	220.97	0.00	0.45				0.45	100.00
	220.97	222.50	0.08	0.15				0.23	65.22
	222.50	223.72	0.20	0.14				0.34	41.18
	223.72	225.86	0.67	0.96	2.74			1.63	58.90
7	79.39	80.38	0.28	0.35				0.63	55.56
	82.02	83.66	0.35	0.43				0.78	55.13
	83.66	85.30	0.52	0.64				1.16	55.17
	88.91	89.89	0.18	0.26				0.44	59.09
	92.50	94.80	0.12	0.31				0.43	72.09
	96.13	98.09	0.14	0.15				0.29	51.72
	98.09	100.06	0.13	0.17				0.30	56.67
	100.06	102.03	0.22	0.49				0.71	69.01
	102.03	104.00	0.31	0.86				1.17	73.50
	104.00	105.97	0.26	0.38				0.64	59.38
	113.52	115.45	0.12	0.16				0.28	57.14
	115.45	116.41	0.34	0.37				0.71	52.11
	116.41	119.42	0.20	0.35				0.55	63.64
	119.42	121.39	0.12	1.70				1.82	93.41
	121.39	123.34	0.12	1.20				1.32	90.91
	123.34	125.33	0.10	0.37				0.47	78.72
	125.33	127.29	0.24	0.41				0.65	63.08
	127.29	129.23	0.60	0.50				1.10	45.45
	129.23	134.23	0.28	0.39				0.67	58.21
	133.20	135.17	0.25	0.33				0.58	56.90
	134.23	133.20	0.57	0.61				1.18	51.69
	135.17	137.30	0.40	0.91				1.31	69.47
	137.30	139.11	0.15	0.55				0.70	78.57
	139.11	141.07	0.16	0.18				0.34	52.94
	141.07	143.04	0.17	0.34				0.51	66.67
	143.04	145.01	0.17	0.32				0.49	65.31
	145.01	146.98	0.11	0.46				0.57	80.70
	146.98	148.95	0.13	0.14				0.27	51.85
	148.95	150.92	0.21	0.27				0.48	56.25
	150.92	152.89	0.16	0.19				0.35	54.29

HOLE	FROM	TO	LEAD	ZINC	SILVER	COPPER	GOLD	Pb+Zn	Zn ratio
7	152.89	154.86	0.22	0.21				0.43	48.84
	154.86	156.83	0.25	0.36				0.61	59.02
	156.83	158.80	0.07	0.27				0.34	79.41
	158.80	160.85	0.12	0.12				0.24	50.00
	160.85	162.72	0.08	0.13				0.21	61.90
	162.72	164.69	0.06	0.05				0.11	45.45
	164.69	166.66	0.18	0.24				0.42	57.14
	166.66	168.63	0.13	0.72				0.85	84.71
	232.71	234.58	2.21	4.22				6.43	65.63
	234.58	236.22	1.82	2.69				4.51	59.65
	236.22	237.86	2.19	3.32				5.51	60.25
	237.86	239.50	1.42	1.81				3.23	56.04
	239.50	241.15	1.22	1.92				3.14	61.15
9	10.05	11.58	0.61	1.16	4.79			1.77	65.54
	11.58	13.10	0.62	1.56	4.79			2.18	71.56
	13.10	14.63	0.57	0.42	4.11			0.99	42.42
	14.63	16.15	1.21	2.10	4.79			3.31	63.44
	16.15	17.67	2.09	3.02	6.17			5.11	59.10
	17.67	19.20	1.16	3.12	4.11			4.28	72.90
	19.20	20.42	1.87	3.74	9.25			5.61	66.67
	20.42	21.94	3.98	9.24	15.09			13.22	69.89
	21.94	23.77	3.27	7.82	10.63			11.09	70.51
	23.77	25.29	2.58	4.63	7.88			7.21	64.22
	25.29	26.82	2.00	4.35	8.23			6.35	68.50
	26.82	28.34	2.03	2.79	8.23			4.82	57.88
	28.34	29.87	0.98	1.57	4.79			2.55	61.57
	29.87	31.39	0.89	2.38	4.79			3.27	72.78
	31.39	32.61	0.91	1.35	5.48			2.26	59.73
	32.61	33.52	0.70	1.51	5.48			2.21	68.33
	33.52	35.05	2.46	6.76	9.25			9.22	73.32
	35.05	36.57	1.98	4.54	7.54			6.52	69.63
	36.57	38.10	2.96	10.08	10.63			13.04	77.30
	38.10	39.62	2.12	5.49	6.86			7.61	72.14
	39.62	41.75	1.48	4.82	2.74			6.30	76.51
	41.75	43.28	0.34	0.71	1.37			1.05	67.62
	43.28	44.81	0.38	0.68	2.06			1.06	64.15
	44.81	46.32	0.46	1.21	3.43			1.67	72.46
	46.32	47.85	0.51	0.82	2.06			1.33	61.65
	47.85	49.37	0.30	0.90	1.37			1.20	75.00
	49.37	50.90	0.31	1.04	2.74			1.35	77.04
	50.90	52.12	0.52	0.75	2.74			1.27	59.06
	52.12	53.34	0.04	0.10				0.14	71.43
	53.34	54.86	0.64	2.67				3.31	80.66
	54.86	56.38	0.06	0.30				0.36	83.33
	56.38	57.91	0.17	0.54				0.71	76.06
	57.91	59.43	0.02	0.07				0.09	77.78
	59.43	60.96	0.03	0.07				0.10	70.00
	60.96	62.48	0.05	0.10				0.15	66.67
	62.48	64.00	0.05	0.12				0.17	70.59
	64.00	65.53	0.02	0.03				0.05	60.00
	65.53	67.05	0.00	0.02				0.02	100.00
	67.05	68.58	0.03	0.11				0.14	78.57
	68.58	70.10	0.02	0.08				0.10	80.00
	70.10	71.63	0.02	0.07				0.09	77.78
	71.63	73.15	0.04	0.14				0.18	77.78

HOLE	FROM	TO	LEAD	ZINC	SILVER	COPPER	GOLD	Pb+Zn	Zn ratio
9	73.15	74.67	0.06	0.24				0.30	80.00
	74.67	76.20	0.23	0.54				0.77	70.13
	76.20	77.72	0.05	0.16				0.21	76.19
	77.72	79.25	0.30	0.25				0.55	45.45
	79.25	80.77	0.15	0.35				0.50	70.00
	80.77	82.29	0.22	0.36				0.58	62.07
	82.29	83.82	0.36	0.33				0.69	47.83
	83.82	85.64	0.02	0.16				0.18	88.89
	85.64	87.17	0.02	0.03				0.05	60.00
	87.17	88.64	0.01	0.04				0.05	80.00
	88.69	90.22	0.34	0.64	2.06			0.98	65.31
	90.22	91.74	0.31	0.74	2.06			1.05	70.48
	91.74	93.27	0.76	1.07	3.43			1.83	58.47
	93.27	94.79	0.14	0.10	1.71			0.24	41.67
	94.79	96.31	1.10	0.81	5.82			1.91	42.41
	96.31	97.84	0.07	0.06	0.34			0.13	46.15
	97.84	99.36	0.06	0.06	0.34			0.12	50.00
	99.36	100.88	0.20	0.24	1.37			0.44	54.55
	100.88	102.41	0.20	0.17	2.06			0.37	45.95
	102.31	104.54	0.20	0.34	2.06			0.54	62.96
	104.54	106.07	0.63	0.80	2.39			1.43	55.94
	106.07	107.59	1.42	1.95	4.11			3.37	57.86
	107.59	109.12	0.37	0.77	1.71			1.14	67.54
	109.12	110.95	1.23	2.18	3.43			3.41	63.93
	110.95	112.47	0.65	1.68	2.06			2.33	72.10
	112.47	113.99	1.45	1.21	4.11			2.66	45.49
	113.99	115.52	1.40	1.53	3.43			2.93	52.22
	115.52	117.05	0.78	0.97	2.39			1.75	55.43
	117.05	118.26	1.17	1.10	3.77			2.27	48.46
	118.26	119.78	2.66	4.23	6.51			6.89	61.39
	119.78	121.31	1 70	2.12	4.46			3.82	55.50
	121.31	122.83	1.49	3.65	5.14			5.14	71.01
	122.83	124.36	0.72	1.65	3.08			2.37	69.62
	124.36	125.57	1.14	2.77	4.79			3.91	70.84
	125.57	127.09	1.24	2.47	3.77			3.71	66.58
	127.09	128.62	0.99	3.20	3.43			4.19	76.37
	128.62	130.14	0.80	2.33	2.74			3.13	74.44
	130.14	131.66	0.88	1.48	2.39			2.36	62.71
	131.66	133.19	1.02	0.38	2.39			1.40	27.14
	133.19	134.71	0.25	0.44	1.71			0.69	63.77
	134.71	136.23	0.59	1.35	2.06			1.94	69.59
	136.23	137.76	2.19	3.49	4.79			5.68	61.44
	137.76	139.28	1.15	1.18	2.74			2.33	50.64
	139.28	140.51	0.41	0.26	1.03			0.67	38.81
	140.51	142.34	0.45	1.06	1.03			1.51	70.20
	142.34	144.17	0.95	0.87	2.39			1.82	47.80
	144.17	145.99	0.63	1.70	1.37			2.33	72.96
	145.99	147.51	0.67	1.34	1.71			2.01	66.67
	147.51	149.03	0.53	1.58	1.03			2.11	74.88
	149.03	150.56	0.41	1.31	1.03			1.72	76.16
	150.56	152.08	0.94	1.23	2.74			2.17	56.68
	152.02	153.61	1.03	1.94	0.08			2.97	65.32
	153.61	155.13	0.11	0.23	1.37			0.34	67.65
	155.13	156.66	0.14	0.56	1.71			0.70	80.00
	156.66	158.18	0.06	0.46	1.71			0.52	88.46

HOLE	FROM	TO	LEAD	ZINC	SILVER	COPPER	GOLD	Pb+Zn	Zn ratio
9	158.18	159.70	0.02	2.37	1.03			2.39	99.16
	159.70	161.23	0.03	0.64	1.37			0.67	95.52
	161.23	162.75	0.04	1.47	0.68			1.51	97.35
	162.75	164.27	1.42	5.54	7.19			6.96	79.60
	164.27	165.80	1.08	3.78	4.45			4.86	77.78
	165.80	167.32	0.06	2.28	1.03			2.34	97.44
	167.32	168.85	0.10	1.32	1.37			1.42	92.96
	168.85	170.07	0.02	1.61	1.03			1.63	98.77
	170.07	171.59	0.04	1.40	1.03			1.44	97.22
	171.59	173.12	0.02	1.24	1.37			1.26	98.41
	173.12	174.64	0.02	0.10	1.71			0.12	83.33
	174.64	176.16	0.01	0.65	0.68			0.66	98.48
	176.16	177.69	0.01	0.33	1.03			0.34	97.06
	177.69	178.91	0.60	0.81				1.41	57.45
	178.91	180.44	0.38	0.75				1.13	66.37
	180.44	181.96	0.44	0.98				1.42	69.01
	181.96	183.48	0.02	0.02				0.04	50.00
	183.48	185.01	0.02	0.08				0.10	80.00
	185.01	186.53	0.02	0.03				0.05	60.00
	186.53	188.06	0.03	0.02				0.05	40.00
	188.06	189.58	0.02	0.03				0.05	60.00
	189.58	191.11	0.02	0.04				0.06	66.67
	191.11	192.63	0.01	0.03				0.04	75.00
	192.63	194.15	0.01	0.01				0.02	50.00
	194.15	195.68	0.01	0.01				0.02	50.00
	195.68	197.21	0.01	0.03				0.04	75.00
	197.21	198.73	0.08	0.45				0.53	84.91
	198.73	200.23	0.02	0.06				0.08	75.00
	200.25	200.86	0.04	1.50				1.54	97.40
	200.86	202.08	0.01	0.02				0.03	66.67
	202.08	203.30	0.01	0.16				0.17	94.12
	203.30	203.91	0.04	1.08				1.12	96.43
	203.91	205.43	0.01	0.10				0.11	90.91
	205.43	206.80	0.00	0.01				0.01	100.00
10	9.14	11.88	0.40	0.06				0.46	13.04
	11.88	13.71	0.27	0.05				0.32	15.63
	13.71	14.93	0.25	0.04				0.29	13.79
	14.93	17.06	0.17	0.07				0.24	29.17
	17.06	18.89	0.16	0.07				0.23	30.43
	18.89	20.42	0.30	0.20				0.50	40.00
	20.42	21.94	0.76	0.22				0.98	22.45
	21.94	23.46	0.08	0.06				0.14	42.86
	23.46	24.99	0.11	0.06				0.17	35.29
	24.99	26.51	0.18	0.08				0.26	30.77
	26.51	28.04	0.16	0.07				0.23	30.43
	28.04	29.56	0.05	0.06				0.11	54.55
	29.56	31.08	0.11	0.27				0.38	71.05
	31.08	32.61	0.03	0.37				0.40	92.50
	32.61	34.14	0.02	0.16				0.18	88.89
	34.14	35.66	0.02	0.13				0.15	86.67
	35.66	37.18	0.02	0.14				0.16	87.50
	37.18	38.71	0.02	0.11				0.13	84.62
	38.71	40.23	0.03	0.16				0.19	84.21
	40.23	41.76	0.42	1.72				2.14	80.37
	41.76	43.28	0.36	0.59				0.95	62.11

HOLE	FROM	TO	LEAD	ZINC	SILVER	COPPER	GOLD	Pb+Zn	Zn ratio
10	43.28	44.81	0.06	0.23				0.29	79.31
	44.81	46.32	0.05	0.15				0.20	75.00
	46.23	47.85	0.09	0.23				0.32	71.88
	47.85	49.68	0.08	0.37				0.45	82.22
	49.68	51.21	0.03	0.06				0.09	66.67
	51.21	52.73	0.01	0.08				0.09	88.89
	52.73	54.56	0.12	0.24				0.36	66.67
	54.56	56.08	0.08	0.27				0.35	77.14
	56.08	57.61	0.41	0.32				0.73	43.84
	57.61	59.13	0.24	0.37				0.61	60.66
	59.13	60.65	1.16	0.20				1.36	14.71
	60.65	62.18	0.70	1.45				2.15	67.44
	62.18	63.39	0.45	0.39				0.84	46.43
	63.39	64.62	0.22	0.27				0.49	55.10
	64.42	66.12	1.60	2.02	4.79			3.62	55.80
	66.14	67.67	0.83	2.05	2.74			2.88	71.18
	67.67	69.19	1.15	0.86	2.74			2.01	42.79
	69.19	70.71	1.04	1.46	4.11			2.50	58.40
	70.71	72.24	0.90	3.11	4.11			4.01	77.56
	72.24	73.76	0.62	1.06	3.43			1.68	63.10
	73.76	75.29	0.51	1.24	2.06			1.75	70.86
	75.29	76.81	0.58	1.34	2.06			1.92	69.79
	76.81	78.33	1.23	1.57	2.74			2.80	56.07
	78.33	79.86	0.39	0.72	1.37			1.11	64.86
	79.86	81.38	1.15	3.51	2.06			4.66	75.32
	81.38	82.91	1.36	3.09	4.11			4.45	69.44
	82.91	84.43	1.12	1.42	2.06			2.54	55.91
	84.43	85.95	0.36	1.03	1.37			1.39	74.10
	85.95	87.48	0.40	0.81				1.21	66.94
	87.48	89.00	0.30	0.39				0.69	56.52
	89.00	90.52	0.21	0.34				0.55	61.82
	90.52	92.05	0.18	0.17				0.35	48.57
	92.05	93.27	0.11	0.18				0.29	62.07
	93.27	94.49	0.26	0.18				0.44	40.91
	94.49	96.01	0.16	0.39	2.06			0.55	70.91
	96.01	97.54	0.58	1.20	1.37			1.78	67.42
	97.54	99.06	0.85	1.32	1.37			2.17	60.83
	99.06	100.58	0.87	1.76	2.74			2.63	66.92
	100.58	102.11	1.25	2.03	3.43			3.28	61.89
	102.11	103.63	2.54	3.66	7.54			6.20	59.03
	103.63	105.16	2.12	2.28	5.48			4.40	51.82
	105.16	106.68	0.27	0.29	0.68			0.56	51.79
	106.68	108.20	0.41	0.24	2.06			0.65	36.92
	108.21	109.93	0.54	1.61	2.06			2.15	74.88
	109.93	111.25	2.38	5.72	6.85			8.10	70.62
	111.25	112.78	1.86	4.42	7.54			6.28	70.38
	112.78	114.30	0.92	1.68	3.43			2.60	64.62
	114.31	115.82	1.41	2.21	4.11			3.62	61.05
	115.82	117.35	0.66	1.40	2.74			2.06	67.96
	117.35	118.87	0.55	1.07	2.06			1.62	66.05
	118.87	120.39	0.43	0.78	1.37			1.21	64.46
	120.39	121.92	0.18	0.09	0.68			0.27	33.33
	121.92	123.44	0.26	0.30	0.68			0.56	53.57
	123.44	124.97	0.53	1.39	1.71			1.92	72.40
	124.97	126.49	0.67	0.98	1.37			1.65	59.39

HOLE	FROM	TO	LEAD	ZINC	SILVER	COPPER	GOLD	Pb+Zn	Zn ratio
10	126.49	128.02	0.96	1.42	2.74			2.38	59.66
	128.02	129.54	0.98	2.04	3.43			3.02	67.55
	129.54	131.06	1.18	2.33	3.43			3.51	66.38
	131.06	132.59	1.50	2.90	3.43			4.40	65.91
	132.59	134.11	0.55	0.93	2.06			1.48	62.84
	134.11	135.64	0.78	1.22	2.79			2.00	61.00
	135.64	137.16	0.61	0.61	2.06			1.22	50.00
	137.16	138.68	0.30	0.46				0.76	60.53
	138.68	140.51	1.16	1.50				2.66	56.39
	140.51	142.03	0.24	0.27				0.51	52.94
	142.03	143.56	0.32	0.59				0.91	64.84
	143.56	145.08	0.00	0.15				0.15	100.00
	145.08	146.61	0.07	0.15				0.22	68.18
	146.61	148.13	0.02	0.06				0.08	75.00
	148.13	149.66	0.03	0.06				0.09	66.67
	149.66	151.18	0.18	0.21				0.39	53.85
	151.18	152.71	0.08	0.12				0.20	60.00
	152.71	154.23	1.25	2.32				3.57	64.99
	154.23	155.75	0.34	0.55				0.89	61.80
	155.75	157.28	0.42	0.48				0.90	53.33
	157.28	158.80	0.13	0.29				0.42	69.05
	158.80	160.23	0.07	0.19				0.26	73.08
	160.23	161.85	0.02	0.10				0.12	83.33
	161.85	163.37	0.11	0.20				0.31	64.52
	163.37	165.89	0.04	0.09				0.13	69.23
	165.89	166.42	0.08	0.11				0.19	57.89
	166.42	167.94	0.24	0.57				0.81	70.37
	167.94	169.77	0.25	0.63				0.88	71.59
	169.77	170.07	0.99	19.00				19.99	95.05
	170.07	171.60	0.09	0.30				0.39	76.92
	171.60	173.13	0.14	0.34				0.48	70.83
	173.13	174.65	0.12	0.14				0.26	53.85
	174.65	175.17	0.32	0.48				0.80	60.00
	176.17	177.70	0.10	0.32				0.42	76.19
	177.70	179.22	0.21	0.46				0.67	68.66
	179.22	180.75	0.54	1.04				1.58	65.82
	180.75	182.27	0.51	0.57				1.08	52.78
	182.27	183.79	0.44	0.72				1.16	62.07
	183.79	185.32	0.17	0.40				0.57	70.18
	185.32	186.84	0.05	0.30				0.35	85.71
	186.84	188.36	0.07	0.14				0.21	66.67
	188.36	191.14	0.08	0.23				0.31	74.19
	191.41	192.94	0.20	0.30				0.50	60.00
	192.24	194.16	0.32	0.23				0.55	41.82
11	25.59	26.57	0.11	0.04				0.15	26.67
	26.57	27.55	0.20	0.05				0.25	20.00
	27.55	28.87	0.20	0.38				0.58	65.52
	28.87	30.51	0.19	0.39				0.58	67.24
	30.51	32.15	0.06	0.14				0.20	70.00
	32.15	32.81	0.16	0.13				0.29	44.83
	32.81	34.45	0.46	0.73	4.45			1.19	61.34
	34.45	36.08	0.22	0.60	4.79			0.82	73.17
	36.08	37.73	0.36	1.21	7.89			1.57	77.07
	37.73	39.37	0.21	0.75	5.14			0.96	78.13
	39.37	41.01	0.10	0.34	2.39			0.44	77.27

HOLE	FROM	TO	LEAD	ZINC	SILVER	COPPER	GOLD	Pb+Zn	Zn ratio
11	41.01	42.65	0.20	0.58	2.74			0.78	74.36
	42.65	44.29	0.16	0.39	3.08			0.55	70.91
	44.29	45.93	0.07	0.29	2.39			0.36	80.56
	45.93	47.57	0.27	0.60	3.08			0.87	68.97
	47.57	49.21	0.22	0.85	3.08			1.07	79.44
	49.21	50.85	0.33	0.80	3.43			1.13	70.80
	50.85	52.49	1.77	1.35	4.45			3.12	43.27
	52.49	54.13	2.18	2.97	6.17			5.15	57.67
	54.13	55.77	1.29	2.65	4.45			3.94	67.26
	55.77	57.09	1.91	2.28	5.83			4.19	54.42
	57.09	58.39	1.04	1.95	3.77			2.99	65.22
	57.09	58.39	1.04	1.95	4.11			2.99	65.22
	58.39	60.04	0.27	0.58				0.85	68.24
	60.04	61.68	0.40	0.74				1.14	64.91
	61.68	63.32	0.17	0.15				0.32	46.88
	63.32	64.96	0.03	0.07				0.10	70.00
	64.96	66.60	0.03	0.14				0.17	82.35
	66.60	68.24	0.36	0.04				0.40	10.00
	68.24	69.88	0.68	0.61				1.29	47.29
	69.88	71.52	0.02	0.07				0.09	77.78
	71.52	73.56	0.46	0.21				0.67	31.34
	73.56	74.80	0.04	0.02				0.06	33.33
	74.80	76.44	0.06	0.05				0.11	45.45
	76.44	77.43	0.32	0.14				0.46	30.43
	77.43	78.74	1.10	1.35				2.45	55.10
	78.74	80.05	0.70	1.18				1.88	62.77
	80.05	81.69	0.45	0.61				1.06	57.55
	81.69	83.33	0.39	0.51				0.90	56.67
	83.33	84.97	0.11	0.03				0.14	21.43
	84.97	86.61	0.21	0.08				0.29	27.59
	86.61	88.25	0.52	0.57				1.09	52.29
	88.25	89.89	0.56	1.02				1.58	64.56
	89.89	91.53	0.42	1.62				2.04	79.41
	91.53	93.18	1.12	1.14	3.08			2.26	50.44
	93.18	94.82	0.63	1.00	2.39			1.63	61.35
	94.82	95.80	0.39	0.86	1.71			1.25	68.80
	95.80	97.11	0.56	1.08	2.39			1.64	65.85
	97.11	98.43	0.84	0.68				1.52	44.74
	98.43	99.41	0.85	0.93				1.78	52.25
	99.41	100.55	0.68	1.70	2.74			2.38	71.43
	100.55	102.03	0.85	0.82				1.67	49.10
	102.03	103.67	0.35	0.78	2.06			1.13	69.03
	103.67	105.32	0.44	0.34	1.37			0.78	43.59
	105.32	106.95	0.56	0.56	1.71			1.12	50.00
	106.95	108.92	0.19	0.35	0.68			0.54	64.81
	108.92	109.58	0.32	0.40	1.37			0.72	55.56
	109.58	110.56	1.40	2.50	4.79			3.90	64.10
	110.56	112.21	0.45	1.12	1.71			1.57	71.34
	112.21	114.17	0.81	1.72	3.08			2.53	67.98
	114.17	114.83	1.52	4.40	6.17			5.92	74.32
	128.61	130.25	0.17	0.42				0.59	71.19
	130.25	131.89	0.04	0.09				0.13	69.23
	131.89	133.53	0.05	0.25				0.30	83.33
	133.53	135.17	0.06	0.20				0.26	76.92
	135.17	136.81	0.05	0.07				0.12	58.33

HOLE	FROM	TO	LEAD	ZINC	SILVER	COPPER	GOLD	Pb+Zn	Zn ratio
12	42.65	44.29	0.16	0.28				0.44	63.64
	44.29	45.93	0.08	0.08				0.16	50.00
	45.93	46.91	0.21	0.14				0.35	40.00
	46.91	48.55	0.66	0.34	1.37			1.00	34.00
	48.55	50.52	0.32	0.35				0.67	52.24
	50.52	52.16	0.36	0.54				0.90	60.00
	52.16	53.81	0.82	1.02	3.43			1.84	55.43
	53.81	55.45	3.48	4.94	14.06			8.42	58.67
	55.45	57.01	0.57	0.94	0.34			1.51	62.25
	57.01	58.73	1.47	0.32	4.79			1.79	17.88
	58.73	60.04	0.97	0.25	5.83			1.22	20.49
	60.04	60.69	4.10	9.55	15.09			13.65	69.96
	60.09	62.66	0.40	0.72	2.06			1.12	64.29
	62.66	64.63	0.69	0.67	3.08			1.36	49.26
	64.63	66.60	0.41	0.18	2.06			0.59	30.51
	66.60	68.57	1.01	0.29	2.06			1.30	22.31
	68.57	70.21	0.96	1.06	3.08			2.02	52.48
	70.21	71.85	0.45	1.24	1.71			1.69	73.37
	71.85	73.82	0.83	1.66	2.74			2.49	66.67
	76.12	77.76	1.02	2.88	3.77			3.90	73.85
	91.86	93.50	1.17	1.52	2.74			2.69	56.51
	93.50	95.14	0.32	0.62	1.03			0.94	65.96
	95.14	96.78	0.58	1.75	1.03			2.33	75.11
	96.78	98.43	1.23	1.64	2.39			2.87	57.14
	98.43	100.07	0.96	1.43	2.06			2.39	59.83
	108.27	109.91	1.01	2.23	2.74			3.24	68.83
	109.91	111.55	1.15	2.92	3.08			4.07	71.74
	111.55	113.19	0.89	3.04	2.74			3.93	77.35
	113.19	114.83	0.63	2.23	2.06			2.86	77.97
	114.83	116.47	0.24	1.33	1.37			1.57	84.71
	116.47	118.11	0.23	0.66	1.71			0.89	74.16
	118.11	119.75	0.45	0.50	1.71			0.95	52.63
	119.75	121.39	0.38	1.10	1.71			1.48	74.32
	121.39	123.03	0.73	1.72	3.08			2.45	70.20
	123.03	124.67	0.74	2.62	2.74			3.36	77.98
13	54.13	57.71	0.03	0.11				0.14	78.57
	57.71	59.06	0.04	0.17				0.21	80.95
	59.06	59.87	0.43	0.38				0.81	46.91
	59.87	60.53	1.52	9.39				10.91	86.07
	60.53	61.35	0.90	0.47				1.37	34.31
	61.35	62.00	1.10	0.85				1.95	43.59
	62.00	62.34	0.90	4.59				5.49	83.61
	62.34	63.65	0.83	0.50				1.33	37.59
	63.65	65.62	0.75	0.45				1.20	37.50
	65.62	66.27	0.42	0.14				0.56	25.00
	66.27	68.57	0.18	0.27				0.45	60.00
	68.57	70.21	0.45	0.75				1.20	62.50
	70.21	71.85	0.31	0.85				1.16	73.28
	71.85	73.49	0.02	0.10				0.12	83.33
	81.69	83.33	0.03	0.10				0.13	76.92
	83.33	84.97	0.09	0.39				0.48	81.25
	84.97	86.61	0.14	0.11				0.25	44.00
	86.61	87.92	0.31	0.38				0.69	55.07
	87.92	88.91	0.36	0.54				0.90	60.00
	88.91	90.22	0.72	2.71				3.43	79.01

HOLE	FROM	TO	LEAD	ZINC	SILVER	COPPER	GOLD	Pb+Zn	Zn ratio
13	90.22	91.54	0.50	2.56				3.06	83.66
	91.54	93.83	0.41	1.04				1.45	71.72
	93.83	96.13	0.80	1.81				2.61	69.35
	96.13	97.77	0.39	0.41				0.80	51.25
	97.77	99.41	0.26	0.10				0.36	27.78
	99.41	101.05	0.16	0.68				0.84	80.95
	101.05	102.69	0.11	0.18				0.29	62.07
	102.69	104.00	0.04	0.09				0.13	69.23
	104.00	105.64	0.08	0.06				0.14	42.86
	105.64	105.64	0.08	0.06				0.14	42.86
	105.64	107.28	1.81	0.68				2.49	27.31
	107.28	108.26	1.81	0.68				2.49	27.31
	108.26	109.58	1.58	5.24				6.82	76.83
	109.58	110.89	1.14	3.85				4.99	77.15
	110.89	112.86	0.54	1.27				1.81	70.17
	112.86	114.50	0.05	0.21				0.26	80.77
	114.50	116.47	0.07	0.17				0.24	70.83
	116.47	117.78	0.71	1.34				2.05	65.37
	117.78	119.09	1.52	3.27				4.79	68.27
	119.09	120.73	1.33	2.16				3.49	61.89
	120.73	122.37	0.83	0.94				1.77	53.11
	122.37	124.02	0.76	1.70				2.46	69.11
	124.02	125.98	2.54	6.96				9.50	73.26
	125.98	126.31	0.97	1.10				2.07	53.14
	126.31	127.62	4.16	7.10				11.26	63.06
	127.62	128.93	2.87	5.70				8.57	66.51
	128.93	130.25	4.98	7.20				12.18	59.11
	130.25	131.56	2.01	1.09				3.10	35.16
	131.56	132.87	0.57	2.77				3.34	82.93
	132.87	134.51	0.79	1.27				2.06	61.65
	134.51	136.15	0.73	0.47				1.20	39.17
	136.15	137.79	1.30	1.77				3.07	57.65
	137.79	139.43	0.38	0.22				0.60	36.67
	139.43	141.08	1.01	1.65				2.66	62.03
	141.08	142.72	3.39	2.81				6.20	45.32
	142.72	144.36	0.99	1.02				2.01	50.75
	144.36	145.99	0.44	0.43				0.87	49.43
	145.99	147.64	0.86	0.74				1.60	46.25
	147.64	149.28	1.00	1.51				2.51	60.16
	149.28	150.92	0.12	0.13				0.25	52.00
	150.92	152.56	0.42	0.42				0.84	50.00
	152.56	154.19	0.32	1.12				1.44	77.78
	154.19	155.84	0.57	1.57				2.14	73.36
	155.84	157.48	1.28	2.70				3.98	67.84
	157.48	159.12	0.64	0.33				0.97	34.02
	159.12	160.76	0.12	0.20				0.32	62.50
	187.00	188.65	0.13	0.07				0.20	35.00
	188.65	190.29	0.34	0.18				0.52	34.62
	190.29	191.93	0.05	0.05				0.10	50.00
	191.93	192.91	0.38	0.15				0.53	28.30
	192.91	194.55	0.88	1.74				2.62	66.41
	194.55	196.19	0.41	0.76				1.17	64.96
	196.19	196.85	1.51	0.71				2.22	31.98
	196.85	198.16	0.07	0.22				0.29	75.86
	198.16	198.49	0.07	4.96				5.03	98.61

HOLE	FROM	TO	LEAD	ZINC	SILVER	COPPER	GOLD	Pb+Zn	Zn ratio
13	198.49	200.15	0.35	1.31				1.66	78.92
	200.15	201.77	0.15	0.30				0.45	66.67
	201.77	203.41	0.18	0.09				0.27	33.33
	203.41	205.05	0.21	0.20				0.41	48.78
	205.05	206.69	0.18	0.30				0.48	62.50
	206.69	208.33	0.03	0.10				0.13	76.92
	208.33	209.97	0.15	0.02				0.17	11.76
	209.97	211.61	0.03	0.03				0.06	50.00
	221.13	222.77	0.12	0.24				0.36	66.67
	222.77	224.41	0.18	0.39				0.57	68.42
	224.41	226.05	0.13	0.32				0.45	71.11
	226.05	227.69	0.28	0.56				0.84	66.67
	227.69	229.33	0.32	0.77				1.09	70.64
	229.33	230.97	0.21	0.96				1.17	82.05
	230.97	232.61	0.30	0.69				0.99	69.70
	232.61	234.25	0.27	1.01				1.28	78.91
	234.25	237.21	0.28	0.74				1.02	72.55
14	30.18	31.82	0.05	0.16				0.21	76.19
	31.82	33.46	0.34	0.38				0.72	52.78
	33.46	35.10	0.24	0.25				0.49	51.02
	35.10	36.75	0.39	1.02				1.41	72.34
	36.75	38.39	1.63	1.76				3.39	51.92
	38.39	40.03	0.51	1.08				1.59	67.92
	40.03	41.34	2.00	3.66				5.66	64.66
	41.34	42.65	1.87	3.83				5.70	67.19
	42.65	44.29	0.97	2.22				3.19	69.59
	44.29	45.93	0.84	1.43				2.27	63.00
	45.93	47.24	0.27	0.41				0.68	60.29
	46.24	48.88	0.26	0.32				0.58	55.17
	48.88	50.85	0.28	0.36				0.64	56.25
	50.85	52.49	0.44	0.66				1.10	60.00
	52.49	54.13	0.43	0.38				0.81	46.91
	54.13	55.77	0.19	0.12				0.31	38.71
	55.77	57.41	0.12	0.14				0.26	53.85
	57.41	59.38	0.06	0.04				0.10	40.00
	59.38	61.35	0.03	0.07				0.10	70.00
	61.35	62.66	0.13	0.09				0.22	40.91
	62.66	62.69	1.26	0.38				1.64	23.17
	62.69	63.64	0.39	0.21				0.60	35.00
	63.64	65.29	1.44	1.98				3.42	57.89
	65.29	66.93	0.74	1.99				2.73	72.89
	66.93	68.57	1.68	0.99				2.67	37.08
	68.57	70.21	0.27	0.53				0.80	66.25
	70.21	72.18	0.27	0.53				0.80	66.25
	72.18	74.15	0.52	0.97				1.49	65.10
	74.15	75.46	0.24	0.25				0.49	51.02
	75.46	77.09	0.31	0.52				0.83	62.65
	77.09	78.74	0.14	0.19				0.33	57.58
	78.74	80.38	0.19	0.29				0.48	60.42
	80.38	82.02	0.13	0.11				0.24	45.83
	82.02	83.66	0.12	0.05				0.17	29.41
	83.66	85.31	0.13	0.31				0.44	70.45
	85.31	86.94	0.17	0.36				0.53	67.92
	86.94	88.58	0.14	0.35				0.49	71.43
	88.58	90.22	0.05	0.15				0.20	75.00

HOLE	FROM	TO	LEAD	ZINC	SILVER	COPPER	GOLD	Pb+Zn	Zn ratio
14	90.22	91.86	0.06	0.15				0.21	71.43
	91.86	93.50	0.08	0.13				0.21	61.90
	93.50	95.14	0.09	0.26				0.35	74.29
	95.14	96.78	0.34	0.33				0.67	49.25
	96.78	98.43	0.24	0.22				0.46	47.83
	98.43	100.06	0.79	0.53				1.32	40.15
	100.06	101.71	0.23	0.43				0.66	65.15
	101.71	103.35	0.23	0.25				0.48	52.08
	103.35	104.99	0.20	0.55				0.75	73.33
	104.99	106.63	0.21	0.52				0.73	71.23
	106.63	108.27	0.02	0.07				0.09	77.78
	108.27	109.91	0.20	0.18				0.38	47.37
	109.91	111.55	0.08	0.11				0.19	57.89
	111.55	113.19	0.26	0.55				0.81	67.90
	113.19	114.83	0.55	0.72				1.27	56.69
	114.83	116.47	0.51	0.87				1.38	63.04
	116.47	118.11	0.77	1.27				2.04	62.25
	118.11	119.75	0.50	1.24				1.74	71.26
	119.75	120.41	0.76	2.13				2.89	73.70
	120.41	121.71	0.99	2.25				3.24	69.44
	121.71	123.03	0.59	1.21				1.80	67.22
	123.03	124.67	0.07	0.12				0.19	63.16
	124.67	128.61	0.58	1.13				1.71	66.08
	128.61	130.25	0.50	1.85				2.35	78.72
	130.25	131.89	0.38	0.92				1.30	70.77
	131.89	133.53	0.22	0.35				0.57	61.40
	133.53	134.84	0.11	0.32				0.43	74.42
	133.53	134.84	0.11	0.32				0.43	74.42
	134.84	136.86	0.33	0.85				1.18	72.03
	136.86	138.45	0.30	0.42				0.72	58.33
	138.45	139.11	0.42	1.53				1.95	78.46
	139.11	139.76	0.10	0.08				0.18	44.44
	139.76	140.09	0.05	0.09				0.14	64.29
	140.09	141.08	1.28	1.82				3.10	58.71
	141.08	142.72	1.22	2.78				4.00	69.50
	142.72	144.36	2.20	4.32				6.52	66.26
	144.36	145.99	2.20	3.16				5.36	58.96
	145.99	147.64	1.53	3.58				5.11	70.06
	147.64	149.28	2.61	6.14				8.75	70.17
	149.28	150.91	1.74	3.26				5.00	65.20
	150.91	152.23	2.63	4.80				7.43	64.60
	152.23	153.31	1.05	3.22				4.27	75.41
	153.31	154.86	0.28	0.34				0.62	54.84
	154.86	155.18	1.17	3.42				4.59	74.51
	155.18	156.82	0.38	0.58				0.96	60.42
	156.82	158.46	0.19	0.22				0.41	53.66
	158.46	160.11	0.46	1.20				1.66	72.29
	160.11	161.75	0.51	1.56				2.07	75.36
	161.75	163.39	0.36	0.71				1.07	66.36
	163.39	165.03	0.50	1.14				1.64	69.51
	165.03	166.67	0.66	1.08				1.74	62.07
	166.67	168.31	0.56	1.51				2.07	72.95
	168.31	170.28	0.63	1.54				2.17	70.97
	170.28	171.92	0.20	0.34				0.54	62.96
	171.92	173.56	0.06	0.18				0.24	75.00

HOLE	FROM	TO	LEAD	ZINC	SILVER	COPPER	GOLD	Pb+Zn	Zn ratio
14	173.56	175.19	0.13	0.28				0.41	68.29
	175.19	176.18	0.64	1.25				1.89	66.14
	176.18	180.45	0.17	0.23				0.40	57.50
	180.45	182.09	0.06	0.22				0.28	78.57
16	44.29	45.93	0.13	0.12				0.25	48.00
	45.93	47.57	0.75	2.44				3.19	76.49
	47.57	49.21	1.41	2.05				3.46	59.25
	49.21	50.85	1.15	2.91				4.06	71.67
	50.85	52.49	1.00	1.06				2.06	51.46
	52.49	54.13	1.28	1.20				2.48	48.39
	54.13	55.77	1.72	0.62				2.34	26.50
	55.77	57.41	1.21	2.07				3.28	63.11
	57.41	59.06	3.07	1.35				4.42	30.54
	59.06	60.69	1.75	2.70				4.45	60.67
	60.69	62.33	0.34	0.43				0.77	55.84
	62.33	63.98	0.62	0.74				1.36	54.41
	63.98	65.62	0.09	0.10				0.19	52.63
	65.62	67.26	0.05	0.05				0.10	50.00
	67.26	68.89	0.04	0.06				0.10	60.00
	68.89	70.54	0.17	0.44				0.61	72.13
	70.54	72.18	0.70	2.35				3.05	77.05
	72.18	73.82	0.58	1.07				1.65	64.85
	73.82	75.45	0.19	0.29				0.48	60.42
	75.45	77.09	0.45	0.32				0.77	41.56
	77.09	78.74	0.18	0.27				0.45	60.00
	78.74	80.38	0.45	0.32				0.77	41.56
	80.38	82.02	0.43	0.46				0.89	51.69
	82.02	83.66	1.99	3.53				5.52	63.95
	83.66	85.30	0.56	0.55				1.11	49.55
	85.30	86.94	0.08	0.07				0.15	46.67
	86.94	88.58	0.38	0.89				1.27	70.08
	88.58	90.22	0.24	0.22				0.46	47.83
	90.22	91.86	0.30	0.39				0.69	56.52
	91.86	93.50	0.27	0.21				0.48	43.75
	93.50	95.14	0.41	0.82				1.23	66.67
	95.14	96.78	0.98	2.13				3.11	68.49
	96.78	98.43	0.09	0.05				0.14	35.71
	98.43	100.06	0.22	0.70				0.92	76.09
	100.06	101.71	0.33	0.75				1.08	69.44
	101.71	103.35	0.15	0.20				0.35	57.14
	103.35	104.98	0.06	0.11				0.17	64.71
	104.98	106.63	0.05	0.07				0.12	58.33
	106.63	108.27	0.09	0.17				0.26	65.38
	108.27	109.91	0.13	0.12				0.25	48.00
	109.91	111.55	0.17	0.21				0.38	55.26
	111.55	113.19	0.07	0.06				0.13	46.15
	113.19	114.83	0.09	0.11				0.20	55.00
	114.83	116.47	0.19	0.16				0.35	45.71
	116.47	118.11	0.34	0.47				0.81	58.02
	118.11	119.75	0.53	1.46				1.99	73.37
	119.75	121.39	0.96	0.94				1.90	49.47
	121.39	123.03	0.67	0.91				1.58	57.59
	123.03	124.67	0.95	0.92				1.87	49.20
	124.67	126.31	0.21	0.38				0.59	64.41
	126.31	127.95	0.38	0.45				0.83	54.22

HOLE	FROM	TO	LEAD	ZINC	SILVER	COPPER	GOLD	Pb+Zn	Zn ratio
16	127.95	129.59	1.23	1.75				2.98	58.72
	129.59	131.23	1.79	1.21				3.00	40.33
	131.23	132.87	0.53	0.52				1.05	49.52
	132.87	134.51	0.17	0.27				0.44	61.36
	134.51	136.15	0.22	0.34				0.56	60.71
	136.15	137.79	0.12	0.28				0.40	70.00
	150.92	152.56	0.18	0.25				0.43	58.14
	152.56	154.21	0.57	1.13				1.70	66.47
	154.21	155.84	0.19	0.24				0.43	55.81
	155.84	157.48	0.21	0.61				0.82	74.39
	157.48	159.12	0.41	1.15				1.56	73.72
	159.12	160.76	0.04	0.12				0.16	75.00
	160.76	162.40	0.17	0.34				0.51	66.67
	162.40	164.04	0.15	0.56				0.71	78.87
	164.04	165.68	0.38	1.00				1.38	72.46
	165.68	167.32	0.13	0.31				0.44	70.45
	167.32	168.96	0.09	0.18				0.27	66.67
	168.96	170.60	0.13	0.25				0.38	65.79
	170.60	172.24	0.15	0.33				0.48	68.75
	172.24	173.88	0.14	0.38				0.52	73.08
	173.88	175.52	0.14	0.38				0.52	73.08
	175.52	177.17	1.80	1.32				3.12	42.31
	177.17	178.81	0.76	0.95				1.71	55.56
	178.81	180.45	0.43	0.69				1.12	61.61
	180.45	182.09	0.49	0.73				1.22	59.84
	182.09	183.73	0.31	0.67				0.98	68.37
	183.73	185.37	0.34	1.15				1.49	77.18
	185.37	187.00	1.62	2.12				3.74	56.68
	187.00	188.65	0.57	1.77				2.34	75.64
	188.65	190.29	0.13	0.12				0.25	48.00
17	70.10	71.63	0.16	0.37				0.53	69.81
	71.63	73.15	0.15	0.48				0.63	76.19
	73.15	74.67	0.18	0.40				0.58	68.97
	74.67	76.20	0.65	0.61				1.26	48.41
	76.20	77.72	0.61	0.93				1.54	60.39
	77.72	79.95	0.87	1.44				2.31	62.34
	79.95	80.77	0.06	0.07				0.13	53.85
	80.77	82.29	0.01	0.02				0.03	66.67
	82.29	83.82	0.01	0.03				0.04	75.00
	83.82	85.34	0.18	0.57				0.75	76.00
	85.34	86.87	0.28	0.62				0.90	68.89
	86.87	88.39	0.39	0.69				1.08	63.89
	88.39	89.91	0.30	0.23				0.53	43.40
	89.91	91.44	0.98	1.91				2.89	66.09
	91.44	92.96	1.01	1.67				2.68	62.31
	92.96	94.49	1.42	2.11				3.53	59.77
	94.49	96.01	0.93	1.33				2.26	58.85
	96.01	97.54	0.69	1.53				2.22	68.92
	97.54	99.06	0.21	1.01				1.22	82.79
	99.06	100.58	0.13	1.10				1.23	89.43
	100.58	102.11	0.46	0.58				1.04	55.77
	102.11	103.68	0.15	0.29				0.44	65.91
	103.68	105.16	0.16	0.20				0.36	55.56
	105.16	106.68	0.17	1.58				1.75	90.29
	106.68	108.20	0.03	0.05				0.08	62.50

HOLE	FROM	TO	LEAD	ZINC	SILVER	COPPER	GOLD	Pb+Zn	Zn ratio
17	108.20	109.73	0.03	0.18				0.21	85.71
	109.73	111.25	0.02	1.18				1.20	98.33
22	9.18	10.51	0.15	0.21	1.03			0.36	58.33
	10.51	11.81	0.14	0.07	1.03			0.21	33.33
	11.81	13.12	0.10	0.08	1.37			0.18	44.44
	13.12	14.76	0.31	0.12	1.37			0.43	27.91
	14.76	16.40	0.26	0.16	0.69			0.42	38.10
	16.40	18.04	0.65	0.13	1.71			0.78	16.67
	18.04	19.68	0.16	0.10	3.43			0.26	38.46
	19.68	21.32	1.10	1.75	4.46			2.85	61.40
	21.32	22.31	4.91	8.08	9.26			12.99	62.20
	22.31	24.28	2.94	3.90	4.80			6.84	57.02
	24.28	26.25	1.73	3.40	4.46			5.13	66.28
	26.25	28.22	3.30	6.42	5.14			9.72	66.05
	28.22	29.86	0.22	0.19	1.03			0.41	46.34
	29.86	31.50	0.19	0.90	0.34			1.09	82.57
	31.50	33.14	0.50	0.39	0.69			0.89	43.82
	33.14	34.78	0.85	1.12	1.71			1.97	56.85
	34.78	36.42	1.01	1.56	1.71			2.57	60.70
	36.42	38.06	0.97	1.31	2.74			2.28	57.46
	38.06	39.70	0.82	1.53	2.74			2.35	65.11
	39.70	41.34	0.53	1.09	2.06			1.62	67.28
	41.34	42.98	0.84	1.34	1.37			2.18	61.47
	42.98	44.62	1.08	2.18	1.03			3.26	66.87
	44.62	46.26	0.92	1.50	1.03			2.42	61.98
	46.26	47.91	0.41	0.73	0.69			1.14	64.04
	47.91	49.55	0.30	0.60	1.03			0.90	66.67
	49.55	51.19	0.14	0.21	1.03			0.35	60.00
	51.19	52.83	0.25	0.54	0.69			0.79	68.35
	52.83	54.47	0.48	0.76	0.69			1.24	61.29
	54.47	56.11	0.55	1.09	1.03			1.64	66.46
	56.11	57.75	1.14	2.23	1.37			3.37	66.17
	57.75	59.39	0.61	1.35	2.40			1.96	68.88
	59.39	61.35	0.78	1.50	1.71			2.28	65.79
	61.35	62.99	0.85	1.25	1.37			2.10	59.52
	62.99	64.96	0.21	1.95	2.40			2.16	90.28
	64.96	66.60	0.02	0.09	1.71			0.11	81.82
	66.60	67.91	0.02	1.78	1.37			1.80	98.89
	67.91	69.22	0.24	2.35	0.69			2.59	90.73
	69.22	70.21	1.70	6.13	7.89			7.83	78.29
	70.21	71.85	0.16	0.42	0.69			0.58	72.41
	71.85	73.49	0.99	2.96	12.00			3.95	74.94
	73.49	75.13	0.20	0.72	0.69			0.92	78.26
	75.13	76.77	0.13	0.22	1.03			0.35	62.86
	76.77	78.41	0.48	0.46	2.74			0.94	48.94
	78.41	80.05	0.06	0.77	2.06			0.83	92.77
	80.05	81.69	0.04	1.68	1.71			1.72	97.67
	81.69	83.33	0.04	0.41	1.37			0.45	91.11
	83.33	84.97	0.06	0.08	0.34			0.14	57.14
	101.38	102.69	0.02	0.02	1.71			0.04	50.00
	102.69	104.33	0.10	0.82	1.71			0.92	89.13
	104.33	105.97	0.40	0.81	1.71			1.21	66.94
	105.97	108.26	0.55	1.10	2.40			1.65	66.67
	108.26	109.90	0.28	0.53	1.03			0.81	65.43
	109.90	111.54	0.18	0.25	0.69			0.43	58.14

HOLE	FROM	TO	LEAD	ZINC	SILVER	COPPER	GOLD	Pb+Zn	Zn ratio
22	111.54	113.18	0.03	0.72	1.03			0.75	96.00
	119.75	121.39	0.07	0.10	1.37			0.17	58.82
	121.39	123.03	0.58	0.80	1.03			1.38	57.97
	123.03	124.67	0.44	0.77	1.71			1.21	63.64
	124.67	126.31	0.30	0.52	1.03			0.82	63.41
	126.31	127.95	0.45	0.91	0.69			1.36	66.91
	127.95	129.59	1.00	1.01	3.43			2.01	50.25
	129.59	131.23	1.15	5.32	3.43			6.47	82.23
	131.23	132.87	0.51	3.54	2.06			4.05	87.41
	132.87	134.51	0.38	0.25	1.71			0.63	39.68
	134.51	136.15	0.10	0.93	1.03			1.03	90.29
	136.15	137.79	0.01	0.08	0.69			0.09	88.89
25	109.73	111.25	0.07	0.13	0.68			0.20	65.00
	111.25	112.78	0.06	0.22	2.05			0.28	78.57
	112.78	114.30	0.01	0.03	0.68			0.04	75.00
	114.30	115.82	0.06	0.10	1.03			0.16	62.50
	115.82	117.35	0.17	0.27	4.79			0.44	61.36
	117.35	118.87	0.21	0.61	16.46			0.82	74.39
	120.39	121.42	0.14	0.47	17.49			0.61	77.05
	121.92	123.44	0.12	0.22	12.34			0.34	64.71
	134.11	135.64	1.44	8.00	8.91			9.44	84.75
	135.16	138.68	0.13	0.31	2.06			0.44	70.45
	135.64	137.16	0.55	1.02	4.11			1.57	64.97
	138.68	140.21	0.44	0.18	3.43			0.62	29.03
	140.21	141.73	1.78	0.25	6.17			2.03	12.32
	141.73	143.26	1.11	0.71	7.89			1.82	39.01
	152.09	153.92	0.37	0.81	2.39			1.18	68.64
	153.62	155.45	0.31	1.25	3.77			1.56	80.13
	155.45	156.97	0.07	0.23	0.34			0.30	76.67
	156.97	158.51	0.11	0.50	2.06			0.61	81.97
	158.51	160.02	0.10	0.29	1.03			0.39	74.36
	160.02	161.54	0.24	0.48	2.06			0.72	66.67
	161.54	163.07	0.29	0.83	2.74			1.12	74.11
	169.16	170.69	0.50	1.14	3.08			1.64	69.51
	172.21	173.44	0.33	0.64	2.06			0.97	65.98
	173.74	175.26	0.40	0.85	2.06			1.25	68.00
	175.26	176.78	0.25	0.38	2.06			0.63	60.32
	176.78	178.31	0.15	0.20	1.03			0.35	57.14
	178.31	179.83	0.17	0.15	0.68			0.32	46.88
	179.83	181.36	0.08	0.11	1.37			0.19	57.89
	193.55	195.07	0.18	0.14	1.03			0.32	43.75
	195.07	196.61	0.22	0.43	1.37			0.65	66.15
	196.61	198.12	1.06	1.30	3.43			2.36	55.08
	198.12	199.64	0.26	0.68	4.11			0.94	72.34
	199.64	201.17	0.24	0.56	1.37			0.80	70.00
	201.17	202.69	0.35	0.60	1.37			0.95	63.16
	202.69	204.22	0.22	0.54	2.74			0.76	71.05
	204.22	205.74	1.52	4.02	4.11			5.54	72.56
	205.74	207.26	1.64	2.04	3.43			3.68	55.43
	207.26	208.79	0.59	0.69	2.39			1.28	53.91
	207.89	210.31	0.12	0.15	1.03			0.27	55.56
	210.31	211.84	0.26	0.66	2.39			0.92	71.74
	211.84	213.36	0.36	0.75	1.37			1.11	67.57
	213.36	214.88	0.45	0.96	2.74			1.41	68.09
	214.88	216.41	0.48	1.46	3.43			1.94	75.26

HOLE	FROM	TO	LEAD	ZINC	SILVER	COPPER	GOLD	Pb+Zn	Zn ratio
25	216.41	217.93	0.45	2.72	2.74			3.17	85.80
	217.93	219.46	0.57	2.70	3.08			3.27	82.57
	219.46	220.98	0.11	0.86	4.45			0.97	88.66
	220.98	222.50	0.46	0.50	3.08			0.96	52.08
	222.50	224.03	0.26	0.82	4.79			1.08	75.93
	224.03	225.55	0.28	0.56	3.77			0.84	66.67
	225.55	227.08	0.19	0.46	2.74			0.65	70.77
	227.08	228.62	0.63	1.36	4.11			1.99	68.34
	228.60	230.12	0.29	0.56	3.77			0.85	65.88
	230.12	231.65	0.42	0.97	5.83			1.39	69.78
	231.65	233.17	0.45	1.54	5.14			1.99	77.39
	237.74	239.27	0.10	0.15	1.71			0.25	60.00
	239.27	240.79	0.14	0.16	4.45			0.30	53.33
	240.79	242.32	0.22	0.12	3.43			0.34	35.29
	242.32	243.84	0.06	0.07	2.06			0.13	53.85
	243.84	245.36	0.08	0.10	2.06			0.18	55.56
26	46.92	48.56	0.24	0.30	1.37	0.01		0.54	55.56
	48.56	50.20	0.26	0.45	1.03	0.01		0.71	63.38
	50.20	51.84	0.19	0.22	1.37	0.02		0.41	53.66
	51.84	53.48	0.14	0.14	0.69	0.01		0.28	50.00
	53.48	55.12	0.17	0.35	0.69	0.01		0.52	67.31
	55.12	56.76	0.10	0.24	2.06	0.01		0.34	70.59
	56.76	58.40	0.30	0.24	1.71	0.02		0.54	44.44
	58.40	60.04	0.32	0.91	8.57	0.04		1.23	73.98
	60.04	61.68	0.37	0.40	7.54	0.02		0.77	51.95
	61.68	63.32	0.25	0.62	1.37	0.01		0.87	71.26
	63.32	64.96	0.76	2.18	6.86	0.01		2.94	74.15
	64.96	66.60	1.26	2.38	12.00	0.02		3.64	65.38
	66.60	68.24	0.32	0.39	1.37			0.71	54.93
	68.24	69.88	0.15	0.20	0.69			0.35	57.14
	69.88	71.52	0.54	0.75	1.37	0.01		1.29	58.14
	71.52	73.16	0.14	0.23	0.34			0.37	62.16
	73.16	74.80	0.16	0.22	0.34			0.38	57.89
	74.80	76.44	0.14	0.29	0.69			0.43	67.44
	76.44	78.08	0.05	0.18	0.34			0.23	78.26
	78.08	79.72	0.31	0.34	1.03			0.65	52.31
	79.72	81.36	1.70	0.61	3.43	0.01		2.31	26.41
	81.36	83.01	0.14	0.11	0.69			0.25	44.00

Correlation Co-efficients

Pb on Zn 0.81

Pb on Ag 0.75

Zn on Ag 0.33

Appendix 2c: Assay data from drill holes cutting the hanging wall

HOLE	FROM	TO	LEAD	ZINC	SILVER	COPPER	GOLD	Pb+Zn	Zn ratio
2	13.78	15.42	0.010	0.028	1.37	0.002		0.04	73.68
	15.42	17.06	0.002	0.018	1.03	0.002		0.02	90.00
	20.34	21.98	0.003	0.014	0.69	0.003		0.02	82.35
	21.98	23.62	0.002	0.020	1.03	0.003		0.02	90.91
	23.62	25.26	0.002	0.010	1.03	0.003		0.01	83.33
	25.26	26.90	0.006	0.014	0.69	0.003		0.02	70.00
	26.90	28.54	0.021	0.031	2.74	0.003		0.05	59.62
	28.54	30.18	0.058	0.061	2.74	0.004		0.12	51.26
	30.18	31.82	0.051	0.098	3.09	0.005		0.15	65.77
	31.82	33.46	0.023	0.054	2.06	0.006		0.08	70.13
	33.46	35.11	0.044	0.098	2.74	0.010		0.14	69.01
	35.10	36.75	0.032	0.063	1.71	0.006		0.10	66.32
	36.75	38.39	0.098	0.115	4.11	0.006	0.34	0.21	53.99
	38.39	40.03	0.081	0.177	3.43	0.005	0.34	0.26	68.60
	40.03	41.67	0.081	0.061	2.74	0.004		0.14	42.96
	45.93	47.57	0.009	0.006	1.03	0.003		0.02	40.00
	47.57	49.21	0.011	0.026	1.37	0.003		0.04	70.27
	49.21	50.85	0.022	0.019	1.03	0.004		0.04	46.34
	50.85	52.49	0.003	0.009	0.69	0.003		0.01	75.00
	59.06	60.70	0.013	0.062	0.34	0.004		0.08	82.67
	60.70	62.34	0.018	0.037	1.71	0.004		0.06	67.27
	62.34	63.98	0.019	0.025	0.69	0.003		0.04	56.82
	63.98	65.62	0.004	0.013	1.03	0.003		0.02	76.47
	72.18	73.82	0.007	0.030	2.40	0.003		0.04	81.08
	73.82	75.46	0.004	0.009	0.69	0.003		0.01	69.23
	75.46	77.10	0.004	0.006	0.34	0.003		0.01	60.00
	77.10	78.74	0.011	0.021	2.06	0.003		0.03	65.63
	78.74	80.38	0.058	0.135	2.74	0.004	1.37	0.19	69.95
	80.38	82.02	0.072	0.215	3.77	0.005	0.34	0.29	74.91
	82.02	83.66	0.026	0.055	1.71	0.002		0.08	67.90
	83.66	85.30	0.041	0.158	2.40	0.002		0.20	79.40
	85.30	88.15	0.005	0.047	1.03	0.001	0.34	0.05	90.38
	88.15	90.22	0.039	0.035	3.09	0.001	0.34	0.07	47.30
	90.22	91.86	0.025	0.061	2.74	0.003	0.34	0.09	70.93
	91.86	93.50	0.039	0.092	3.09	0.003		0.13	70.23
	93.50	95.14	0.205	0.33	0.34	0.007	0.34	0.54	61.68
	95.14	96.78	0.145	0.408	3.77	0.008	0.34	0.55	73.78
	96.78	98.43	0.093	0.103	1.71	0.004		0.20	52.55
	98.43	100.07	0.015	0.039	1.03	0.003		0.05	72.22
	133.53	135.17	0.016	0.011	0.34	0.004	0.34	0.03	40.74
	135.17	136.81	0.014	0.022	0.34	0.006		0.04	61.11
	136.81	138.45	0.008	0.008	0.69	0.009		0.02	50.00
	138.45	140.09	0.006	0.007	0.34	0.003		0.01	53.85
	140.09	141.73	0.007	0.010	0.34	0.005		0.02	58.82
	141.73	143.37	0.023	0.026	0.34	0.003		0.05	53.06
	143.37	145.01	0.003	0.005	0.34	0.004		0.01	62.50
	145.01	146.65	0.270	0.670	3.09	0.009		0.94	71.28
	146.65	148.29	0.165	0.220	3.09	0.015		0.39	57.14
	148.29	149.93	0.555	0.155	0.62	0.026		0.71	21.83
	149.93	151.57	0.150	0.190	6.17	0.014	0.17	0.34	55.88
	151.57	153.22	0.190	0.150	2.74	0.020	0.17	0.34	44.12

HOLE	FROM	TO	LEAD	ZINC	SILVER	COPPER	GOLD	Pb+Zn	Zn ratio
2	153.22	154.86	0.160	0.290	2.74	0.020	0.17	0.45	64.44
	154.86	156.50	0.069	0.230	1.71	0.016	0.17	0.30	76.92
	156.50	158.14	0.070	0.090	2.40	0.009		0.16	56.25
	158.14	159.78	0.080	0.111	2.06	0.014		0.19	58.12
	159.78	161.42	0.092	0.345	3.09	0.008	0.34	0.44	78.95
	161.42	163.06	0.015	0.051	1.71	0.005	0.34	0.07	77.27
	163.06	164.70	0.026	0.200	2.06	0.002	0.34	0.23	88.50
	164.70	166.34	0.016	0.049	0.34	0.002		0.07	75.38
	172.57	174.21	0.013	0.004	1.71	0.003		0.02	23.53
	190.73	192.50	0.002	0.003	0.34	0.002		0.01	60.00
	202.10	203.74	0.005	0.017	0.34	0.005		0.02	77.27
	206.69	208.33	0.051	0.104	0.34	0.006		0.16	67.10
	216.54	218.18	0.023	0.052	0.69	0.003		0.08	69.33
	251.97	253.61	0.014	0.068	0.34	0.002		0.08	82.93
4	179.79	181.43	0.005	0.049	0.34	0.009		0.05	90.74
	181.43	183.07	0.009	0.032	1.03	0.014		0.04	78.05
	201.61	203.25	0.002	0.051	0.69	0.007		0.05	96.23
	207.02	208.66	0.012	0.048	1.71	0.022		0.06	80.00
	208.66	210.30	0.014	0.112	2.40	0.025		0.13	88.89
	210.30	211.94	0.008	0.064	0.69	0.006		0.07	88.89
	211.94	213.58	0.016	0.075	1.71	0.008		0.09	82.42
	213.58	215.22	0.056	0.080	2.06	0.008		0.14	58.82
	215.22	216.86	0.009	0.329	0.69	0.035		0.34	97.34
	216.86	218.50	0.008	0.039	0.69	0.009		0.05	82.98
	218.50	220.14	0.032	0.410	0.34	0.010		0.44	92.76
	220.14	221.78	0.010	0.078	0.69	0.008		0.09	88.64
	221.78	223.43	0.015	0.055	0.34	0.010		0.07	78.57
	223.43	225.07	0.003	0.041	0.34	0.009		0.04	93.18
	225.07	226.71	0.013	0.212	0.34	0.010		0.23	94.22
	226.71	228.35	0.009	0.068	0.34	0.007		0.08	88.31
	228.35	229.99	0.001	0.007	0.34	0.006		0.01	87.50
LCO-3	22.50	24.00	0.079	0.091	6.00			0.17	53.53
	27.00	28.50	0.089	0.143	3.00		0.69	0.23	61.64
	34.50	36.00	0.063	0.091	4.00		0.86	0.15	59.09
	36.00	37.50	0.155	0.231	7.50		0.86	0.39	59.84
	37.50	39.00	0.134	0.119	8.00		0.86	0.25	47.04
	39.00	40.50	0.134	0.182	10.50		0.86	0.32	57.59
	40.50	42.00	0.082	0.093	5.50		0.69	0.18	53.14
	42.00	43.50	0.086	0.099	5.50		1.88	0.19	53.51
	43.50	45.00	0.214	0.570	11.00		0.86	0.78	72.70
	45.00	46.50	0.061	0.086	4.00		0.17	0.15	58.50
24	21.65	23.29	0.23	0.59	0.34			0.82	71.95
	23.29	24.93	0.15	0.50	1.03			0.65	76.92
	24.93	26.57	0.12	0.06	0.34			0.18	33.33
	26.57	28.22	0.06	0.05	0.34			0.11	45.45
	28.22	29.86	0.20	0.11	1.03			0.31	35.48
	29.86	31.50	0.07	0.08	1.37			0.15	53.33
	31.50	33.14	0.11	0.05	0.34			0.16	31.25
	36.42	38.06	0.06	0.04	0.34			0.10	40.00
	38.06	39.70	0.20	0.02	1.03			0.22	9.09
	39.70	41.34	0.41	0.04	2.06			0.45	8.89
	41.34	41.99	0.09	0.07	1.03			0.16	43.75
	91.86	93.50	0.77	1.48	4.11			2.25	65.78
	93.50	95.14	0.35	0.33	3.09			0.68	48.53
	95.14	96.78	1.00	1.92	2.74			2.92	65.75

HOLE	FROM	TO	LEAD	ZINC	SILVER	COPPER	GOLD	Pb+Zn	Zn ratio
24	96.78	98.43	0.96	1.12	4.11			2.08	53.85
	98.43	100.07	0.36	0.64	2.40			1.00	64.00
	103.35	104.99	0.46	0.82	1.71			1.28	64.06
	104.99	106.63	0.75	1.59	2.06			2.34	67.95
	106.63	107.61	0.36	0.54	2.74			0.90	60.00
	119.75	121.39	0.26	0.83	2.06			1.09	76.15
8	31.16	32.81	0.02	0.04				0.06	66.67
	32.81	34.45	0.04	0.12				0.16	75.00
	34.45	36.09	0.00	0.08				0.08	100.00
	36.09	37.73	0.01	0.05				0.06	83.33
	37.73	39.37	0.03	0.08				0.11	72.73
	39.37	41.67	4.20	7.88	15.09			12.08	65.23
	41.67	42.65	0.26	0.57				0.83	68.67
	42.65	43.63	0.22	0.12	0.68			0.34	35.29
	43.63	45.60	0.58	0.91	1.37			1.49	61.07
	45.60	47.57	0.15	0.10	1.37			0.25	40.00
	47.57	49.21	0.22	0.22	1.37			0.44	50.00
	49.21	50.85	0.15	0.37				0.52	71.15
	50.85	52.49	0.22	0.44	1.37			0.66	66.67
	52.49	54.14	0.05	0.05				0.10	50.00
	54.14	55.77	0.01	0.09	0.34			0.10	90.00
	55.77	57.42	0.10	0.18				0.28	64.29
	80.38	82.02	0.05	0.24				0.29	82.76
	82.02	83.66	0.19	0.25				0.44	56.82
	83.66	85.31	0.09	0.55				0.64	85.94
	85.31	86.94	0.04	0.06				0.10	60.00
	86.94	87.92	0.03	0.03				0.06	50.00
	87.92	89.56	0.09	0.09				0.18	50.00
	89.56	91.21	0.07	0.04				0.11	36.36
	91.21	92.85	1.82	0.49	2.74			2.31	21.21
	92.85	94.49	0.29	0.25	0.68			0.54	46.30
	94.49	95.80	0.15	0.37				0.52	71.15
	95.80	97.44	0.92	1.02	1.37			1.94	52.58
	97.44	99.08	0.44	0.57	0.68			1.01	56.44
	99.08	100.72	0.24	0.60	0.68			0.84	71.43
	100.72	102.36	0.08	0.25	0.68			0.33	75.76
	102.36	103.67	0.10	0.13				0.23	56.52
	129.26	130.91	0.16	0.26				0.42	61.90
	130.91	132.55	0.06	0.07				0.13	53.85
	132.55	134.18	0.07	0.11				0.18	61.11
	134.18	135.83	0.03	0.04				0.07	57.14
	135.83	137.47	0.03	0.05				0.08	62.50
	137.47	139.11	0.13	0.28				0.41	68.29
	139.11	140.75	0.11	0.17				0.28	60.71
	140.75	142.39	0.24	0.18				0.42	42.86
	142.39	143.37	0.10	0.88				0.98	89.80
	143.37	145.01	0.52	0.89	1.37			1.41	63.12
	145.01	146.65	1.50	0.15	2.74			1.65	9.09
	146.65	148.29	0.67	2.24	1.37			2.91	76.98
	148.29	151.25	0.44	0.54	0.68			0.98	55.10
	151.25	152.88	0.56	1.17	1.37			1.73	67.63
	152.88	154.53	0.06	0.09				0.15	60.00
	208.66	210.30	0.02	0.04				0.06	66.67
	210.30	211.94	0.02	0.06				0.08	75.00
	211.94	213.58	0.00	0.09				0.09	100.00

HOLE	FROM	TO	LEAD	ZINC	SILVER	COPPER	GOLD	Pb+Zn	Zn ratio
8	213.58	215.22	0.03	0.13				0.16	81.25
	223.09	224.74	0.19	0.48				0.67	71.64
	224.74	226.38	0.13	0.41				0.54	75.93
	226.38	228.02	0.08	0.33				0.41	80.49
	228.02	229.66	0.09	0.10				0.19	52.63
	229.66	230.97	0.47	1.42				1.89	75.13
	230.97	232.28	0.44	0.90	2.06			1.34	67.16
	232.28	233.59	0.53	1.58	2.74			2.11	74.88
	233.59	235.24	0.01	0.08				0.09	88.89
	235.24	236.87	0.01	0.07				0.08	87.50

Correlation Co-efficients

Pb on Zn 0.88
Pb on Ag 0.49
Zn on Ag 0.48

Footnotes

1. Depths in metres
2. Values in percent
3. Values in grams per tonne
4. Abbreviated form for Amoco Canada Petroleum Co. drill holes (prefix: NB-T-O)
5. Abbreviated form for Lac Minerals Ltd. 1984 drilling (prefix: LCO-)
6. Lac Mineral 1983 drilling

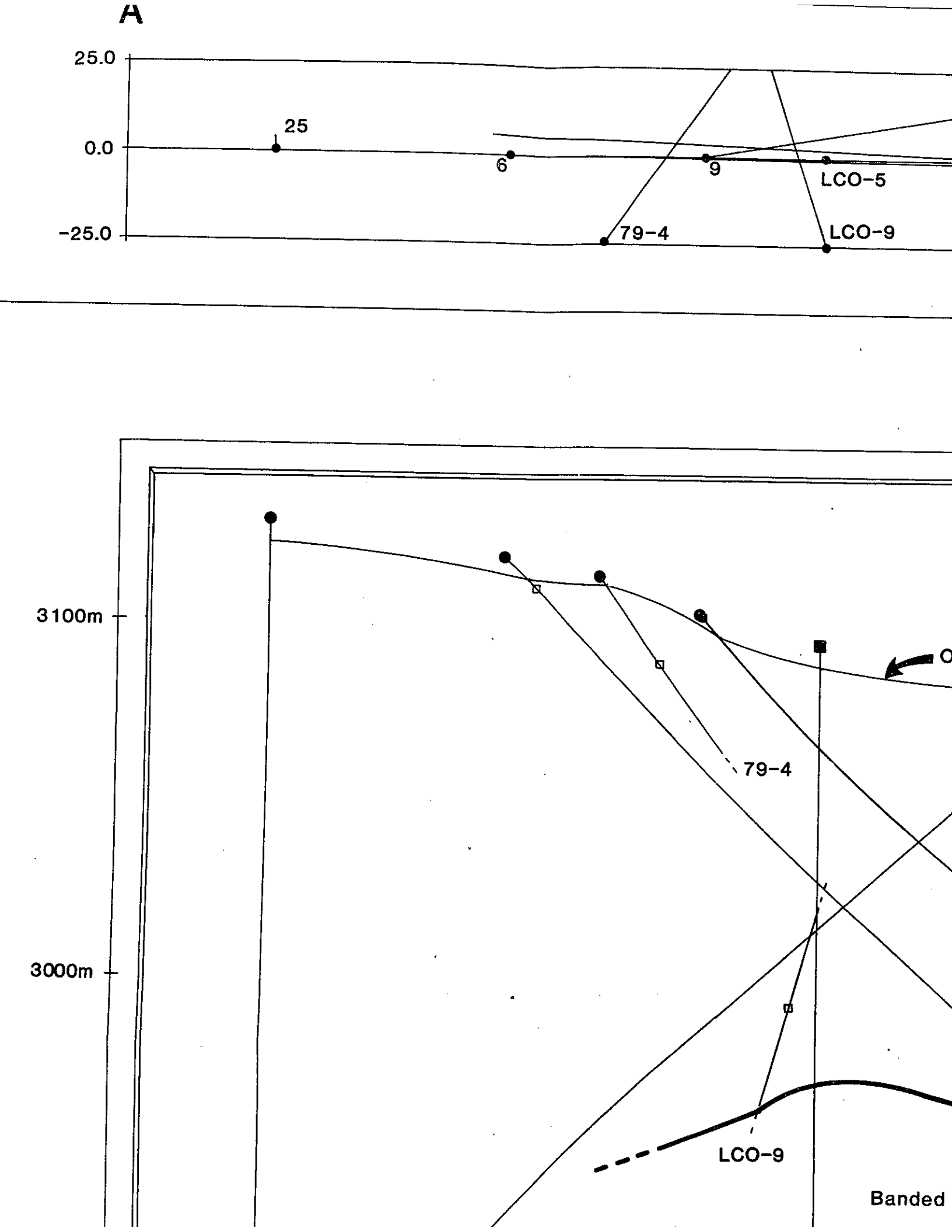
A
25.0
0.0
-25.0
25
6
9
LCO-5
79-4
LCO-9
3100m
3000m
79-4
LCO-9
Banded

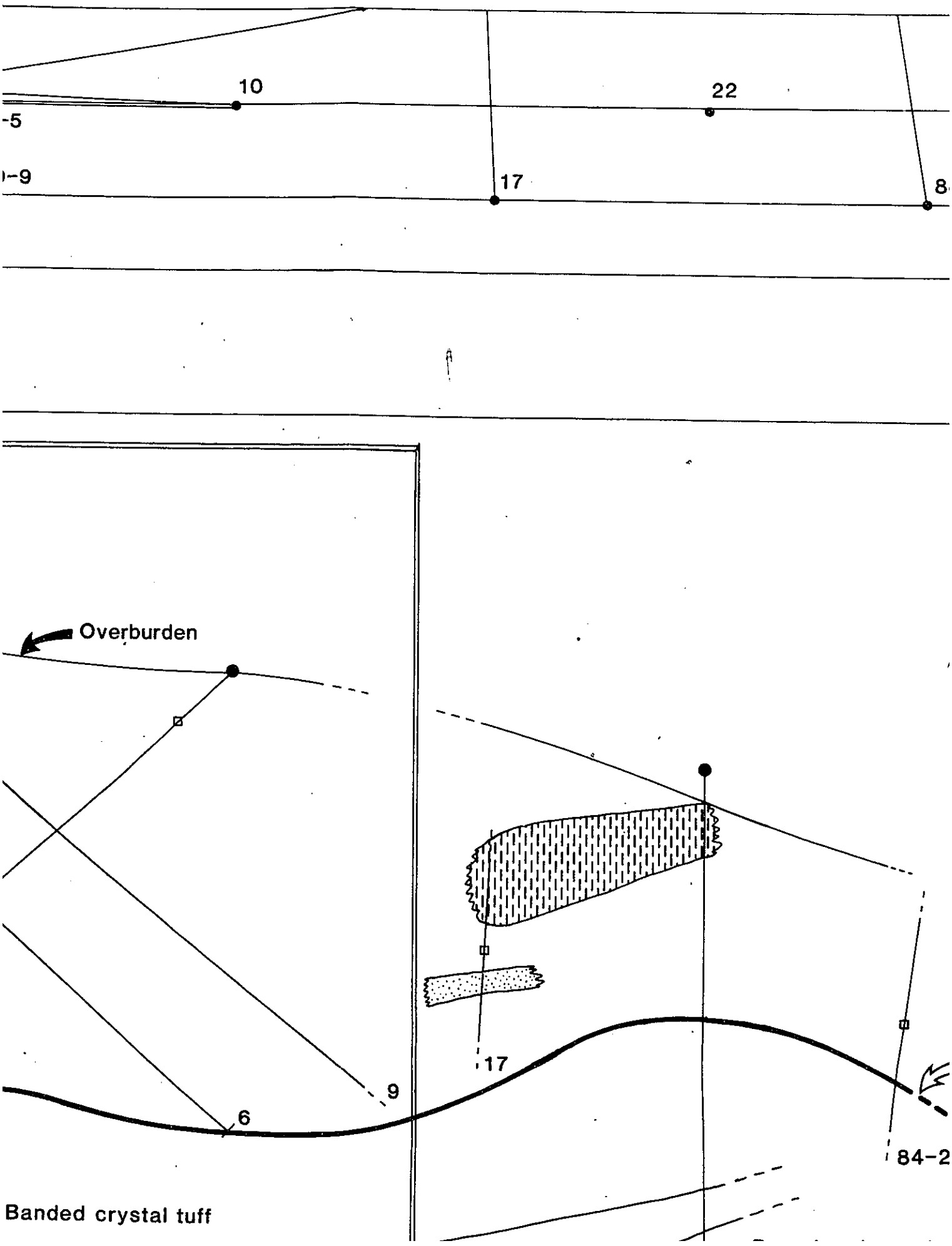
10
22
-5
-9
17
8
Overburden
9
6
17
84-2
Banded crystal tuff

A'

84-1

84-2

Topographic profile for cross-sections A and B

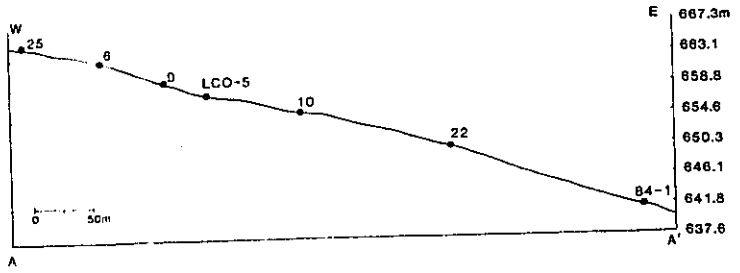

3100m

3000m

Approximate
base of main breccia

84-2

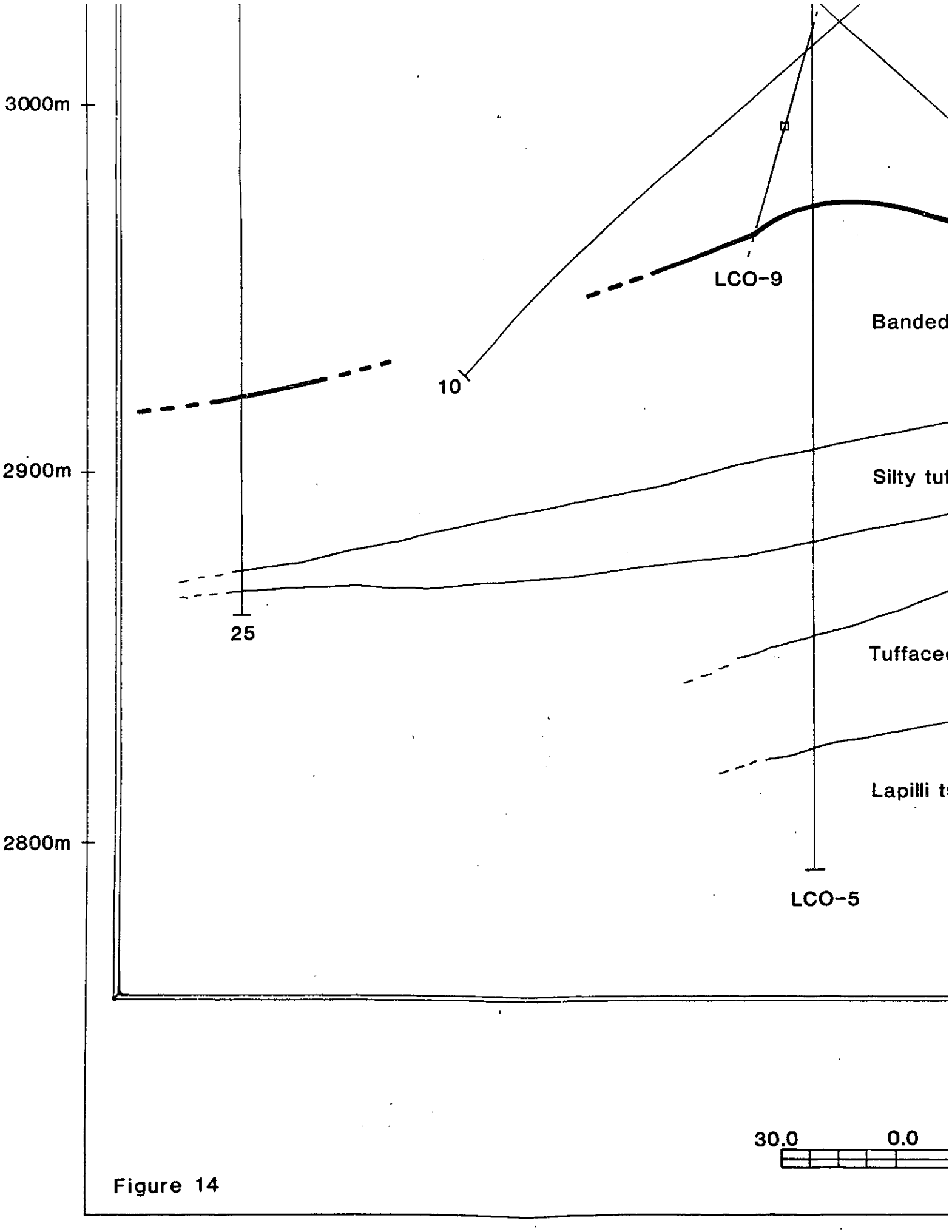
3000m
2900m
2800m
LCO-9
10
25
LCO-5
Banded
Silty tuf
Tufface
Lapilli t
30.0
0.0

Figure 14

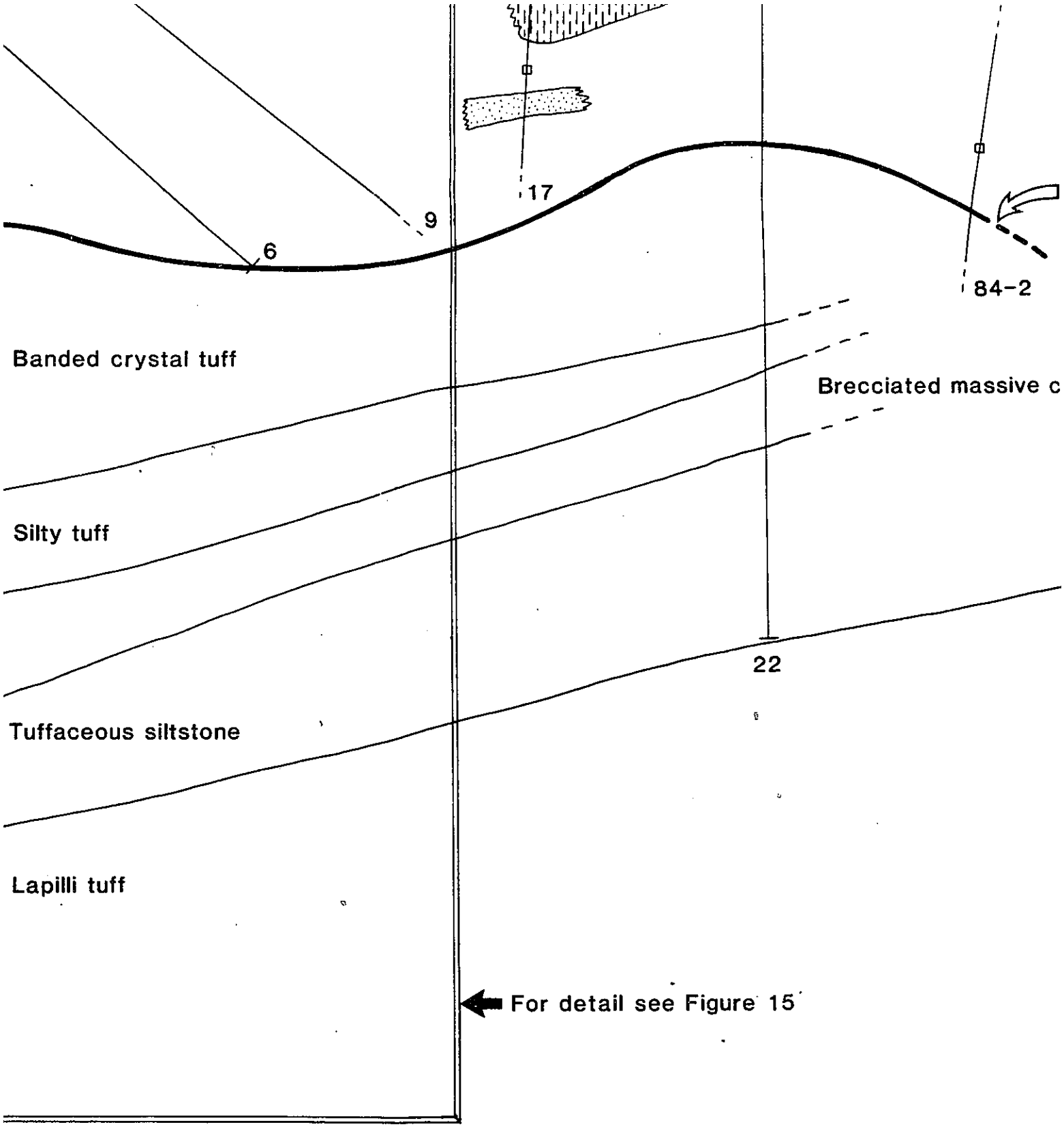

MOUNT COSTI

Geology, long E

0.0 30.0 60.0 m

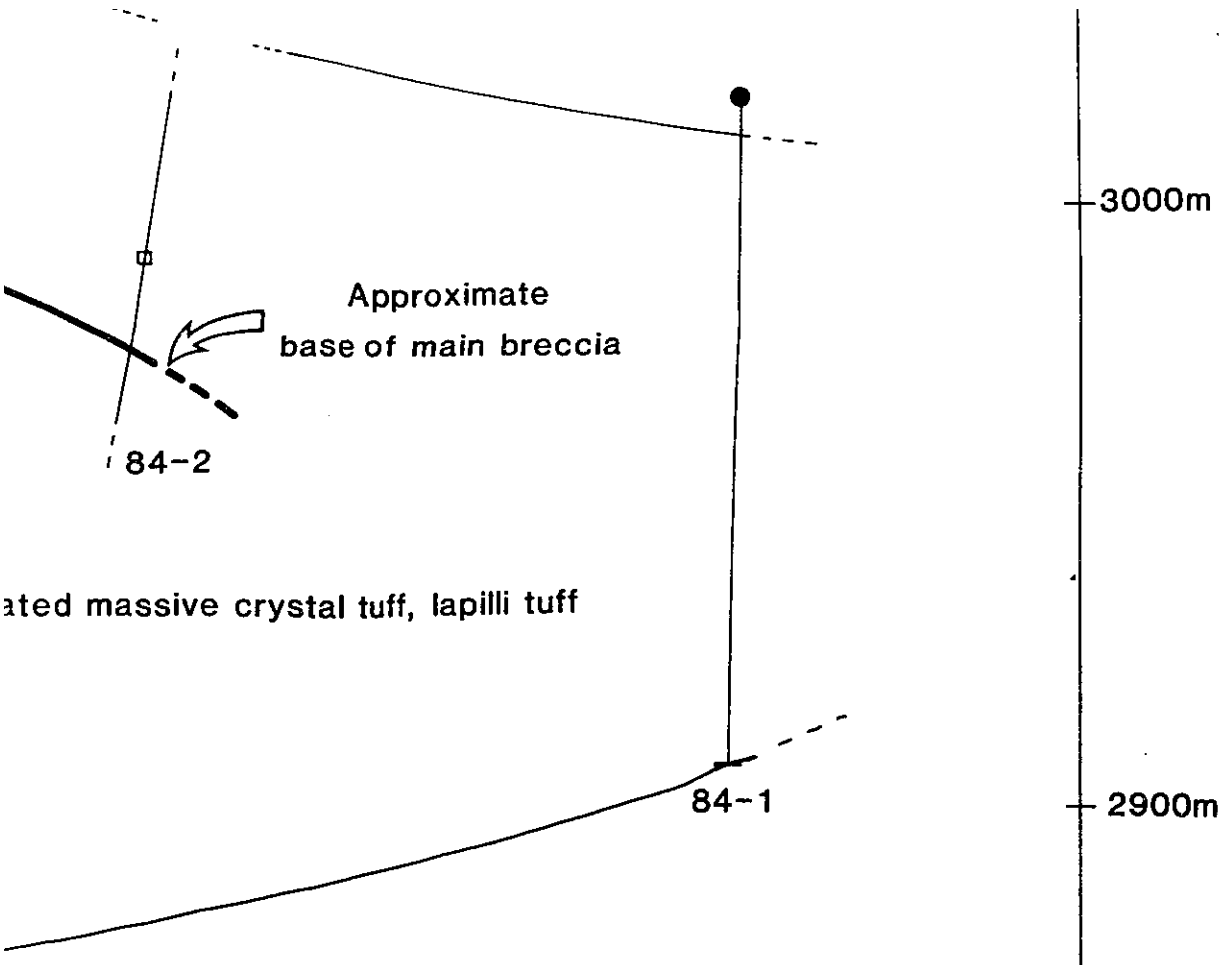

LEGEND

- Spherulitic to Banded Rhyolite
- Massive Rhyolite, Siltstone
- Banded to massive Crystal Tuff
- Lapilli Tuff, Siltstone, minor Rhyolite
- Lapilli Tuff & Banded Crystal Tuff
- Tuffaceous Siltstone

COSTIGAN Pb-Zn DEPOSIT

gy, long E-W section (S080E, 90)

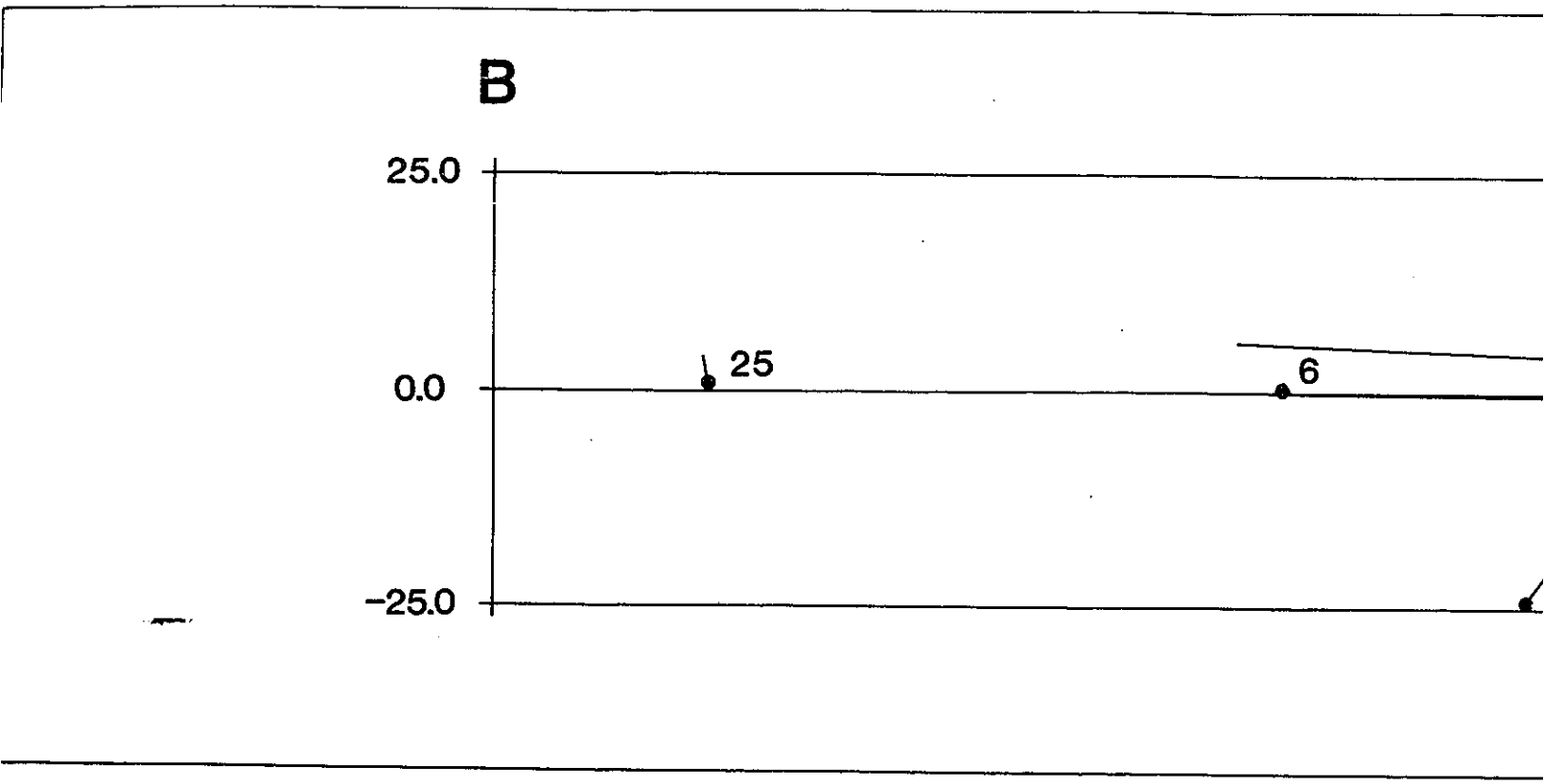
B
25.0
0.0
-25.0
25
6

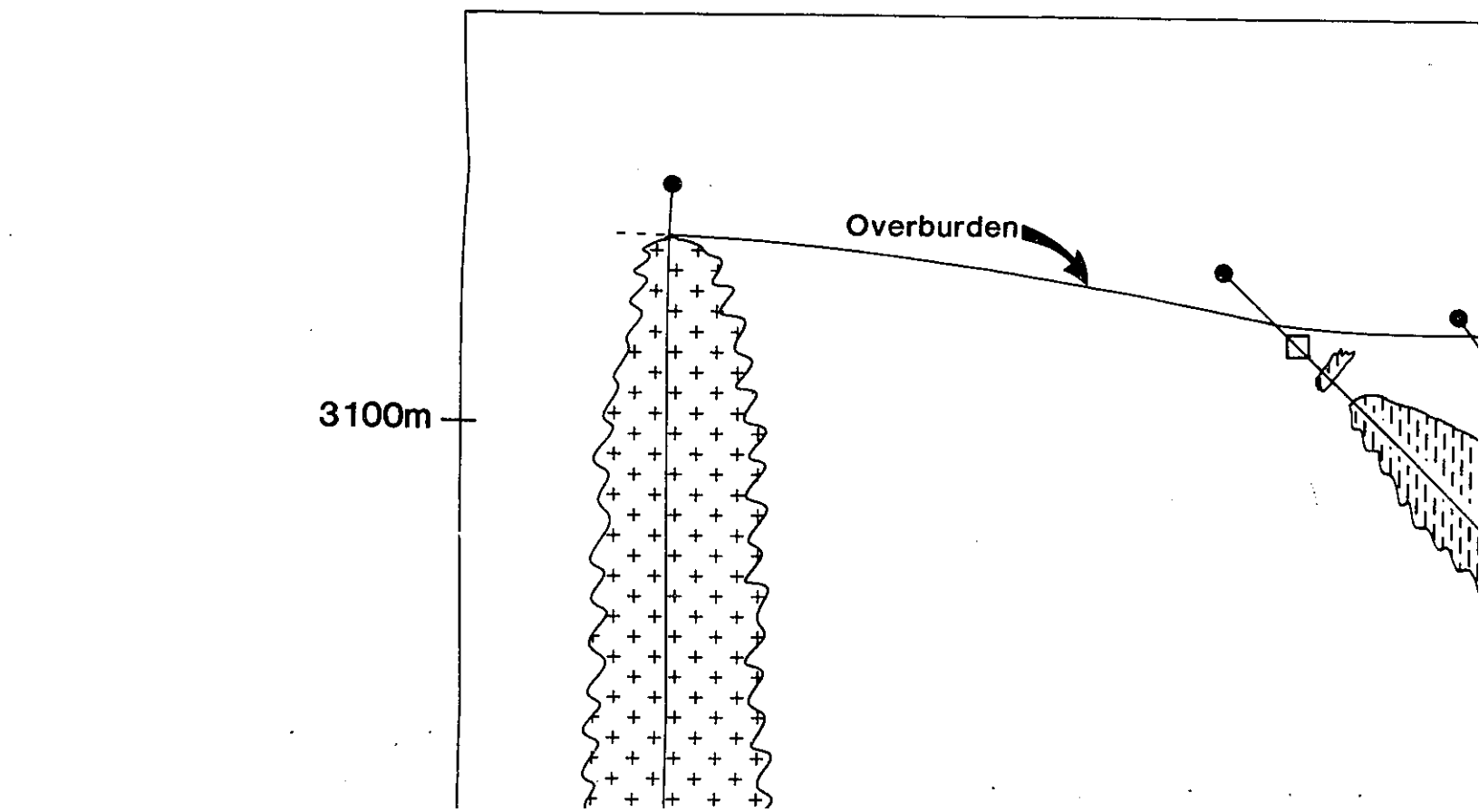
Overburden
3100m

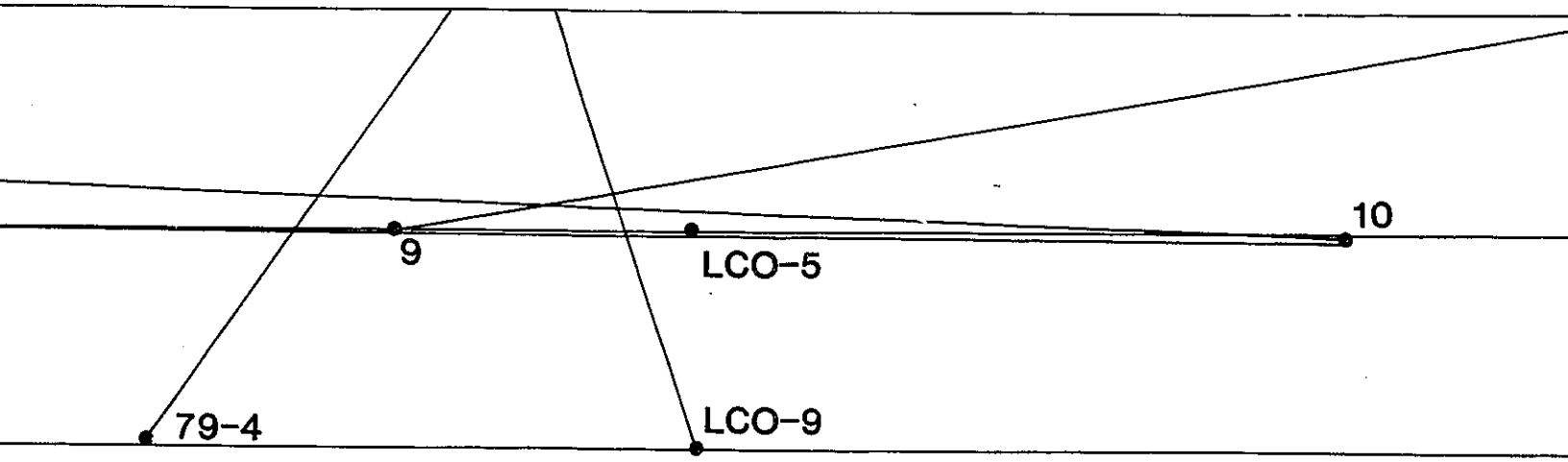
9
10
LCO-5
79-4
LCO-9

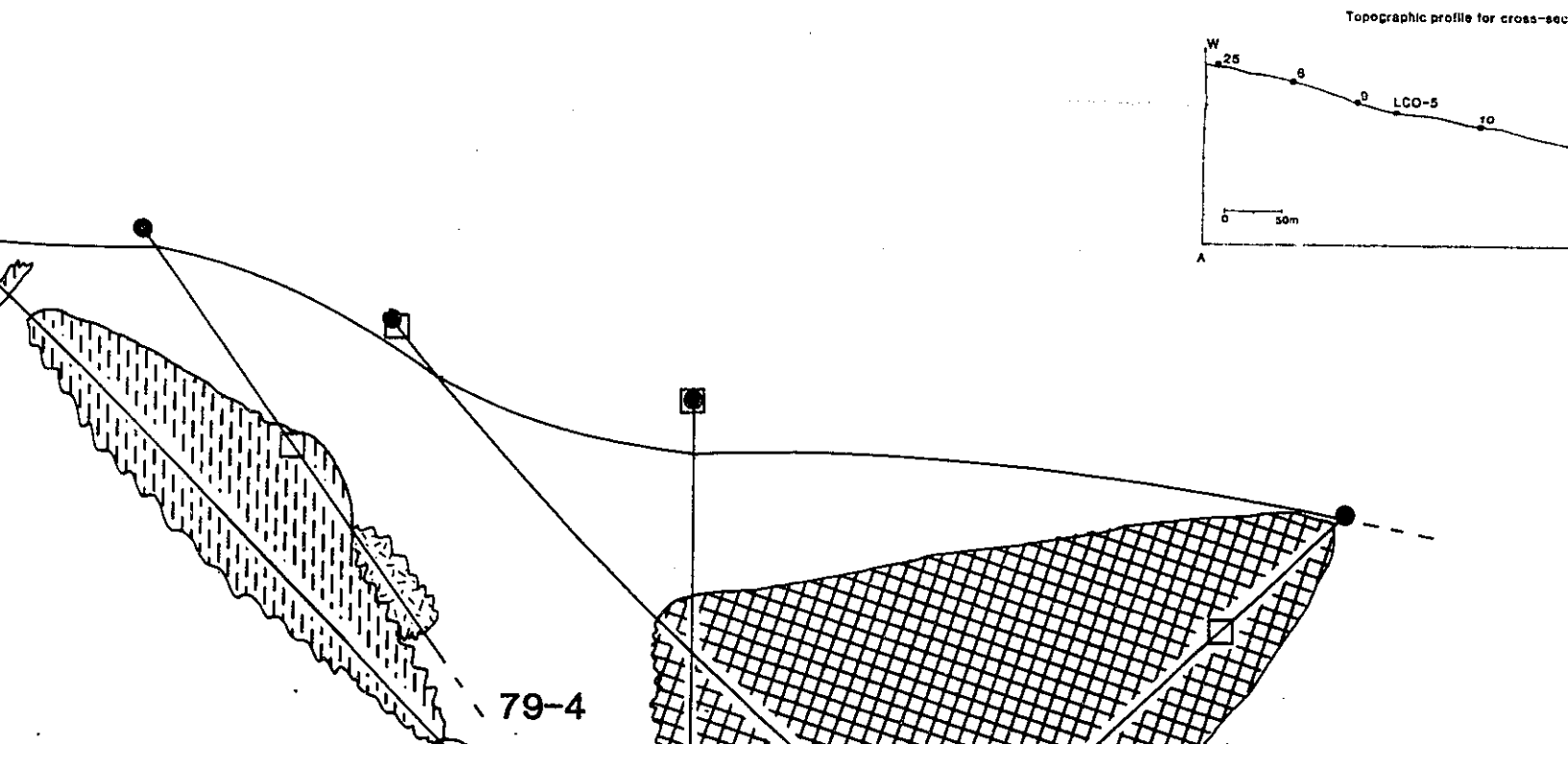
Topographic profile for cross-sec
W
25
8
0
LCO-5
10
0
50m
A
79-4

B′

10

17

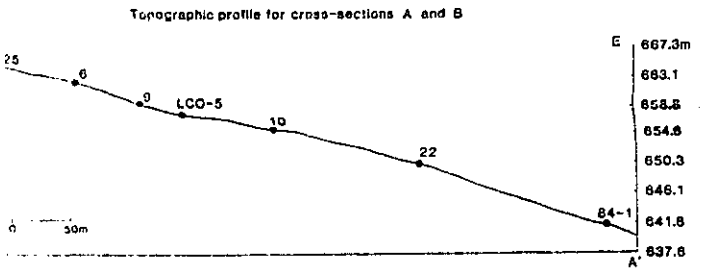
Topographic profile for cross-sections A and B
25
6
9
LCO-5
19
22
84-1
30m
E
667.3m
663.1
658.8
654.6
650.3
646.1
641.8
637.6
A′

3100m

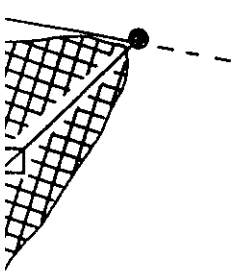

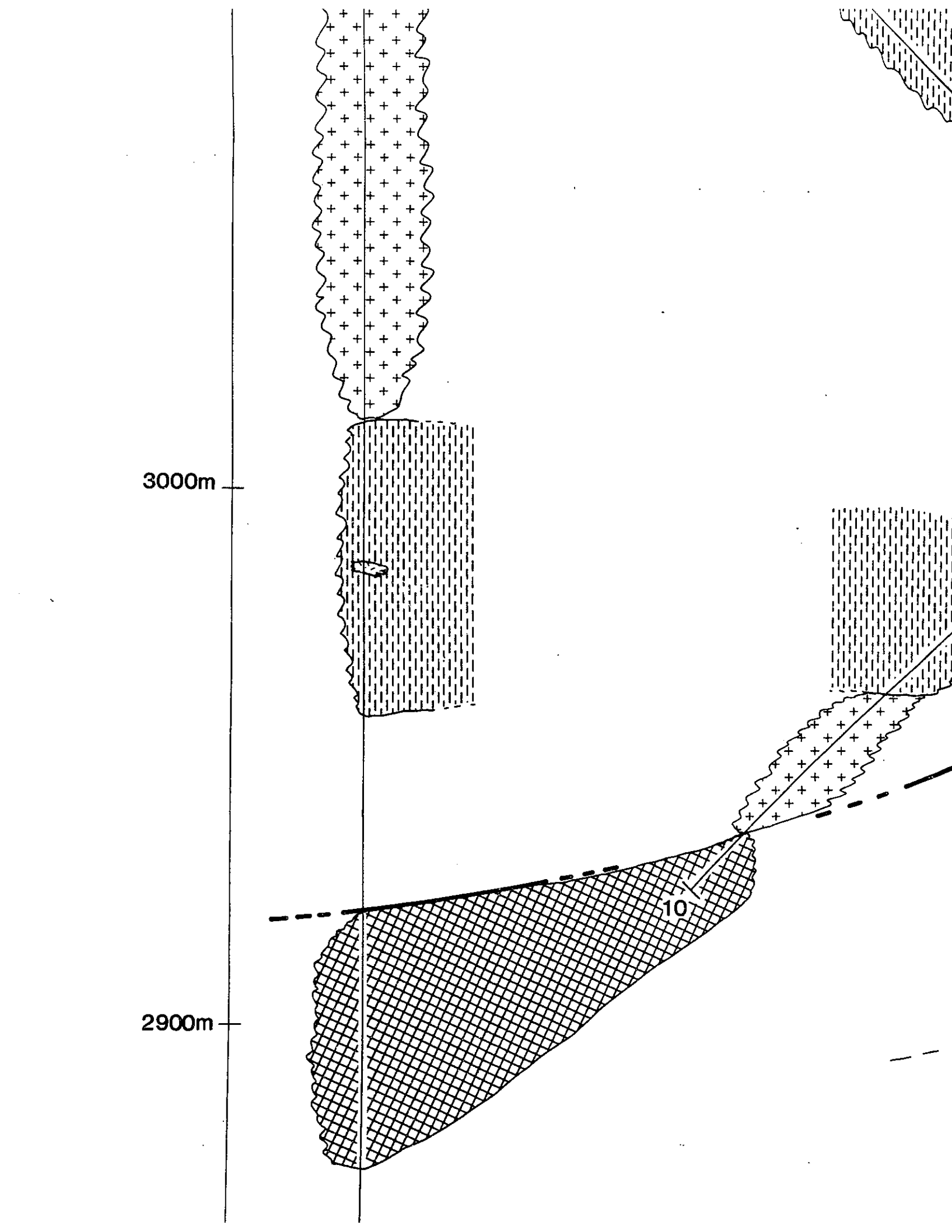
3000m
2900m
10

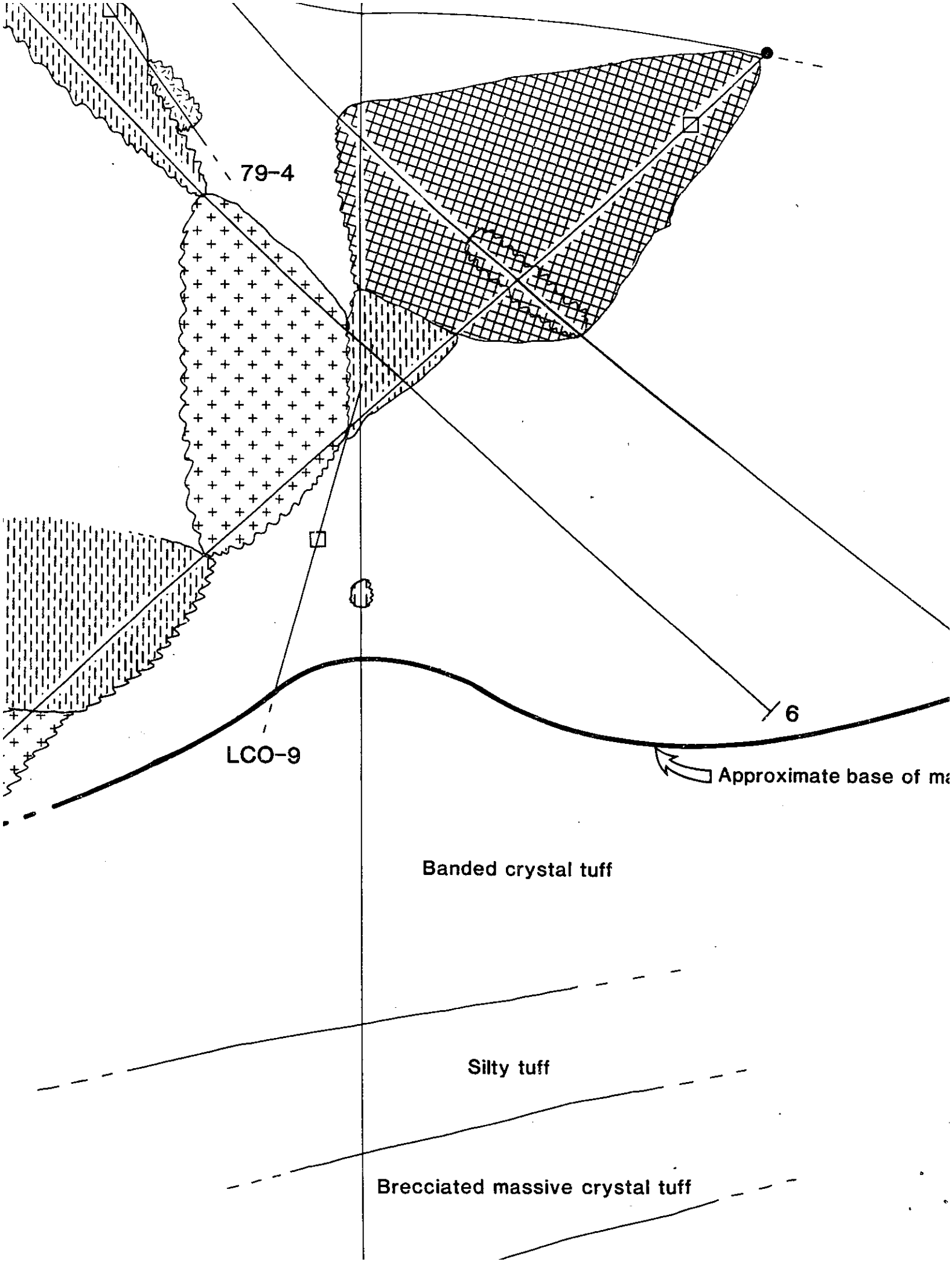
79-4
6
LCO-9
Approximate base of ma
Banded crystal tuff
Silty tuff
Brecciated massive crystal tuff

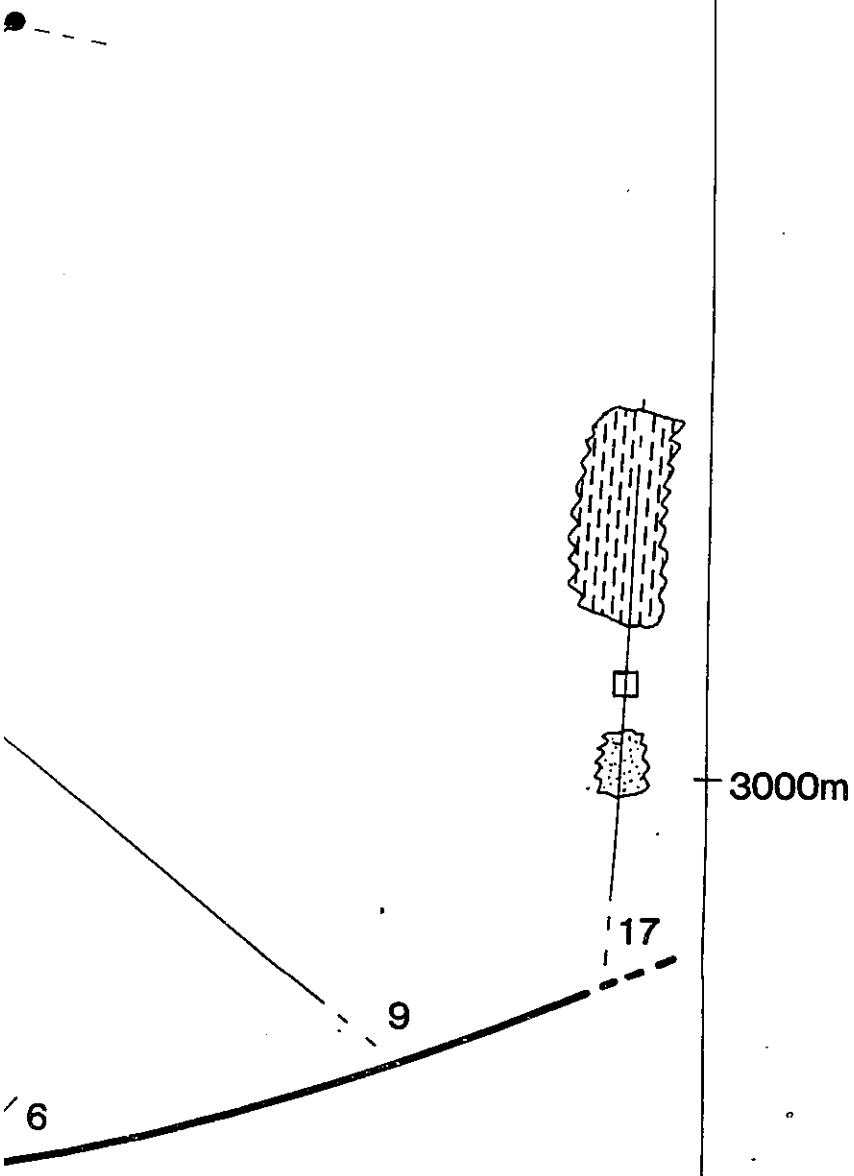

ximate base of main breccia

2900m

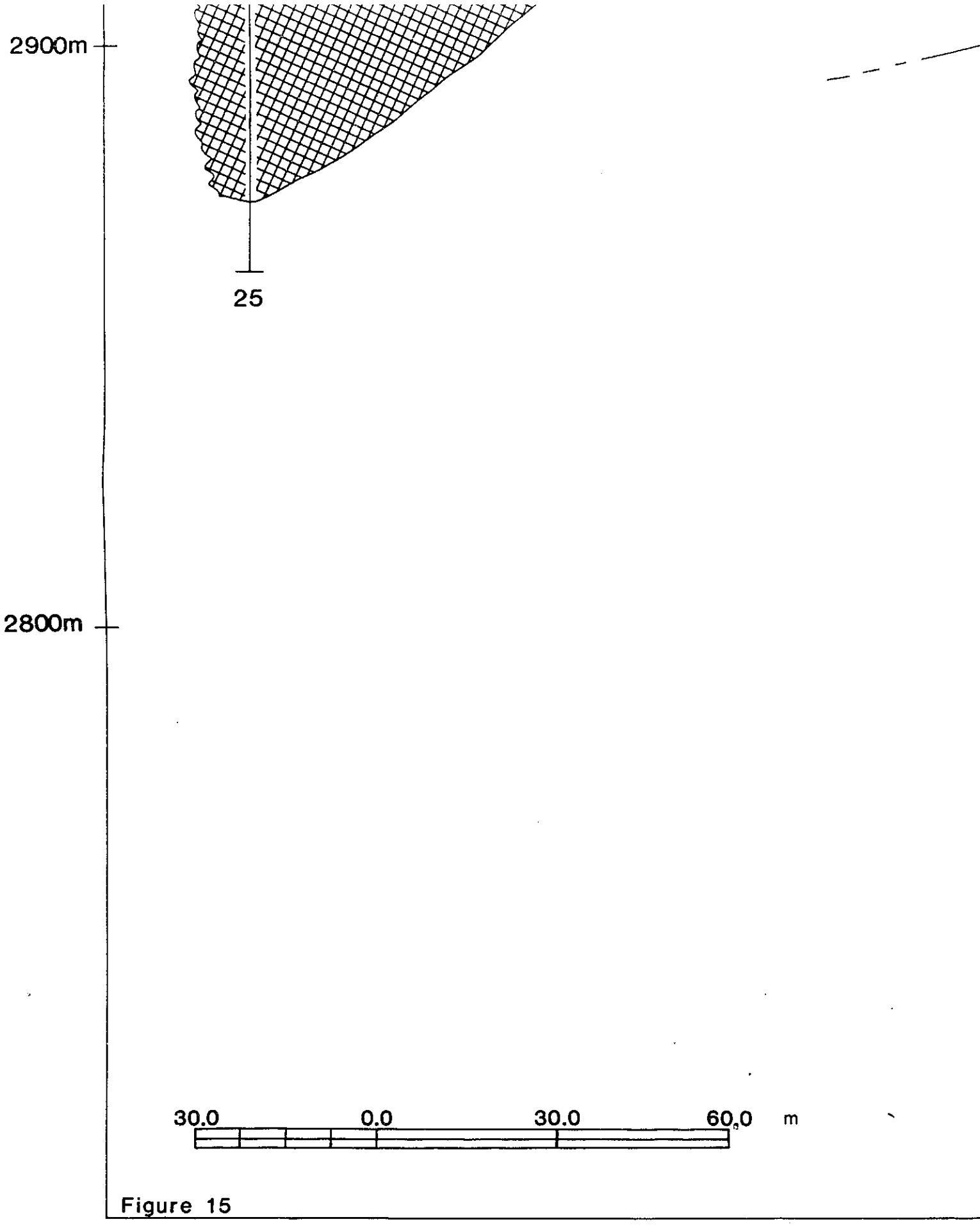

Figure 15

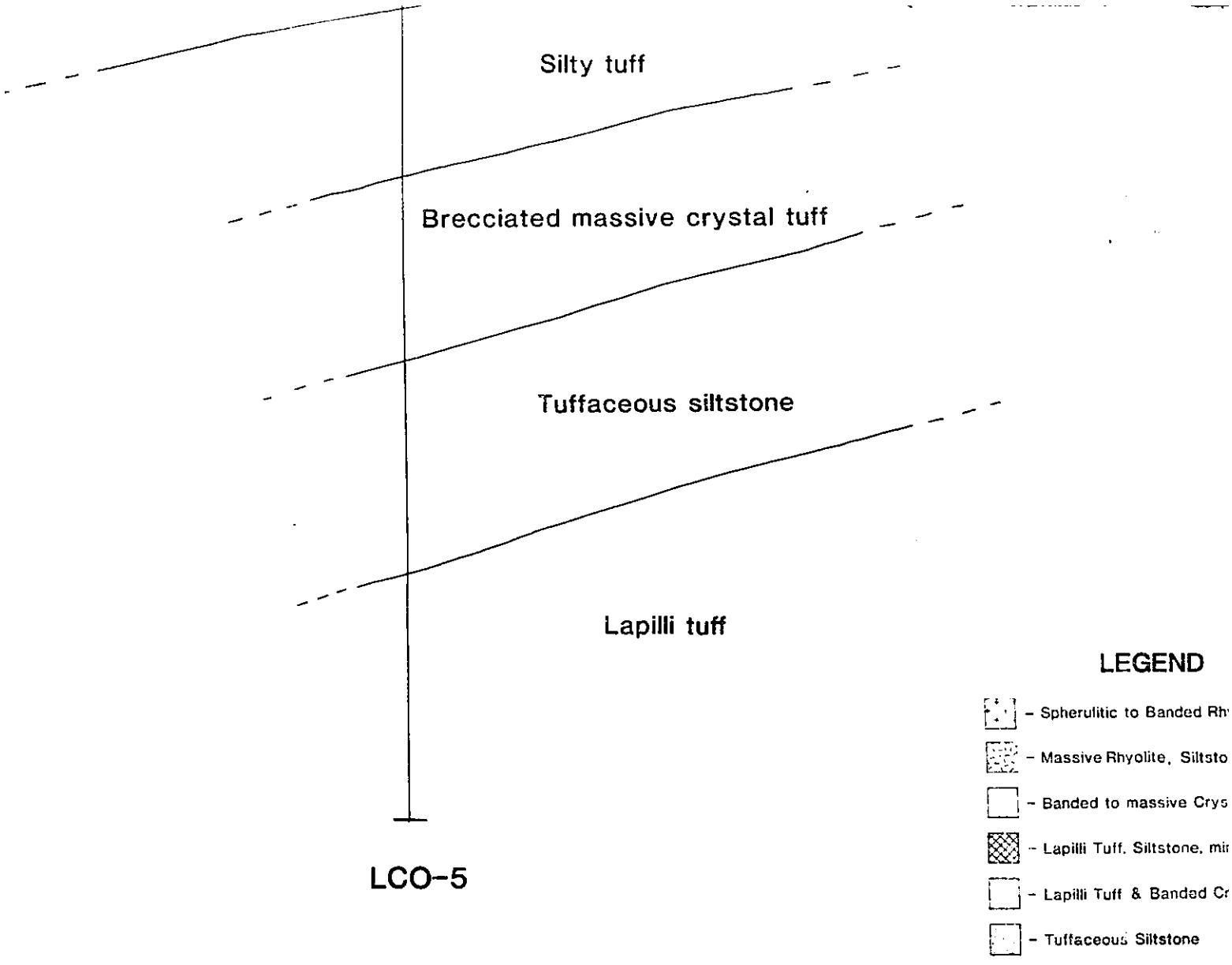

MOUNT COSTIGAN Pb–Zn DEPO

Geology, short E–W section (S080E,9(

2900m

2800m

LEGEND

- Spherulitic to Banded Rhyolite
- Massive Rhyolite, Siltstone
- Banded to massive Crystal Tuff
- Lapilli Tuff, Siltstone, minor Rhyolite
- Lapilli Tuff & Banded Crystal Tuff
- Tuffaceous Siltstone

Pb–Zn DEPOSIT

section (S080E,90)

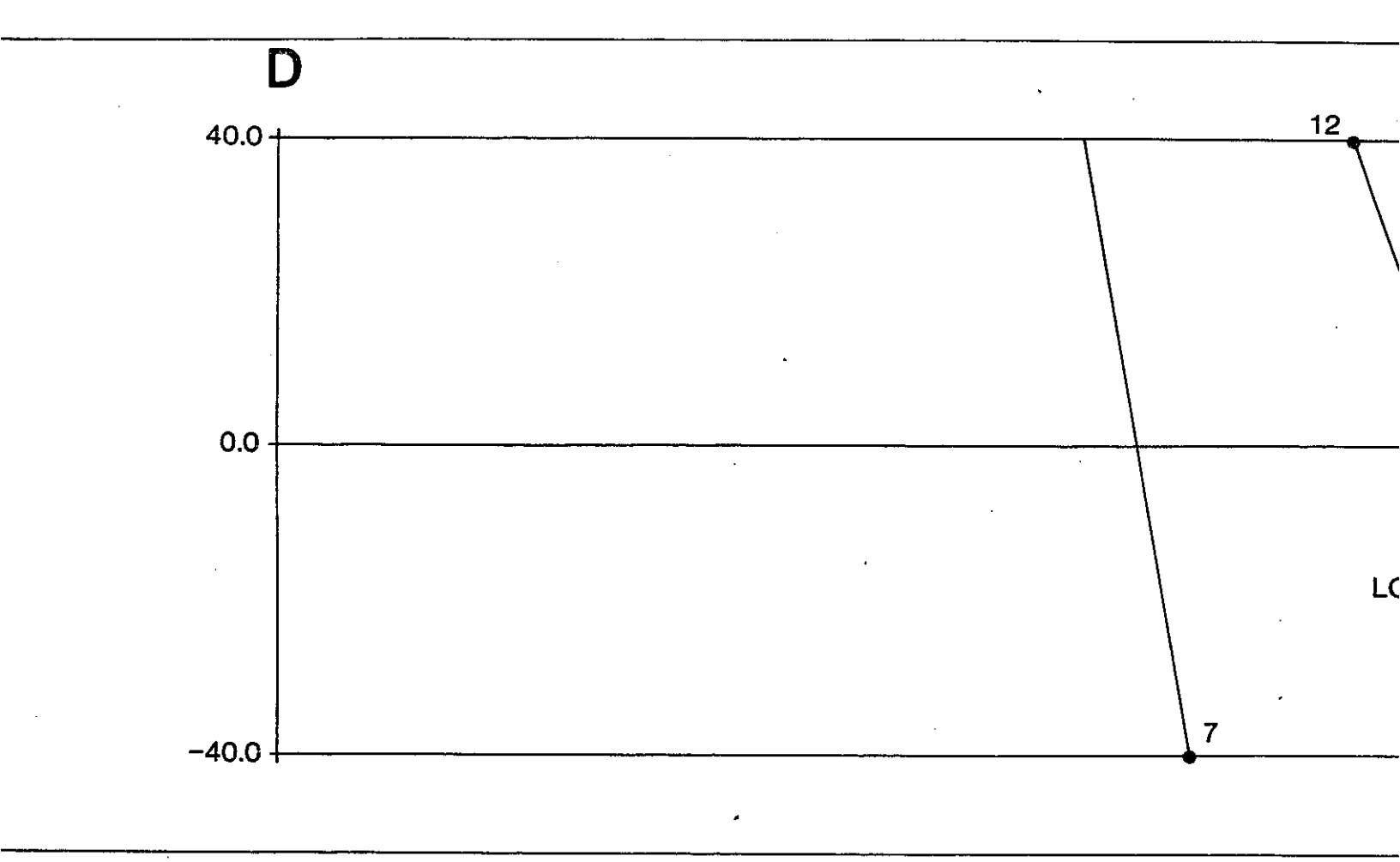
D
40.0
0.0
-40.0
12
7
LC

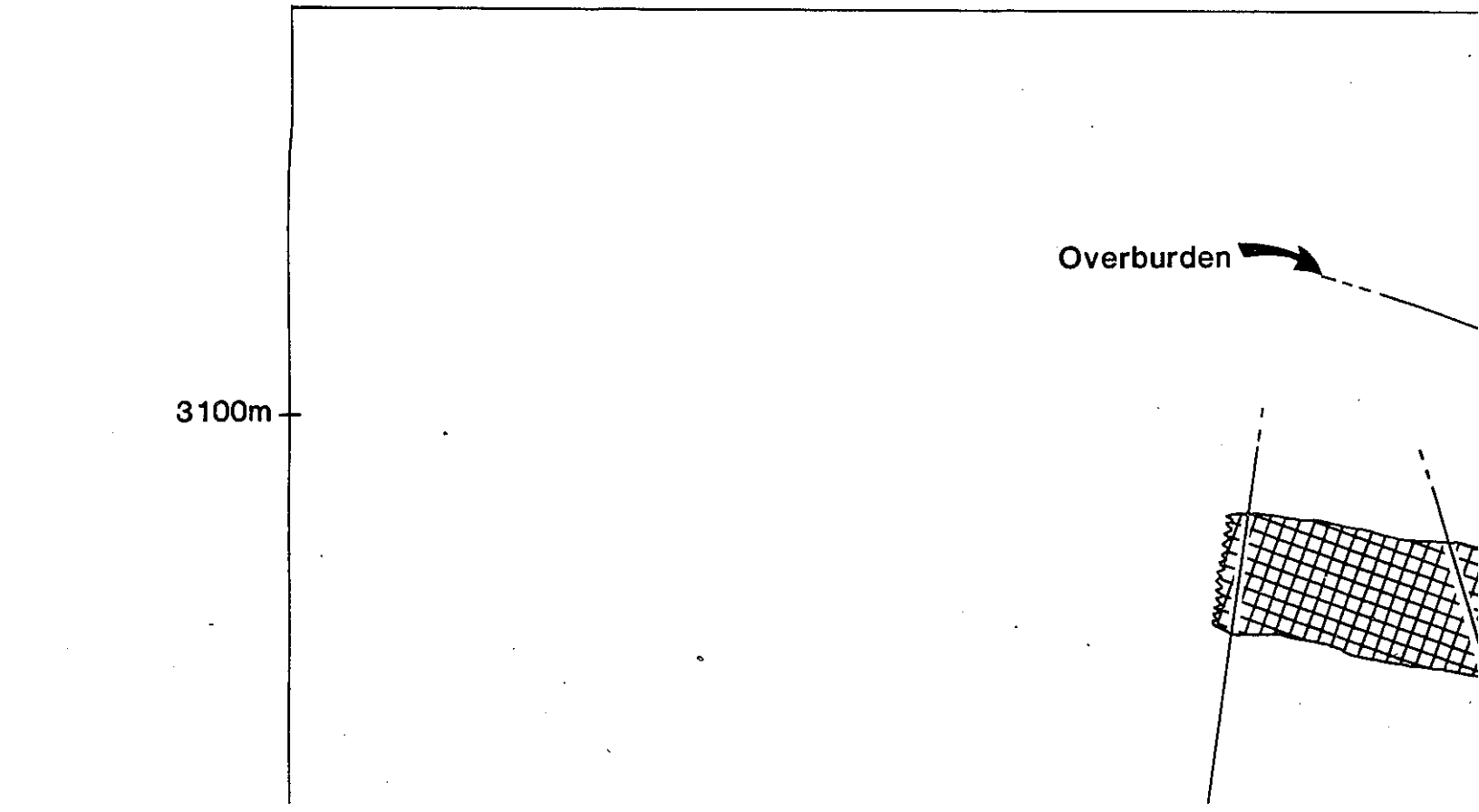
Overburden
3100m

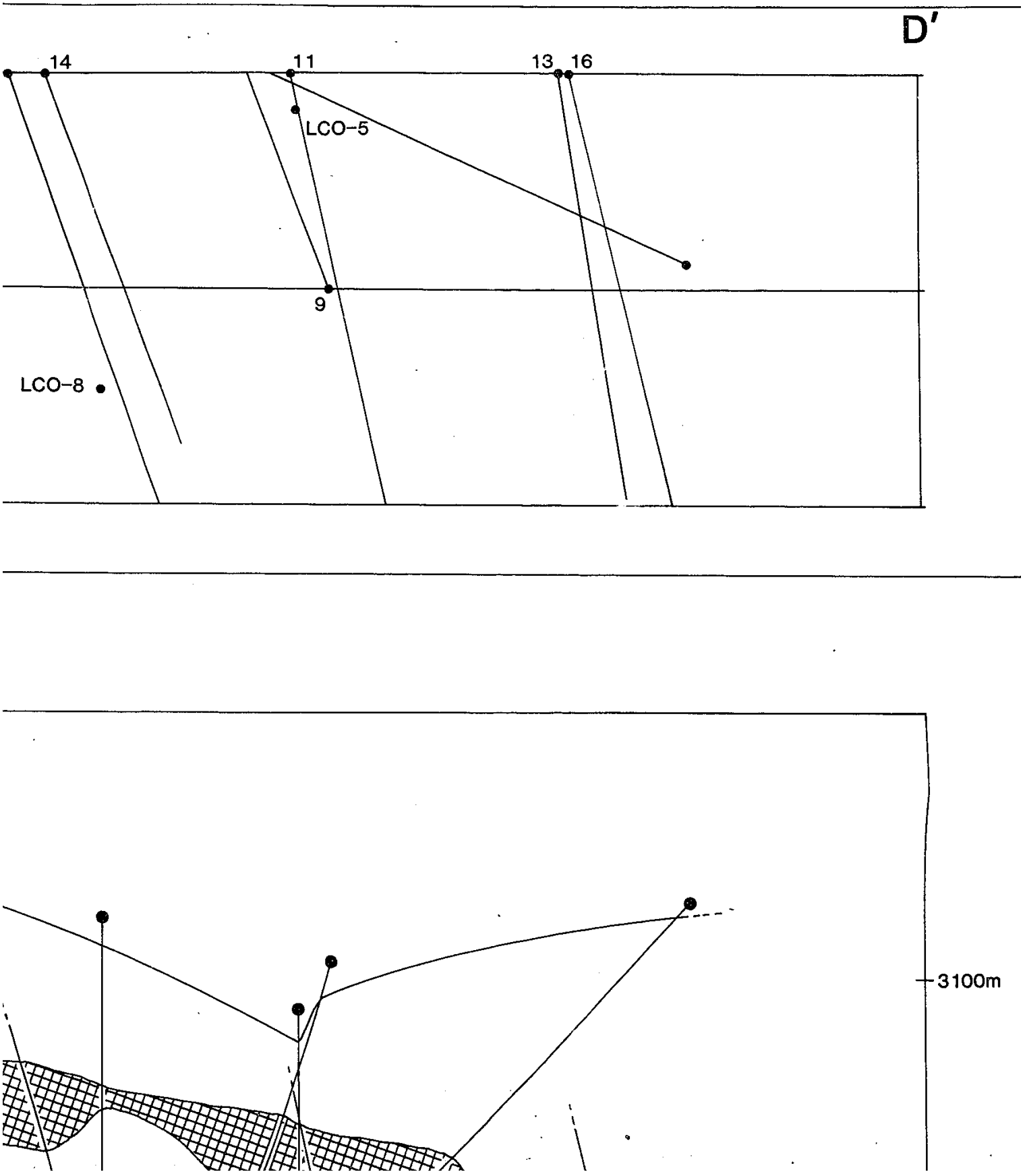
D′
14
11
13
16
LCO-5
9
LCO-8
3100m

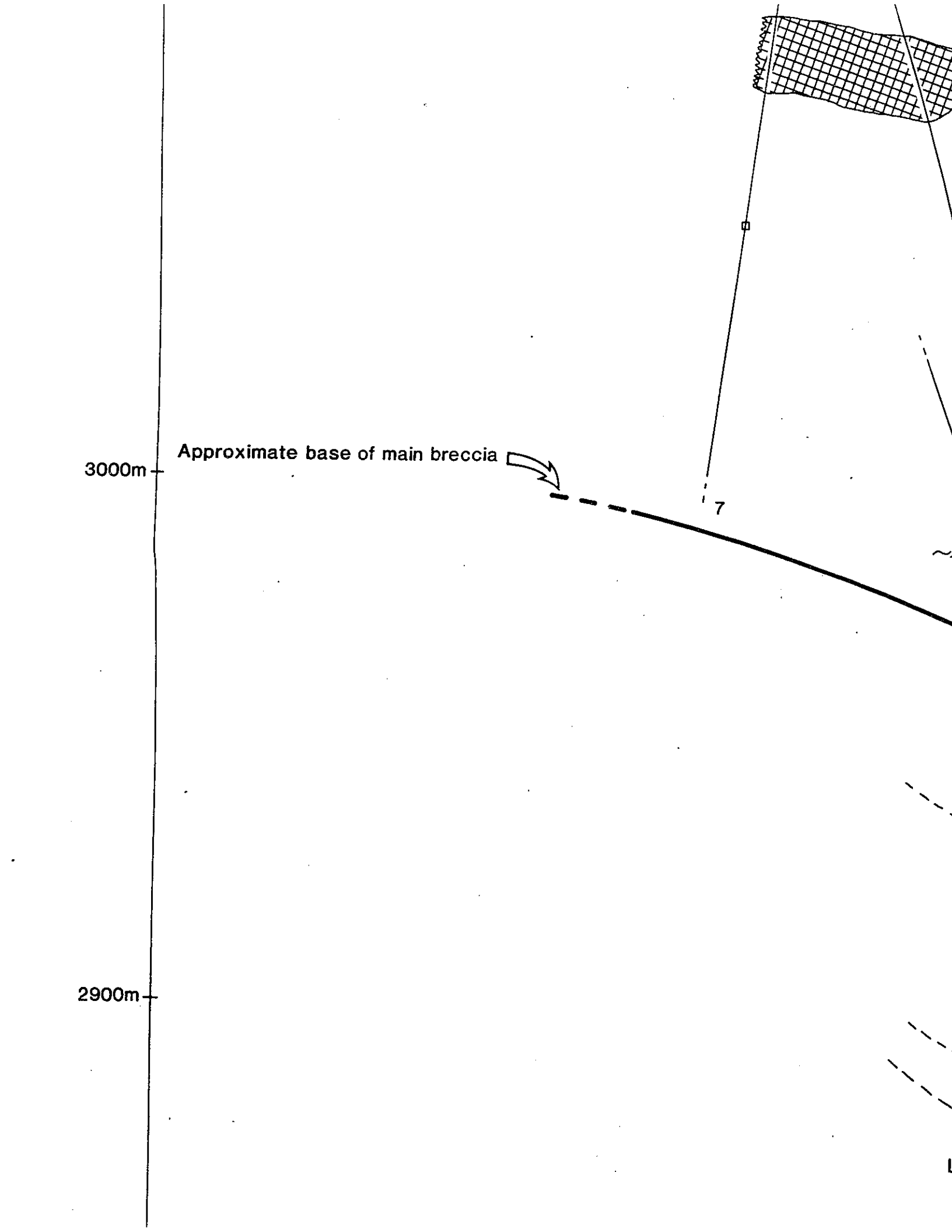
Approximate base of main breccia
3000m
2900m
7

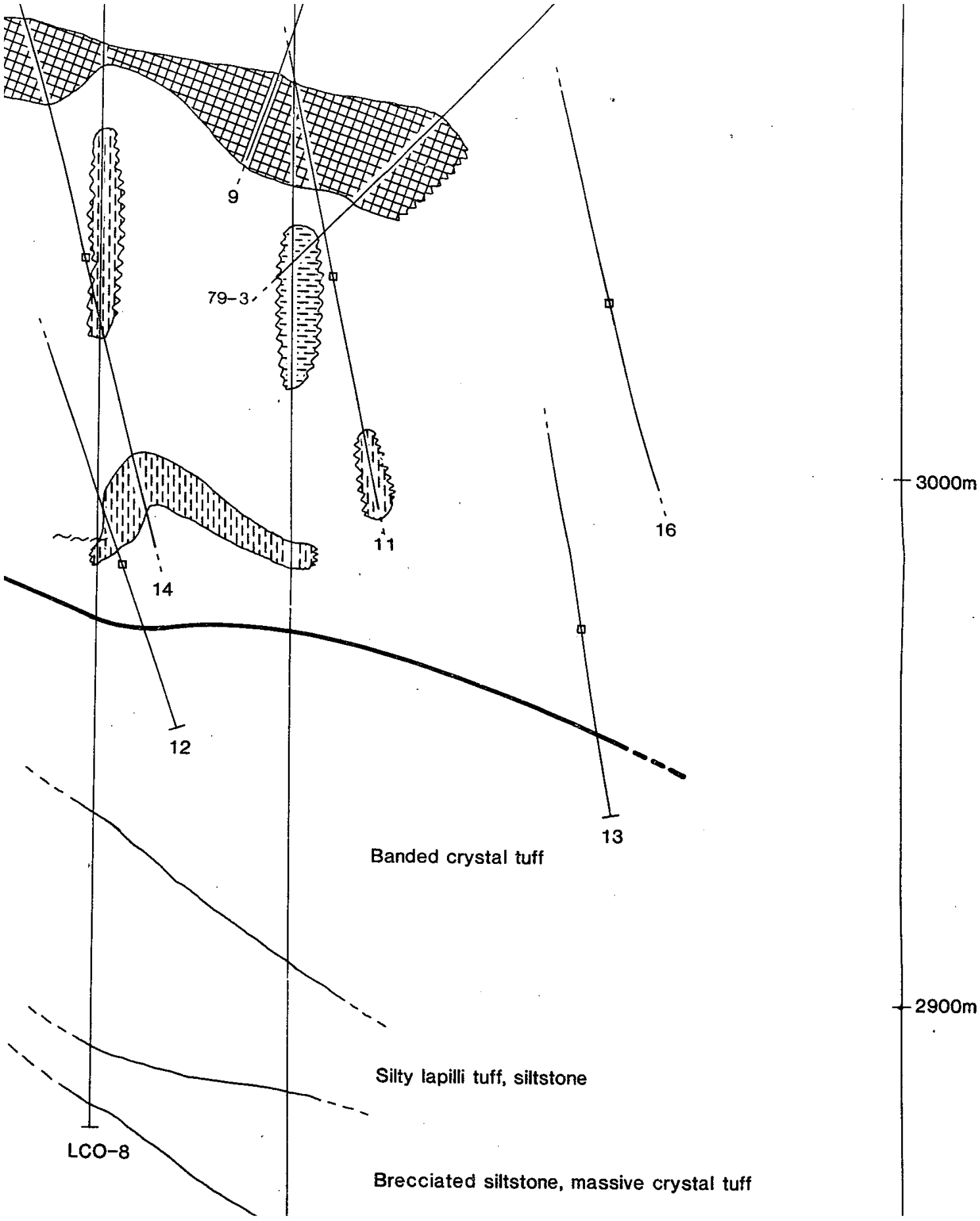
9
79-3
11
16
14
12
13
3000m
2900m
Banded crystal tuff
Silty lapilli tuff, siltstone
LCO-8
Brecciated siltstone, massive crystal tuff

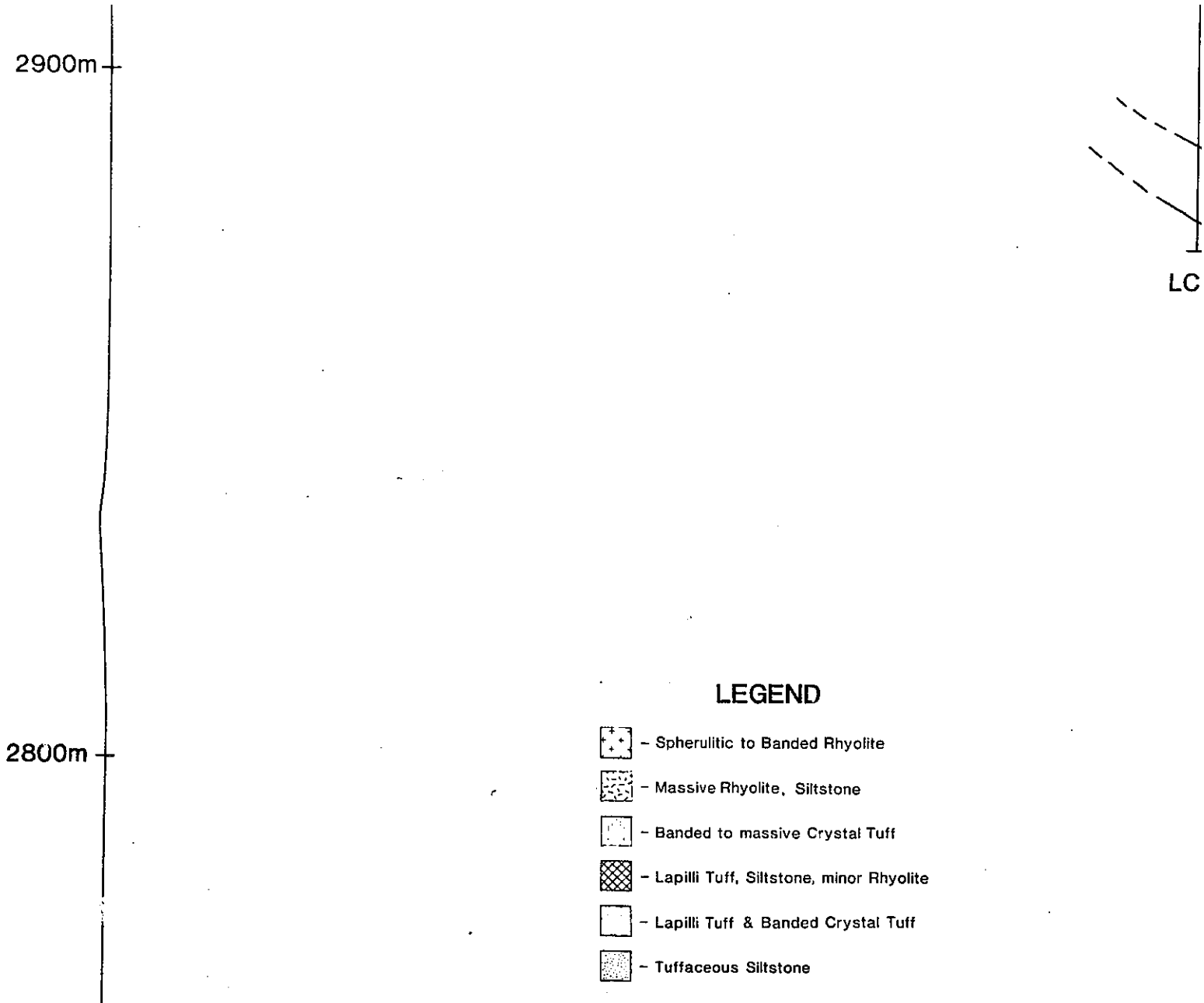

MOUNT COSTIGAN Pb–Zn DEPOSIT

Geology, short N–S section (N020, 90)

Figure 16

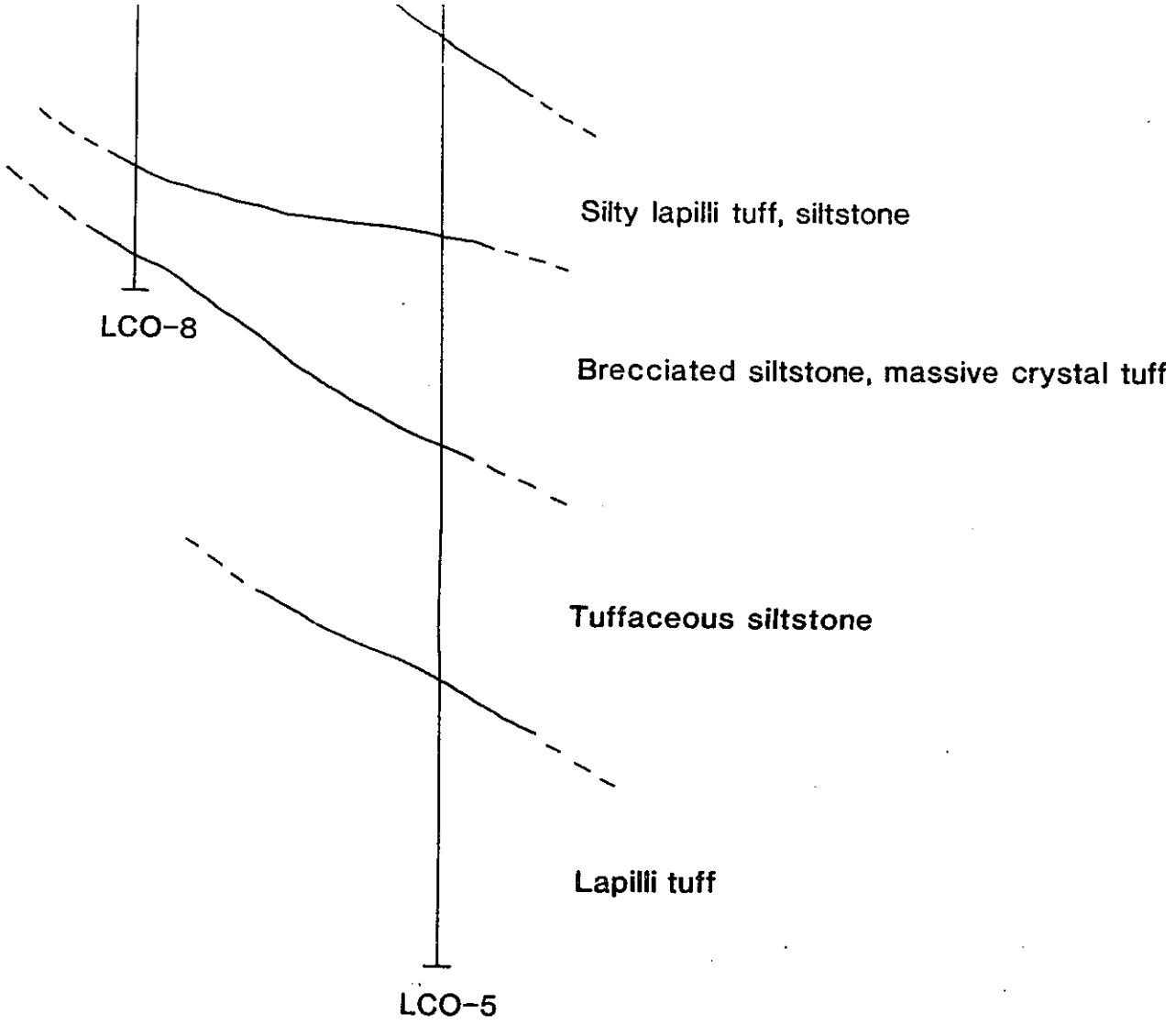
Silty lapilli tuff, siltstone
LCO-8
Brecciated siltstone, massive crystal tuff
Tuffaceous siltstone
Lapilli tuff
LCO-5

29

28

OSIT

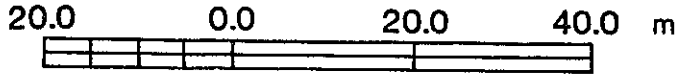
20.0
0.0
20.0
40.0
m

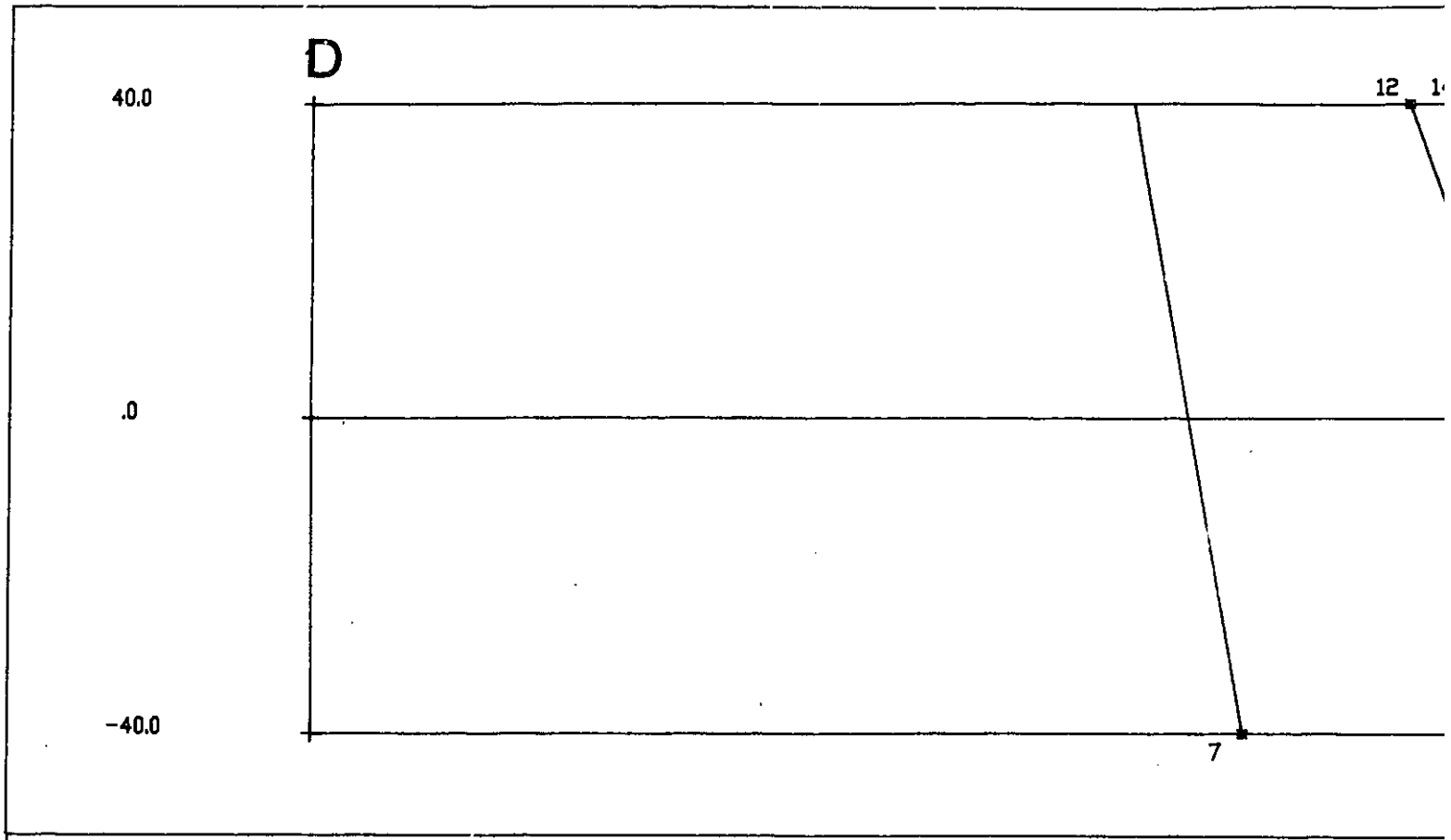
D
40.0
.0
-40.0
12
7

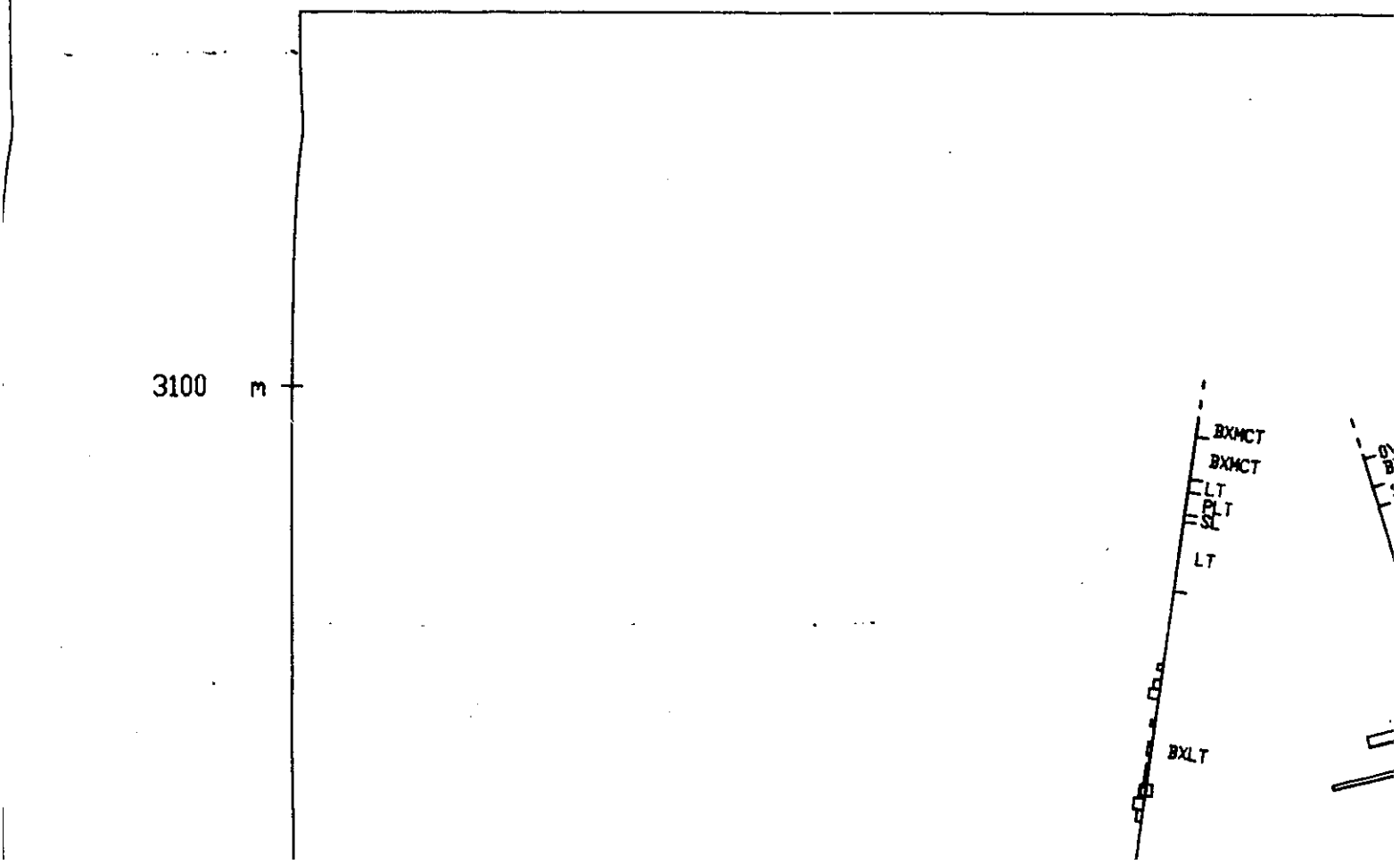
3100
m
BXMCT
BXMCT
LT
PLT
SL
LT
BXLT

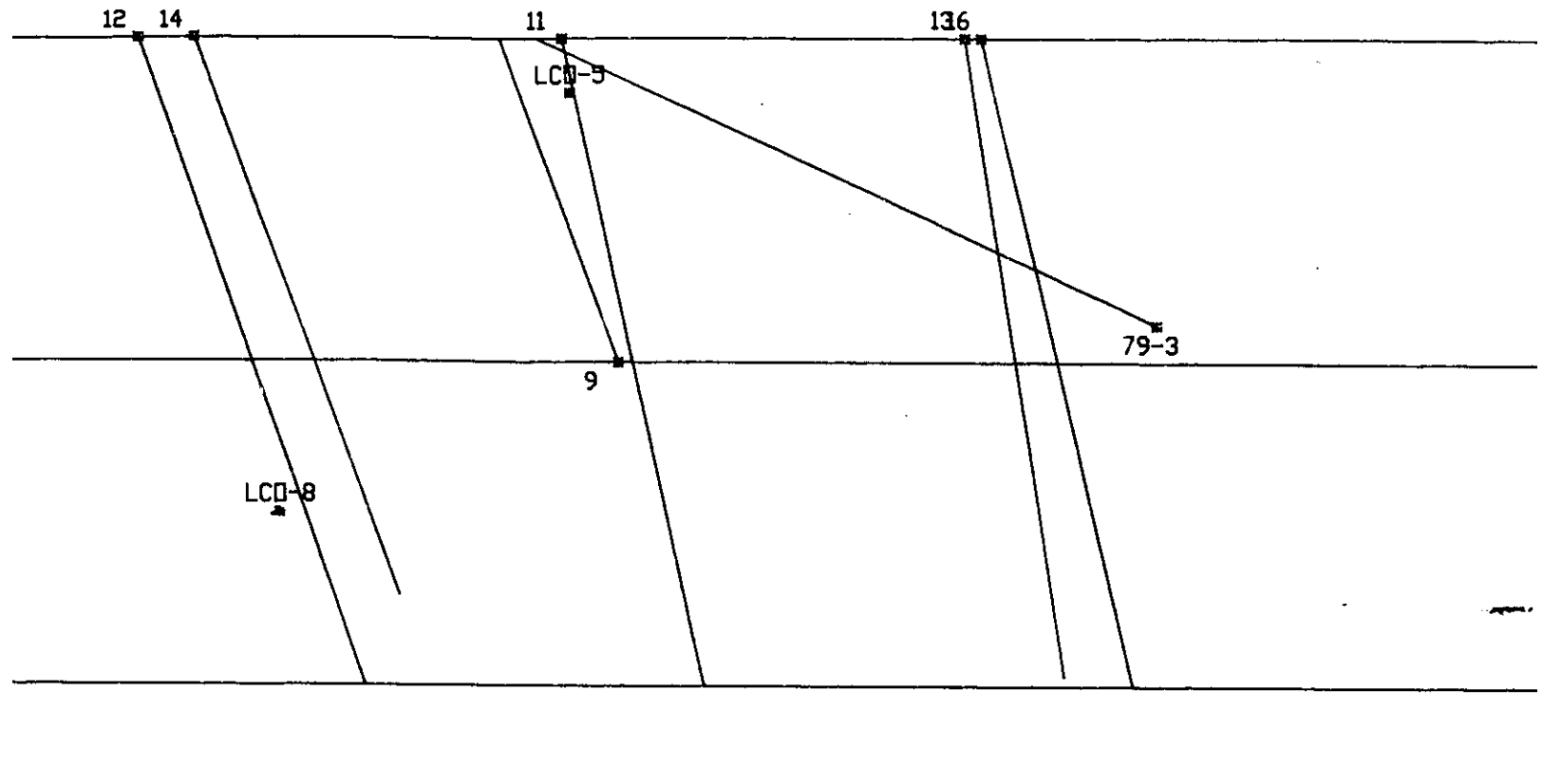
12
14
11
136
LCD-5
79-3
9
LCD-8

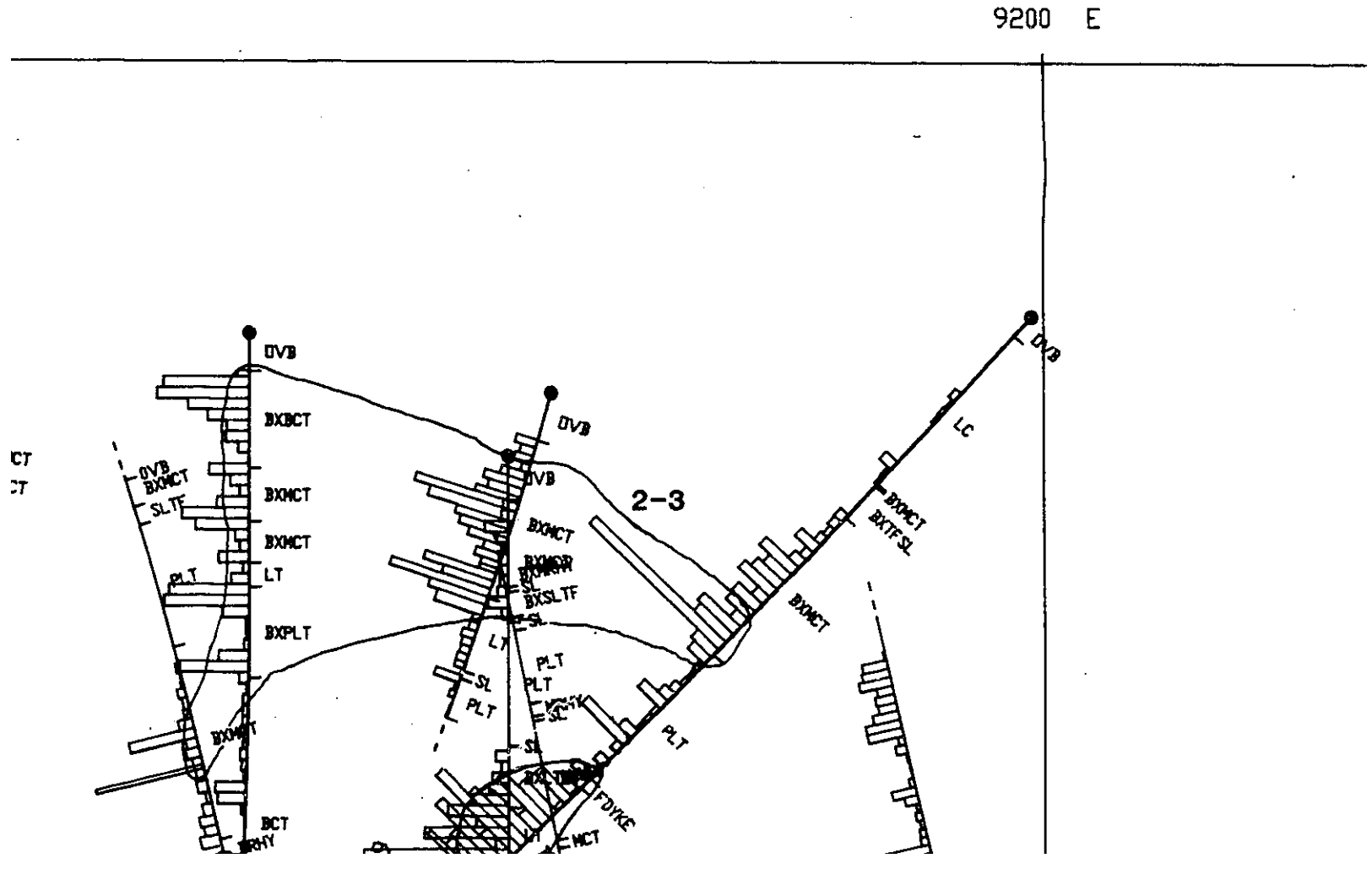
9200 E
DVB
BXBCT
BXMCT
SLTF
PLT
LT
BXPLT
BCT
2-3
BXSLTF
SL
PL_T
FDYKE
MCT
LC
BXTF-SL

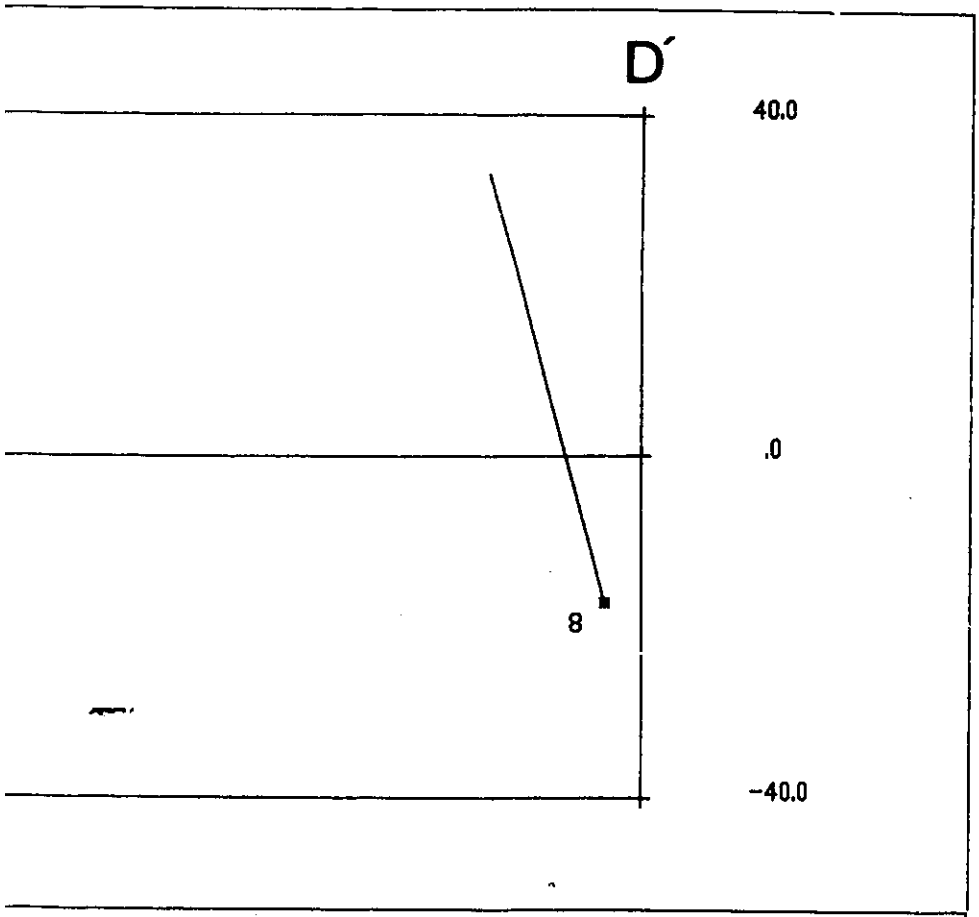
D´
40.0
.0
-40.0
8

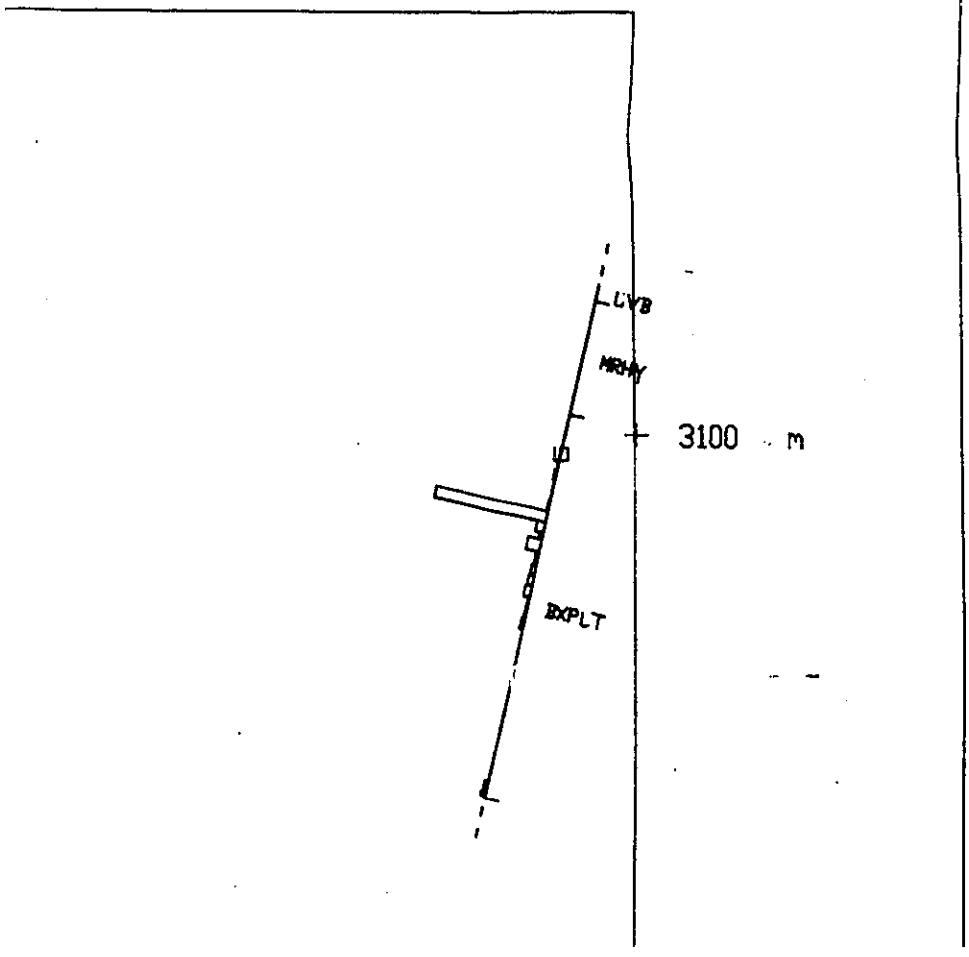
LVB
MRHy
3100 m
EXPLT

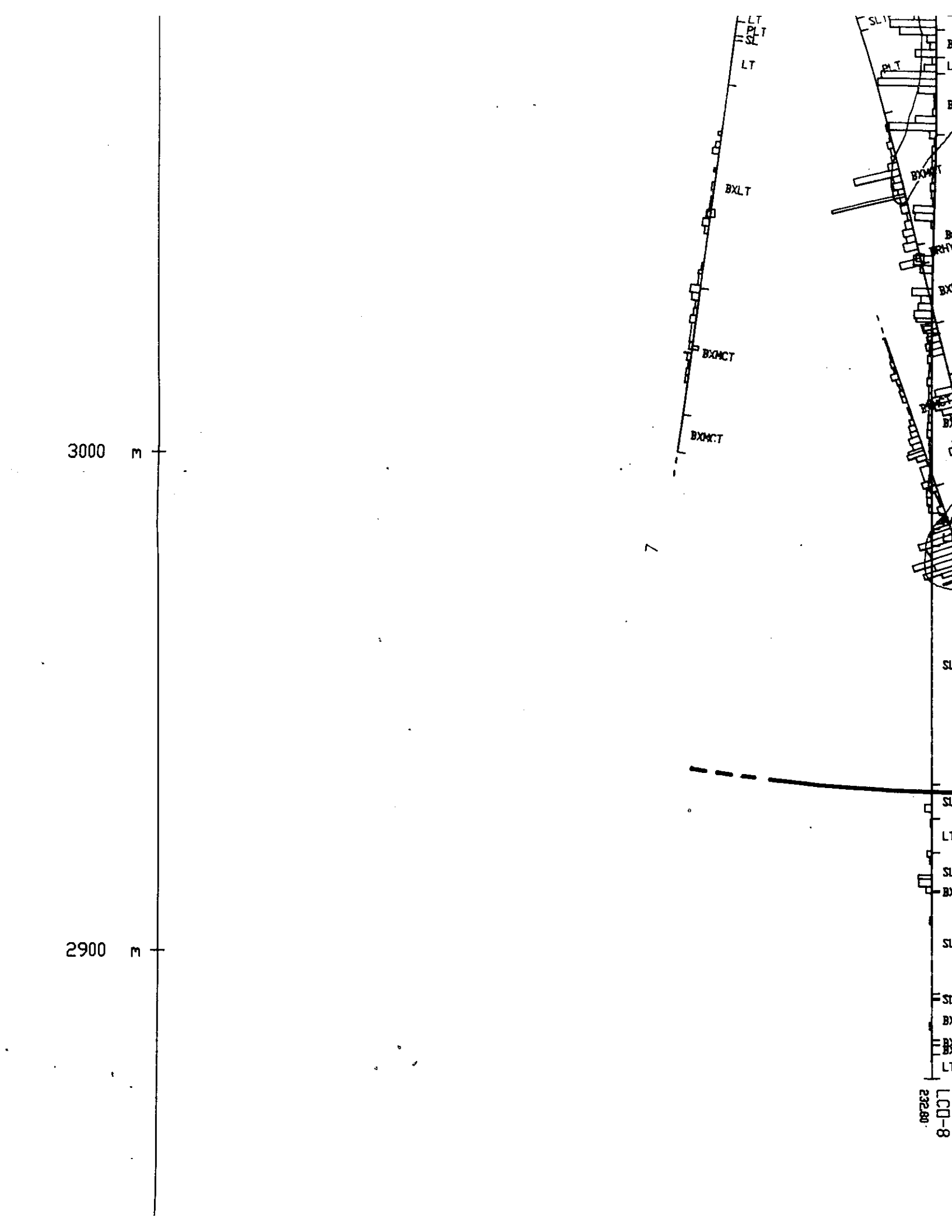
3000 m
2900 m
BXLT
BXMCT
BXMCT
LT
PLT
SLT
LCD-8

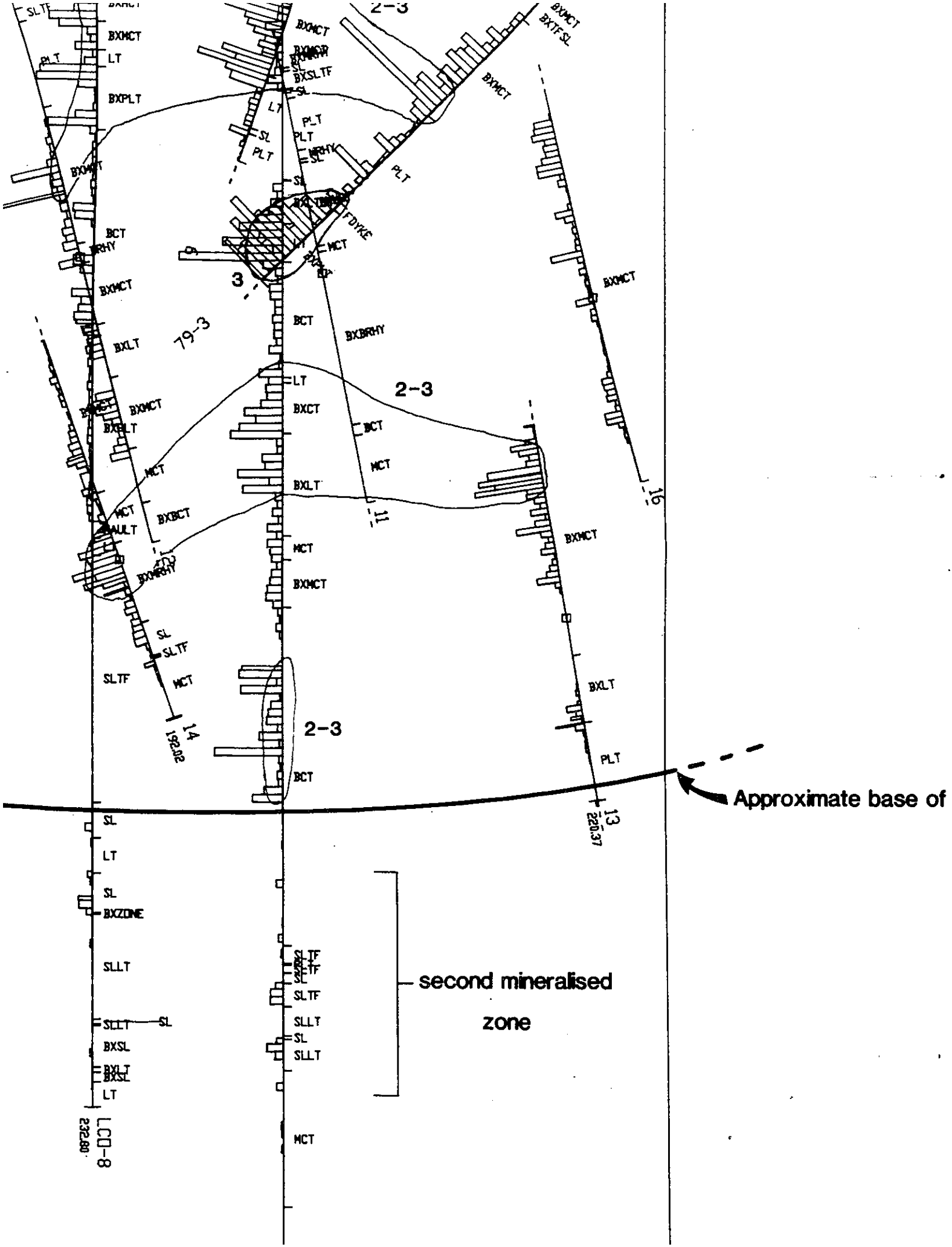
Approximate base of
second mineralised
zone
2-3
79-3
LCD-8
232.80
14
192.02
13
220.37
11
16
BXMCT
BXLT
BXSL
BXZONE
BXCT
BXBCT
BXBRHY
BXXMCT
BXTF-SL
BXSLTF
BXPLT
BCT
MCT
PLT
LT
SL
SLTF
SLLT
FAULT
F'DYKE

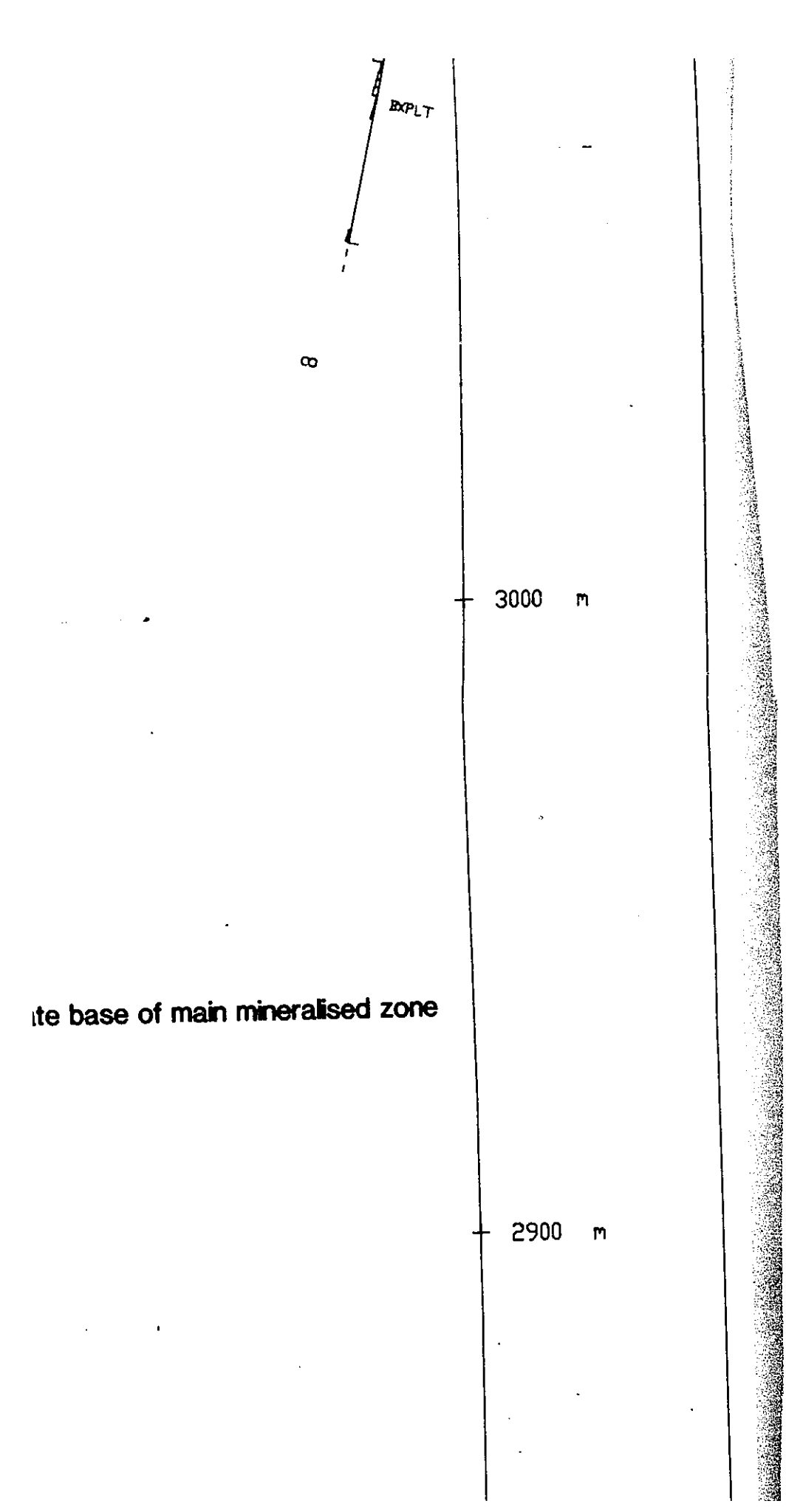

ıte base of main mineralised zone

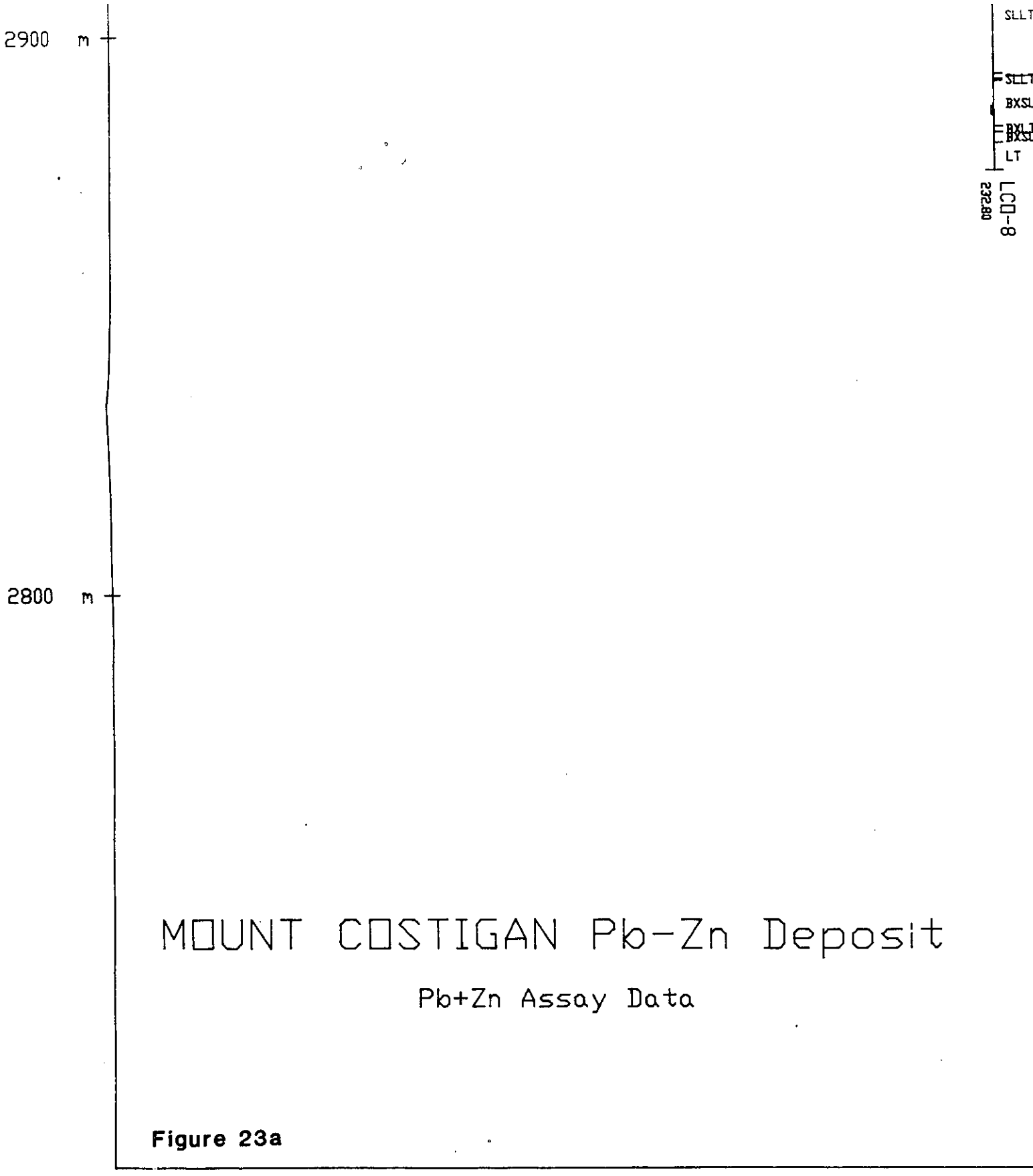

MOUNT COSTIGAN Pb-Zn Deposit

Pb+Zn Assay Data

Figure 23a

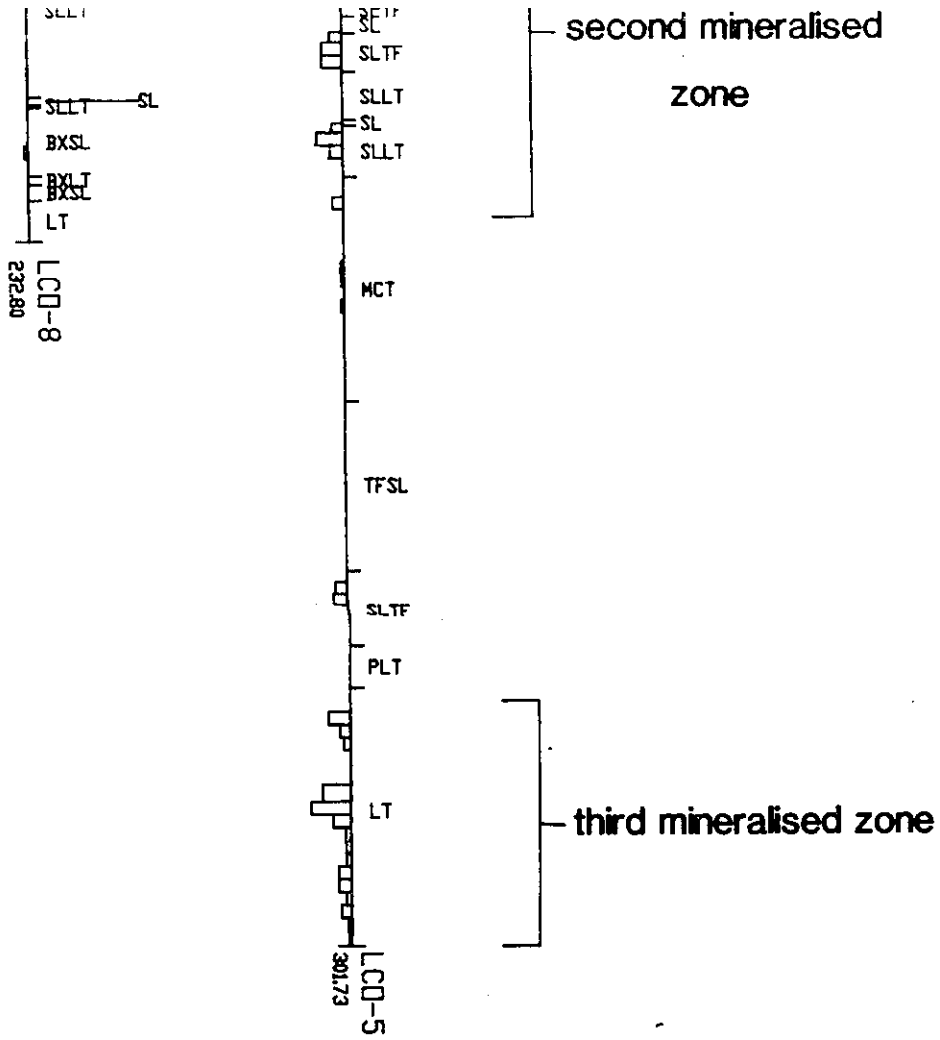

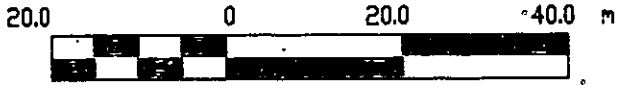

Legend

1 – Low Grade:

2 – Medium Gra

3 – High Grade:

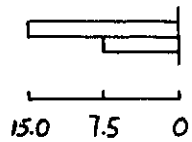

OVB - Overburden
LC - Lost Core
MLNG - Melange
BCT - Banded Crystal Tuff
MCT - Massive Crystal Tuf
LT - Lapilli Tuff
PLT - Polymictic Lapilli Tu
BRHY - Flow-banded Rhyc
MRHY - Massive Rhyolite
SRHY - Spherulitic Rhyolit
SBRHY - Spherulitic, Flow
SL - Siltstone
SLTF - Silty Tuff
SLLT - Silty Lapilli Tuff
TFSL - Tuffaceous Siltston

Note: Prefix "BX" denotes the above lithologies.

9200 E

2900 m

Legend

1 – Low Grade: <4 g/t

2 – Medium Grade: 4–10 g/t

3 – High Grade: >10 g/t

2800 m

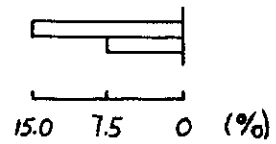

OVB - Overburden
LC - Lost Core
MLNG - Melange
BCT - Banded Crystal Tuff
MCT - Massive Crystal Tuff
LT - Lapilli Tuff
PLT - Polymictic Lapilli Tuff
BRHY - Flow-banded Rhyolite
MRHY - Massive Rhyolite
SRHY - Spherulitic Rhyolite
SBRHY - Spherulitic, Flow-banded Rhyolite
SL - Siltstone
SLTF - Silty Tuff
SLLT - Silty Lapilli Tuff
TFSL - Tuffaceous Siltstone

Note: Prefix "BX" denotes brecciated varieties of the above lithologies.

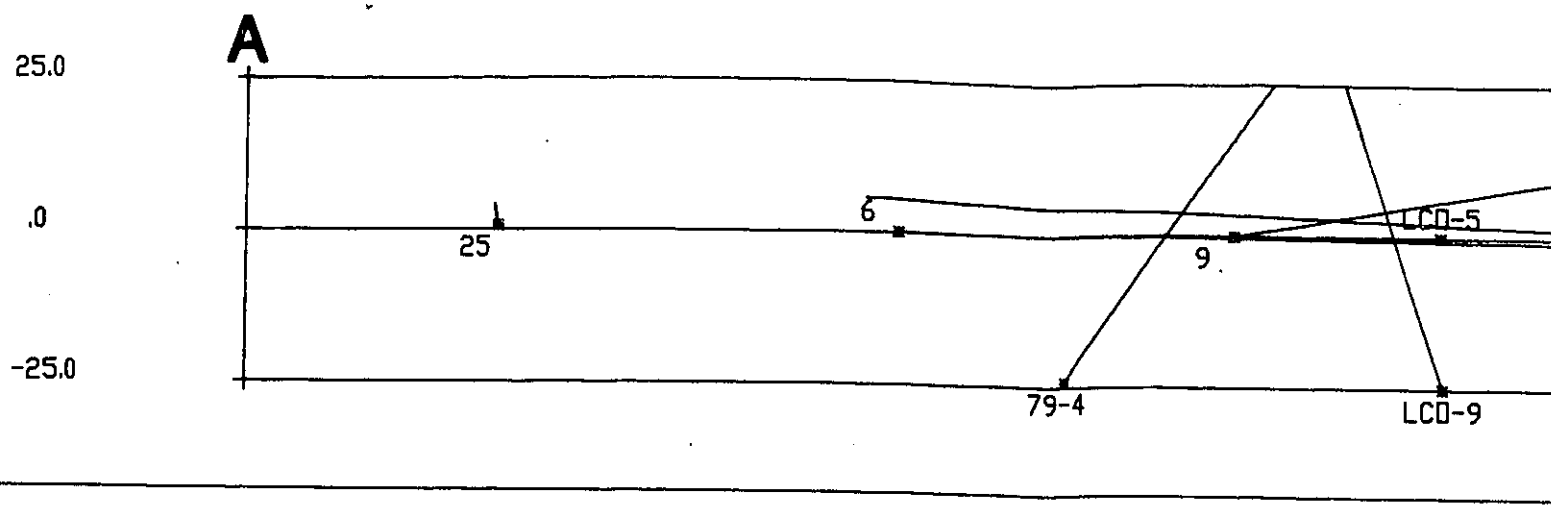
A
25.0
.0
-25.0
25
6
9
LCD-5
79-4
LCD-9

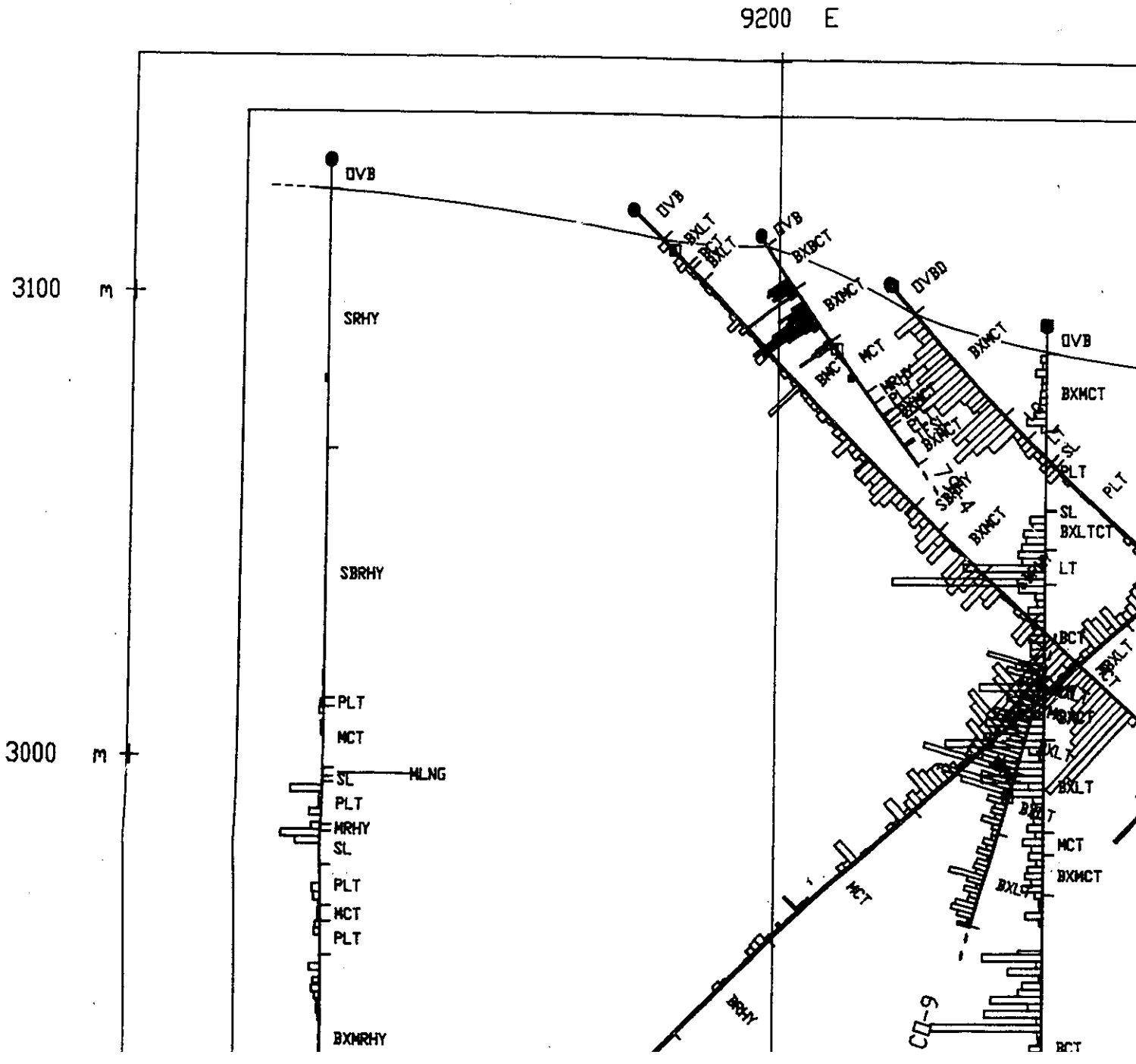
9200 E
3100 m
3000 m
DVB
SRHY
SBRHY
PLT
MCT
SL
MLNG
PLT
MRHY
SL
PLT
MCT
PLT
BXMRHY
BXLT
BXMCT
BXLTCT
LT
MRHY
CD-9

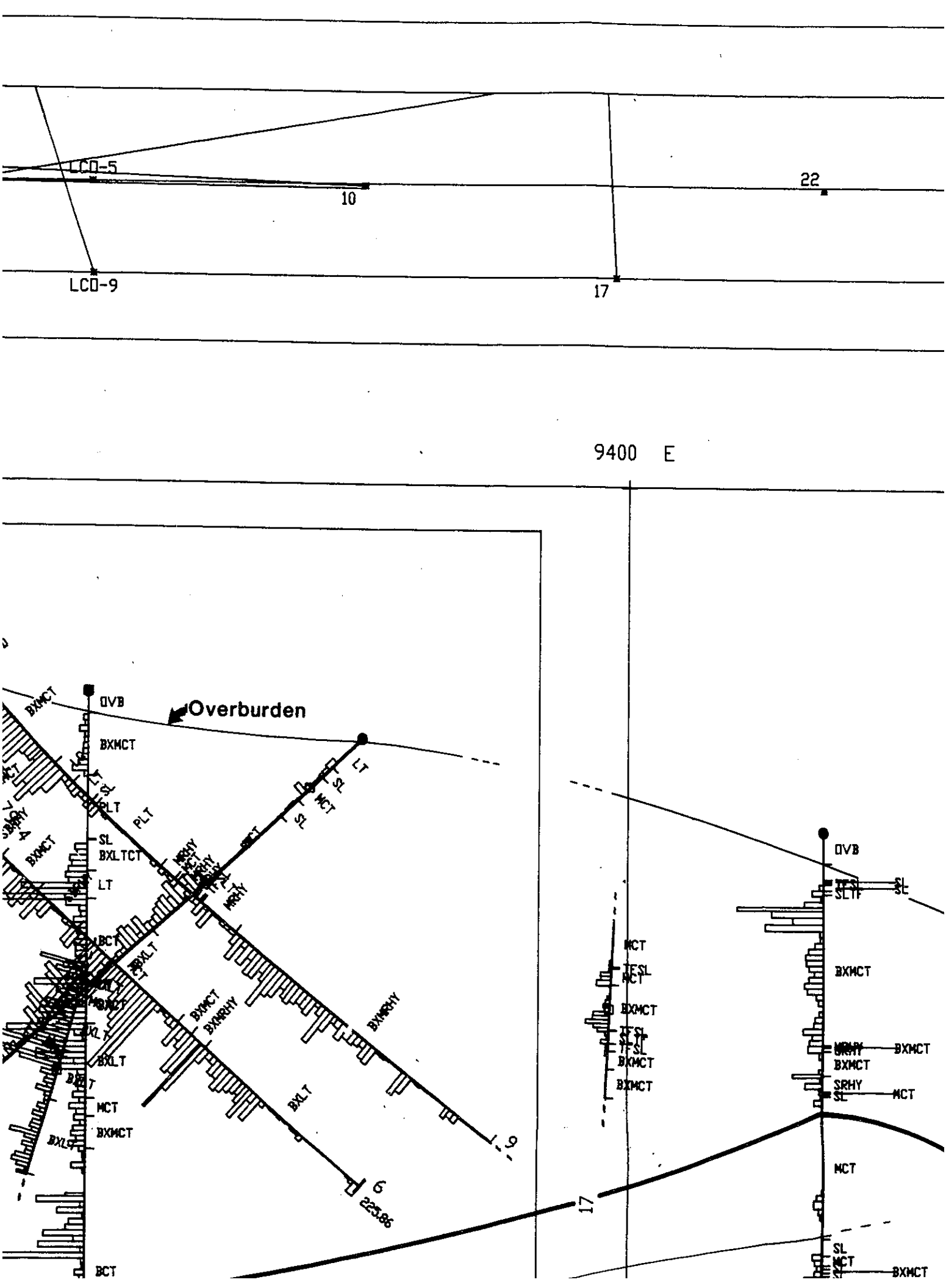
LCO-5
10
22
LCO-9
17
9400 E
Overburden
OVB
BXMCT
LT
SL
PLT
BXLTCT
MCT
MRHY
BCT
BXLT
BXMRHY
9
6
22586
17
TFSL
SLTF
SRHY

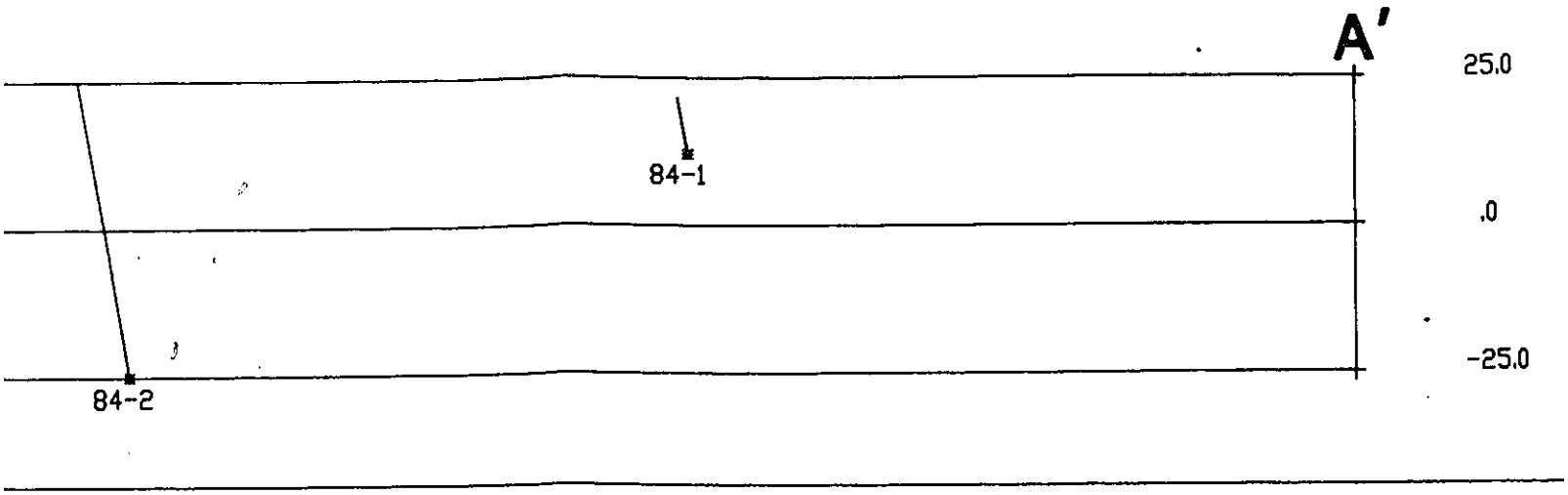
A'
25.0
.0
-25.0
84-1
84-2

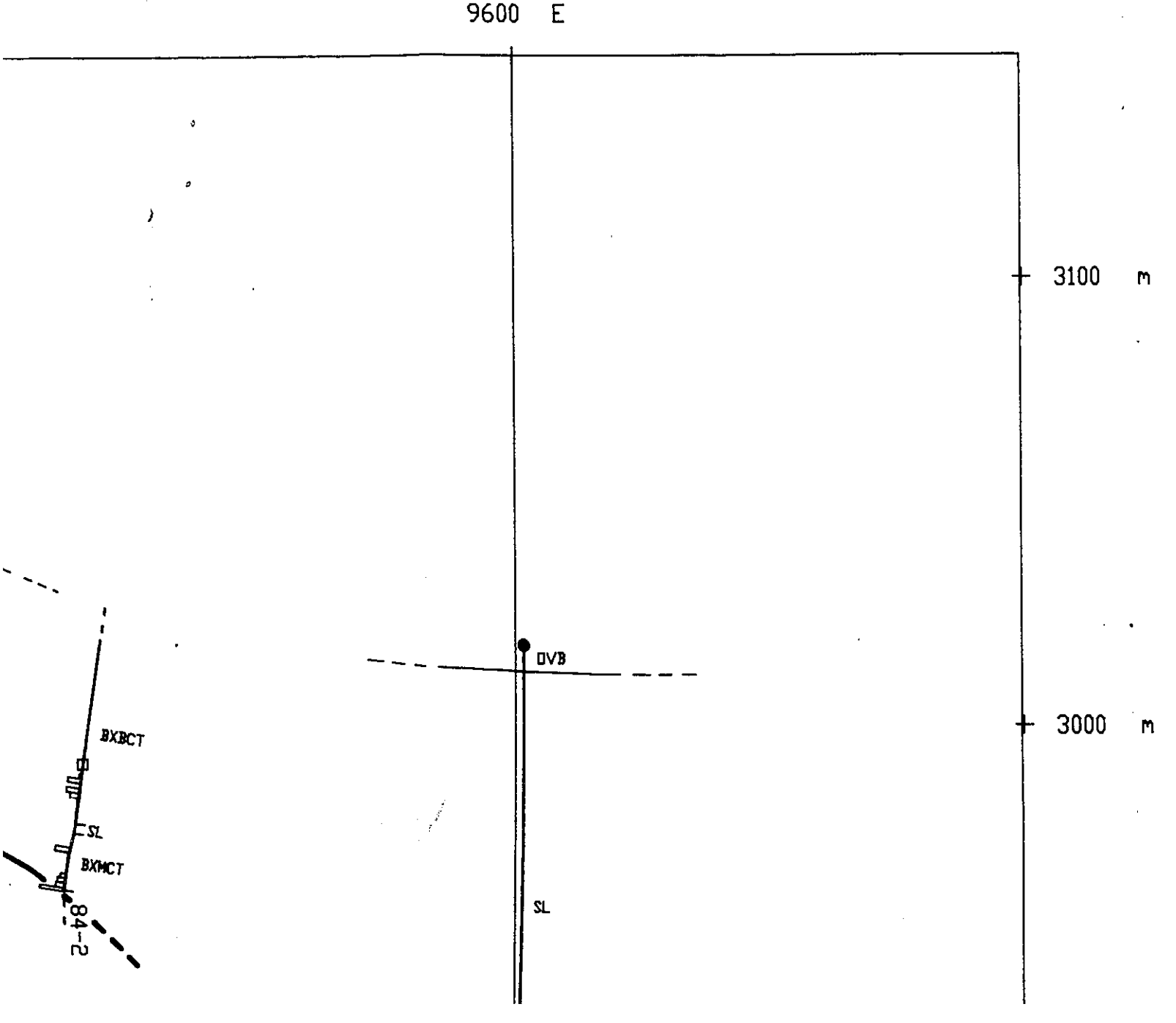
9600 E
3100 m
3000 m
DVB
BXBCT
SL
BXMCT
84-2
SL

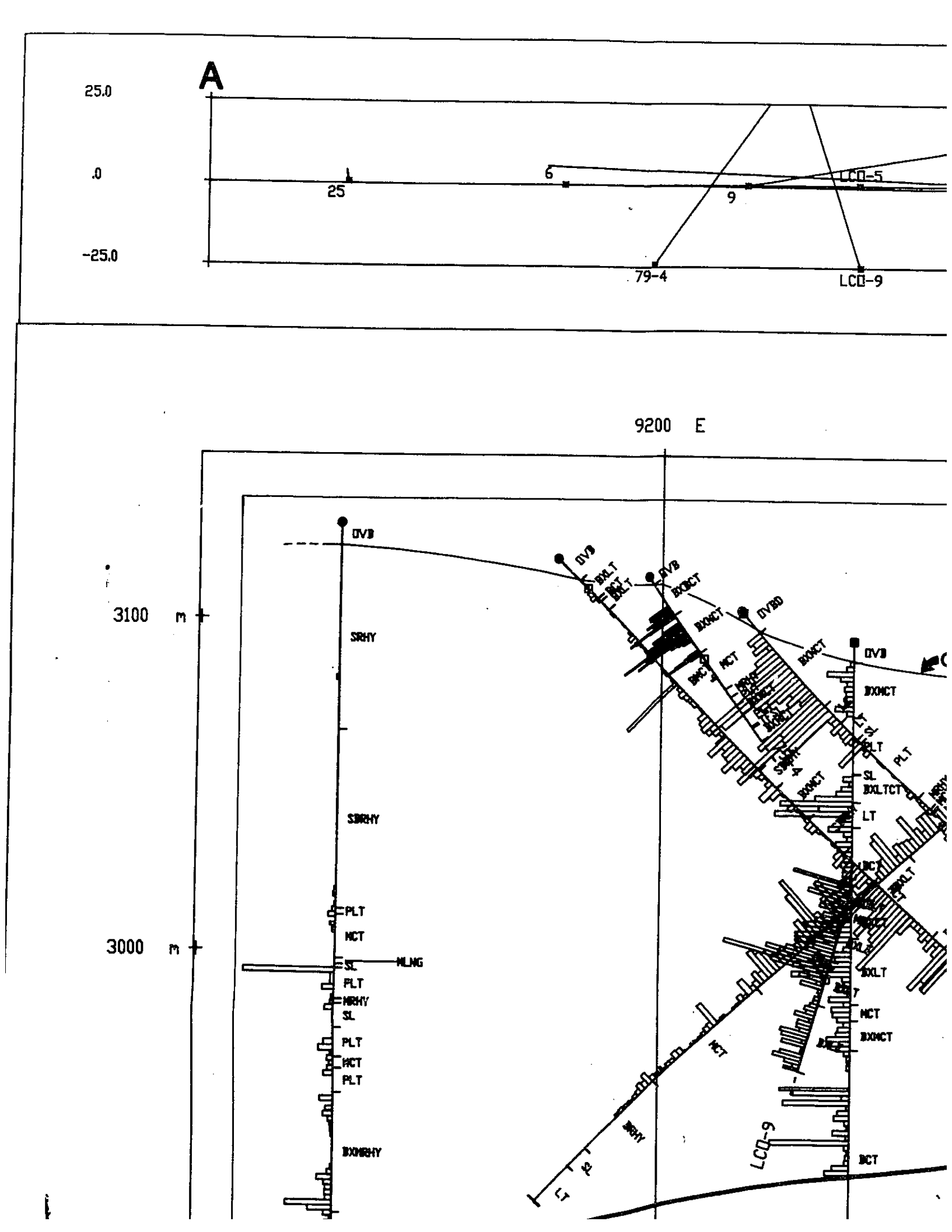
A
25.0
.0
-25.0
25
6
9
LCD-5
79-4
LCD-9
9200 E
3100 m
3000 m
DVB
SRHY
SBRHY
PLT
MCT
SL
MLMG
MRHY
BXMRHY
BXLT
BXMCT
LT
LCD-9

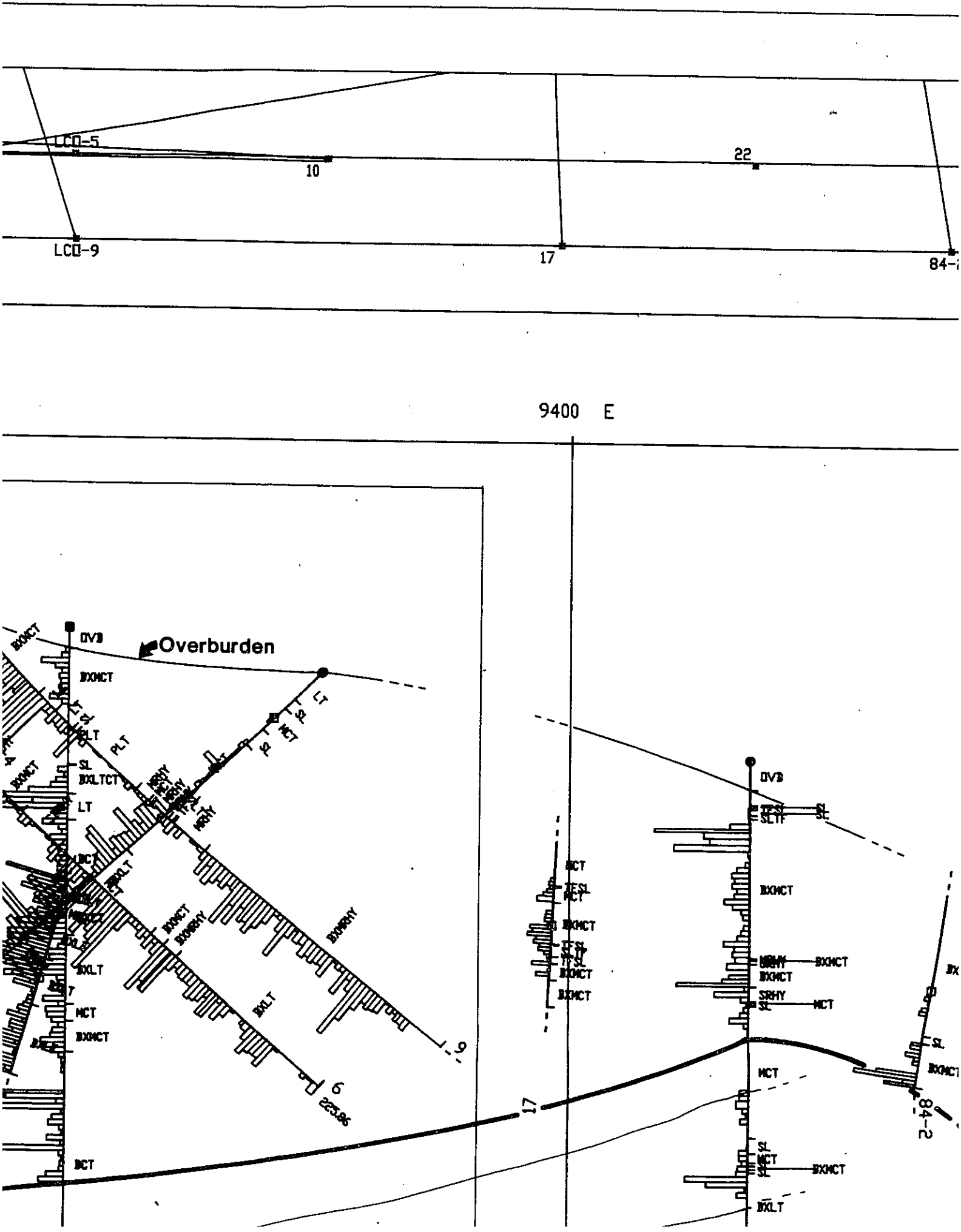
LCD-5
10
22
LCD-9
17
9400 E
Overburden
DVB
BXHCT
BXLTCT
BXLT
MCT
SL
LT
PLT
MSHY
BXMSHY
SRHY
TESL
SLTF
17
6
225.86
84-2

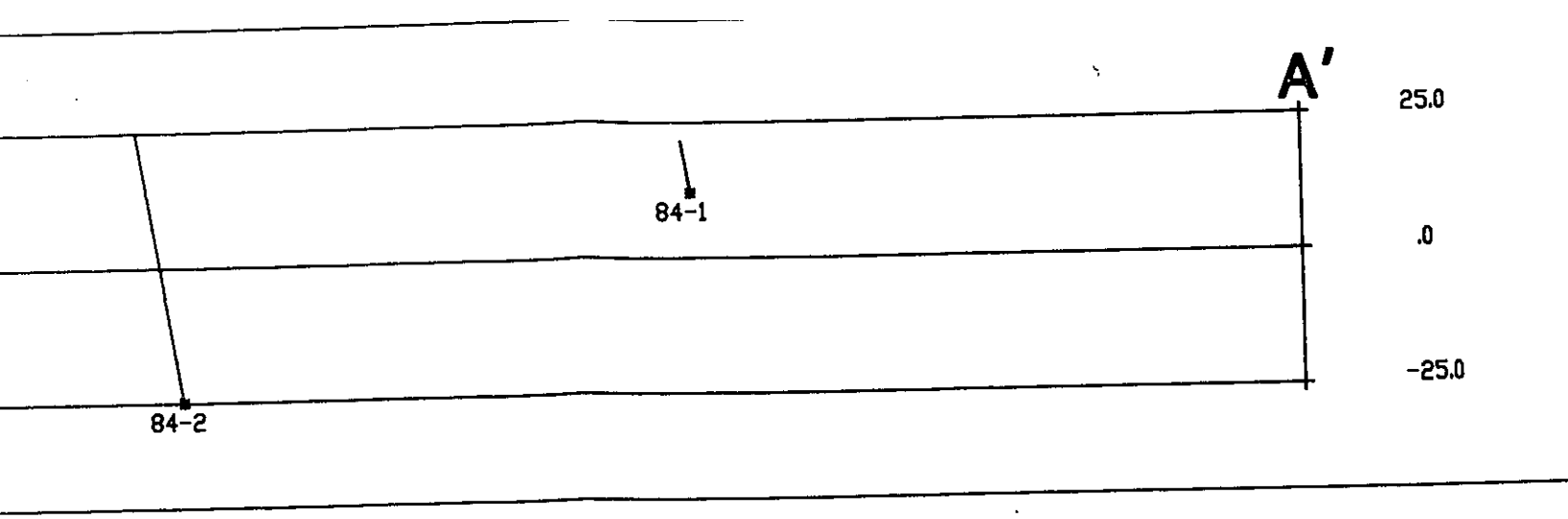

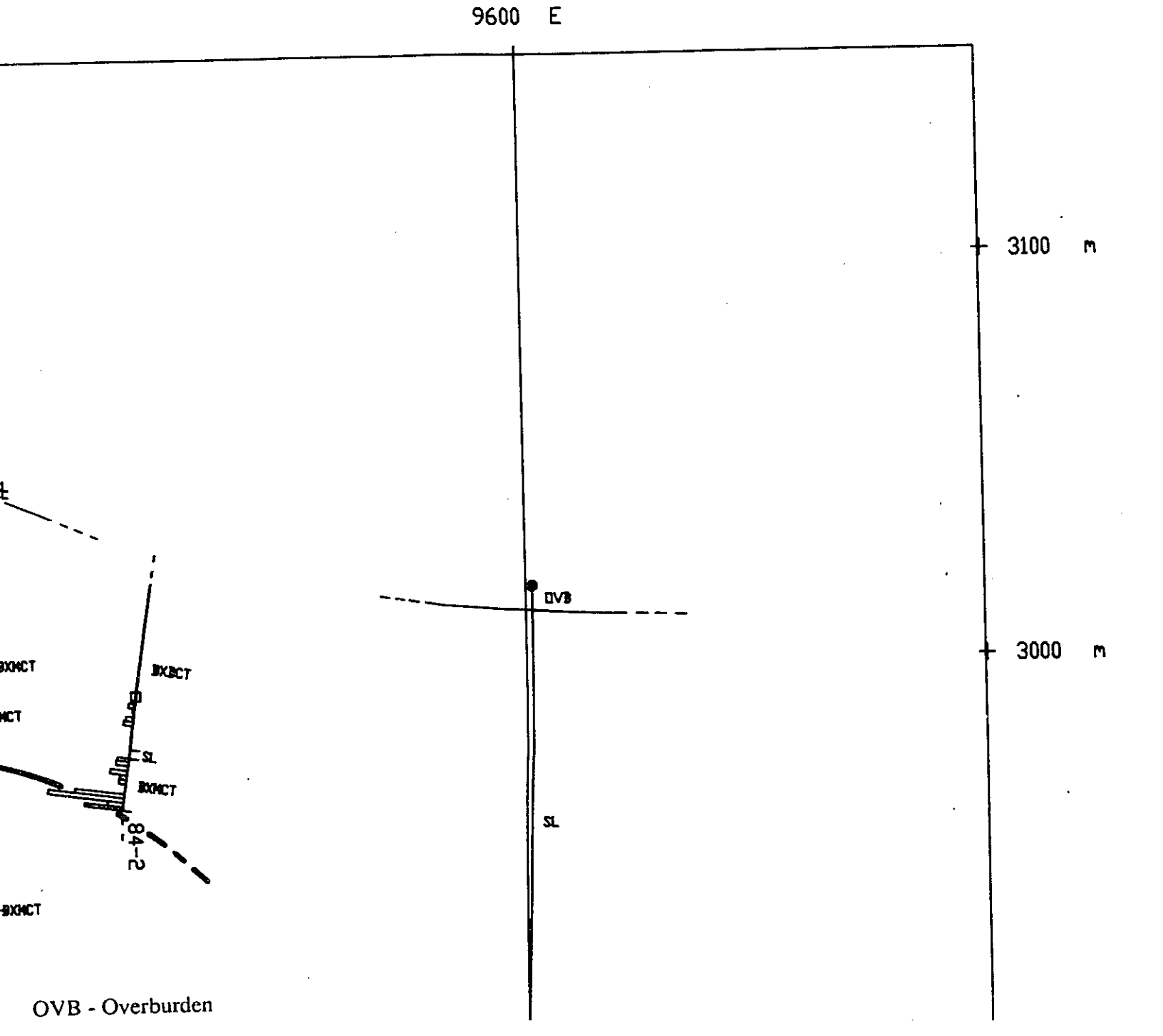

OVB - Overburden

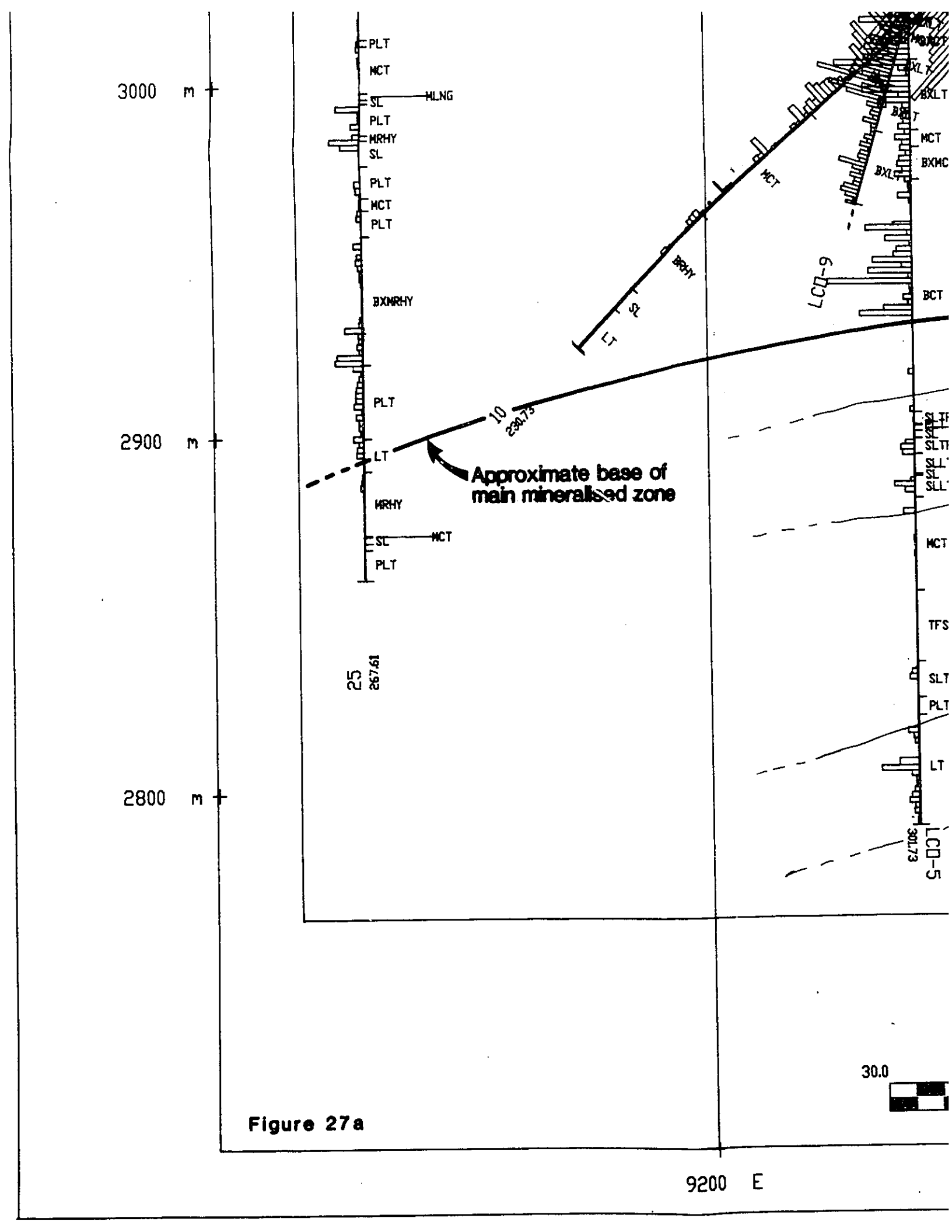
3000 m
2900 m
2800 m
9200 E
PLT
MCT
SL
MLNG
PLT
MRHY
SL
PLT
MCT
PLT
BXMRHY
PLT
LT
MRHY
SL
MCT
PLT
25
267.61
10
230.75
LT
SL
BRHY
MCT
LCD-9
BXL
BXLT
MCT
BXMC
BCT
MCT
TFS
SLT
PLT
LT
LCD-5
30.73
Approximate base of
main mineralised zone
30.0

Figure 27a

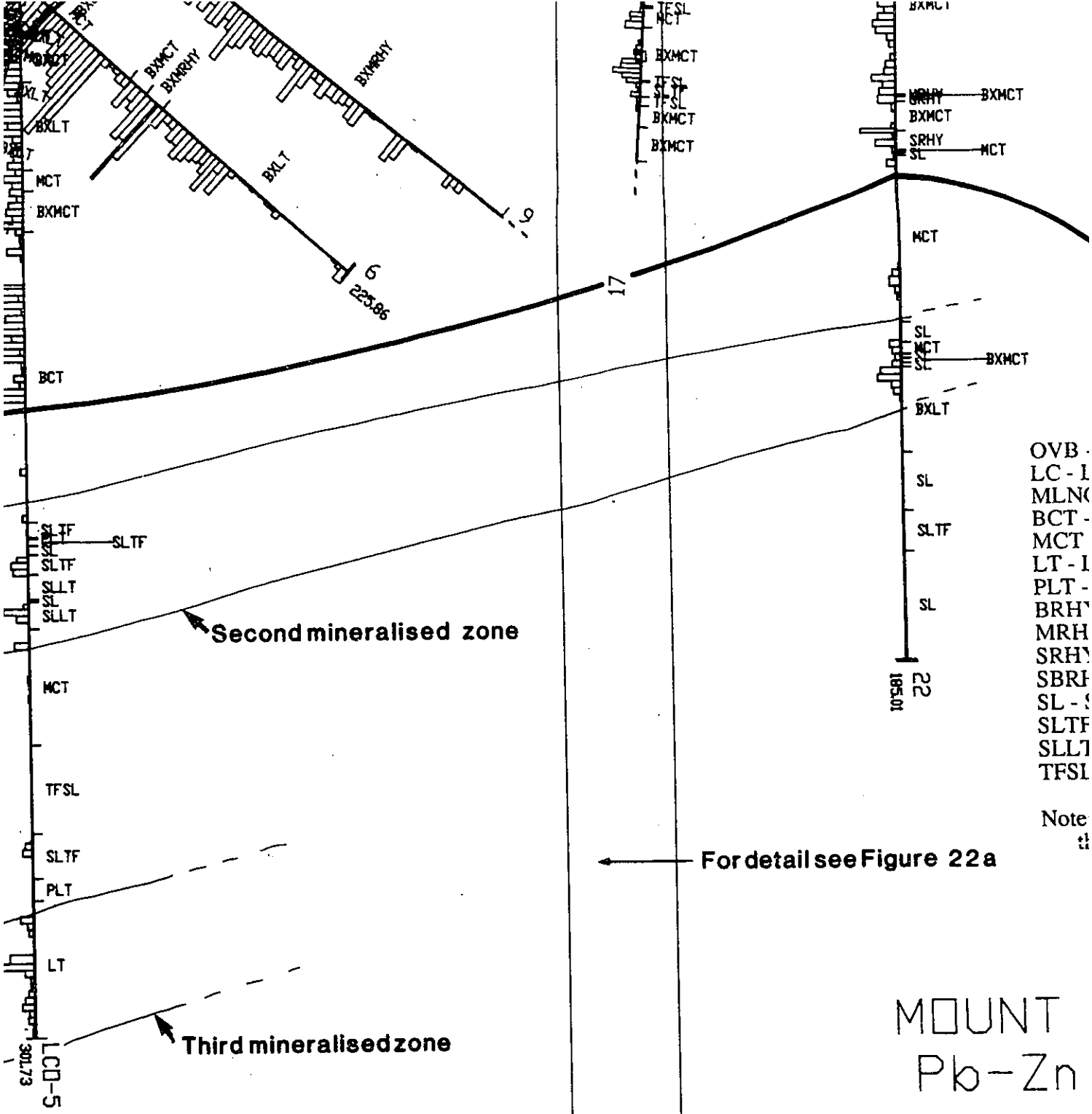

OVB -
LC - L
MLN(
BCT -
MCT
LT - L
PLT -
BRH
MRH
SRH
SBR
SL -
SLTF
SLLT
TFSL

Note
t

MOUNT
Pb-Zn

Pb Assc

5.0

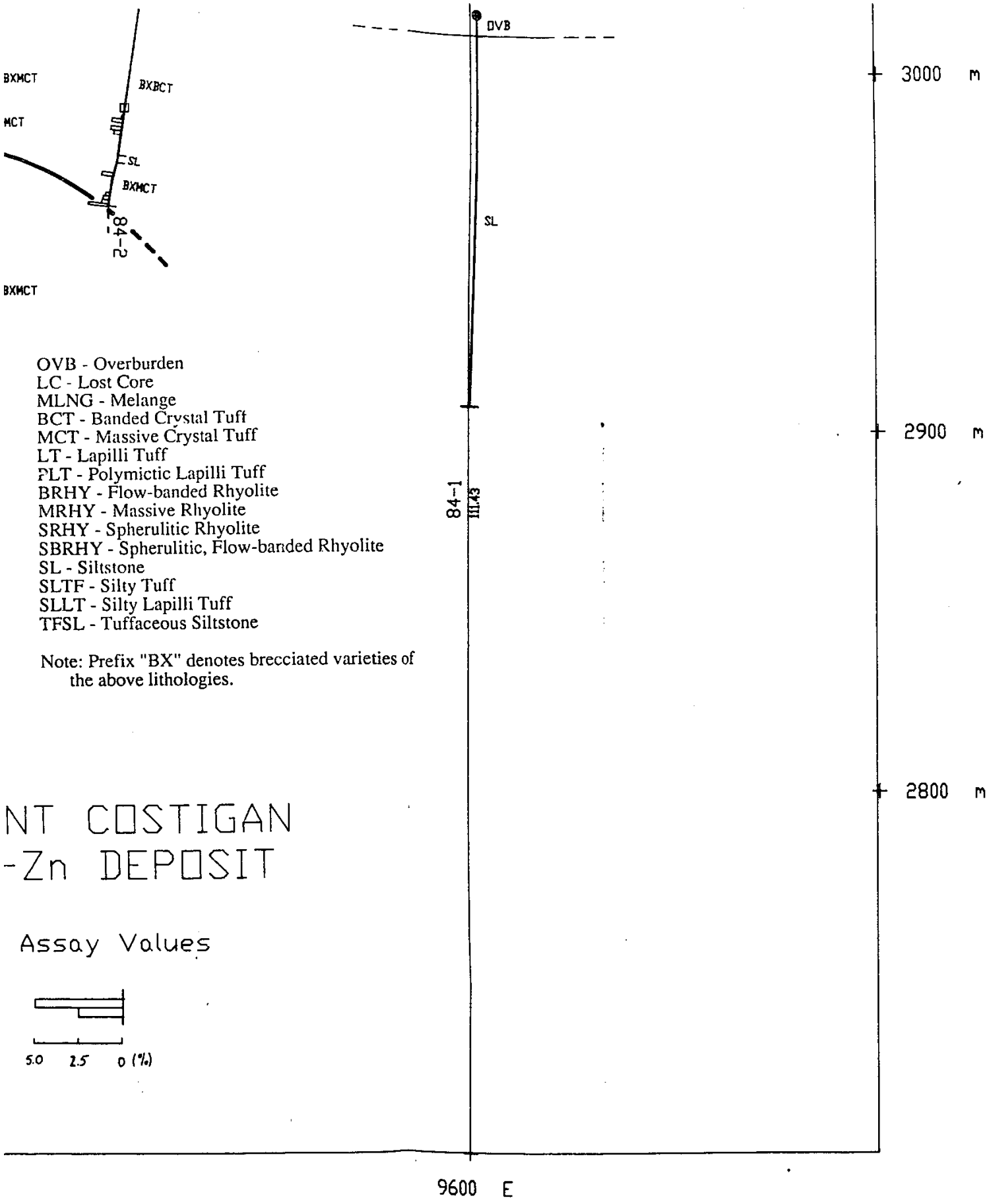

OVB - Overburden
LC - Lost Core
MLNG - Melange
BCT - Banded Crystal Tuff
MCT - Massive Crystal Tuff
LT - Lapilli Tuff
PLT - Polymictic Lapilli Tuff
BRHY - Flow-banded Rhyolite
MRHY - Massive Rhyolite
SRHY - Spherulitic Rhyolite
SBRHY - Spherulitic, Flow-banded Rhyolite
SL - Siltstone
SLTF - Silty Tuff
SLLT - Silty Lapilli Tuff
TFSL - Tuffaceous Siltstone

Note: Prefix "BX" denotes brecciated varieties of the above lithologies.

NT COSTIGAN -Zn DEPOSIT

Assay Values

5.0 2.5 0 (%)

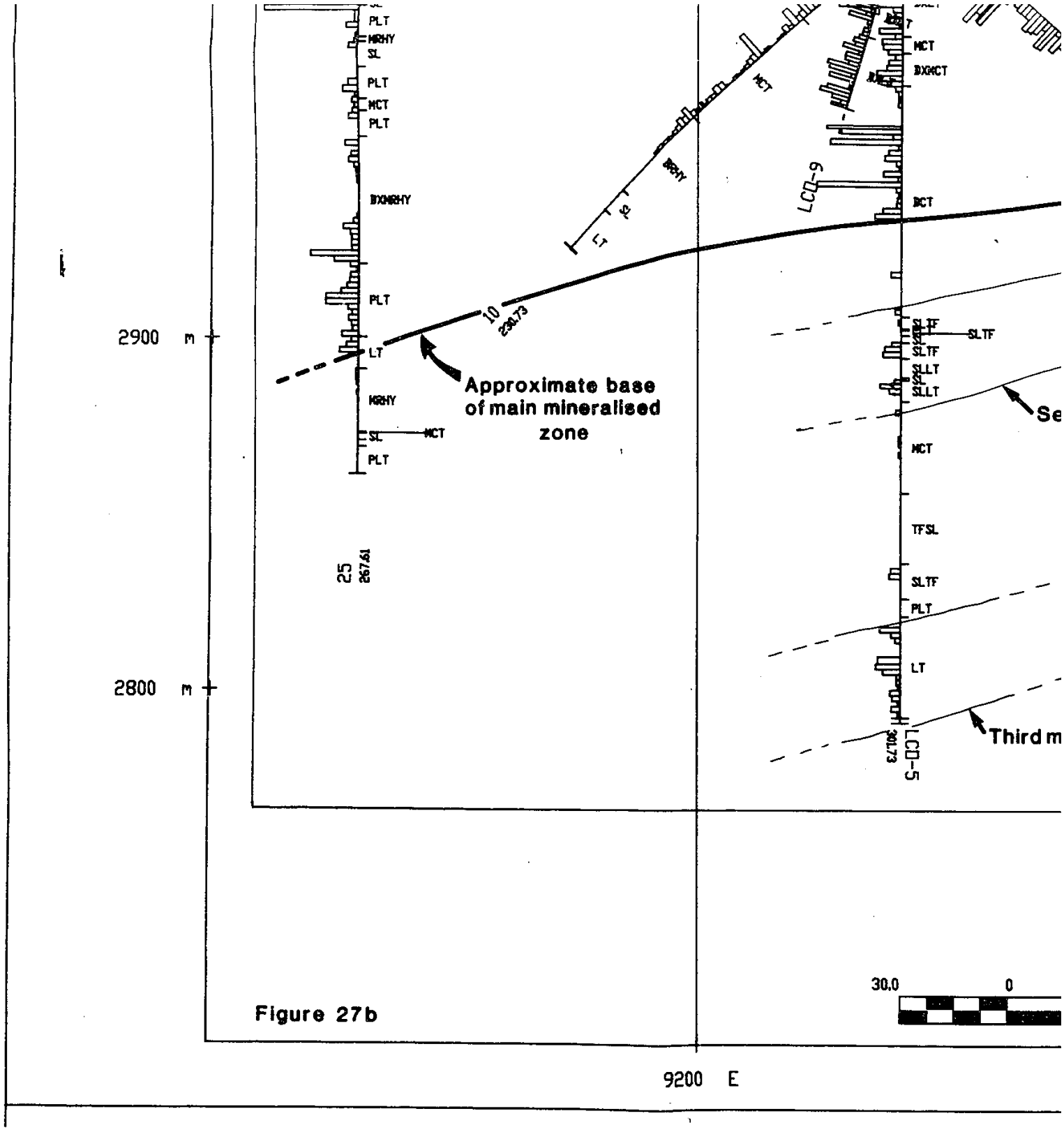
2900 m
2800 m
9200 E
PLT
MRHY
SL
PLT
MCT
PLT
BXMRHY
PLT
LT
MRHY
SL
MCT
PLT
25
267.61
10
230.73
LT
MRHY
LCD-9
MCT
BXMCT
BCT
SLTF
SLTF
SLLT
SLLT
MCT
TFSL
SLTF
PLT
LT
LCD-5
Approximate base of main mineralised zone
Se
Third m
30.0
0

Figure 27b

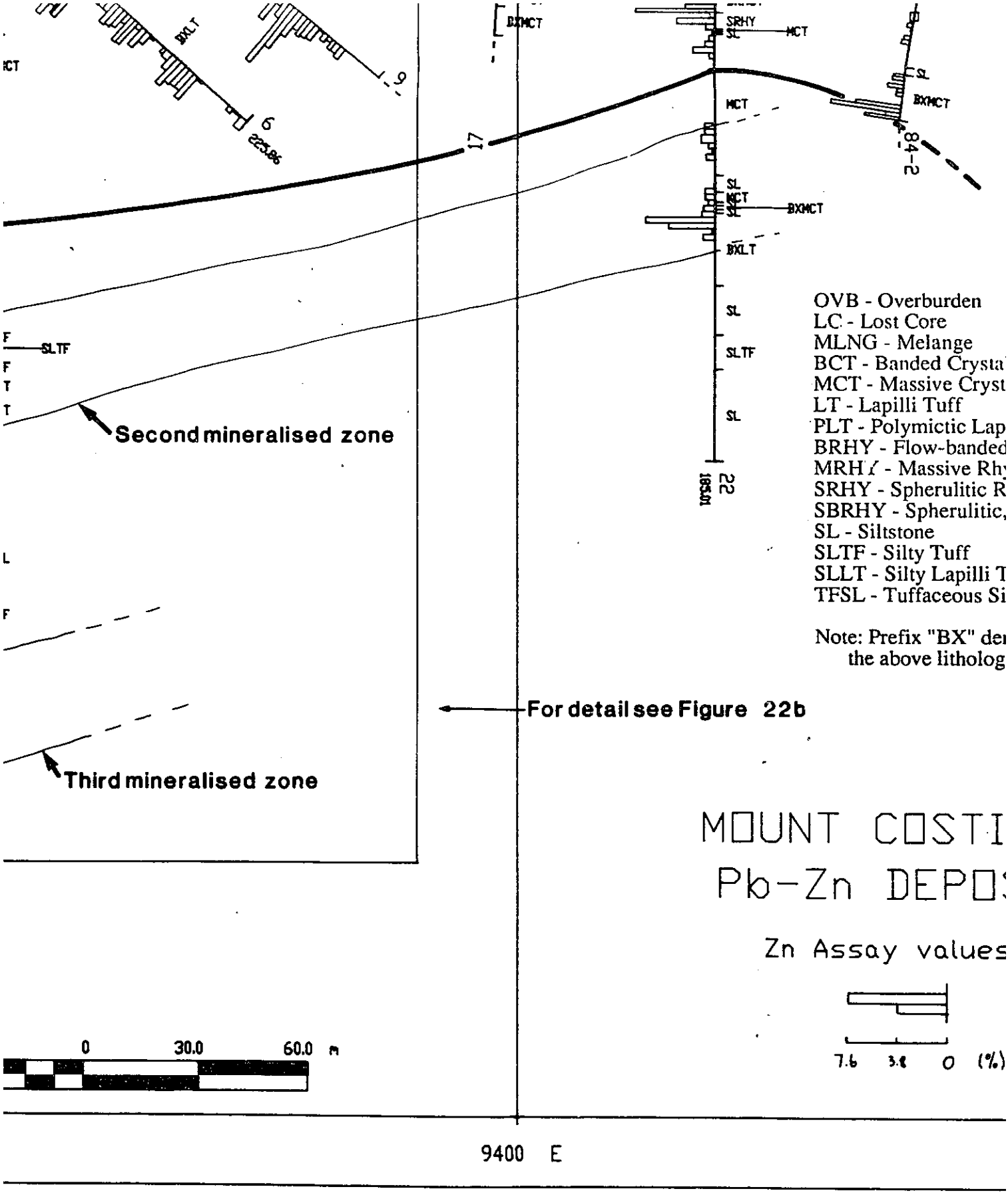
Second mineralised zone
Third mineralised zone
For detail see Figure 22b
OVB - Overburden
LC - Lost Core
MLNG - Melange
BCT - Banded Crysta
MCT - Massive Cryst
LT - Lapilli Tuff
PLT - Polymictic Lap
BRHY - Flow-banded
MRHY - Massive Rh
SRHY - Spherulitic R
SBRHY - Spherulitic,
SL - Siltstone
SLTF - Silty Tuff
SLLT - Silty Lapilli T
TFSL - Tuffaceous Si
Note: Prefix "BX" de
the above litholog
MOUNT COSTI
Pb-Zn DEPO
Zn Assay values
0
30.0
60.0 m
7.6
3.8
0
(%)
9400 E

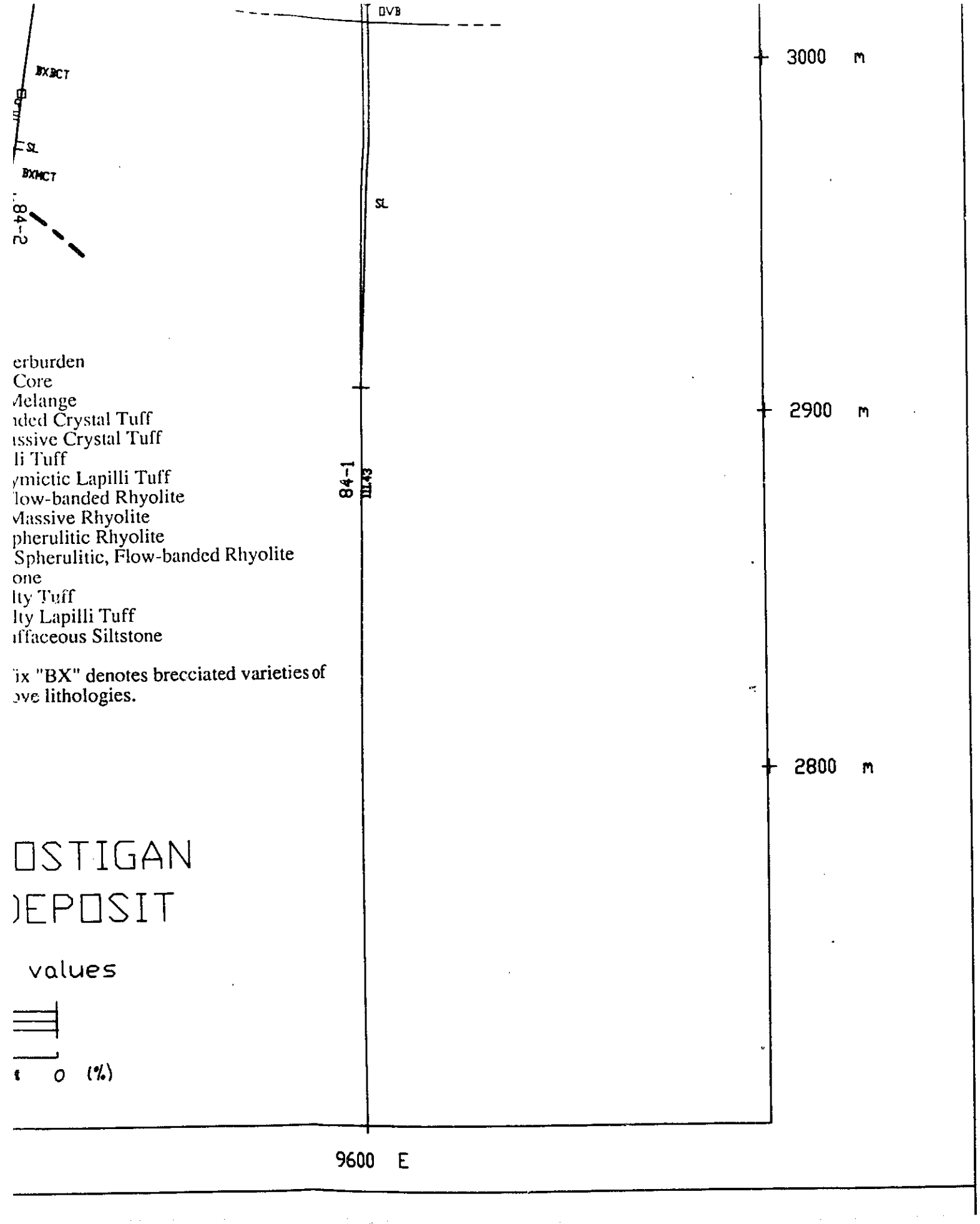

erburden
Core
Melange
ıded Crystal Tuff
ıssive Crystal Tuff
li Tuff
ymictic Lapilli Tuff
low-banded Rhyolite
Massive Rhyolite
pherulitic Rhyolite
Spherulitic, Flow-banded Rhyolite
one
lty Tuff
lty Lapilli Tuff
ıffaceous Siltstone

ix "BX" denotes brecciated varieties of
ove lithologies.

OSTIGAN
)EPOSIT

values

t 0 (%)

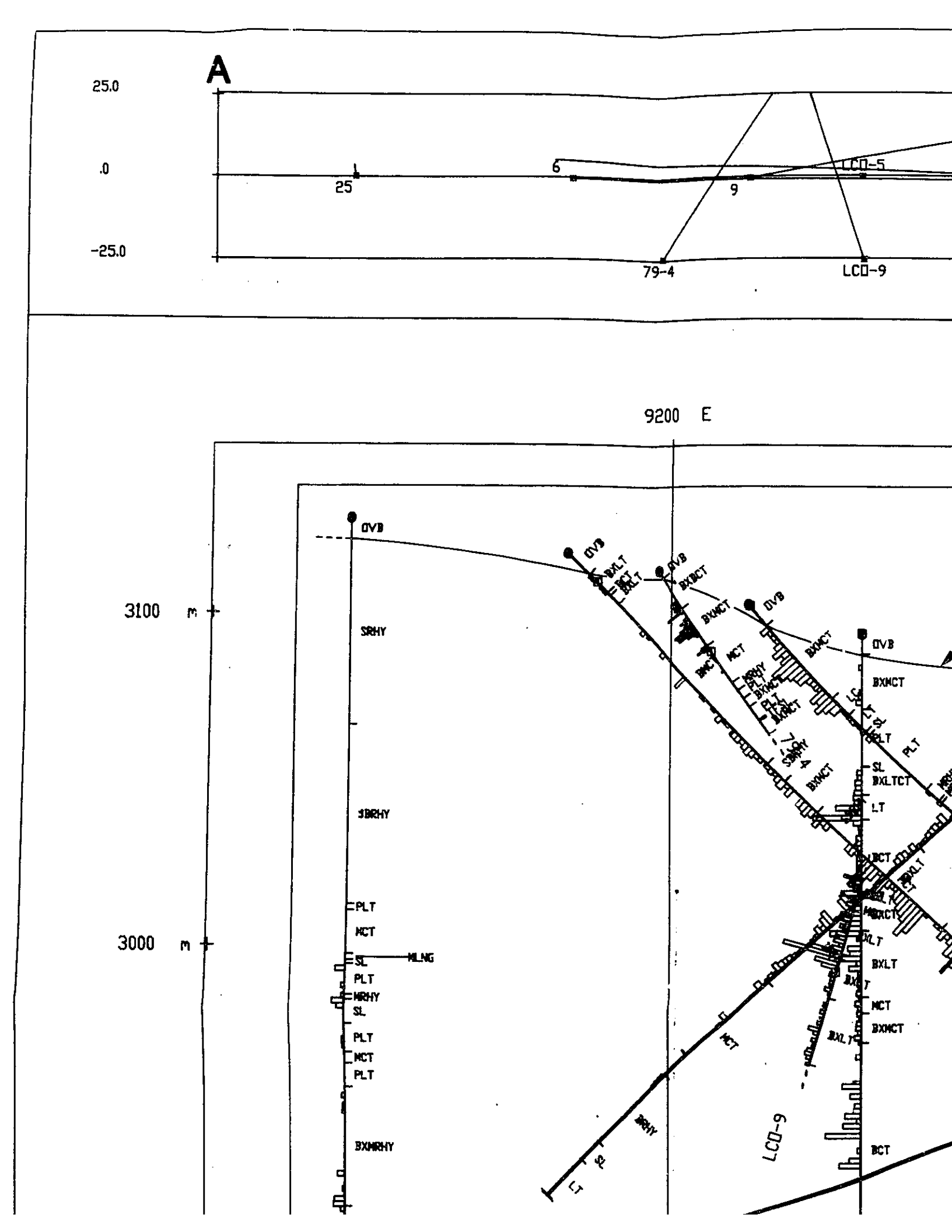
A
25.0
.0
-25.0
25
6
9
LCD-5
79-4
LCD-9
9200 E
3100 m
3000 m
OVB
SRHY
3BRHY
PLT
MCT
SL
MLNG
MRHY
BXMRHY
BXMCT
BXLTCT
BXLT
BCT
LT
LCD-9

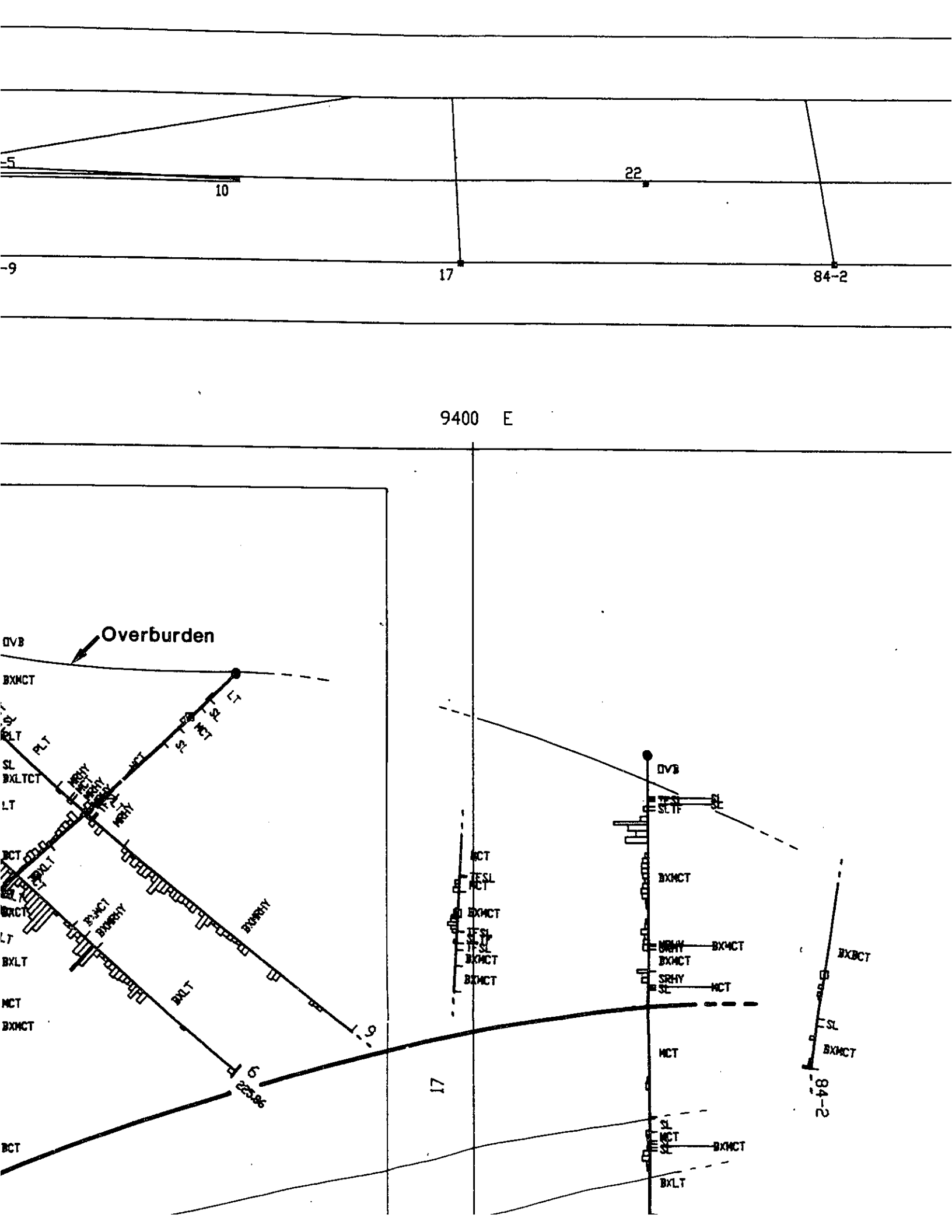
-5
10
22
-9
17
84-2
9400 E
Overburden
OVB
BXMCT
PLT
SL
BXLTCT
LT
MCT
MRHY
BXMRHY
BXLT
BCT
17
84-2
SRHY
BXBCT

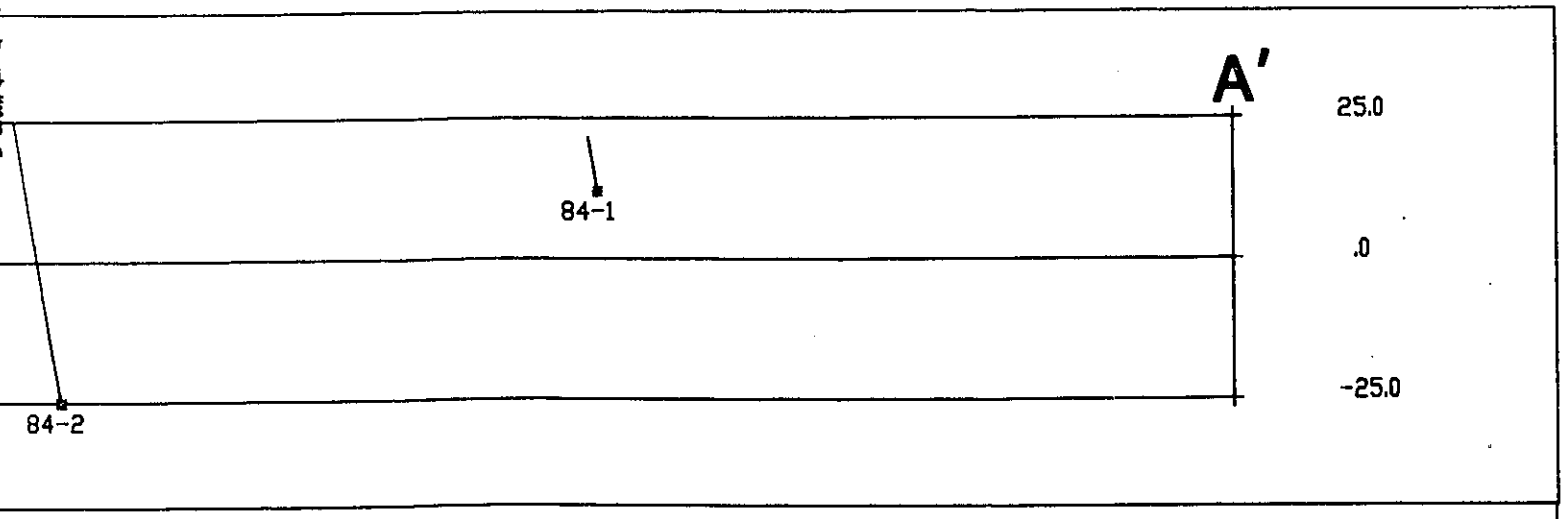
A'
25.0
.0
-25.0
84-1
84-2

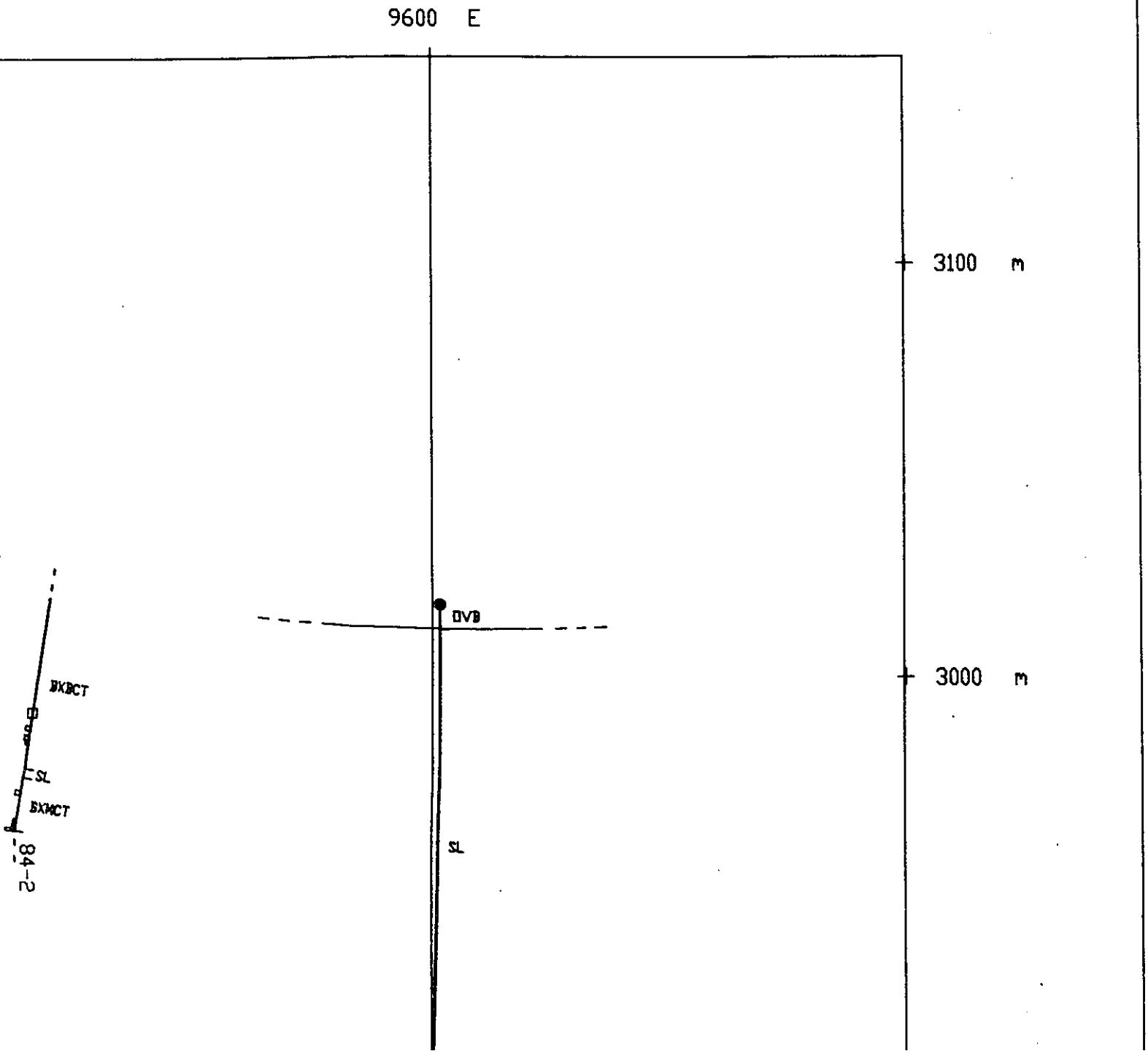
9600 E
3100 m
3000 m
DVB
SL
BXBCT
SL
BXMCT
84-2

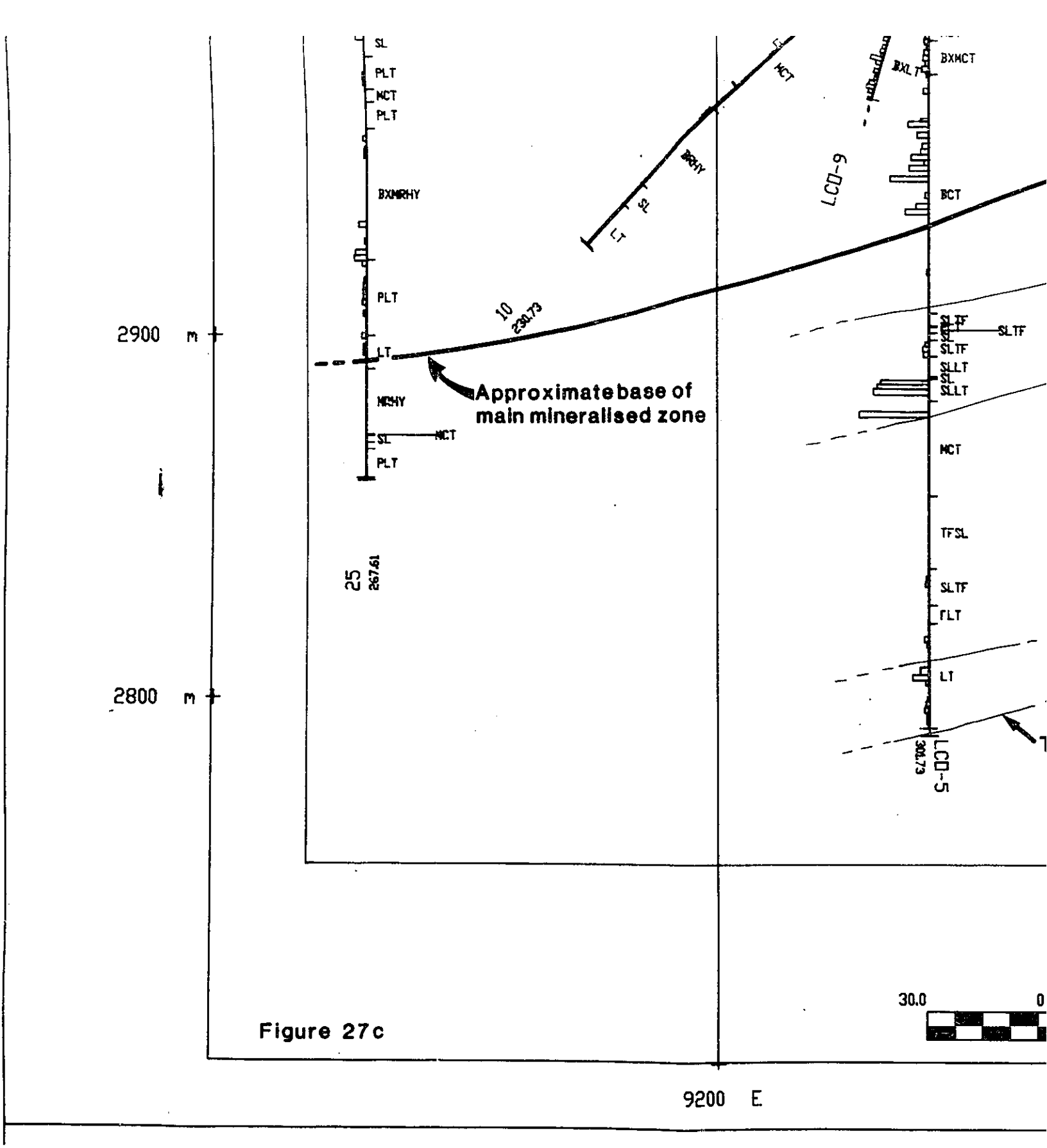
2900 m
2800 m
9200 E
SL
PLT
MCT
PLT
BXMRHY
PLT
LT
MRHY
SL
MCT
PLT
10
239.73
Approximate base of
main mineralised zone
25
267.61
LT
SL
MRHY
LCD-9
BXMCT
BXL
BCT
SLTF
SLTF
SLTF
SLLT
SL
SLLT
MCT
TFSL
SLTF
FLT
LT
LCD-5
304.73
30.0
0

Figure 27c

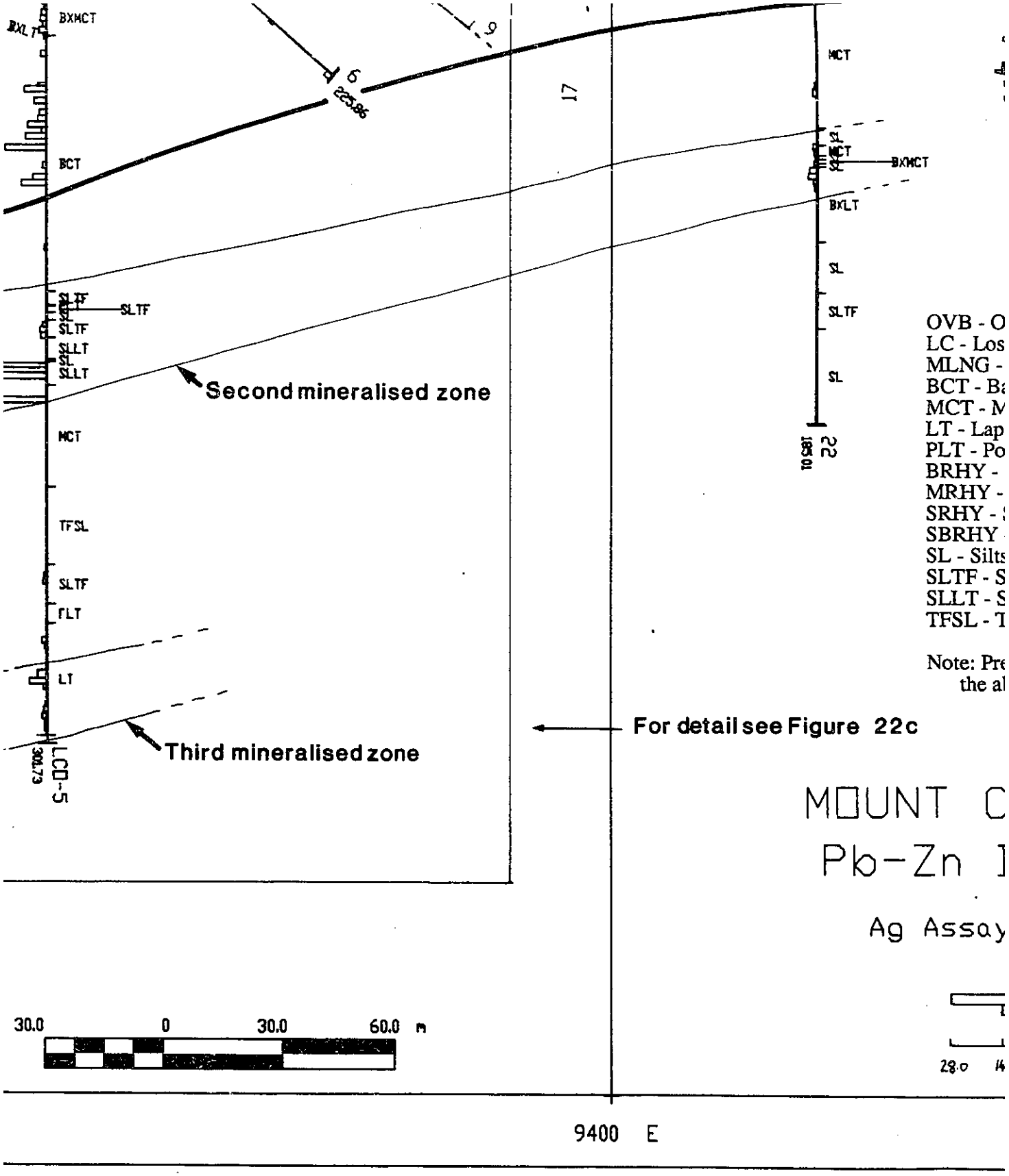
BXMCT
BXLT
BCT
SLTF
SLTF
SLTF
SLLT
SL
SLLT
MCT
TFSL
SLTF
FLT
LT
LCD-5
Second mineralised zone
Third mineralised zone
For detail see Figure 22c
MCT
BXMCT
BXLT
SL
SLTF
SL
22
17
9
6
30.0
0
30.0
60.0 m
9400 E
OVB - O
LC - Los
MLNG -
BCT - Ba
MCT - M
LT - Lap
PLT - Po
BRHY -
MRHY -
SRHY -
SBRHY
SL - Silts
SLTF - S
SLLT - S
TFSL - T
Note: Pre
the al
MOUNT C
Pb-Zn
Ag Assay

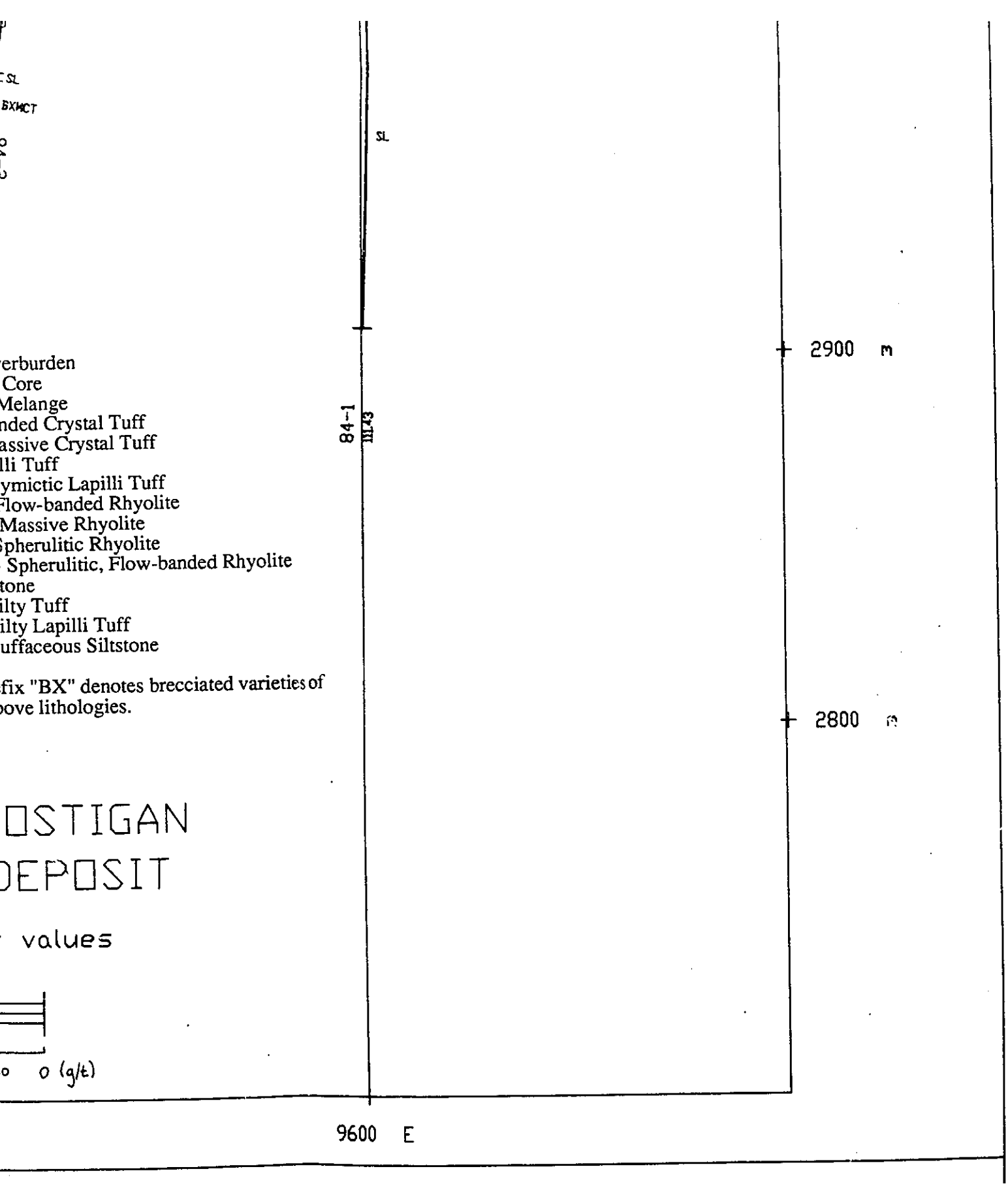

erburden
Core
Melange
nded Crystal Tuff
assive Crystal Tuff
lli Tuff
ymictic Lapilli Tuff
Flow-banded Rhyolite
Massive Rhyolite
Spherulitic Rhyolite
Spherulitic, Flow-banded Rhyolite
tone
ilty Tuff
ilty Lapilli Tuff
uffaceous Siltstone

fix "BX" denotes brecciated varieties of
ove lithologies.

OSTIGAN
DEPOSIT

values

0 (g/t)